PREPARATION OF ICETEXANE DITERPENOIDS: SYNTHESIS OF BREAST CANCER CELL GROWTH INHIBITORS

by

Daniel Jun Moon

A thesis submitted to the Faculty of the University of Delaware in partial fulfillment of the requirements for the degree of Master of Science in Chemistry and Biochemistry

Summer 2016

PREPARATION OF

ICETEXANE DITERPENOIDS

SYNTHESIS OF BREAST CANCER CELL

GROWTH INHIBITORS

by

Daniel Jun Moon

Approved: _____

William J. Chain, Ph.D.
Professor in charge of thesis on behalf of the Advisory Committee

Approved: _____

Murray V. Johnston, Ph.D.
Chair of the Department of Chemistry and Biochemistry

Approved: _____

George H. Watson, Ph.D.
Dean of the College of Arts & Sciences

Approved: _____

Ann L. Ardis, Ph.D.
Senior Vice Provost for Graduate and Professional Education

ACKNOWLEDGMENTS

I would like to express my sincere appreciation to Ms. Heather Green, my high school chemistry teacher, whose expertise and excitement to teach organic chemistry sparked my interest.

I am greatly indebted to Dr. Kevin Minbiole for opening up the opportunity to pursue graduate school. If it weren't for his captivating lectures, I do not think I would have held an interest and made it this far.

I am grateful for Dr. Christine Hughey, whose patience, support, and generous guidance helped me pursue my passions during and after my time at James Madison University.

I am thankful for every single one of my colleagues, both in Hawaii and Delaware, for the encouragements and memories we have shared.

Lastly, I am sincerely thankful for Dr. William Chain, who has had faith in me for the past two years. In times when I did not think I could go further in my studies, his trust in me urged me to do better. It was a pleasure working with him.

TABLE OF CONTENTS

LIST OF TABLES

LIST OF FIGURES

LIST OF ABBREVIATIONS

Å	angstrom(s)
Ac	acetyl
BINAP	2,2'-Bis(diphenylphosphino)-1,1'-binaphthyl
Bu	butyl
°C	degrees Celsius
Calcd.	calculated
CAM	ceric ammonium molybdate
CI+	chemical ionization
cm	centimeter(s)
δ	chemical shift (parts per million)
d	doublet
dd	doublet of doublet
ddd	doublet of doublet of doublet
dddd	doublet of doublet of doublet of doublet
ddt	doublet of doublet of triplet
DMAP	4-(dimethylamino)pyridine
DME	1,2-dimethoxyethane
DMF	*N*,*N*-dimethylformamide
DMSO	dimethyl sulfoxide
dppf	1,1'-Bis(diphenylphosphino)ferrocene
dt	doublet of triplet
EI+	electron impact ionization
ES+ (or ESI+)	electrospray ionization

equiv	equivalence
Et	ethyl
FD+	field desorption
FTIR	Fourier transform infrared spectroscopy
g	gram(s)
h	hour(s)
HPLC	high performance liquid chromatography
HRMS	high resolution mass spectrum
Hz	hertz(s)
I	current
IC_{50}	half maximal inhibitory concentration
J	coupling constant
K	kelvin
kcal	kilocalorie(s)
kV	kilovolts
λ	wavelength
L	liter(s)
LAH	lithium aluminum hydride
m	multiplet
M	molarity (mol L^{-1})
$[M]^+$	molecular ion (positive)
mA	milliamp(s)
mg	milligram(s)
MHz	megahertz(s)

min	minute(s)
μL	microliter(s)
mL	milliliter(s)
μM	micromolar
mm	millimeter(s)
μmol	micromole(s)
mmol	millimole(s)
mol	mole(s)
N	normality (concentration)
nM	nanomolar
NMI	*N*-methylimidazole
NMR	nuclear magnetic resonance
NOESY	nuclear Overhauser effect spectroscopy
*o*QM	*ortho*-quinone methide
Ph	phenyl
pyr	pyridine
q	quartet
qd	quartet of doublet
qt	quartet of triplet
R_f	retention factor
s	singlet or second(s)
s.m. (or sm)	starting material
SN_{Ar}	nucleophilic aromatic substitution
t	triplet

TBAF	tetra-*n*-butylammonium fluoride
TBS	*tert*-butyldimethylsilyl
td	triplet of doublet
tdd	triplet of doublet of doublet
Temp	temperature
TEMPO	(2,2,6,6-Tetramethyl-piperidin-1-yl)oxyl
TLC	thin-layer chromatography
TMAF	tetramethylammonium fluoride
TMPO	(2,2,6,6-Tetramethyl-piperidin-1-yl)oxyl
Tf	triflic
THF	tetrahydrofuran
TMS	trimethylsilyl
TMSCl	trimethylsilyl chloride
Ts	tosyl
UV	ultraviolet

ABSTRACT

Breast cancer is one of the most common cancers among women worldwide. Late stage treatment for breast cancer involves a chemotherapeutic, doxorubicin, which has earned the nickname “the red death” due to the detrimental side effects associated with this drug. Therefore, it is urgent that we identify and study recently discovered breast cancer drugs capable of treating cancer patients. Premnalatifolin A, an icetexane diterpene dimer, was recently isolated and evaluated against multiple cancer cell lines, in particular MCF-7 breast cancer cells (IC_{50} = 1.77 μM), outperforming doxorubicin (IC_{50} = 3.68 μM). The monomeric unit was also found to be selectively cytotoxic against MCF-7 cell line (IC_{50} = 3.53 μM).

Given that both the dimer and monomer exhibited anti-cancer activity, our goal was to develop synthetic pathways for the tricyclic backbone of the monomer. We have developed two synthesis pathways to forming the 3-vinyl siloxybenzyl halide and a one-step synthesis of both the unsubstituted and 4,4-dimethyl-substituted vinylated silyl enol ether, and during the course of our work we developed optimized conditions for the Suzuki-Miyaura coupling of an aryl chloride. We attempted utilizing the enolate–*ortho*-quinone methide Michael addition, a reaction sequence notable in our group, to join the two cyclic fragments. Due to complications resulting from an unproductive hemiacetal formation, we revised the synthesis by diverting to a classic alkylation reaction sequence. The classical enolate alkylation was highly diastereoselective, giving the desired 1,2-*trans* alkylation product, which was followed by a ring-closing metathesis reaction to construct the 7-membered ring and complete the core structure of these important natural products. Furthermore, we explored the

hydrogenation of the cycloheptene ring, opening up the synthesis to generate a small library of icetexane model compounds.

Chapter 1

INTRODUCTION

Icetexane diterpenoids have been described in the literature since 1976, and to date over 40 icetexanes have been isolated from a variety of terrestrial plant species.[1,2] Icetexane natural products consist of a 6-7-6 tricyclic system with variations in oxidation levels in each ring. The unique structural variety of icetexane natural products have exhibited an array of biological activity, such as antioxidant, hepatoprotective, cytotoxic[3], anti-inflammatory, antibacterial[4], and trypanocidal[5] activity (Figure 1.1).

The genus *Premna* are distributed throughout tropical and sub-tropical environments in Asia, Africa, Australia, and Pacific Islands. The various *Premna*

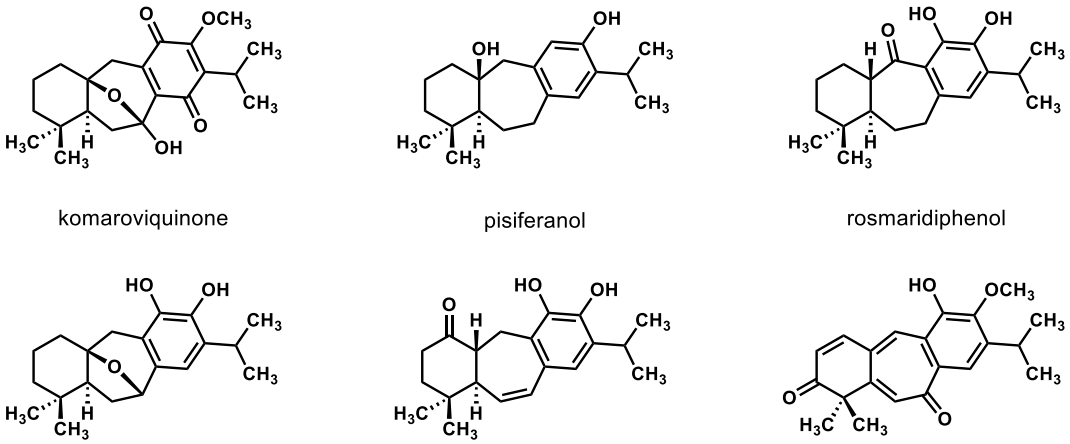

Figure 1.1 Isolated icetexanes exhibiting vast array of biological activity.[1]

species have been known to be used as Indian traditional medicine.[4,6]

Premnalatifolin A (**1**) is a dimeric icetexane diterpenoid that was recently isolated from the dry stem-bark of *Premna latifolia*, a plant known to Indian traditional medicine. This compound and several other related icetexanes (Figure 1.2) were isolated and evaluated for cytotoxicity against various human cancer cell lines. Premnalatifolin A was found to be a selective growth inhibitor of breast cancer cells in vitro (MCF-7, IC_{50} = 1.77 μM), which is comparable to doxorubicin (Adriamycin®, IC_{50} = 3.70 μM), one of the current standards of care. Premnalatifolin A was also found to be active against a human colon cancer cell line (HT-29, IC_{50} = 19.4 μM) outperforming doxorubicin (HT-29, IC_{50} = 39.6 μM).[7] The monomeric unit (**2**) was also found to be selectively cytotoxic (MCF-7, IC_{50} = 3.53 μM and HT-29, IC_{50} = 127 nM).[8] The detailed mechanism of action of doxorubicin is still not fully understood,[9] and though it is the standard of care in several human cancers, doxorubicin is quite toxic and is associated with several detrimental side effects and a high mortality rate. This has earned doxorubicin the nickname of "the red death" among patients;[10] thus

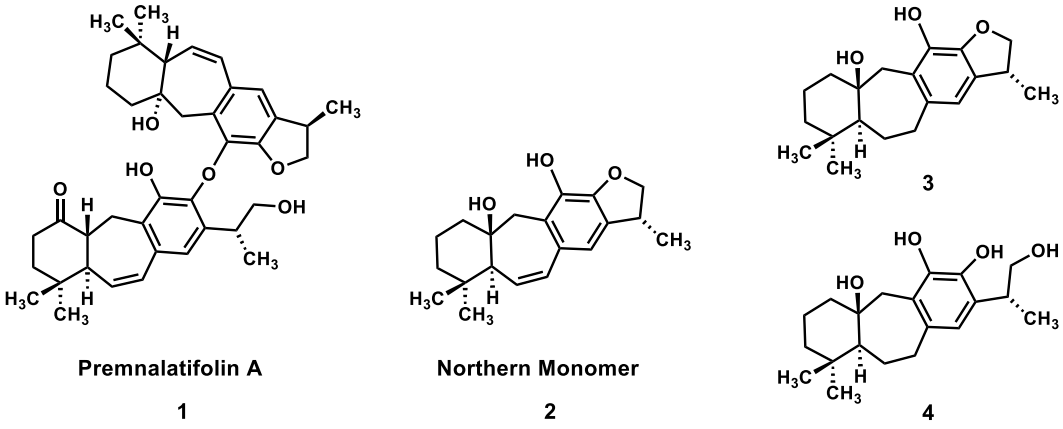

Figure 1.2 Natural products isolated from *Premna latifolia*.[8, 11]

there is a clear, urgent need for new chemotherapeutics for the treatment of breast cancer. Premnalatifolin A is a promising lead compound for the discovery of new, less toxic chemotherapeutics.

Premnalatifolin A is a dimeric icetexane diterpene, with each tricyclic monomer varying slightly in oxidation levels, (**2**) and (**5**) (Figure 1.3). Given that both monomeric and dimeric icetexane terpenoids have significant anti-cancer activity, our

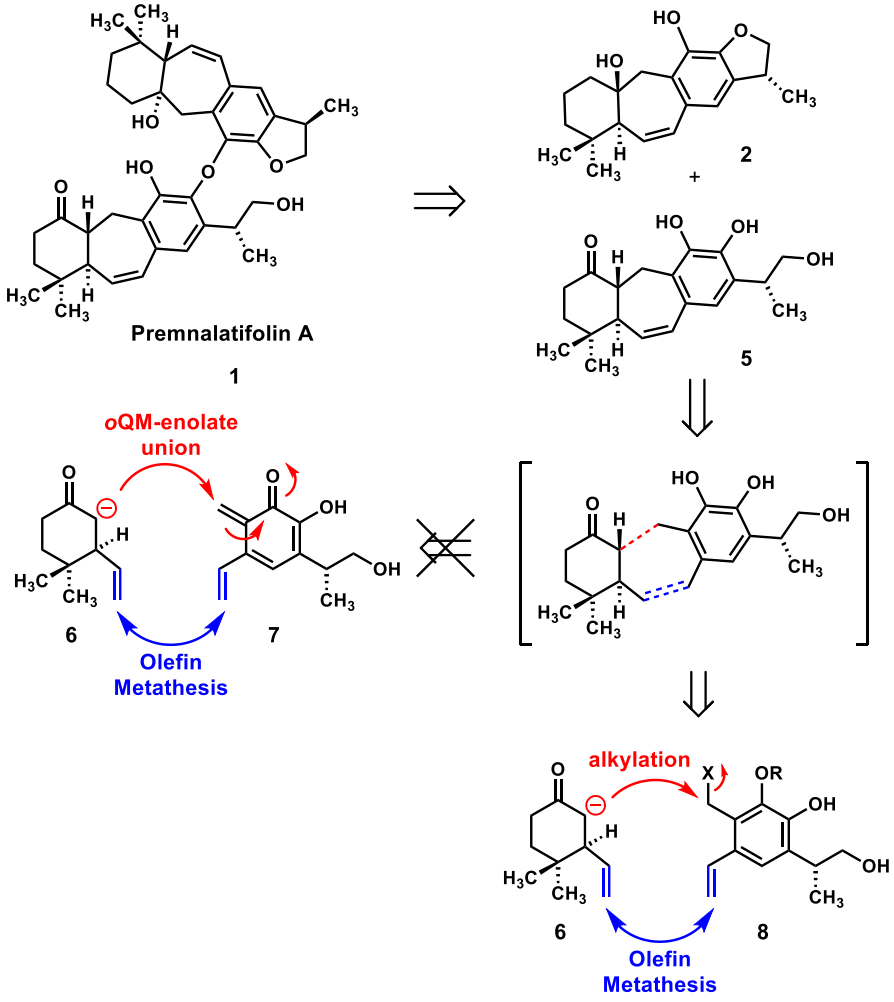

Figure 1.3 Retrosynthetic analysis of premnalatifolin A.

goal is to develop a flexible, modular synthesis of the tricyclic monomer units. Thus, we will enable further exploration of cytotoxic icetexane diterpenes as new cytotoxic agents, and enable the generation of libraries of compounds for screening against human cancer cell lines.

The tricyclic monomers (**2**) and (**5**) are composed of an oxidized aromatic ring and a dimethylcyclohexane fused by a cycloheptene ring. In this chapter, synthetic strategies relying upon an enolate–*ortho*-quinone methide reaction are explored for the synthesis of these monomers via the formation of the key seven-membered ring utilizing a two-step sequence – a Michael addition of enolate (**6**) to a reactive *ortho*-quinone methide (the coumarin derivative (**7**)), and a ring-closing metathesis (Figure 1.2). We have developed our synthetic strategy utilizing a model system (Figure 1.4), focusing on the carbocyclic backbone (**9**) of premnalatifolin A, and we have demonstrated the difficulties of the *ortho*-quinone methide reaction sequence, forming an undesirable hemiacetal. However, we successfully formed the model monomeric unit by redirecting the focus to an alkylation reaction sequence of the vinyl silyl enol ether (**10**) and conveniently the *ortho*-quinone methide precursor (**11**).

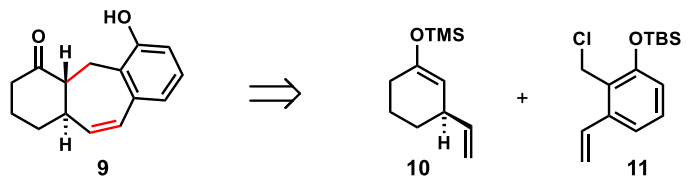

Figure 1.4 Retro-synthesis of the model system.

Chapter 2

SYNTHESIS

The group is deeply interested in approaching natural product synthesis utilizing carbonyl-enabled carbon–carbon bond formations.[12,13] In this chapter, a synthetic strategy employing the enolate–*ortho*-quinone methide Michael addition to initiate the formation of the seven-membered ring. In doing so, we developed synthetic pathways to making the precursors, a silyl-enol ether and an *ortho*-quinone methide precursor.

2.1 Silyl-Enol Ether

A straightforward 1,4-addition of vinyl cuprate [formed from a vinyl Grignard reagent and Cu(I)] to cyclohexenone (**12**) followed by trapping of the resultant enolate with chlorotrimethylsilane gave the silyl enol ether unit (**10**) in 96% yield in a one-pot reaction (Figure 2.1).[14–17] The same procedure was successfully applied to the more sterically crowded 4,4-dimethylcyclohex-2-ene-1-one substrate (**13**) to give the 4,4-

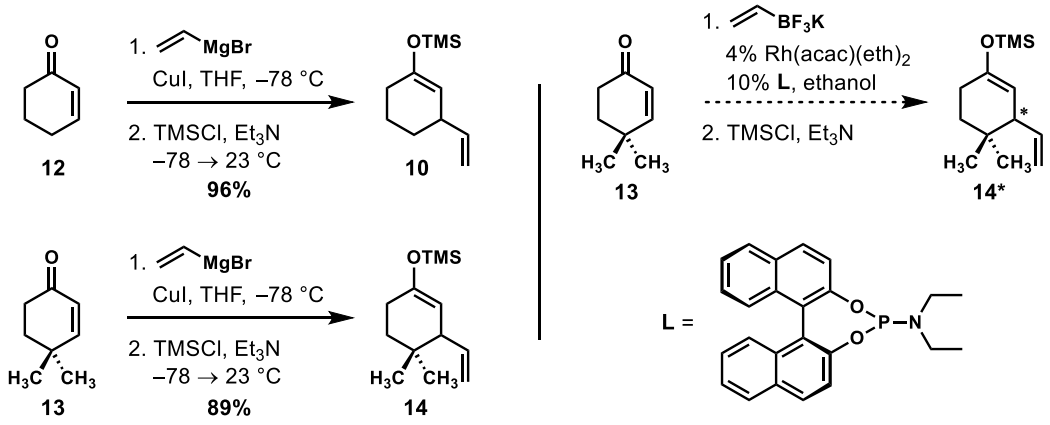

Figure 2.1 Vinylated silylenol ether one-pot synthesis.

dimethyl-substituted silyl enol ether (**14**) in 89% yield. In due course, we will reevaluate the 1,4-addition reaction. We will employ an enantioselective conjugate addition of potassium vinyltrifluoroborate to dimethylcyclohexanone (**13**) mediated by a rhodium catalyst featuring a monodentate phosphoramidite ligand to give the enantiomeric TMS-enolate upon trapping with chlorotrimethylsilane.[18]

2.2 *Ortho*-Quionone Methide Precursor

Two routes were developed toward the trisubstituted aromatic ring that comprised the right hand piece of the model system. In the first, we employed commercially available 2,6-dihydroxybenzoic acid, and in the second we employed 2-chloro-6-fluorobenzaldehyde.

2.2.1 Route A

Adapting the methods of Shaw[19] and Murphy[20], Route A (Figure 2.2) started with commercially available 2,6-dihydroxybenzoic acid (**15**). Reaction of (**15**) with acetone in the presence of thionyl chloride and 4-dimethylaminopyridine was a straightforward acetonide protection reported by Shaw *et al.*.[19] Compound (**16**), thus obtained in 84% yield, was converted to the aryl triflate (**17**) under the action of triflic anhydride in the presence of pyridine (80% yield).[19,20] The aryl triflate underwent a Suzuki-Miyaura cross-coupling reaction with potassium vinyl trifluoroborate, cesium carbonate base, and ($PdCl_2$[dppf]) as the palladium catalyst under conditions developed by Molander *et al.*, providing compound (**18**) at 87% yield.[21] Deprotection of acetonide (**18**) by a straightforward lithium aluminum hydride reduction gave the diol (**19**) in 92% yield.[19] The benzylic hydroxide group converted to the corresponding aldehyde (**20**) by selective aerobic oxidation in the presence of Cu(I), (2,2,6,6-

tetramethylpiperidin-1-yl)oxyl [TEMPO]), and methylimidazole catalysts to give compound (**20**) at 98% yield.[22] Stahl reported free phenols inhibiting oxidation, possibly due to the formation of inactive Cu-phenolate species. However, due to the *ortho*-position of phenol and aldehyde, we presume the intramolecular hydrogen-bonding bridge prevented the Cu(I) from coordinating with the phenol group. After the protection of compound (**20**) using *tert*- butyldimethylsilyl trifluoromethanesulfonate[23] (98% yield), the reduction of the benzaldehyde group using a mild reducing agent in protic solvent, sodium borohydride in methanol, gave compound (**22**) at 92% yield. Utilizing stronger reducing agents or aprotic solvents, such as lithium aluminum hydride or THF, additionally facilitated protecting group migration, resulting in the free phenol and protected primary alcohol. A NOESY was collected to ensure that the silyl group did not migrate to the primary alcohol after the exposure to a mild reducing

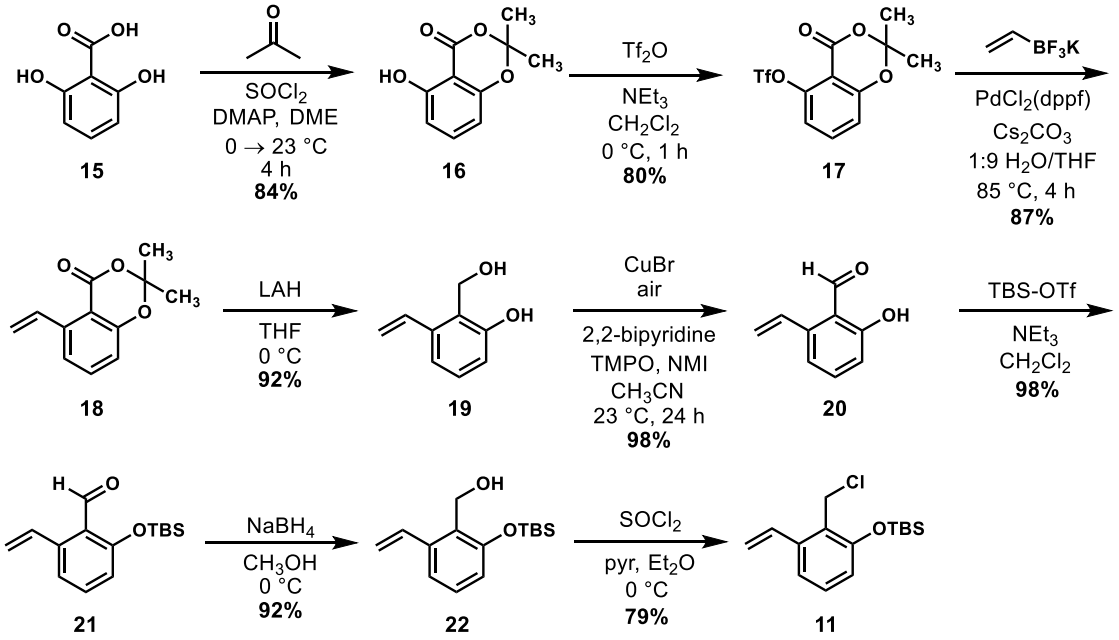

Figure 2.2 Route A to *ortho*-quinone methide model intermediate.

agent (Figure 2.3). Magnesium borohydride, although not a typical reducing agent, worked as well, but in moderate yield (53% yield). The benzylic hydroxyl group was then converted to the corresponding chloride under the action of thionyl chloride and pyridine, making 3-vinylsiloxybenzyl halide (**11**) (79% yield), the precursor to the *ortho*-quinone methide.

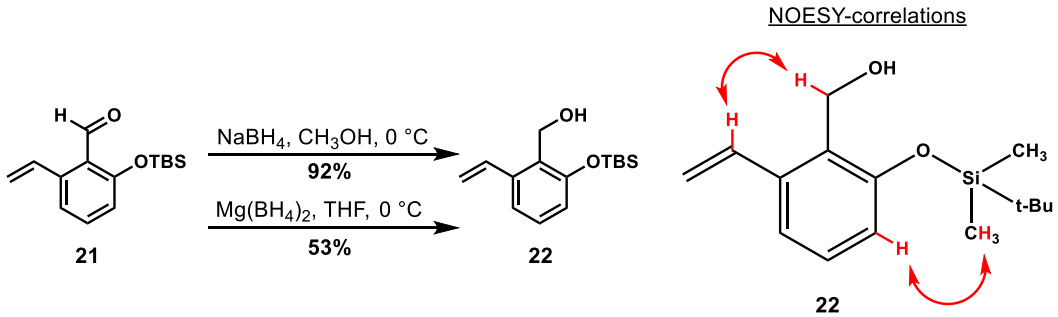

Figure 2.3 Reducing benzaldehyde and NOESY of (**22**).

2.2.2 Route B

The 8-step synthesis of the aryl portion of the monomer unit unfortunately required several steps of protecting group manipulation. In order to further streamline the synthesis of the model system, we addressed the liability of protecting group manipulations by beginning with an alternate starting material.

Most of the protecting group manipulations were around the benzoic acid functional group of (**15**) (Figure 2.4). Therefore, it was in our interest to avoid the acetonide protecting group and the reduction/oxidation sequence, so we sought out an inexpensive, commercially available benzaldehyde derivative starting material. The 2-chloro-6-fluorobenzaldehyde (**23**) was an optimal starting material to switch our focus to avoid the need for the use of acetonide protecting group. Additionally, unlike (**15**)

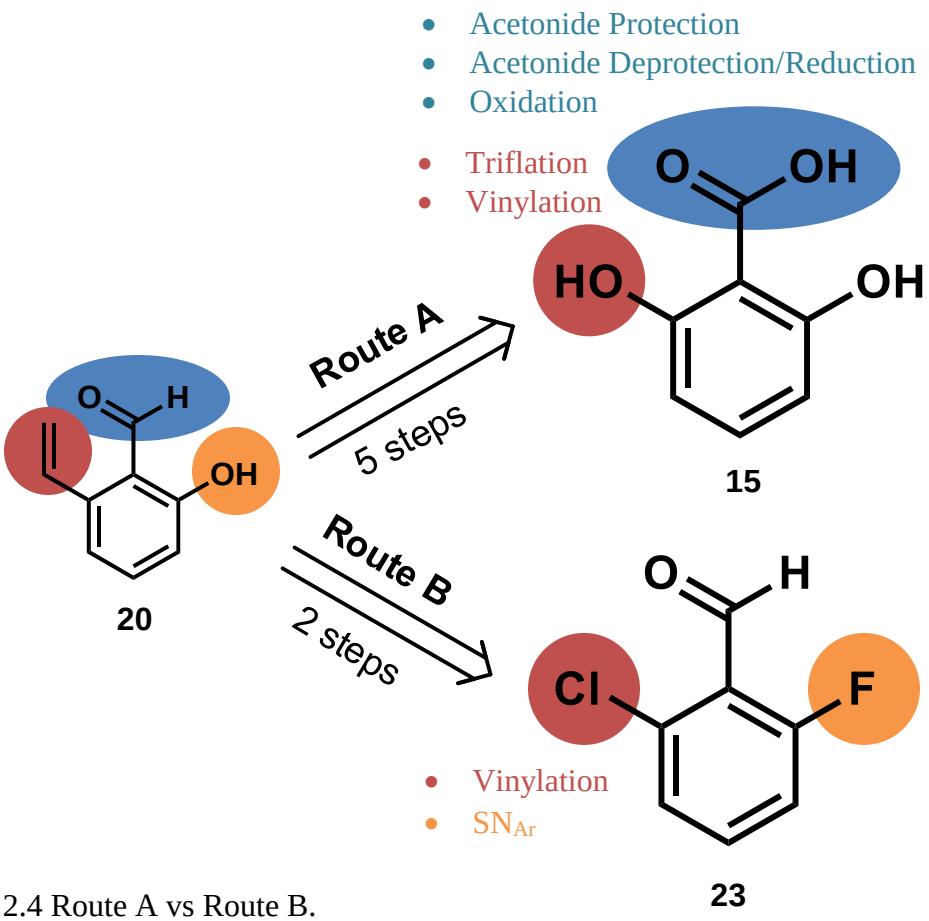

Figure 2.4 Route A vs Route B.

where the free phenol underwent triflation in order to undergo vinylation via Suzuki-Miyaura reaction, an aryl halide should provide a suitable synthetic handle for cross coupling manipulation to install the required vinyl group without the need for activation. However, an extra step was required to install the phenol group by a selective nucleophilic aromatic substitution by displacing the fluoride halogen. Eventually, we were able to truncate the synthesis to 5-steps (Figure 2.5).

Starting with 2-chloro-6-fluorobenzaldehyde (**23**), potassium hydroxide selectively displaced the fluoride halogen by a simple nucleophilic aromatic substitution reaction to give compound (**24**) in 91% yield. Due to its volatile nature,

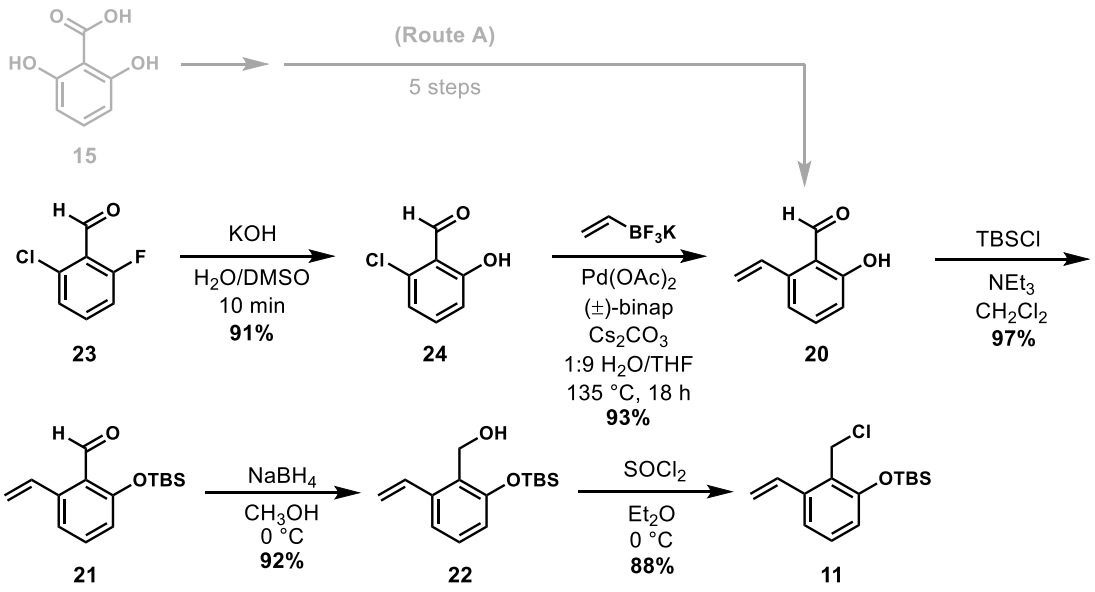

Figure 2.5 Route B of *ortho*-quinone methide model intermediate.

we were cautious in drying the compound under vacuum over a long period of time. Conveniently, the subsequent coupling reaction was run under wet conditions. The Suzuki-Miyaura coupling reaction did not occur under the same parameters from route A, and required some study in order to engage the less reactive aryl chloride. Aryl triflates generally undergo oxidative addition to low-valent palladium at rates much higher than the corresponding aryl chlorides, reflecting the significant difference in bond energy between σ C–OTf and σ C–Cl. The successful engagement of aryl chlorides in Suzuki-Miyaura cross coupling reactions was described by Nájare[24] and coworkers when they employed an unorthodox catalyst system and low valent palladium. In their work, they utilized a different bidentate ligand, (*S*)-BINAP, in the presence of $Pd(OAc)_2$ and cesium carbonate base in *N*,*N*-dimethylformamide at 120 °C. In our hands, a successful coupling reaction of aryl chloride (**24**) and potassium vinyl trifluoroborate in the presence of catalytic $Pd(OAc)_2$, (±)-BINAP ligand, and

cesium carbonate base in 10% H_2O/THF required an elevated reaction temperature of 135 °C. When using 1,1'- Bis(diphenylphosphino)ferrocene (dppf) ligand, the ligand used in coupling aryl triflates (Route A), there was no reaction.[25] The success with BINAP ligand over dppf ligand for aryl chlorides can be attributed to the natural bite angle of the bidentate diphosphine ligand. The wider natural bite angle of dppf ligand does not generally facilitate oxidative addition, an acceptable ligand for coupling a more reactive aryl triflate. BINAP has a narrower natural bite angle, facilitating the oxidative addition of Pd(II)BINAP with less reactive aryl halides.[26] The last three steps of our synthesis required only slight adaptations of chemistry employed in our first approach (Route A). The less reactive *tert*-butyldimethylsilyl chloride gave the corresponding silyl ether (**21**) in similar yield to before which required the *tert*-butyldimethylsilyl trifluoromethanesulfonate. Followed by the reduction of the benzaldehyde (**21**) using sodium borohydride in methanol, the benzylic alcohol (**22**) underwent chlorination using thionyl chloride in the absence of pyridine, resulting in higher yields. We have encountered complications with pyridine in the past with *ortho*-quinone methide precursors where prolonged exposure to the reaction conditions resulted in displacement of the chloride by pyridine to give mixtures of salts.

2.2.2.1 Suzuki-Miyaura Coupling Reaction

In Route A, the aryl triflate (**17**) underwent a smooth Suzuki cross-coupling with 1 eq. potassium vinyl trifluoroborate, 1% mol ($PdCl_2$[dppf]), 2 eq. Cs_2CO_3, in 0.5 M 10% H_2O/THF solvent on a 20-mmol scale heated at reflux for 18 hours. This was straightforward, owing to the high reactivity of aryl triflates, bromides, and iodides toward low-valent palladium. The high reactivity of aryl triflate was generally

attributed to the weaker σ C–OTf bond strength, accelerating the often rate-limiting oxidative addition step of the catalytic cycle (bond dissociation energies for σ Ph−X: I: 65 kcal mol^{-1}; Br: 81 kcal mol^{-1}; Cl: 96 kcal mol^{-1}).[27–29] On the other hand, aryl chlorides, having a stronger σ C−Cl bond, exhibit poor reactivity or increased tendency toward side reactions as reported by Molander[25]. However, the presence of electron-withdrawing groups at the *ortho* and *para* positions active aryl chlorides towards oxidative addition, allowing the coupling reaction to proceed in comparable yields at substantially higher reaction temperatures.[21,30] The benzaldehyde group in (**24**) acts as the electron-withdrawing group, *ortho* to the aryl chloride. Therefore, adapting conditions described by Nájera,[24] we executed a straightforward solvent screen in search of a more efficient cross coupling reaction. On a 0.6-mmol scale, reactions conducted in 1.2 mL *N*,*N*-dimethylformamide gave poor yield and an equal ratio of the proto-dechlorinated side product (**25**) (Table 2.1, entry 1). The next reasonable solvent was the high boiling DMSO solvent (entry 2). The desired product (**20**) was more favored over (**25**), but 18 hours was not sufficient for completion. We hypothesized that DMSO may have acted as a ligand, binding to Pd(II) and therefore disrupting the metal and displacing other ligands required in the catalytic cycle. Therefore, DMSO was not further tested due to the potential complication as well as the need for longer reaction times. The active transmetallating reagent in the Suzuki-Miyaura cross-coupling reaction is a boronic acid, formed by hydrolysis of our trifluoroborate salt.[31–34] Therefore, to increase the rate of the hydrolysis of the trifluoroborate salt to the boronic acid coupling partner, we explored varying moisture levels in the reactions (entries 3-4). After seeing an increase in the desired yield from dry *N*,*N*-dimethylformamide (entry 1) to *N*,*N*-dimethylformamide containing a single

Table 2.1 Suzuki-Miyaura coupling solvent screening. 0.100 g (**24**), 1.2 equiv potassium vinyl trifluoroborate[a], 3 mol% palladium acetate, 6 mol% (±)-BINAP, 3 equiv cesium carbonate, 0.25 M in a sealed pressure tube.

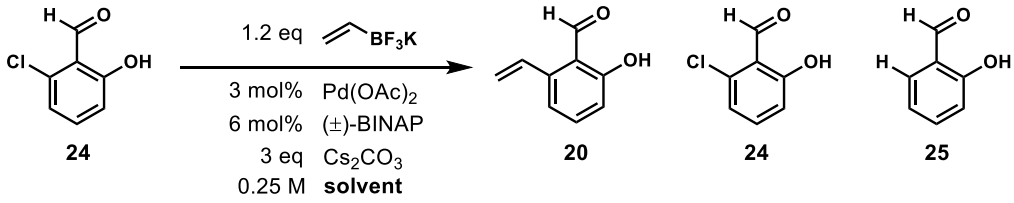

Entry	Solvent	Time (h)	Temp (°C)	Isolated (20) yield (%)	Products ratio (20) : (24) : (25)
1	DMF	17	120	16	43 : 14 : 43
2	DMSO	17	120	10	28 : 69 : 3
3	wet DMF	19	120	21	74 : 13 : 13
4	wet CH_3CN	18	120	9	20 : 80 : 0
5	9:1 CH_3CN:H_2O	18	120	47	67 : 33 : 0
6	9:1 THF:H_2O	18.5	120	66	only (**20**)
7[b]	9:1 THF:H_2O	18.5	135	93	only (**20**)

drop of water (wet solvent) (entry 3), we proceeded to adding 10% water to the solvents (entry 5), creating biphasic mixtures. Due to the dramatic increase in yield of the desired product, we also tested the solvent system used in Route A (entry 6). Upon further increase in the reaction temperature, we found the optimized condition: 1.2 equiv potassium vinyl trifluoroborate, 3 mol% palladium acetate, 6 mol% (±)-BINAP, 3 equiv cesium carbonate, 0.25 M of 9:1 THF:H_2O solvent on a 16 mmol (2.5 gram) scale at 135 °C for 18 hours (entry 7).

[a] Increased equivalence of trifluoroborate salt gave increased desired yields, but this adjustment was not necessary.

[b] 16 mmol scale

2.3 *Ortho*-Quinone Methide Michael Addition

We successfully joined the enol ether (**10**) and the *ortho*-quinone methide precursor (**11**) under the action of tetramethylammonium fluoride at low temperature, by employing the reaction conditions developed in our group.[12] While the enolate–*ortho*-quinone methide coupling was efficient and diastereoselective, we were not able to isolate the desired ketophenol (**26**), instead observing a ring-closed hemiacetal (**27**) at 36% yield. Initially, the reaction (Figure 2.6) looked promising, showing a bright yellow color as the reaction was stirring and revealing three spots on the TLC plate, R_f = 0.75, 0.50, 0.20, where R_f = 0.20 was consistent with the expected behavior of the desired product (**26**).[12] However, a crude ^{13}C NMR did not indicate the presence of ketone of any sort, instead suggesting the ketone function had been derivitized. After

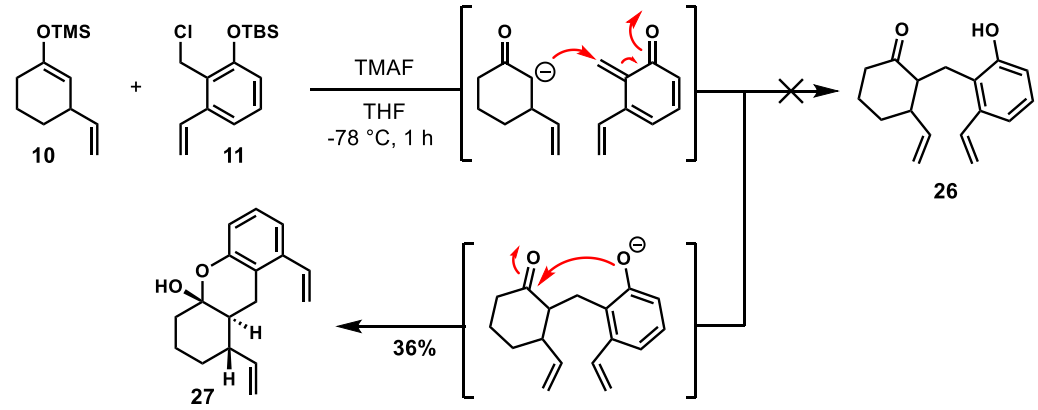

Figure 2.6 *Ortho*-quinone methide reaction.

purifying and isolating the three spots, only R_f = 0.50 (hemiacetal product) was characterizable. The isolated product was a diastereomeric mixture of hemiacetals, with both isomers clearly visible by ^1H NMR analysis. The diastereomers were

seperable by HPLC[c], but immediately equilibrated to a diastereomeric mixture when dissolved in solution. However, one diastereomer was selectively crystallized and characterized by x-ray diffraction.

During the course of development of the enolate–*ortho*-quinone methide reaction, the problem of hemiacetal formation from ketophenol adducts was previously encounterd. Conditions were developed to open the hemiacetals and capture the ketophenols for characterization purposes. In all cases, hemiacetals could be opened and captured by deprotonation with potassium carbonate and subsequently trapping the ketophenol with iodomethane in DMSO.[12] Therefore, we attempted to open the hemiacetal, adapting the mentioned conditions (Table 2.2). Under basic

Table 2.2 Opening hemiacetal (**27**).

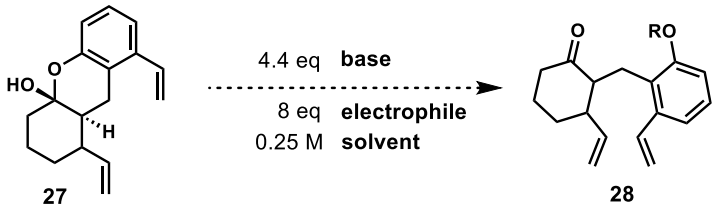

27 **28**

Entry	Solvent	Base	Electrophile	Product
1	DMSO	K_2CO_3	CH_3I	s.m.
2	DMSO	K_2CO_3	$(CH_3)_2SO_4$	s.m.
3	DMF	K_2CO_3	CH_3I	s.m.
4	THF	BuLi	CH_3I	s.m.
5[d]	DMSO	TsOH	—	side products
6	CH_2Cl_2	NMI	TBSCl	s.m. + side product

[c] Agilent Poroshell 120 EC-C18, 4.6 × 50 mm, 2.7 μm. Isocratic 65% CH_3CN, 35% H_2O flow at 1 mL/min. Wavelength of detection at 254 nm. t_{R1} = 1.48 min, t_{R2} = 1.65 min.

[d] Heated to 60 °C under acidic condition.

conditions, there was no success in opening the hemiacetal (entries 1-4). Utilizing *tert*-butyldimethylsilyl chloride to trap the desired product also gave undesirable results (entry 8).[35] Under acidic conditions (entry 5), there were multiple side products, each of which were difficult to isolate and characterize.

2.4 Alkylation Reaction

Due to the unforeseen stability of the hemiacetal, we looked into a new strategy. Instead of deprotecting both silyl groups, causing the free phenol to attack the adjacent carbonyl function, we retreated to a traditional enolate alkylation strategy, proceeding by attack of an enolate on a classical electrophile, in our case the *ortho*-quinone methide precursor (**11**) (Figure 2.7). Separately, enol ethers (**10**) and (**14**) were desilylated upon exposure to methyllithium[36], and the subsequent alkylation took place upon addition of the electrophile (**11**) to the corresponding enolates (Figure 2.8).

Both reactions using the chloride electrophile (**11**) did not undergo complete alkylation during the lifetime of the enolates, giving moderate yields. Moreover, the reaction was favoring an unexpected side product (**31**) and (**33**). Presumably, the slow alkylation allows for the enolate to isomerize during the time of reaction. To circumvent the slow reactivity of the electrophile, we switched out the chloride atom

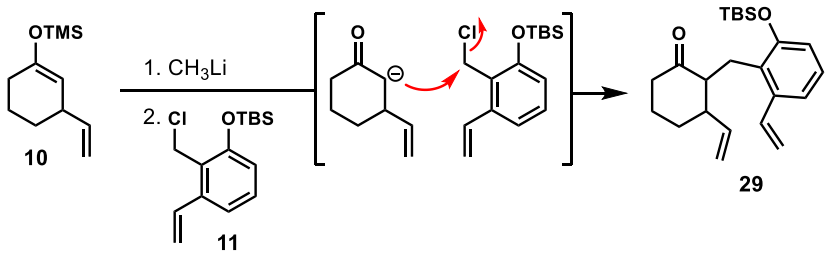

Figure 2.7 Desilylated alkylation addition one-pot synthesis.

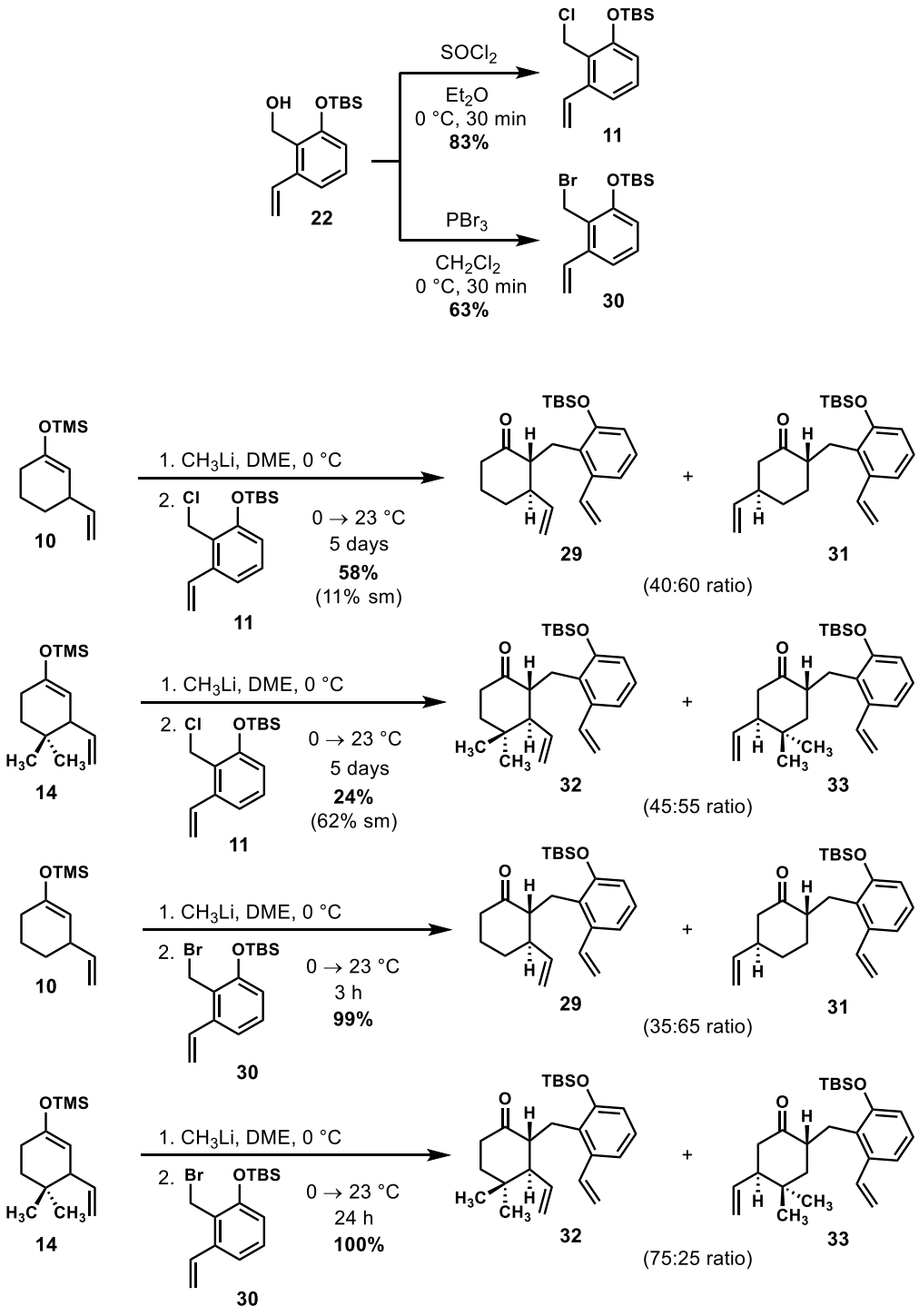

Figure 2.8 Alkylation reaction scope.

for a bromide atom (**30**) to act as a better leaving group. Under the same alkylation conditions, the reaction went to completion, giving better yields and favoring the desired products (**29**) and (**32**). The bromide leaving group enhanced the rate of reaction. However, the enolate intermediate was still vulnerable to isomerization during the reaction, facilitating the formation of side products (**31**) and (**33**).

Initially, the side product from the alkylation reaction was thought to be the undesired *cis*-diastereomeric product. In order to confirm the structures of the desired alkylated product and the side product, we formed the ring-closed hemiacetal of each product by exposure to tetra-*n*-butylammonium fluoride[37] (Figure 2.9). The resulting crystalline hemiacetal (**27**) confirmed (**29**) to be the desired *trans*-product. However, crystalline hemiacetal (**34**) determined side product (**31**) to be an unexpected constitutional isomer and not the 1,2-*cis*-diastereomeric alkylation product.

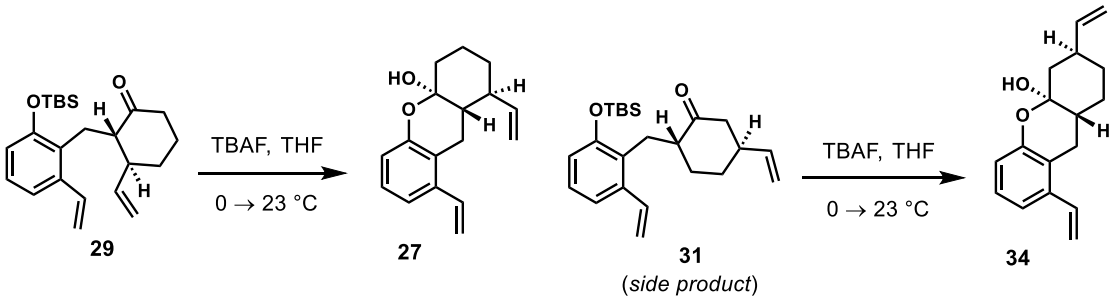

Figure 2.9 Confirming alkylation products via hemiacetal formation.

2.5 Completing the Backbone

Separating the two alkylation products was tedious, ultimately achievable, but not necessary for the subsequent reaction. Olefin metathesis of (**29**) and (**32**), using Grubbs 2nd Generation Catalyst[38], completed the formation of the 7-membered ring,

(**35**) and (**36**) respectively (Figure 2.10). The alkylation side product (**31**) did not undergo transformation in the presence of Grubbs 2nd Generation Catalyst, and was easier to separate by flash column chromatograph after the metathesis reaction. We sought to explore multiple oxidation levels with respect to the seven membered ring, as icetexane natural products have been described with saturation and with an oxygen bridge. Therefore, we prepared (**37**) and (**38**) for future biological testing by hydrogenation of the alkene bond using palladium on activated carbon and hydrogen gas at greater than 90% yields. The *tert*-butyldimethylsilyl ether groups were deprotected upon exposure to tetra-*n*-butylammonium fluoride[37], to give our final products (**39**), (**40**), (**41**), (**42**) with varying yields (53–99%). Testing the final products for cytotoxicity against cancer cell lines is being coordinated with the Helen F. Graham Cancer Center and Research Institute at Christiana Care.

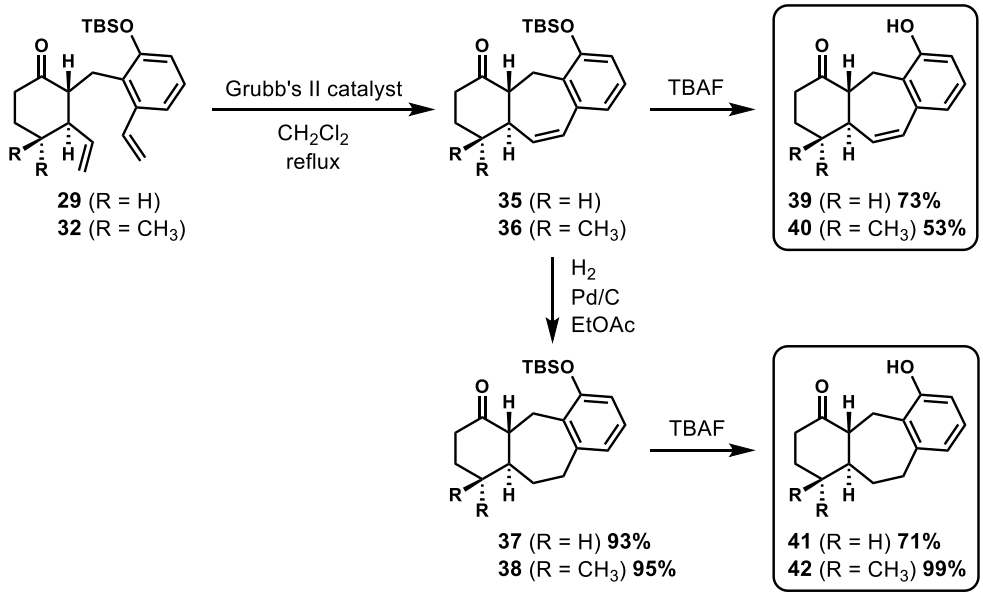

Figure 2.10 Completing the divergent synthesis of the model system.

Chapter 3

CONCLUSION

A one-pot synthesis was developed in making both the unsubstituted and 4,4-dimethyl-substituted silyl-enol ether racemate. Once the synthesis of the premnalatifolin A monomeric unit is determined, we will engage in enantioselective 1,4-addition reaction in the presence of a rhodium catalyst and monodentate phosphoramidite ligand to launch an asymmetric synthesis to the natural product.

Two generations of synthetic pathways were developed in making the electrophilic portion of the alkylation reaction, originally the *ortho*-quinone methide precursor. The first generation synthesis required superfluous steps of protecting group manipulations, starting from a dihydroxybenzoic acid. The second generation synthesis, starting from a dihalobenzaldehyde, truncated the number of steps from 8 steps to 5 steps. Coupling an activated aryl chloride substrate with a vinyl group was successful when using a different palladium catalyst source and ligands under more extreme conditions compared to coupling an aryl triflate substrate. The enolate–*ortho*-quinone methide reaction sequence joined the silyl-enol ether and *ortho*-quinone methide precursor to form a stable ring-closed hemiacetal. However, due to the difficulties of re-opening the hemiacetal, the approach was deemed ineffective. We changed our focus to an alkylation approach, preventing the formation of the hemiacetal and allowing us to proceed in the synthesis of the model system. The o*rtho*-quinone methide precursor was not optimal for the alkylation reaction with the chloride leaving group. Therefore, the leaving group was switched to a bromide, resulting in a much higher yield and shorter reaction time.

After the seven-membered ring formation by olefin metathesis, we proceeded to reducing the cycloheptene ring by a simple hydrogenation. The silyl ether group was displaced from both the unsubstituted and the 4,4-dimethyl-substituted set of the cycloheptane and cycloheptene monomers, resulting in four simple monomeric unit derivatives to be tested for cytotoxicity against numerous cancer cell lines. Overall, the synthesis of the model system of the monomeric premnalatifolin A tricyclic backbone was successful.

REFERENCES

1. Simmons, E. M.; Sarpong, R. *Nat. Prod. Rep.*, **2009**, *26*, 1195–1217.
2. Watson, W. H.; Taira, Z. *Tetrahedron Lett.*, **1976**¸ *29*, 2501–2502.
3. V.G.M., N.; Atmakur, H.; Katragadda, S.B.; Devabakthuni, B.; Kota, A.; S., C.K.R.; Kuncga, M.; M.V.P.S., V.V.; Kulkami, P. Janaswamy, M. R.; Sistla, R. *Phytomedicine*, **2014**, *21*, 497–505.
4. Salae, A.; Rodjun, A.; Karalai, C.; Ponglimanont C.; Chantrapromma S.; Kanjana-Opas, A.; Tewtrakul, S.; Fun, H. *Tetrahedron*, **2012**, *68*, 819–829.
5. Uchiyama, N.; Kiuchi, F.; Ito, M.; Honda, G.; Takeda, Y.; Khodzhimatov, O. K.; Ashurmetov, O. A. *J. Nat. Prod.*, **2003**, *66*, 128–131.
6. Rekha, K. Richa, P. Babu, K. S.; Rao, J. M. *Int. J. Pharm. Chem. Biol. Sci.*, **2015**, *4*, 317–325.
7. Suresh, G.; Babu, K.; Rao, M.; Rao, V.; Yadav, P.; Nayak V.; Ramakrishna, S.*Tetrahedron Lett.*, **2011**, *52*, 5016–5019.
8. Suresh, G.; Babu, K.; Rao, V.; Rao, M.; Nayak, V.; Ramakrishna S. *Tetrahedron Lett.*, **2011**, *52*, 1273–1276.
9. Chatterjee, K.; Zhang, J.; Honbo, N.; Karliner, J. S. *Cardiology*, **2010**, *115*, 115–162.
10. Groopman, J. in "How Doctors Think" Boston: Houghton Mifflin, **2007**.
11. Hymavathi, A., Babu, K. S.; Naidu, V. G. M.; Krishna, S. R.; Diwan, P. V.; Rao, J. M. *Bioorg. Med. Chem. Lett.*, **2009**, *19*, 5727–5731.
12. Lewis, R. S.; Garza, C. J.; Dang, A. T.; Pedro, T. K. A.; Chain, W. J. *Org. Lett.*, **2015**, *17*, 2278–2281.
13. Li, Z.; Nakashige, M.; Chain W. J. *J. Am. Chem. Soc.*, **2011**, *133*, 6553–6556.
14. Chen, Y.; Huang, J.; Liu, B. *Tetrahedron Lett.*, **2010**, *51*, 4655–4657.
15. Jones, T. K.; Denmark, S. E. *J. Org. Chem.*, **1985**, *50*, 4037–4045.

16. Bergmann, E. D.; Ginsburg, D.; Pappo, R. "The Michael Reaction." *Organic Reactions*, R. Adams, Ed., John Wiley & Sons, Inc.: New York, **1959**, *Vol. 10*, pp. 179–563.

17. Little, R. D.; Masjedizadeh, M. R.; Wallquist, O.; McLoughlin, J. I. "The intramolecular Michael reaction" *Organic Reactions*, L. A. Paquette, Ed., John Wiley & Sons, Inc.: New York, **1995**, Vol. *47*, pp. 316–552.

18. Duursma, A.; Boiteau, J.; Lefort, L.; Boogers, J. A. F.; de Vries, A. H. M.; de Vries, J. G.; Minnaard, A. J.; Feringa, B. L. *J. Org. Chem.*, **2004**, *69*, 8045–8052.

19. Kumar, V.; Shaw, A. K. *J. Org. Chem.*, **2008**, *73*, 7526–7531.

20. Zhou, J.; Matos, M.; Murphy, P. V. *Org. Lett.*, **2011**, *13*, 5716–5719.

21. Molander, G. A.; Rivero, M. R. *Org. Lett.*, **2002**, *4*, 107–109.

22. Hoover, J. M.; Stahl, S. S. *J. Am. Chem. Soc.*, **2011**, *133*, 16901–16910.

23. Corey, E. J.; Cho, H.; Rucker, C.; Hua, D. H. *Tetrahedron Lett.*, **1981**, *22*, 3455–3458.

24. Alacid, E.; Nájera, C. *J. Org. Chem.*, **2009**, *74*, 8191–8195.

25. Molander, G. A.; Brown, A. R. *J. Org. Chem.*, **2006**, *71*, 9681–9686.

26. Birkholz, M.-N.; Freixa, Z.; van Leeuwen P. *Chem. Soc. Rev.*, **2009**, *38*, 1099–1118.

27. Miyaura, N.; Suzuki, A. *Chem. Rev.*, **1995**, *95*, 2457–2483.

28. Gushin, V. V.; Alper, H. *Chem. Rev.*, **1994**, *94*, 1047–1062.

29. Littke, A. F.; Fu, G. C. *Angew. Chem., Int. Ed.*, **2002**, 41, 4176–4211.

30. Littke, A. F.; Dai, C.; Fu, G. C. *J. Am. Chem. Soc.*, **2000**, *112*, 4020–4028.

31. Lennox, A. J.; Lloyd-Jones, G. C. *Chem. Soc. Rev.*, **2014**, *43*, 412–443.

32. Lennox, A. J.; Lloyd-Jones, G. C. *J. Am. Chem. Soc.*, **2012**, *134*, 7431–7441.

33. Molander, G. A.; Canturk, B. *Angew. Chem., Int. Ed.*, **2009**, *48*, 9240–9261.

34. Butters, M.; Harvey, J. N.; Jover, J.; Lennox, A. J.; Lloyd-Jones, G. C.; Murray, P. M. *Angew. Chem., Int. Ed.*, **2010**, *49*, 5156–5160.

35. Opalka, S. M.; Steinbacher, J. L.; Lambiris, B. A.; McQuade, D. T. *J. Org. Chem.*, **2011**, *76*, 6503–6517.

36. Stork, G.; Hudrlik, P. F. *J. Am. Chem. Soc.*, **1968**, *90*, 4464–4465.

37. Corey, E. J.; Venkateswarlu, A. *J. Am. Chem. Soc.*, **1972**, *94*, 6190–6191.

38. Grubbs, R. H.; Vougioukalakis, G. C. *Chem. Rev.*, **2010**, *110*, 1746–1787.

Appendix A

EXPERIMENTAL SECTION

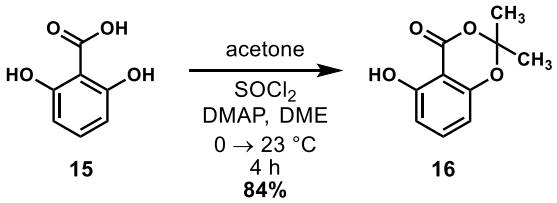

Thionyl chloride (0.650 mL, 9.00 mmol, 1.39 equiv) was added to a precooled (0 °C) solution of 4-(dimethylamino)pyridine (0.047 g, 0.38 mmol, 0.059 equiv), 2,6-dihydroxybenzoic acid (**15**) (1.00 g, 6.49 mmol, 1 equiv), and dry acetone (0.650 mL, 8.78 mmol, 1.35 equiv) in 1,2-dimethoxyethane (5 mL). The resultant mixture was stirred at 0 °C for 4 h. Excess thionyl chloride was quenched by the addition of water (20 mL). The resultant mixture was extracted with ethyl ether (3 × 20 mL). The combined organic layers were washed with saturated aqueous sodium chloride solution and then were dried over anhydrous sodium sulfate. The dried solution was concentrated, and the residue was purified by flash column chromatography (5% ethyl acetate−hexanes) afforded 5-hydroxy-2,2-dimethyl-4H-benzo[δ][1,3]dioxin-4-one (**16**) (1.06 g, 5.46 mmol, 84%) as a white solid.

5-hydroxy-2,2-dimethyl-4H-benzo[δ][1,3]dioxin-4-one (**16**): TLC: 20% ethyl acetate−hexanes, R_f = 0.68 (UV, $KMnO_4$). ^{1}H NMR (300 MHz, $CDCl_3$) δ: 10.32 (s, 1H), 7.39 (t, *J* = 8.3 Hz, 1H), 6.61 (d, *J* = 8.4 Hz, 1H), 6.43 (d, *J* = 8.1 Hz, 1H), 1.73 (s, 6H). ^{13}C NMR (75 MHz, $CDCl_3$) δ: 165.6, 161.5, 155.7, 138.0, 110.9, 107.4, 107.2, 99.5, 25.8. FTIR (NaCl, thin film), cm^{-1}: 3200, 3000, 2945, 1696, 1632, 1230, 1207, 1078. HRMS: ES+ $[M+Na]^+$ Calcd. For $C_{10}H_{10}O_4Na$: 217.0477. Found: 217.0483.

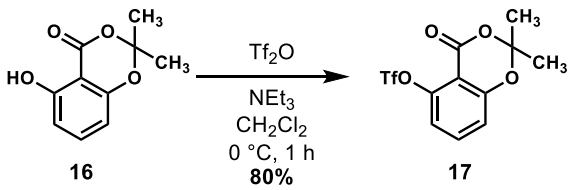

Trifluoromethanesulfonic anhydride (1.26 mL, 7.49 mmol, 1.99 equiv) was added to a precooled (0 °C) solution of 5-hydroxy-2,2-dimethyl-4H-benzo[δ][1,3]dioxin-4-one (**16**) (0.730 g, 3.76 mmol, 1 equiv), and triethylamine (1.60 mL, 11.5 mmol, 3.06 equiv) in dichloromethane (7 mL). The mixture was stirred at 0 °C for 1 h, then excess trifluoromethanesulfonic anhydride was quenched by the addition of water (20 mL). The resultant mixture was extracted with ethyl ether (3 × 20 mL). The combined organic layers were washed with saturated aqueous sodium chloride solution and then were dried over anhydrous sodium sulfate. The dried solution was concentrated, and the residue was purified by flash column chromatography (5% ethyl acetate−hexanes) afforded 2,2-dimethyl-4-oxo-4H-benzo[δ][1,3]dioxin-5-yl trifluoromethanesulfonate (**17**) (984 mg, 3.02 mmol, 80.3%) as a white solid.

2,2-dimethyl-4-oxo-4H-benzo[δ][1,3]dioxin-5-yl trifluoromethanesulfonate (**17**): TLC: 20% ethyl acetate−hexanes, R_f = 0.36 (UV, $KMnO_4$). ^{1}H NMR (300 MHz, $CDCl_3$) δ: 7.60 (t, J = 8.4 Hz, 1H), 7.06 (dd, J_1 = 8.5 Hz, J_2 = 1.0 Hz, 1H), 7.00 (d, J = 8.3 Hz, 1H), 1.76 (s, 6H). ^{13}C NMR (75 MHz, $CDCl_3$) δ: 157.5, 157.3, 148.7, 136.5, 118.8 (q, J = 319.5 Hz), 118.1, 116.6, 108.3, 107.0, 25.5. FTIR (NaCl, thin film), cm^{-1}: 3110, 2997, 2947, 1747, 1623, 1477, 1434, 1210, 1024. HRMS: ES+ $[M+Na]^+$ Calcd. For $C_{11}H_9F_3O_6SNa$: 348.9970. Found: 348.9979.

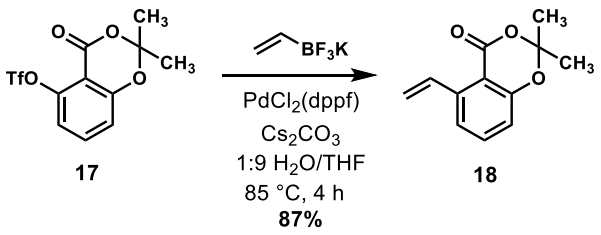

A solution of potassium vinyltrifluoroborate (2.45 g, 18.3 mmol, 1 equiv), [1,1′-Bis(diphenylphosphino)ferrocene]dichloropalladium(II) (0.144 g, 0.197 mmol, 0.011 equiv), cesium carbonate (10.8 g, 33.1 mmol, 1.81 equiv), and 2,2-dimethyl-4-oxo-4H-benzo[δ][1,3]dioxin-5-yl trifluoromethanesulfonate (**17**) (5.96 g, 18.3 mmol, 1 equiv), in tetrahydrofuran/water (9:1, 40 mL) was degassed by bubbling with argon for 15 min. The reaction mixture was heated at reflux for 4 h, then was cooled to 23 °C and diluted with water (30 mL). The solution was extracted with ethyl acetate (3 × 20 mL). The combined organic layers were washed with saturated aqueous sodium chloride solution and then were dried over anhydrous sodium sulfate. The dried solution was concentrated, and the resultant residue was purified by flash column chromatography (4% ethyl acetate−hexanes) afforded 2,2-dimethyl-5-vinyl-4H-benzo[δ][1,3]dioxin-4-one (**18**) (3.23 g, 15.8 mmol, 87%) as a white solid.

2,2-dimethyl-5-vinyl-4H-benzo[δ][1,3]dioxin-4-one (**18**): TLC: 20% ethyl acetate−hexanes, R_f = 0.58 (UV, $KMnO_4$). ^{1}H NMR (300 MHz, $CDCl_3$) δ: 7.72 (dd, J_1 = 17.4 Hz, J_2 = 10.9 Hz, 1H), 7.47 (t, J = 7.7 Hz, 1H), 7.26 (dd, J_1 = 7.8 Hz, J_2 = 0.6 Hz, 1H), 6.88 (dd, J_1 = 8.2 Hz, J_2 = 1.1 Hz, 1H), 5.71 (dd, J_1 = 17.4 Hz, J_2 = 1.3 Hz, 1H), 5.42 (dd, J_1 = 11.0 Hz, J_2 = 1.4 Hz, 1H), 1.71 (s, 6H). ^{13}C NMR (75 MHz, $CDCl_3$) δ: 160.5, 156.8, 142.5, 135.5, 135.4, 121.5, 117.9, 116.7, 111.0, 105.4, 25.8. FTIR (NaCl, thin film), cm^{-1}: 2999, 1692, 1474, 1229, 1207. HRMS: ES+ $[M+Na]^+$ Calcd. For $C_{12}H_{12}O_3Na$: 227.0684. Found: 227.0683.

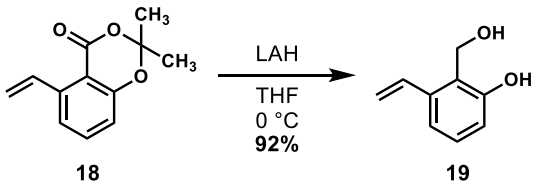

18 19

Lithium aluminum hydride (1.70 g, 44.8 mmol, 4.07 equiv) was added to a precooled (0 °C solution of 2,2-dimethyl-5-vinyl-4H-benzo[δ][1,3]dioxin-4-one (**18**) (2.24 g, 11.0 mmol, 1 equiv) in tetrahydrofuran (80 mL). The mixture was stirred at 0 °C for 5 min, then excess lithium aluminum hydride was quenched by the slow addition of acetic acid (1 mL). Upon diluting the mixture with water (50 mL), the resultant mixture was extracted with ethyl ether (3 × 100 mL). The combined organic layers were washed with saturated aqueous sodium chloride solution and then were dried over anhydrous sodium sulfate. The dried solution was concentrated, and the residue was purified by flash column chromatography (20% ethyl acetate–hexanes) to afford 2-(hydroxymethyl)-3-vinylphenol (**19**) (1.52 g, 10.1 mmol, 91.8%) as a clear, yellow oil.

2-(hydroxymethyl)-3-vinylphenol (**19**): TLC: 20% ethyl acetate−hexanes, R_f = 0.10 (UV, $KMnO_4$). ^{1}H NMR (300 MHz, $CDCl_3$) δ: 7.11 (t, J = 7.9 Hz, 1H), 7.00 (d, J = 7.8 Hz, 1H), 6.86 (dd, J_1 = 17.3 Hz, J_2 = 10.9 Hz, 1H), 6.75 (d, J = 8.0 Hz, 1H), 5.57 (dd, J_1 = 17.3 Hz, J_2 = 1.3 Hz, 1H), 5.31 (dd, J_1 = 11.0 Hz, J_2 = 1.2 Hz, 1H), 4.86 (s, 2H). ^{13}C NMR (75 MHz, $CDCl_3$) δ: 155.7, 138.0, 133.9, 129.0, 122.4, 118.6, 117.5, 115.7, 58.9. FTIR (NaCl, thin film), cm^{-1}: 3288, 3086, 2930, 1844, 1577, 1469, 1268. HRMS: CI+ $[M+NH_4]^+$ Calcd. For $C_9H_{10}O_2NH_4$: 168.1024. Found: 168.1018.

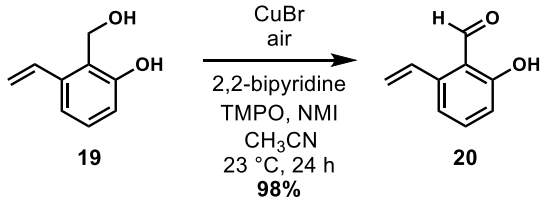

A solution of 2,2′-Bipyridine (0.017 g, 0.11 mmol, 0.10 equiv), (2,2,6,6-tetramethyl-piperidin-1-yl)oxyl (0.019 g, 0.12 mmol, 0.11 equiv), 1-methylimidazole (8 μL, 0.1 mmol, 0.09 equiv), copper (I) bromide (0.024 g, 0.17 mmol, 0.16 equiv) and 2-(hydroxymethyl)-3-vinylphenol (**19**) (0.144 g, 1.06 mmol, 1 equiv), in acetonitrile (1 mL) was bubbled with air for 1 h. The mixture was quenched by the addition of 1 N hydrochloric acid (1 mL), then was extracted with ethyl ether (3 × 10 mL). The combined organic layers were washed with saturated aqueous sodium chloride solution and then were dried over anhydrous sodium sulfate. The dried solution was concentrated, and the residue was purified by flash column chromatography (5% ethyl acetate−hexanes) to afford 2-hydroxy-6-vinylbenzaldehyde (**20**) (0.153 g, 1.03 mmol, 97.2%) as a clear, colorless oil.

2-hydroxy-6-vinylbenzaldehyde (**20**): TLC: 20% ethyl acetate−hexanes, R_f = 0.66 (UV, $KMnO_4$). ^{1}H NMR (400 MHz, $CDCl_3$) δ: 11.86 (s, 1H), 10.27 (s, 1H), 7.42 (t, J = 8.0 Hz, 1H), 7.17 (dd, J_1 = 17.3 Hz, J_2 = 11.0 Hz, 1H), 6.91 (d, J = 7.6 Hz, 1H), 6.86 (d, J = 8.4 Hz, 1H), 5.63 (dd, J_1 = 17.3 Hz, J_2 = 1.3 Hz, 1H), 5.53 (dd, J_1 = 11.0 Hz, J_2 = 1.2 Hz, 1H). ^{13}C NMR (101 MHz, $CDCl_3$) δ: 195.4, 162.7, 143.2, 137.2, 131.9, 121.4, 118.6, 117.2. FTIR (NaCl, thin film), cm^{-1}: 3411, 2956, 2930, 2895, 2858, 1575, 1467, 1272. HRMS: CI+ $[M+NH_4]^+$ Calcd. For $C_9H_8O_2NH_4$: 166.0863. Found: 166.0869.

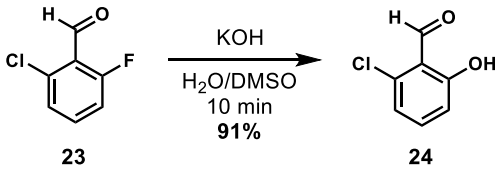

23 **24**

Potassium hydroxide (3.58 g, 63.9 mmol, 2 equiv) was added to a solution of 2-chloro-6-fluorobenzaldehyde (**23**) (5.09 g, 32.1 mmol, 1 equiv) in dimethyl sulfoxide (16 mL). Water (2.5 mL) was added slowly to the resultant yellow solution, ove which time the reaction mixture warmed slightly. The mixture was cooled to 23 °C, whereupon additional potassium hydroxide (1.00 g, 17.8 mmol, 0.554 equiv) was added. The resultant mixture was stirred at 23 °C for 24 h and then was quenched by the addition of 1 N aqueous hydrochloric acid (5 mL) until the solution reached a pH of 1 by litmus paper. The resultant cloudy reaction mixture was extracted with ethyl acetate (2 × 50 mL). The combined organic layers were washed with saturated aqueous sodium chloride solution and then were dried over anhydrous sodium sulfate. The dried solution was concentrated, and the residue was passed through a 2 cm silica gel plug and eluted with hexanes. Concentration of the resultant solution afforded 2-chloro-6-hydroxybenzaldehyde (**24**) (4.60 g, 29.4 mmol, 91%) as a white solid.

2-chloro-6-hydroxybenzaldehyde (**24**): TLC: 20% ethyl acetate−hexanes, R_f = 0.67 (UV, $KMnO_4$). ^{1}H NMR (400 MHz, $CDCl_3$) δ: 11.92 (s, 1H), 10.42 (s, 1H), 7.42 (t, *J* = 8.2 Hz, 1H), 6.96 (d, *J* = 7.9 Hz, 1H), 6.90 (d, *J* = 8.5 Hz, 1H). ^{13}C NMR (101 MHz, $CDCl_3$) δ: 195.6, 164.0, 138.2, 137.6, 121.1, 117.3, 117.1. FTIR (KBr, thin film), cm^{-1}: 3078, 2922, 2852, 1652, 1446, 1169. HRMS: CI+ $[M]^+$ Calcd. For $C_7H_5O_2Cl$: 155.9978. Found: 155.9980.

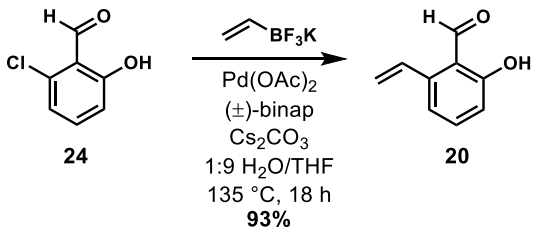

A solution of potassium vinyltrifluoroborate (2.67 g, 19.9 mmol, 1.21 equiv), palladium (II) acetate (0.113 g, 0.505 mmol, 0.030 equiv), 2,2'-bis(diphenylphosphino)-1,1'-binaphthyl (0.605 g, 0.971 mmol, 0.059 equiv), cesium carbonate (17.2 g, 52.6 mmol, 3.2 equiv), and 2-chloro-6-hydroxybenzaldehyde (**24**) (2.57 g, 16.4 mmol, 1 equiv), in tetrahydrofuran/water (9:1, 65 mL) in a 150 mL glass pressure reactor was degassed by bubbling with argon for 15 minutes. The reactor was sealed and the reaction mixture was heated at 135 °C for 18 h. The reaction mixture was cooled to 23 °C and quenched by the slow addition of 1N aqueous hydrochloric acid solution (30 mL) until bubbling ceased after 5 minutes. The solution was extracted with ethyl acetate (3 × 40 mL). The combined organic layers were washed with saturated aqueous sodium chloride solution and then were dried over anhydrous sodium sulfate. The dried solution was concentrated, and the resultant residue was purified by flash column chromatography (4% ethyl acetate−hexanes) afforded 2-hydroxy-6-vinylbenzaldehyde (**20**) (2.27 g, 15.3 mmol, 93%) as a clear, colorless oil.

2-hydroxy-6-vinylbenzaldehyde (**20**): TLC: 20% ethyl acetate−hexanes, R_f = 0.66 (UV, $KMnO_4$). ^{1}H NMR (400 MHz, $CDCl_3$) δ: 11.86 (s, 1H), 10.27 (s, 1H), 7.42 (t, J = 8.0 Hz, 1H), 7.17 (dd, J_1 = 17.3 Hz, J_2 = 11.0 Hz, 1H), 6.91 (d, J = 7.6 Hz, 1H), 6.86 (d, J = 8.4 Hz, 1H), 5.63 (dd, J_1 = 17.3 Hz, J_2 = 1.3 Hz, 1H), 5.53 (dd, J_1 = 11.0 Hz, J_2 = 1.2 Hz, 1H). ^{13}C NMR (101 MHz, $CDCl_3$) δ: 195.37, 162.65, 143.15, 137.15, 131.89, 121.34, 118.60, 117.21, 117.18. FTIR (KBr, thin film), cm^{-1}: 3411, 2956,

2930, 2895, 2858, 1575, 1467, 1272. HRMS: CI+ $[M+NH_4]^+$ Calcd. For $C_9H_8O_2NH_4$: 166.0863. Found: 166.0869.

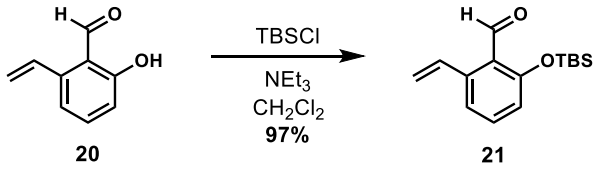

20 **21**

Triethylamine (2.95 mL, 21.2 mmol, 2 equiv) was added to a solution of 2-hydroxy-6-vinylbenzaldehyde (**20**) (1.57 g, 10.59 mmol, 1 equiv) and *tert*-butylchlorodimethylsilane (1.76 g, 11.7 mmol, 1.1 equiv) in dichloromethane (30 mL) at 23 °C. The resultant reaction mixture was stirred for 24 hours and then was quenched by the addition of saturated sodium bicarbonate solution (25 mL). The solution was extracted with ethyl ether (3 × 20 mL). The combined organic layers were washed with saturated aqueous sodium chloride solution and then were dried over anhydrous sodium sulfate. The dried solution was concentrated, and the resultant residue was purified by flash column chromatography (5% ethyl acetate−hexanes) to afford 2-((*tert*-butyldimethylsilyl)oxy)-6-vinylbenzaldehyde (**21**) (2.69 g, 10.3 mmol, 97%) as a clear, yellow oil.

2-((*tert*-butyldimethylsilyl)oxy)-6-vinylbenzaldehyde (**21**): TLC: 20% ethyl acetate−hexanes, R_f = 0.73 (UV, $KMnO_4$). ^{1}H NMR (300 MHz, $CDCl_3$) δ: 10.62 (s, 1H), 7.51 (dd, J_1 = 17.4 Hz, J_2 = 11.0 Hz, 1H), 7.37 (t, J = 8.0 Hz, 1H), 7.13 (d, J = 7.8 Hz, 1H), 6.80 (d, J = 8.9 Hz, 1H), 5.63 (dd, J_1 = 17.4 Hz, J_2 = 1.5 Hz, 1H), 5.35 (dd, J_1 = 10.9 Hz, J_2 = 1.5 Hz, 1H), 1.00 (s, 9H), 0.27 (s, 6H). ^{13}C NMR (75 MHz, $CDCl_3$) δ: 192.6, 159.7, 141.2, 135.9, 134.6, 124.5, 120.4, 119.1, 117.3, 25.8, 18.4, -

4.2. FTIR (KBr, thin film), cm^{-1}: 2958, 2927, 2856, 1690, 1570, 1467, 1400, 1263, 1011. HRMS: ES+ $[M+Na]^+$ Calcd. For $C_{15}H_{22}O_2SiNa$: 285.1287. Found: 285.1289.

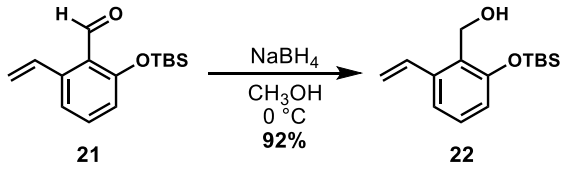

Sodium borohydride (0.372 g, 6.89 mmol, 1.1 equiv) was added to a precooled (0 °C) solution of 2-((*tert*-butyldimethylsilyl)oxy)-6-vinylbenzaldehyde (**21**) (1.64 g, 6.26 mmol, 1 equiv) in anhydrous methanol (40 mL). The resultant reaction mixture warmed to 22 °C and stirred for 1 h. Excess sodium borohydride was quenched by the slow addition of aqueous 1 N hydrochloric acid solution (5 mL) until bubbling ceased. The layers were separated and the aqueous layer was extracted with ethyl acetate (3 × 40 mL). The combined organic layers were washed with saturated aqueous sodium chloride solution and then were dried over anhydrous sodium sulfate, concentrated, and the residue was purified by flash column chromatography (10% ethyl acetate−hexanes) to afford (2-((*tert*-butyldimethylsilyl)oxy)-6-vinylphenyl)methanol (**22**) (1.52 g, 5.75 mmol, 92%) as a clear, yellow oil.

(2-((*tert*-butyldimethylsilyl)oxy)-6-vinylphenyl)methanol (**22**): TLC: 20% ethyl acetate−hexanes, R_f = 0.48 (UV, $KMnO_4$). ^{1}H NMR (300 MHz, $CDCl_3$) δ: 7.19 – 7.04 (m, 3H), 6.77 (dd, J_1 = 7.1 Hz, J_2 = 2.1 Hz, 1H), 5.66 (dd, J_1 = 17.4 Hz, J_2 = 1.4 Hz, 1H), 5.36 (dd, J_1 = 11.0 Hz, J_2 = 1.4 Hz, 1H), 4.78 (d, J = 4.0 Hz, 2H), 1.03 (s, 9H), 0.27 (s, 6H). ^{13}C NMR (75 MHz, $CDCl_3$) δ: 154.2, 139.2, 134.4, 128.7, 128.6, 119.4, 117.9, 117.1, 57.0, 25.8, 18.3, -4.2. FTIR (KBr, thin film), cm^{-1}: 3053, 2925,

1954, 1862, 1662, 1607, 1569, 1452, 1412, 1338, 1311, 1278, 1235, 1194, 1079. HRMS: ES+ $[M+Na]^+$ Calcd. For $C_{15}H_{24}O_2SiNa$: 287.1443. Found: 287.1446.

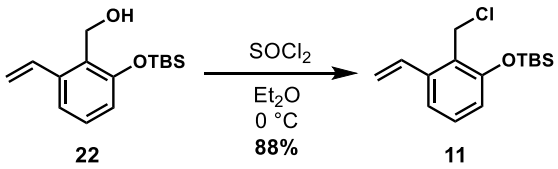

22 **11**

Thionyl chloride (0.121 mL, 1.66 mmol, 1.1 equiv) was added dropwise to a precooled (0 °C) solution of (2-((*tert*-butyldimethylsilyl)oxy)-6-vinylphenyl)methanol (**22**) (0.406 g, 1.54 mmol, 1 equiv) in anhydrous ethyl ether (15 mL). The resultant heterogeneous reaction mixture was warmed up to 23 °C for 15 minutes and then was filtered through a 1 cm silica gel plug. The plug was eluted with ether (25 mL), and the combined filtrates were concentrated and purified by flash column chromatography (hexanes) to afford *tert*-butyl(2-(chloromethyl)-3-vinylphenoxy)dimethylsilane (**11**) (0.383 g, 1.35 mmol, 88%) as a clear, colorless oil.

tert-butyl(2-(chloromethyl)-3-vinylphenoxy)dimethylsilane (**11**): TLC: 20% ethyl acetate−hexanes, R_f = 0.83 (UV, $KMnO_4$). ^{1}H NMR (300 MHz, $CDCl_3$) δ: 7.22 – 7.01 (m, 3H), 6.77 (dd, J_1 = 7.8 Hz, J_2 = 1.4 Hz, 1H), 5.72 (dd, J_1 = 17.3 Hz, J_2 = 1.4 Hz, 1H), 5.41 (dd, J_1 = 11.0, J_2 = 1.4 Hz, 1H), 4.75 (s, 2H), 1.06 (s, 9H), 0.29 (s, 6H). ^{13}C NMR (75 MHz, $CDCl_3$) δ: 154.1, 139.5, 133.8, 129.5, 125.6, 119.0, 117.7, 117.4, 38.0, 25.8, 18.3, -4.2. FTIR (KBr, thin film), cm^{-1}: 2956, 2930, 2858, 1576, 1470, 1285, 1260, 1004. HRMS: EI+ $[M]^+$ Calcd. For $C_{15}H_{23}OClSi$: 282.1207. Found: 282.1219.

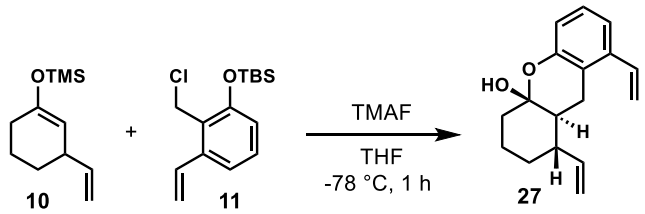

A precooled (–78 °C) solution of tetramethylammonium fluoride (0.48 g, 5.2 mmol, 4.2 equiv) in dichloromethane (10 mL) was added rapidly via cannula to a solution of *tert*-butyl(2-(chloromethyl)-3-vinylphenoxy)dimethylsilane (**11**) (0.350 g, 1.24 mmol, 1 equiv) and trimethyl((3-vinylcyclohex-1-en-1-yl)oxy)silane (**10**) (0.359 g, 1.83 mmol, 1.48 equiv) in dichloromethane (5 mL) at –78 °C. The resultant bright yellow reaction mixture was stirred for 1 h at –78 °C, then was quenched by the addition of acetic acid (60 μL). The mixture was warmed to room temperature and filtered through a 1 cm thick silica gel plug and eluted with ethyl acetate. The combined filtrates were concentrated, and the residue was purified by flash column chromatography (5% ethyl acetate–hexanes) to afford a 1:1 diastereomeric mixture of 1,8-divinyl-1,2,3,4,9,9a-hexahydro-4a*H*-xanthen-4a-ol (**27**) (0.16 g, 0.62, 34%) as a crystalline solid.

1,8-divinyl-1,2,3,4,9,9a-hexahydro-4a*H*-xanthen-4a-ol (diastereomeric mixture) (**27**): TLC: 20% ethyl acetate–hexanes, R_f = 0.50 (UV, CAM). ^{1}H NMR (400 MHz, $CDCl_3$) δ: 7.13 – 7.06 (2H), 6.95 – 6.81 (1H), 6.80 – 6.72 (1H), 5.70 – 5.51 (2H), 5.33 – 5.24 (1H), 5.19 – 4.78 (2H), 2.99 – 2.36 (2H), 2.26 – 2.12 (1H), 2.12 – 1.96 (1H), 1.93 – 1.67 (5H), 1.67 – 1.53 (1H), 1.38 – 1.18 (1H). ^{13}C NMR (101 MHz, $CDCl_3$) δ: 151.7, 151.6*, 141.5*, 141.0, 137.9*, 137.5, 134.03*, 134.01, 127.0, 126.8*, 120.5, 118.4*, 118.1, 118.0*, 116.5, 116.3*, 115.9, 115.83*, 115.76*, 115.4, 96.3, 96.1*, 45.3, 42.8*, 41.9, 40.4*, 38.8*, 38.0, 32.6, 32.1*, 23.8, 22.2*, 22.0, 21.3*. FTIR (KBr, thin film), cm^{-1}: 3447, 3071, 2935, 2850, 2361, 2339, 1576, 1457, 1257,

1243, 1186, 1168, 1154. HRMS: FD+ $[M]^+$ Calcd. For $C_{17}H_{20}O_2$: 256.1463. Found: 256.1456.

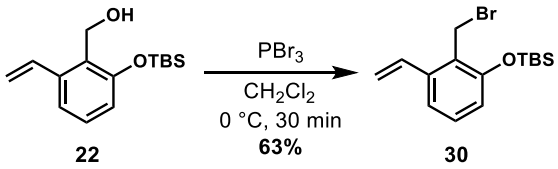

22 **30**

Phosphorus tribromide (0.60 mL, 6.3 mmol, 1.1 equiv) was added to a precooled (0 °C) solution of (2-((*tert*-butyldimethylsilyl)oxy)-6-vinylphenyl)methanol (**22**) (1.52 g, 5.75 mmol, 1 equiv) in anhydrous dichloromethane (50 mL). The resultant heterogeneous reaction mixture was then quickly filtered through a 5 cm alumina (Basic, Brockmann Activity I) pad. The filter pad was eluted with ether (50 mL), and the combined filtrates were concentrated to afford *tert*-butyl(2-(bromomethyl)-3-vinylphenoxy)dimethylsilane (**30**) (1.19 g, 3.64 mmol, 63%) as a clear, colorless oil.

tert-butyl(2-(bromomethyl)-3-vinylphenoxy)dimethylsilane (**30**): TLC: 20% ethyl acetate−hexanes, R_f = 0.71 (UV, $KMnO_4$). ^{1}H NMR (400 MHz, $CDCl_3$) δ: 7.16 (t, J = 7.8 Hz, 1H), 7.12 – 7.02 (m, 2H), 6.75 (dd, J_1 = 7.9 Hz, J_2 = 1.3 Hz, 1H), 5.73 (dd, J_1 = 17.3 Hz, J_2 = 1.4 Hz, 1H), 5.42 (dd, J_1 = 11.0 Hz, J_2 = 1.4 Hz, 1H), 4.66 (s, 2H), 1.06 (s, 9H), 0.30 (s, 6H). ^{13}C NMR (101 MHz, $CDCl_3$) δ: 154.1, 139.4, 133.9, 129.5, 125.8, 119.2, 117.7, 117.4, 26.2, 26.0, 18.5, -4.0. FTIR (KBr, thin film), cm^{-1}: 3080, 3070, 2956, 2930, 2885, 2858, 2363, 2336, 1576, 1470, 1284, 1254, 1218, 1000. HRMS: EI+ $[M]^+$ Calcd. For $C_{15}H_{24}OBrSi$: 327.0774. Found: 327.0768.

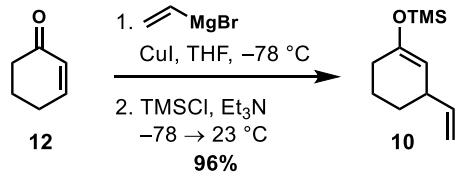

Vinylmagnesium bromide (1.38 M in tetrahydrofuran, 18.1 mL, 25.0 mmol, 2.40 equiv) was added dropwise to a precooled (–78 °C) solution of copper(I) iodide (2.39 g, 12.5 mmol, 1.20 equiv) in tetrahydrofuran (35 mL). The resultant suspension was stirred at –78 °C for 15 minutes whereupon 2-cyclohexene-1-one (**12**) (1.01 mL, 10.4 mmol, 1 equiv) was added dropwise to the mixture. The resultant mixture was stirred at –78 °C for 1 h at which point trimethylamine (4.35 mL, 31.2 mmol, 3.00 equiv) and chlorotrimethylsilane (3.95 mL, 31.1 mmol, 2.99 equiv) were added sequentially dropwise to the reaction mixture. The brown heterogeneous mixture was allowed to warm to 23 °C and stirred for 1 hour. The resulting black mixture was added to a mixture of 9:1 saturated ammonium chloride/ concentrated ammonium hydroxide solution (50 mL). The layers were separated and the aqueous layer was extracted with ethyl ether (3 × 30 mL). The combined organic layers were washed with a mixture of 9:1 saturated ammonium chloride/ concentrated ammonium hydroxide solution (3 × 30 mL) until the aqueous layer was colorless, then washed with water (30 mL) and brine (30 mL), and the combined organic layers were dried over anhydrous sodium sulfate. The dried solution was concentrated to afford trimethyl((3-vinylcyclohex-1-en-1-yl)oxy)silane (**10**) (1.96 g, 9.98 mmol, 96%) as a clear yellow oil.

trimethyl((3-vinylcyclohex-1-en-1-yl)oxy)silane (**10**): TLC: 20% ethyl acetate−hexanes, R_f = 0.78 ($KMnO_4$). ^{1}H NMR (400 MHz, $CDCl_3$) δ: 5.77 (ddd, J_1 = 17.1 Hz, J_2 = 10.1 Hz, J_3 = 6.9 Hz, 1H), 4.99 (dt, J_1 = 17.2 Hz, J_2 = 1.7 Hz, 1H), 4.94 (ddd, J_1 = 10.2 Hz, J_2 = 2.0 Hz, J_3 = 1.1 Hz, 1H), 4.77 (dt, J_1 = 3.2 Hz, J_2 = 1.4 Hz,

1H), 2.89 – 2.79 (m, 1H), 2.10 – 1.85 (m, 2H), 1.78 – 1.66 (m, 2H), 1.63 – 1.51 (m, 1H), 1.33 – 1.24 (m, 1H), 0.19 (s, 9H). ^{13}C NMR (101 MHz, $CDCl_3$) δ: 151.3, 143.5, 113.3, 106.9, 38.9, 30.0, 28.9, 21.0, 0.5. FTIR (KBr, thin film), cm^{-1}: 2932, 2860, 1663, 1367, 1252, 1191. HRMS: ES+ $[M+H]^+$ Calcd. For $C_{11}H_{21}OSi$: 197.1367. Found: 197.1358.

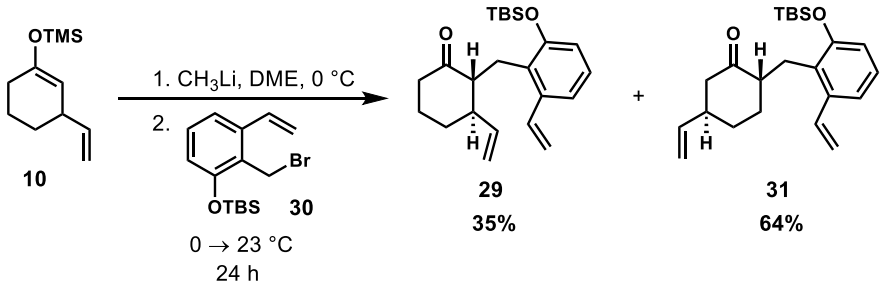

Methyllithium (1.6 M in ethyl ether, 0.53 mL, 0.86 mmol, 1.4 equiv) was added to a precooled (0 °C) solution of trimethyl((3-vinylcyclohex-1-en-1-yl)oxy)silane (**10**) (0.170 g, 0.866 mmol, 1.38 equiv) in 1,2-dimethoxyethane (1.2 mL). The resultant heterogeneous yellow mixture was stirred at 0 °C for 10 minutes whereupon *tert*-butyl(2-(bromomethyl)-3-vinylphenoxy)dimethylsilane (**30**) (0.206 g, 0.629 mmol, 1 equiv) was added dropwise to the mixture. The heterogeneous yellow mixture slowly warmed up to 23 °C and stirred for 24 h, then was followed by filtering through a 5 cm thick neutral silica plug and eluted with ethyl ether (10 mL). The solution was concentrated to afford a 35:65 mixture of 2-(2-((*tert*-butyldimethylsilyl)oxy)-6-vinylbenzyl)-3-vinylcyclohexanone (**29**) and 2-(2-((*tert*-butyldimethylsilyl)oxy)-6-vinylbenzyl)-5-vinylcyclohexanone (**31**) (0.23 g, 0.62 mmol, 99%) as a clear, yellow oil. The ratio of the two products was determined by NMR.

2-(2-((*tert*-butyldimethylsilyl)oxy)-6-vinylbenzyl)-3-vinylcyclohexanone (**29**): TLC: 20% ethyl ether−hexanes, R_f = 0.55 (UV, CAM). ^{1}H NMR (400 MHz, $CDCl_3$) δ: 7.10 – 6.98 (m, 3H), 6.68 (dd, J_1 = 7.3 Hz, J_2 = 1.9 Hz, 1H), 5.64 – 5.53 (m, 2H), 5.27 (dd, J_1 = 10.9 Hz, J_2 = 1.5 Hz, 1H), 4.92 (dt, J_1 = 17.1 Hz, J_2 = 1.3 Hz, 1H), 4.83 (dt, J_1 = 10.4, J_2 = 1.2 Hz, 1H), 3.10 – 3.02 (m, 1H), 2.93 – 2.79 (m, 2H), 2.47 – 2.40 (m, 1H), 2.37 – 2.22 (m, 2H), 2.00 – 1.89 (m, 2H), 1.81 – 1.72 (m, 1H), 1.67 – 1.57 (m, 1H), 1.00 (s, 9H), 0.25 (s, 3H), 0.24 (s, 3H). ^{13}C NMR (101 MHz, $CDCl_3$) δ: 212.7, 154.1, 140.8, 139.4, 136.2, 128.7, 126.6, 119.3, 117.8, 115.7, 114.7, 54.3, 48.4, 41.2, 30.8, 26.4, 26.2, 25.0, 18.6, -3.6, -3.7. FTIR (KBr, thin film), cm^{-1}: 3080, 2955, 2929, 2857, 2361, 2339, 1712, 1572, 1466, 1270. HRMS: FD+ $[M]^+$ Calcd. For $C_{23}H_{34}O_2Si$: 370.2328. Found: 370.2339.

2-(2-((*tert*-butyldimethylsilyl)oxy)-6-vinylbenzyl)-5-vinylcyclohexanone (**31**): TLC: 20% ethyl ether−hexanes, R_f = 0.62 (UV, CAM).^{1}H NMR (400 MHz, $CDCl_3$) δ: 7.11 (dd, J_1 = 7.8 Hz, J_2 = 1.4 Hz, 1H), 7.06 (t, J = 7.8 Hz, 1H), 6.93 (dd, J_1 = 17.3 Hz, J_2 = 11.0 Hz, 1H), 6.73 (dd, J_1 = 7.8 Hz, J_2 = 1.4 Hz, 1H), 5.76 (ddd, J_1 = 16.9 Hz, J_2 = 10.4 Hz, J_3 = 6.2 Hz, 1H), 5.59 (dd, J_1 = 17.3 Hz, J_2 = 1.5 Hz, 1H), 5.24 (dd, J_1 = 11.0 Hz, J_2 = 1.5 Hz, 1H), 5.01 (dt, J_1 = 16.9 Hz, J_2 = 1.4 Hz, 1H), 4.96 (dt, J_1 = 9.9Hz, J_2 = 1.3 Hz, 1H), 3.17 (dd, J_1 = 13.8 Hz, J_2 = 3.3 Hz, 1H), 2.70 (dd, J_1 = 13.8 Hz, J_2 = 10.4 Hz, 1H), 2.63 – 2.51 (m, 1H), 2.47 (ddd, J_1 = 12.3 Hz, J_2 = 3.9 Hz, J_3 = 2.1 Hz, 1H), 2.48 – 2.39 (m, 1H), 2.17 (m, 1H), 1.93 – 1.80 (m, 2H), 1.45 – 1.31 (m, 2H), 0.97 (s, 9H), 0.23 (s, 3H), 0.22 (s, 3H). ^{13}C NMR (101 MHz, $CDCl_3$) δ: 211.9, 154.2, 141.7, 139.2, 135.5, 128.9, 126.7, 119.0, 117.7, 116.0, 113.5, 50.5, 47.6, 44.1, 31.8, 31.7, 26.0, 25.3, 18.4, -3.8, -4.0. FTIR (KBr, thin film), cm^{-1}: 3080, 2955, 2929,

2857, 2361, 2339, 1712, 1572, 1466, 1270. HRMS: FD+ $[M]^+$ Calcd. For $C_{23}H_{34}O_2Si$: 370.2328. Found: 370.2339.

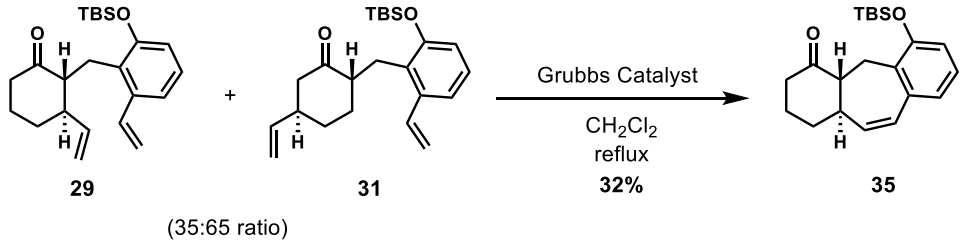

The second generation Grubb's catalyst (15 mg, 0.018 mmol, 0.028 equiv) was added in one portion to a 35:65 mixture of 2-(2-((*tert*-butyldimethylsilyl)oxy)-6-vinylbenzyl)-3-vinylcyclohexanone (**29**) and 2-(2-((*tert*-butyldimethylsilyl)oxy)-6-vinylbenzyl)-5-vinylcyclohexanone (**31**) (0.240 g, 0.648 mmol, 1 equiv) in dichloromethane (6 mL). The resultant red solution was heated at reflux for 24 h, was then cooled and concentrated. Purification of the residue by flash column chromatography (1% ethyl acetate−hexanes) afforded 6-((*tert*-butyldimethylsilyl)oxy)-1,2,3,4a,5,11a-hexahydro-4H-dibenzo[α,δ][7]annulen-4-one (**35**) (0.072 g, 0.21 mmol, 32%) as a colorless crystalline solid.

6-((*tert*-butyldimethylsilyl)oxy)-1,2,3,4a,5,11a-hexahydro-4H-dibenzo[α,δ][7]annulen-4-one (**35**): TLC: 20% ethyl acetate−hexanes, R_f = 0.49 (UV, CAM). ^{1}H NMR (400 MHz, $CDCl_3$) δ: 7.01 (t, J = 7.8 Hz, 1H), 6.79 (d, J = 7.5 Hz, 1H), 6.70 (d, J = 8.0 Hz, 1H), 6.38 (dd, J_1 = 12.5 Hz, J_2 = 2.5 Hz, 1H), 5.70 (dd, J_1 = 12.5 Hz, J_2 = 3.0 Hz, 1H), 4.29 (d, J = 15.2 Hz, 1H), 2.56 (tq, J_1 = 12.2 Hz, J_2 = 3.0 Hz, 1H), 2.44 (m, 1H), 2.41 (dd, J_1 = 12.3 Hz, J_2 = 8.2 Hz, 1H), 2.27 (td, J_1 = 13.7 Hz, J_2 = 6.3 Hz, 1H), 2.10 (dd, J_1 = 15.3 Hz, J_2 = 8.6 Hz, 1H), 2.16 – 2.01 (m, 2H), 1.73 (qt, J_1 = 13.1 Hz, J_2 = 3.8 Hz, 1H), 1.56 (qd, J_1 = 13.0 Hz, J_2 = 3.7 Hz, 1H), 1.05 (s,

9H), 0.18 (d, J = 14.5 Hz, 6H). ^{13}C NMR (101 MHz, $CDCl_3$) δ: 210.7, 152.5, 137.1, 134.6, 130.7, 129.3, 126.4, 124.6, 118.6, 54.4, 50.5, 41.3, 33.1, 26.5, 25.9, 24.1, 18.4, -4.16, -4.21. FTIR (KBr, thin film), cm^{-1}: 3063, 2955, 2929, 2858, 2361, 1715, 1575, 1458, 1278, 1257, 1012. HRMS: CI+ $[M+H]^+$ Calcd. For $C_{21}H_{31}O_2Si$: 343.2093. Found: 343.2102.

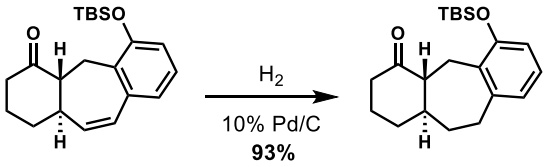

35 **37**

6-((*tert*-butyldimethylsilyl)oxy)-1,2,3,4a,5,11a-hexahydro-4H-dibenzo[α,δ][7]annulen-4-one (**35**) (37 mg, 0.11 mmol, 1 equiv) was added to a mixture of 10% palladium on carbon (1 mg, 6 μmol, 0.05 equiv) in ethyl acetate (0.4 mL). The flask was then purged with hydrogen and held under a hydrogen atmosphere using a hydrogen-filled balloon. The mixture was stirred at room temperature for 3 h and then was filtered through a 1 cm thick silica plug and eluted with ethyl acetate (1 mL). The solution was concentrated to afford 6-((*tert*-butyldimethylsilyl)oxy)-1,2,3,4a,5,10,11,11a-octahydro-4H-dibenzo[α,δ][7]annulen-4-one (**37**) (35 mg, 0.10 mmol, 93%) as a clear, colorless oil.

6-((*tert*-butyldimethylsilyl)oxy)-1,2,3,4a,5,10,11,11a-octahydro-4H-dibenzo[α,δ][7]annulen-4-one (**37**): TLC: 20% ethyl acetate−hexanes, R_f = 0.53 (CAM). ^{1}H NMR (400 MHz, $CDCl_3$) δ: 6.95 (t, J = 7.8 Hz, 1H), 6.70 (d, J = 7.3 Hz, 1H), 6.66 (d, J = 8.0 Hz, 1H), 4.00 (d, J = 14.5 Hz, 1H), 2.85 (t, J = 13.1 Hz, 1H), 2.69 (ddd, J_1 = 14.3 Hz, J_2 = 7.2 Hz, J_3 = 1.4 Hz, 1H), 2.42 (ddt, J_1 = 12.9 Hz, J_2 = 4.3 Hz, J_3 = 2.4 Hz, 1H), 2.29 (tdd, J_1 = 13.0 Hz, J_2 = 6.0 Hz, J_3 = 1.2 Hz, 1H), 2.18 (dd, J_1 =

14.6 Hz, J_2 = 10.3 Hz, 1H), 2.09 – 1.97 (m, 3H), 1.86 – 1.59 (m, 3H), 1.52 – 1.42 (m, 1H), 1.40 – 1.23 (m, 1H), 1.00 (s, 9H), 0.21 (s, 3H), 0.15 (s, 3H). ^{13}C NMR (101 MHz, $CDCl_3$) δ: 212.0, 152.9, 145.5, 131.4, 126.4, 121.5, 117.3, 55.4, 50.2, 42.0, 35.8, 34.7, 34.4, 26.6, 25.9, 24.1, 18.3, -4.1, -4.2. FTIR (KBr, thin film), cm^{-1}: 3066, 3029, 2955, 2928, 2857, 2361, 2337, 1709, 1465, 1264. HRMS: ESI+ $[M+H]^+$ Calcd. For $C_{21}H_{33}O_2Si$: 345.2244. Found: 345.2236.

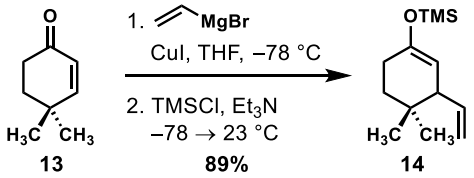

Vinylmagnesium bromide (0.7 M in tetrahydrofuran, 9.6 mL, 9.7 mmol, 2.4 equiv) was added dropwise to a precooled (–78 °C) solution of copper(I) iodide (0.92 g, 4.8 mmol, 1.2 equiv) in tetrahydrofuran (15 mL). The resultant suspension was stirred at –78 °C for 15 minutes whereupon 4,4-dimethylcyclohex-2-en-1-one (**13**) (0.50 mL, 4.0 mmol, 1.0 equiv) was added dropwise to the mixture. The resultant mixture was stirred at –78 °C for 1 h at which point trimethylamine (1.7 mL, 12 mmol, 3.0 equiv) and chlorotrimethylsilane (1.5 mL, 12 mmol, 3.0 equiv) were sequentially added dropwise to the reaction mixture. The brown heterogeneous mixture was allowed to warm to 23 °C and stirred for 1 hour. The resulting black reaction mixture was added to a mixture of 9:1 saturated ammonium chloride/ammonium hydroxide solution (30 mL). The layers were separated and the aqueous layer was extracted with ethyl ether (3 × 25 mL). The combined organic layers were washed with a mixture of 9:1 saturated ammonium chloride/ammonium hydroxide solution (3 × 25 mL) until aqueous layer was colorless, then washed with

water (15 mL) and brine (15 mL), and dried over anhydrous sodium sulfate. The dried solution was concentrated and purified by flash column chromatography using neutral silica (hexanes) to afford ((4,4-dimethyl-3-vinylcyclohex-1-en-1-yl)oxy)trimethylsilane (**14**) (0.80 g, 3.6 mmol, 89%), a clear yellow oil.

((4,4-dimethyl-3-vinylcyclohex-1-en-1-yl)oxy)trimethylsilane (**14**): TLC: 20% ethyl acetate−hexanes, R_f = 0.77 ($KMnO_4$). ^{1}H NMR (400 MHz, $CDCl_3$) δ: 5.71 (ddd, J_1 = 16.8 Hz, J_2 = 10.4 Hz, J_3 = 8.5 Hz, 1H), 5.02 – 4.95 (m, 2H), 4.66 (dt, J_1 = 3.2 Hz, J_2 = 1.4 Hz, 1H), 2.51 – 2.45 (m, 1H), 2.08 – 1.92 (m, 2H), 1.51 – 1.42 (m, 1H), 1.41 – 1.33 (m, 1H), 0.94 (s, 3H), 0.79 (s, 3H), 0.19 (s, 9H).^{13}C NMR (101 MHz, $CDCl_3$) δ: 150.0, 140.3, 115.1, 106.8, 49.8, 35.2, 31.6, 28.1, 27.7, 23.5, 0.5. FTIR (KBr, thin film), cm^{-1}: 2959, 2924, 2867, 1665, 1366, 1252, 1198. HRMS: ES+ $[M+H]^+$ Calcd. For $C_{13}H_{25}OSi$: 225.1680. Found: 225.1669.

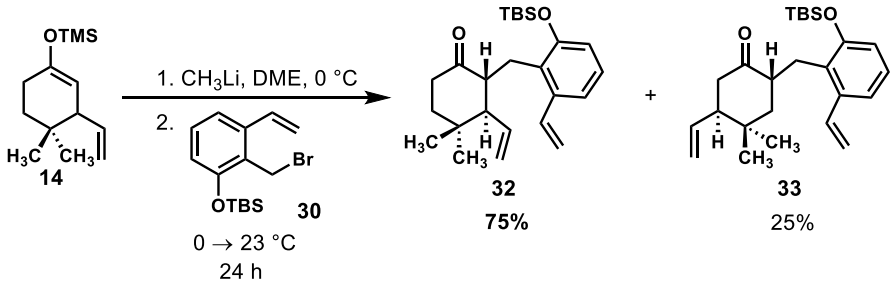

Methyllithium (1.6 M in ethyl ether, 0.33 mL, 0.53 mmol, 1.4 equiv) was added to a precooled (0 °C) solution of ((4,4-dimethyl-3-vinylcyclohex-1-en-1-yl)oxy)trimethylsilane (**14**) (0.125 g, 0.560 mmol, 1.47 equiv) in 1,2-dimethoxyethane (0.8 mL). The resultant heterogeneous yellow mixture was stirred at 0 °C for 10 minutes whereupon *tert*-butyl(2-(bromomethyl)-3-vinylphenoxy)dimethylsilane (**30**) (0.124 g, 0.381 mmol, 1 equiv) was added dropwise to the mixture. The heterogeneous

yellow mixture slowly warmed up to room temperature and stirred for 24 h, then was followed by filtering through a 5 cm thick neutral silica plug and eluted with ethyl ether (10 mL). The solution was concentrated to afford a 75:25 mixture of 2-(2-((*tert*-butyldimethylsilyl)oxy)-6-vinylbenzyl)-4,4-dimethyl-3-vinylcyclohexanone (**32**) and 2-(2-((*tert*-butyldimethylsilyl)oxy)-6-vinylbenzyl)-4,4-dimethyl-5-vinylcyclohexanone (**33**) (0.15 g, 0.38 mmol, 100%). The ratio of the two products were determined by NMR.

2-(2-((*tert*-butyldimethylsilyl)oxy)-6-vinylbenzyl)-4,4-dimethyl-3-vinylcyclohexanone (**32**): TLC: 20% ethyl ether−hexanes, R_f = 0.60 (UV, $KMnO_4$). ^{1}H NMR (400 MHz, $CDCl_3$) δ: 7.17 (dd, J_1 = 17.4 Hz, J_2 = 10.9 Hz, 1H), 7.02 (dd, J_1 = 7.8 Hz, J_2 = 1.7 Hz, 1H), 6.98 (t, J = 7.6 Hz, 1H), 6.66 (dd, J_1 = 7.5 Hz, J_2 = 1.7 Hz, 1H), 5.54 (dd, J_1 = 17.4 Hz, J_2 = 1.7 Hz, 1H), 5.47 (dt, J_1 = 16.6 Hz, J_2 = 10.1 Hz, 1H), 5.25 (dd, J_1 = 10.9 Hz, J_2 = 1.8 Hz, 1H), 4.94 (q, J = 1.9 Hz, 1H), 4.91 (dd, J_1 = 10.0 Hz, J_2 = 1.9 Hz, 1H), 3.12 (ddd, J_1 = 11.7 Hz, J_2 = 7.8 Hz, J_3 = 6.0 Hz, 1H), 3.01 (dd, J_1 = 14.1 Hz, J_2 = 8.0 Hz, 1H), 2.62 (dd, J_1 = 14.1 Hz, J_2 = 5.5 Hz, 1H), 2.46 (td, J_1 = 13.6 Hz, J_2 = 6.1 Hz, 1H), 2.22 (ddd, J_1 = 13.5 Hz, J_2 = 4.7 Hz, J_3 = 3.0 Hz, 1H), 1.97 (dd, J_1 = 11.5 Hz, J_2 = 9.8 Hz, 1H), 1.75 (ddd, J_1 = 13.5 Hz, J_2 = 6.1 Hz, J_3 = 3.0 Hz, 1H), 1.66 (dd, J_1 = 13.8 Hz, J_2 = 4.8 Hz, 1H), 1.05 (s, 3H), 1.00 (s, 9H), 0.90 (s, 3H), 0.26 (s, 3H), 0.24 (s, 3H). ^{13}C NMR (101 MHz, $CDCl_3$) δ: 212.4, 154.0, 139.7, 137.1, 137.1, 129.5, 126.2, 119.2, 117.7, 117.4, 115.0, 60.5, 49.6, 41.8, 38.8, 33.9, 29.8, 26.2, 26.1, 20.5, 18.7, -3.4, -3.7. FTIR (KBr, thin film), cm^{-1}: 3074, 2957, 2930, 2858, 2361, 2337, 1714, 1572, 1466, 1270. HRMS: FD+ $[M]^+$ Calcd. For $C_{25}H_{38}O_2Si$: 398.2641. Found: 398.2636.

2-(2-((*tert*-butyldimethylsilyl)oxy)-6-vinylbenzyl)-4,4-dimethyl-5-vinylcyclohexanone (**33**): TLC: 20% ethyl ether−hexanes, R_f = 0.64 ($KMnO_4$). ^1H NMR (400 MHz, $CDCl_3$) δ: 7.09 (dd, J_1 = 7.8 Hz, J_2 = 1.7 Hz, 1H), 7.06 (t, J = 7.7 Hz, 1H), 6.93 (dd, J_1 = 17.3 Hz, J_2 = 10.9 Hz, 1H), 6.73 (dd, J_1 = 7.6 Hz, J_2 = 1.6 Hz, 1H), 5.70 (ddd, J_1 = 16.9 Hz, J_2 = 10.3 Hz, J_3 = 7.8 Hz, 1H), 5.58 (dd, J_1 = 17.3 Hz, J_2 = 1.6 Hz, 1H), 5.24 (dd, J_1 = 11.0 Hz, J_2 = 1.5 Hz, 1H), 5.04 (ddd, J_1 = 10.2 Hz, J_2 = 1.2 Hz, 1H), 4.98 (ddd, J_1 = 17.1 Hz, J_2 = 1.8 Hz, J_3 = 1.0 Hz, 1H), 3.17 (dd, J_1 = 13.8 Hz, J_2 = 3.4 Hz, 1H), 2.86 – 2.75 (m, 1H), 2.68 (dd, J_1 = 13.7 Hz, J_2 = 10.3 Hz, 1H), 2.40 (t, J = 13.4 Hz, 1H), 2.32 – 2.18 (m, 2H), 1.50 (dd, J_1 = 13.4 Hz, J_2 = 5.5 Hz, 1H), 1.35 (t, J = 13.4 Hz, 1H), 0.98 (s, 9H), 0.87 (s, 3H), 0.87 (s. 3H), 0.23 (s, 3H), 0.23 (s, 3H). ^{13}C NMR (101 MHz, $CDCl_3$) δ: 212.2, 154.1, 139.3, 138.2, 135.6, 128.7, 126.7, 119.0, 117.6, 116.1, 116.0, 52.7, 46.9, 46.8, 43.6, 33.6, 29.3, 26.0, 25.2, 19.3, 18.4, -3.9, -4.0. FTIR (KBr, thin film), cm^{-1}: 3074, 2957, 2930, 2858, 2361, 2337, 1714, 1572, 1466, 1270. HRMS: FD+ $[M]^+$ Calcd. For $C_{25}H_{38}O_2Si$: 398.2641. Found: 398.2636.

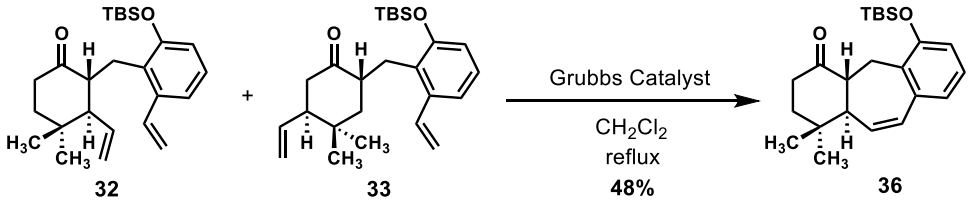

The second generation Grubb's catalyst (15 mg, 0.018 mmol, 0.047 equiv) was added to a 75:25 mixture of 2-(2-((*tert*-butyldimethylsilyl)oxy)-6-vinylbenzyl)-4,4-dimethyl-3-vinylcyclohexanone (**32**) and 2-(2-((*tert*-butyldimethylsilyl)oxy)-6-vinylbenzyl)-4,4-dimethyl-5-vinylcyclohexanone (**33**) (0.151 g, 0.379 mmol, 1 equiv)

in dichloromethane (4 mL). The resultant red solution was heated at reflux for 30 h, was then cooled and concentrated. Purification of the residue by flash column chromatography (1% ethyl acetate−hexanes) afforded 6-((*tert*-butyldimethylsilyl)oxy)-1,1-dimethyl-1,2,3,4a,5,11a-hexahydro-4H-dibenzo[α,δ][7]annulen-4-one (**36**) (0.068 g, 0.18 mmol, 48%) as a colorless crystalline solid.

6-((*tert*-butyldimethylsilyl)oxy)-1,1-dimethyl-1,2,3,4a,5,11a-hexahydro-4H-dibenzo[α,δ][7]annulen-4-one (**36**): TLC: 20% ethyl acetate−hexanes, R_f = 0.53 (UV, CAM). ^{1}H NMR (400 MHz, $CDCl_3$) δ: 7.01 (t, J = 7.8 Hz, 1H), 6.79 (d, J = 7.4 Hz, 1H), 6.69 (dd, J_1 = 8.0 Hz, J_2 = 0.9 Hz, 1H), 6.51 (dd, J_1 = 12.7 Hz, J_2 = 2.4 Hz, 1H), 5.86 (dd, J_1 = 12.7 Hz, J_2 = 3.4 Hz, 1H), 4.20 (dd, J_1 = 15.0 Hz, J_2 = 1.3 Hz, 1H), 2.55 (dd, J_1 = 12.8 Hz, J_2 = 7.7 Hz, 1H), 2.44 (dt, J_1 = 12.7 Hz, J_2 = 2.6 Hz, 2H), 2.34 (ddd, J_1 = 13.9 Hz, J_2 = 4.6 Hz, J_3 = 2.9 Hz, 1H), 2.13 (dd, J_1 = 15.0 Hz, J_2 = 7.7 Hz, 1H), 1.76 (ddd, J_1 = 13.5 Hz, J_2 = 6.5 Hz, J_3 = 3.0 Hz, 1H), 1.74 – 1.59 (m, 1H), 1.14 (s, 3H), 1.07 (s, 9H), 1.02 (s, 3H), 0.22 (s, 3H), 0.18 (s, 3H). ^{13}C NMR (101 MHz, $CDCl_3$) δ: 210.6, 152.3, 137.5, 131.6, 131.2, 131.0, 126.3, 124.0, 118.3, 58.1, 50.8, 41.3, 38.5, 35.0, 29.8, 25.9, 23.8, 20.1, 18.4, -4.1, -4.2. FTIR (KBr, thin film), cm^{-1}: 3020, 2958, 2929, 2859, 2361, 2338, 1716, 1458, 1255, 1019. HRMS: ESI+ $[M+H]^+$ Calcd. For $C_{23}H_{35}O_2Si$: 371.2406. Found: 371.2404.

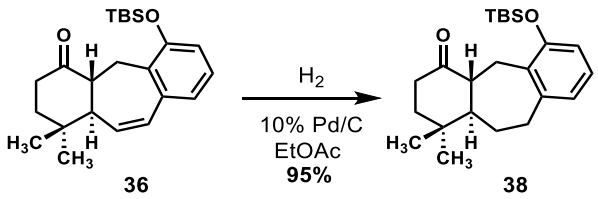

6-((*tert*-butyldimethylsilyl)oxy)-1,1-dimethyl-1,2,3,4a,5,11a-hexahydro-4H-dibenzo[α,δ][7]annulen-4-one (**36**) (33 mg, 0.089 mmol, 1 equiv) was added to a mixture of 10% palladium on carbon (1 mg, 0.005 mmol, 0.05 equiv) in ethyl acetate (0.4 mL). The flask was then purged with hydrogen and held under a hydrogen atmosphere using a hydrogen-filled balloon. The mixture was stirred at room temperature for 3 h and then was filtered through a 1 cm silica plug and eluted with ethyl acetate (1 mL). The solution was concentrated to afford 6-((*tert*-butyldimethylsilyl)oxy)-1,1-dimethyl-1,2,3,4a,5,10,11,11a-octahydro-4H-dibenzo[α,δ][7]annulen-4-one (**38**) (32 mg, 0.085 mmol, 95%) as a clear, colorless oil.

6-((*tert*-butyldimethylsilyl)oxy)-1,1-dimethyl-1,2,3,4a,5,10,11,11a-octahydro-4H-dibenzo[α,δ][7]annulen-4-one (**38**): TLC: 20% ethyl acetate−hexanes, R_f = 0.57 (CAM). ^{1}H NMR (400 MHz, $CDCl_3$) δ: 6.95 (t, J = 7.8 Hz, 1H), 6.70 (d, J_1 = 7.2 Hz, 1H), 6.66 (d, J_1 = 8.1 Hz, 1H), 4.10 (d, J = 13.3 Hz, 1H), 2.83 – 2.68 (m, 2H), 2.49 (td, J_1 = 13.6 Hz, J_2 = 6.8 Hz, 1H), 2.32 (dt, J_1 = 13.6 Hz, J_2 = 3.6 Hz, 1H), 2.20 – 2.03 (m, 3H), 1.78 – 1.59 (m, 3H), 1.23 (ddd, J_1 = 14.5 Hz, J_2 = 9.4 Hz, J_3 = 2.6 Hz, 1H), 1.02 (s, 3H), 1.01 (s, 9H), 0.98 (s, 3H), 0.22 (s, 3H), 0.17 (s, 3H). ^{13}C NMR (101 MHz, $CDCl_3$) δ: 212.1, 153.0, 146.2, 131.1, 126.4, 121.0, 117.2, 58.0, 50.6, 42.6, 38.8, 34.8, 34.4, 29.6, 29.4, 25.9, 24.5, 20.2, 18.3, -4.1, -4.2. FTIR (KBr, thin film), cm^{-1}: 3066, 3034, 2955, 2928, 2856, 2361, 2337, 1716, 1653, 1559, 1464, 1272. HRMS: ESI+ $[M+H]^+$ Calcd. For $C_{23}H_{37}O_2Si$: 373.2557. Found: 373.2552.

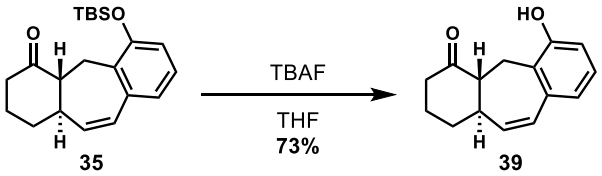

Tetra-*n*-butylammonium fluoride (1.0 M in tetrahydrofuran, 0.12 mL, 0.12 mmol, 1.2 equiv) was added to 6-((*tert*-butyldimethylsilyl)oxy)-1,2,3,4a,5,11a-hexahydro-4H-dibenzo[α,δ][7]annulen-4-one (**35**) (35 mg, 0.10 mmol, 1 equiv) neat. The mixture was stirred at 23 °C for 5 minutes, then was concentrated. Purification of the residue by flash column chromatography (12% ethyl acetate–hexanes) afforded 6-hydroxy-1,2,3,4a,5,11a-hexahydro-4H-dibenzo[α,δ][7]annulen-4-one (**39**) (17 mg, 0.074 mmol, 73%) as a white solid.

6-hydroxy-1,2,3,4a,5,11a-hexahydro-4H-dibenzo[α,δ][7]annulen-4-one (**39**): TLC: 20% ethyl acetate−hexanes, R_f = 0.26 (CAM). ^{1}H NMR (400 MHz, $CDCl_3$) δ: 7.83 (s, 1H), 7.11 (t, J = 7.8 Hz, 1H), 6.86 (d, J = 8.0 Hz, 1H), 6.69 (d, J = 7.5 Hz, 1H), 6.63 (dd, J_1 = 10.3 Hz, J_2 = 2.0 Hz, 1H), 5.95 (dd, J_1 = 10.3 Hz, J_2 = 5.6 Hz, 1H), 3.19 (dd, J_1 = 13.3 Hz, J_2 = 7.1 Hz, 1H), 3.05 (d, J = 14.2 Hz, 1H), 2.49 (dd, J_1 = 14.2 Hz, J_2 = 7.1 Hz, 1H), 2.46 – 2.33 (m, 2H), 2.16 – 1.92 (m, 3H), 1.83 (qd, J_1 = 12.7 Hz, J_2 = 4.0 Hz, 1H), 1.68 – 1.54 (m, 1H). ^{13}C NMR (101 MHz, $CDCl_3$) δ: 215.4, 154.6, 139.9, 134.1, 131.2, 127.2, 125.3, 120.3, 115.9, 65.7, 44.5, 40.6, 30.2, 26.5, 24.1. FTIR (KBr, thin film), cm^{-1}: 3350, 3016, 2924, 2853, 2361, 2338, 1685, 1457, 1252. HRMS: ESI+ $[M+H]^+$ Calcd. For $C_{15}H_{17}O_2$: 229.1223. Found: 229.1221.

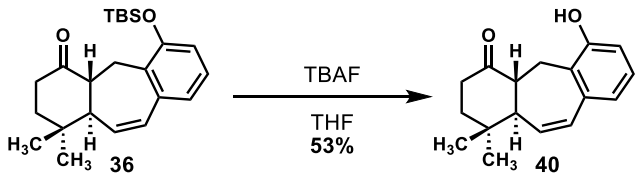

Tetra-*n*-butylammonium fluoride (1.0 M in tetrahydrofuran, 0.13 mL, 0.13 mmol, 1.2 equiv) was added to 6-((*tert*-butyldimethylsilyl)oxy)-1,1-dimethyl-1,2,3,4a,5,11a-hexahydro-4H-dibenzo[α,δ][7]annulen-4-one (**36**) (39 mg, 0.11 mmol, 1 equiv) neat. The mixture was stirred at 23 °C for 5 minutes, then was concentrated. Purification of the residue by flash column chromatography (12% ethyl acetate–hexanes) afforded 6-hydroxy-1,1-dimethyl-1,2,3,4a,5,11a-hexahydro-4H-dibenzo[α,δ][7]annulen-4-one (**40**) (14 mg, 0.055 mmol, 53%) as a white solid.

6-hydroxy-1,1-dimethyl-1,2,3,4a,5,11a-hexahydro-4H-dibenzo[α,δ][7]annulen-4-one (**40**): TLC: 20% ethyl acetate−hexanes, R_f = 0.26 (CAM). ^{1}H NMR (400 MHz, $CDCl_3$) δ: 8.01 (s, 1H), 7.12 (t, J = 7.8 Hz, 1H), 6.87 (d, J = 7.9 Hz, 1H), 6.73 – 6.67 (m, 2H), 6.04 (dd, J_1 = 10.5 Hz, J_2 = 6.1 Hz, 1H), 3.36 (dd, J_1 = 13.9 Hz, J_2 = 7.1 Hz, 1H), 3.10 (d, J = 14.1 Hz, 1H), 2.54 (tdd, J_1 = 14.0 Hz, J_2 = 6.6 Hz, J_3 = 1.3 Hz, 1H), 2.38 – 2.31 (m, 2H), 1.92 (ddd, J_1 = 13.9 Hz, J_2 = 6.1 Hz, J_3 = 1.9 Hz, 1H), 1.77 (ddd, J_1 = 13.6 Hz, J_2 = 6.6 Hz, J_3 = 2.4 Hz, 1H), 1.52 (td, J_1 = 13.9 Hz, J_2 = 4.9 Hz, 1H), 1.27 (s, 3H), 0.91 (s, 3H). ^{13}C NMR (101 MHz, $CDCl_3$) δ: 216.0, 154.7, 140.0, 131.8, 131.1, 127.2, 125.0, 120.2, 115.9, 60.7, 51.6, 41.5, 38.2, 32.7, 29.3, 24.3, 20.0. FTIR (KBr, thin film), cm^{-1}: 3336, 3002, 2957, 2923, 2852, 2361, 2339, 1696, 1457, 1254. HRMS: ESI+ $[M+H]^+$ Calcd. For $C_{17}H_{21}O_2$: 257.1536. Found: 257.1533.

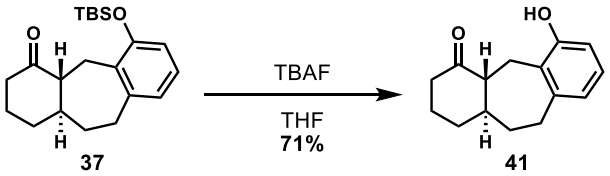

Tetra-*n*-butylammonium fluoride (1.0 M in tetrahydrofuran, 95 μL, 0.095 mmol, 1.2 equiv) was added to 6-((*tert*-butyldimethylsilyl)oxy)-1,2,3,4a,5,10,11,11a-octahydro-4H-dibenzo[α,δ][7]annulen-4-one (**37**) (27 mg, 0.079 mmol, 1 equiv) neat. The mixture was stirred at 23 °C for 5 minutes, then was concentrated. Purification of the residue by flash column chromatography (12% ethyl acetate–hexanes) afforded 6-hydroxy-1,2,3,4a,5,10,11,11a-octahydro-4H-dibenzo[α,δ][7]annulen-4-one (**41**) (13 mg, 0.056 mmol, 71%) as a white solid.

6-hydroxy-1,2,3,4a,5,10,11,11a-octahydro-4H-dibenzo[α,δ][7]annulen-4-one (**41**): TLC: 20% ethyl acetate−hexanes, R_f = 0.19 (CAM). ^{1}H NMR (400 MHz, $(CD_3)_2CO$) δ: 8.10 (s, 1H), 6.87 (t, *J* = 7.7 Hz, 1H), 6.69 (d, *J* = 7.9 Hz, 1H), 6.59 (d, *J* = 7.4 Hz, 1H), 3.89 (d, *J* = 14.5 Hz, 1H), 2.91 – 2.79 (m, 2H), 2.67 (ddd, J_1 = 14.3 Hz, J_2 = 7.3 Hz, J_3 = 2.0 Hz, 1H), 2.49 – 2.36 (m, 1H), 2.26 (ddt, J_1 = 12.8 Hz, J_2 = 4.1 Hz, J_3 = 2.2 Hz, 1H), 2.21 – 2.12 (m, 1H), 2.11 – 1.97 (m, 2H), 1.80 – 1.69 (m, 2H), 1.66 (dt, J_1 = 13.2 Hz, J_2 = 3.8 Hz, 1H), 1.59 – 1.47 (m, 1H), 1.34 – 1.22 (m, 1H). ^{13}C NMR (101 MHz, $(CD_3)_2CO$) δ: 211.8, 155.1, 145.9, 127.5, 127.2, 120.6, 114.2, 55.7, 50.5, 42.2, 36.2, 34.8 (2C), 27.2, 24.0. (FTIR (KBr, thin film), cm^{-1}: 3335, 2923, 2851, 2361, 2339, 1700, 1684, 1653, 1559, 1540, 1507, 1457. HRMS: ESI+ $[M+H]^+$ Calcd. For $C_{15}H_{19}O_2$: 231.1380. Found: 231.1381.

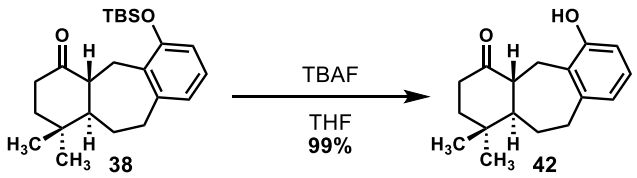

Tetra-*n*-butylammonium fluoride (1.0 M in tetrahydrofuran, 93 μL, 0.093 mmol, 1.2 equiv) was added to 6-((*tert*-butyldimethylsilyl)oxy)-1,1-dimethyl-1,2,3,4a,5,10,11,11a-octahydro-4H-dibenzo[α,δ][7]annulen-4-one (**38**) (29 mg, 0.078 mmol, 1 equiv) neat. The mixture was stirred at 23 °C for 5 minutes, then was concentrated. Purification of the residue by flash column chromatography (12% ethyl acetate–hexanes) afforded 6-hydroxy-1,1-dimethyl-1,2,3,4a,5,10,11,11a-octahydro-4H-dibenzo[α,δ][7]annulen-4-one (**42**) (20 mg, 0.077 mmol, 99%) as a colorless, clear oil.

6-hydroxy-1,1-dimethyl-1,2,3,4a,5,10,11,11a-octahydro-4H-dibenzo[α,δ][7]annulen-4-one (**42**): TLC: 20% ethyl acetate−hexanes, R_f = 0.20 (CAM). ^{1}H NMR (400 MHz, $(CD_3)_2CO$) δ: 8.08 (s, 1H), 6.88 (t, J = 7.7 Hz, 1H), 6.69 (dd, J_1 = 8.1 Hz, J_2 = 1.2 Hz, 1H), 6.59 (d, J_1 = 7.3 Hz, 1H), 3.85 (d, J = 12.6 Hz, 1H), 2.76 (dd, J_1 = 7.0 Hz, J_2 = 4.6 Hz, 2H), 2.62 (td, J_1 = 14.1 Hz, J_2 = 5.9 Hz, 1H), 2.32 – 2.21 (m, 2H), 2.18 (ddd, J_1 = 13.3 Hz, J_2 = 4.2 Hz, J_3 = 2.8 Hz, 1H), 2.16 – 2.09 (m, 1H), 1.75 (ddd, J_1 = 13.3 Hz, J_2 = 5.9 Hz, J_3 = 2.8 Hz, 1H), 1.62 (td, J_1 = 14.1 Hz, J_2 = 4.2 Hz, 1H), 1.53 (td, J_1 = 11.3 Hz, J_2 = 3.1 Hz, 1H), 1.27 – 1.18 (m, 1H), 1.04 (s, 3H), 1.00 (s, 3H). ^{13}C NMR (101 MHz, $(CD_3)_2CO$) δ: 212.3, 155.1, 146.1, 127.3, 126.9, 120.3, 114.3, 57.3, 50.8, 43.1, 39.0, 34.7, 34.4, 29.7 (2C), 24.2, 20.1. FTIR (KBr, thin film), cm^{-1}: 3310, 2956, 2923, 2852, 2361, 2339, 1700, 1684, 1653, 1559, 1540, 1507, 1465, 1457. HRMS: ESI+ $[M+H]^+$ Calcd. For $C_{17}H_{23}O_2$: 259.1693. Found: 259.1696.

Appendix B

CATALOG OF SPECTRA

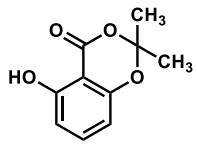
O
O
CH3
CH3
HO
O

16

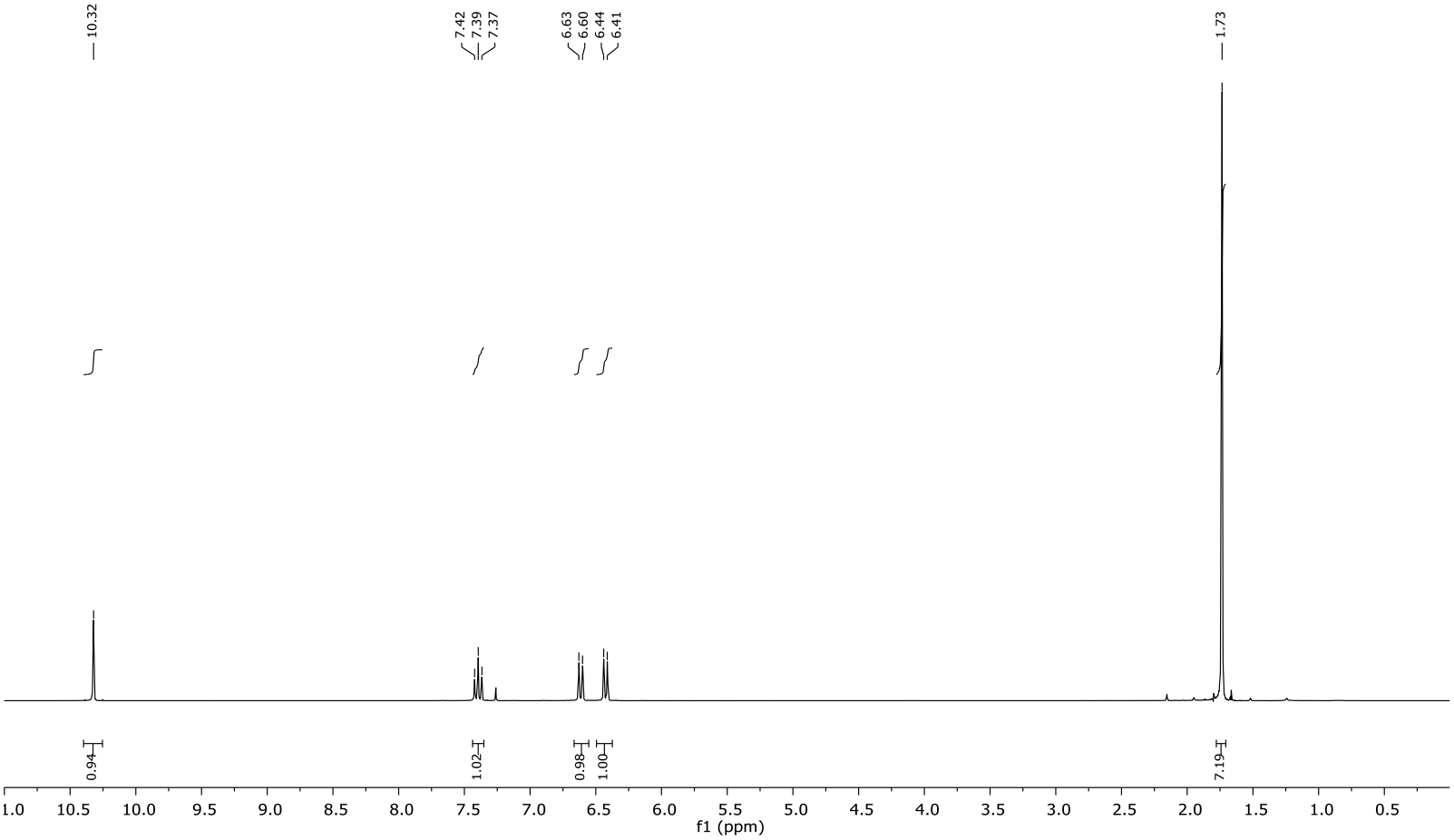
10.32
7.42
7.39
7.37
6.63
6.60
6.44
6.41
1.73
0.94
1.02
0.98
1.00
7.19
1.0
10.5
10.0
9.5
9.0
8.5
8.0
7.5
7.0
6.5
6.0
5.5
5.0
4.5
4.0
3.5
3.0
2.5
2.0
1.5
1.0
0.5
f1 (ppm)

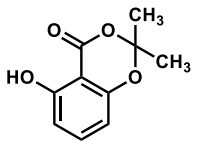
O
O
CH3
CH3
HO
O

16

165.58
161.50
155.67
138.03
110.90
107.36
107.23
99.45
25.75
230 220 210 200 190 180 170 160 150 140 130 120 110 100 90 80 70 60 50 40 30 20 10 0 -10
f1 (ppm)

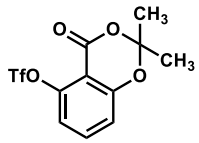
O
O
CH3
CH3
TfO
O

17

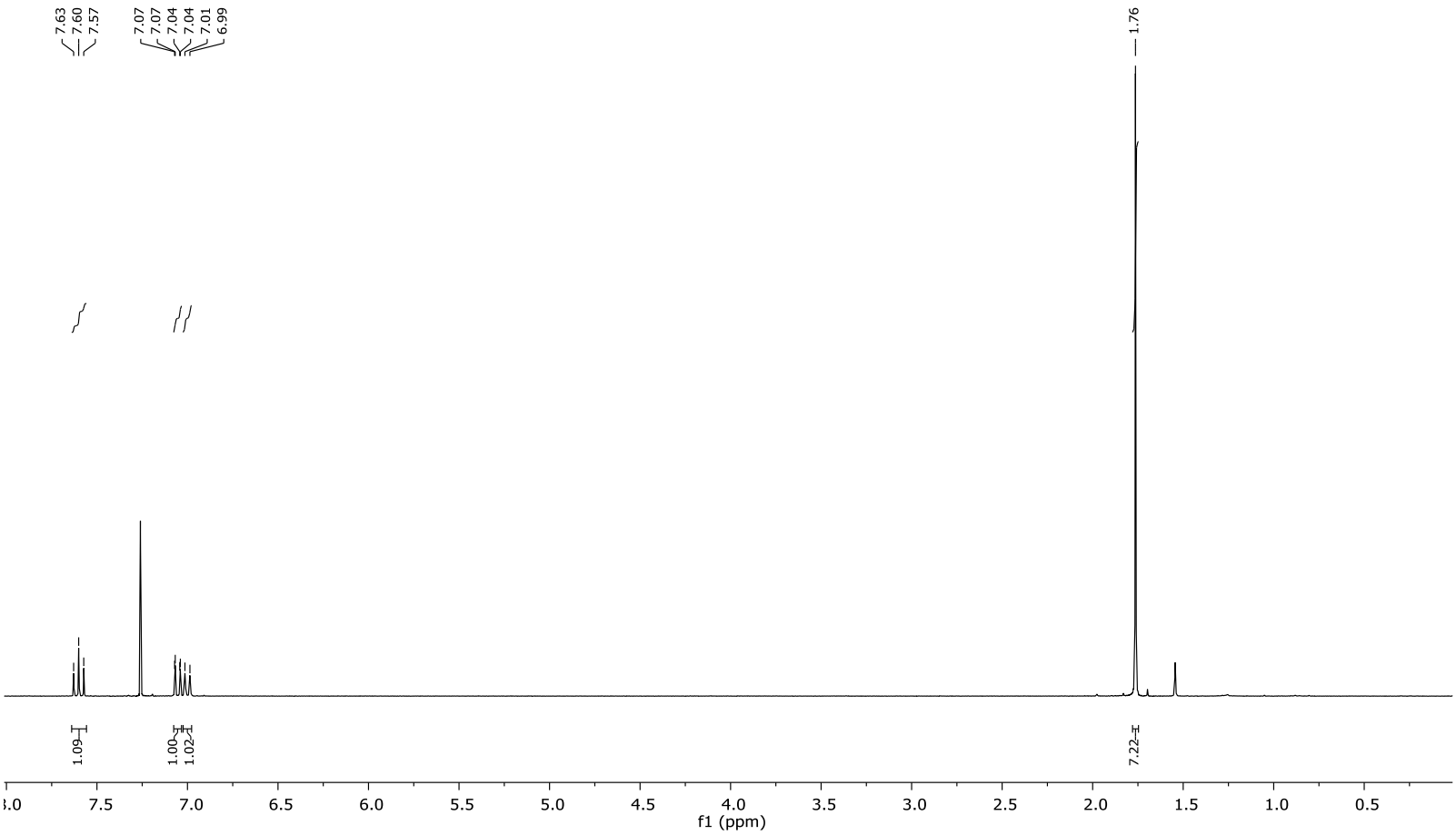
7.63
7.60
7.57
7.07
7.07
7.04
7.04
7.01
6.99
1.76
1.09
1.00
1.02
7.22
f1 (ppm)

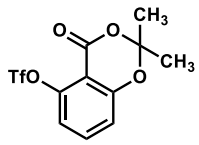
O
O
CH3
CH3
TfO
O

17

157.50
157.25
148.66
136.49
125.20
120.94
118.07
116.69
116.62
112.43
108.32
106.98
25.52
230 220 210 200 190 180 170 160 150 140 130 120 110 100 90 80 70 60 50 40 30 20 10 0 -10
f1 (ppm)

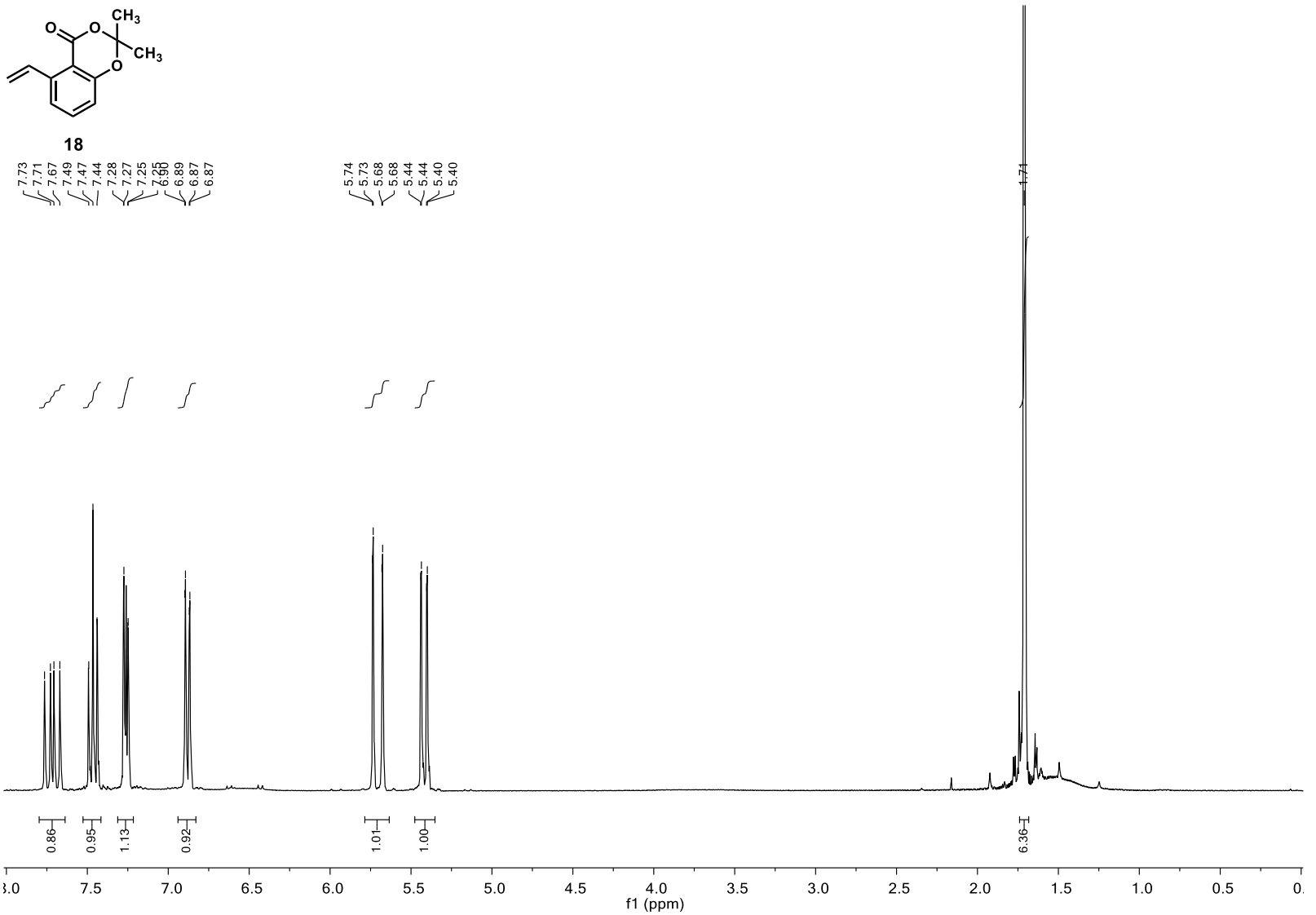
18
7.73
7.71
7.67
7.49
7.47
7.44
7.28
7.27
7.25
6.90
6.89
6.87
6.87
5.74
5.73
5.68
5.68
5.44
5.44
5.40
5.40
1.71
0.86
0.95
1.13
0.92
1.01
1.00
6.36
7.5
7.0
6.5
6.0
5.5
5.0
4.5
4.0
3.5
3.0
2.5
2.0
1.5
1.0
0.5
f1 (ppm)

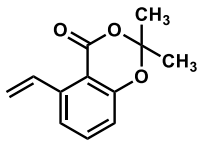
O
O
CH3
CH3
O

18

160.45
156.84
142.46
135.46
135.43
121.51
117.91
116.67
111.04
105.43
25.77
230 220 210 200 190 180 170 160 150 140 130 120 110 100 90 80 70 60 50 40 30 20 10 0 -10
f1 (ppm)

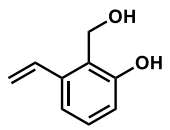
OH
OH

19

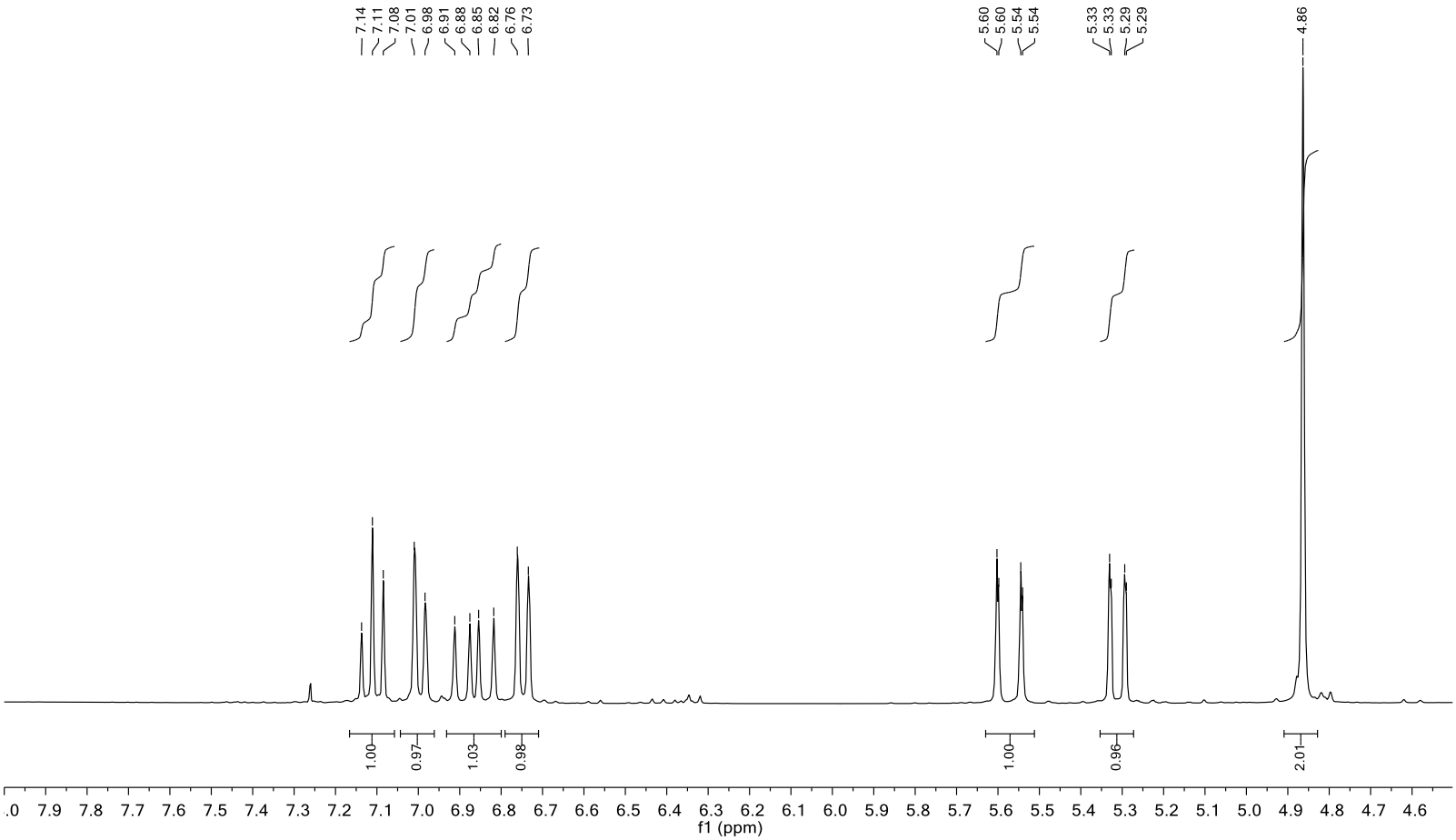
7.14
7.11
7.08
7.01
6.98
6.91
6.88
6.85
6.82
6.76
6.73
5.60
5.60
5.54
5.54
5.33
5.33
5.29
5.29
4.86
1.00
0.97
1.03
0.98
1.00
0.96
2.01
f1 (ppm)

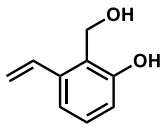
OH
OH

19

155.72
137.95
133.93
129.06
122.41
118.60
117.52
115.65
58.92
230 220 210 200 190 180 170 160 150 140 130 120 110 100 90 80 70 60 50 40 30 20 10 0 -10
f1 (ppm)

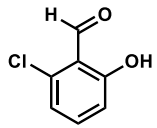
H
O
Cl
OH

24

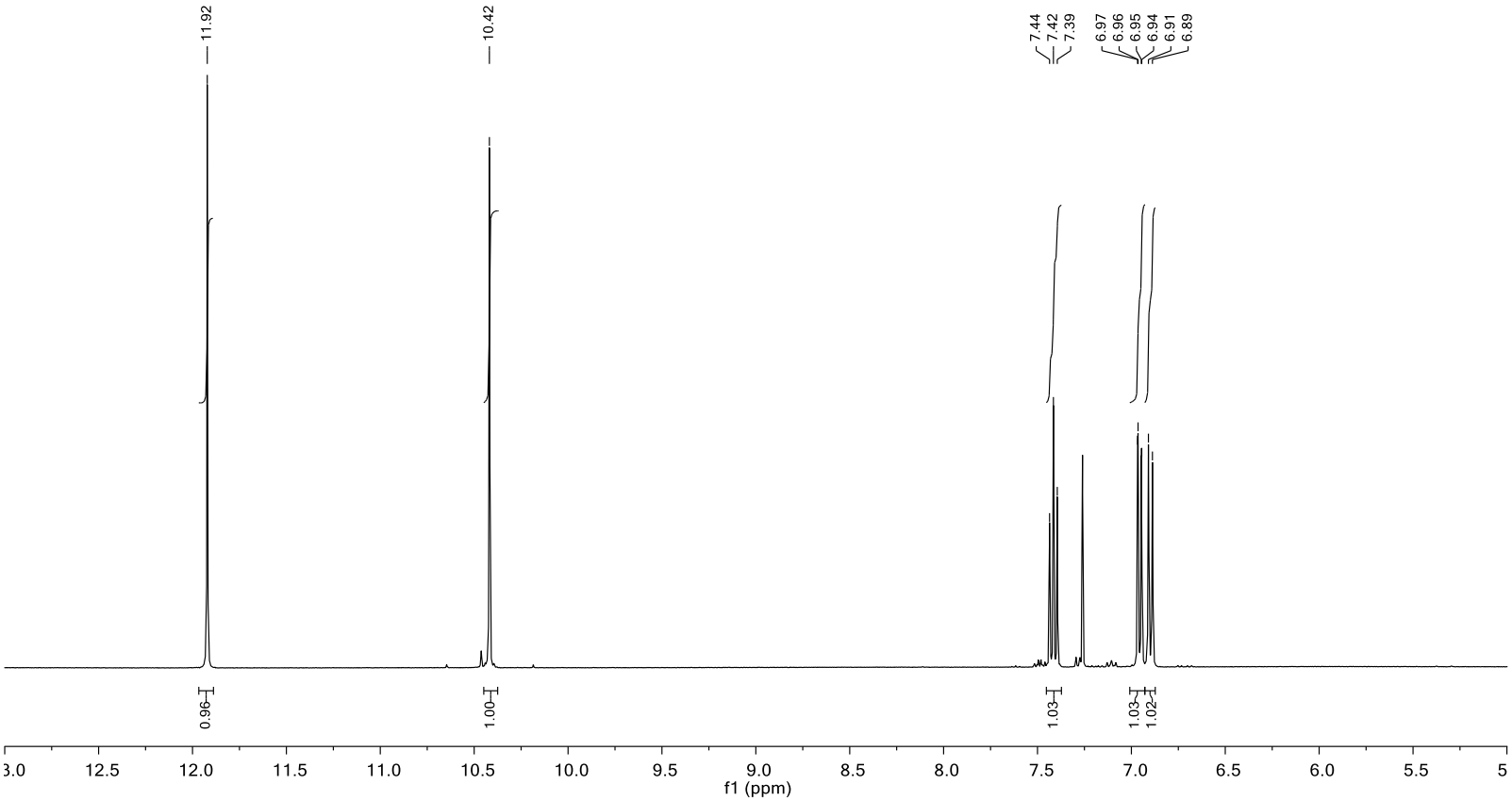
11.92
10.42
7.44
7.42
7.39
6.97
6.96
6.95
6.94
6.91
6.89
0.96
1.00
1.03
1.03
1.02
3.0
12.5
12.0
11.5
11.0
10.5
10.0
9.5
9.0
8.5
8.0
7.5
7.0
6.5
6.0
5.5
5
f1 (ppm)

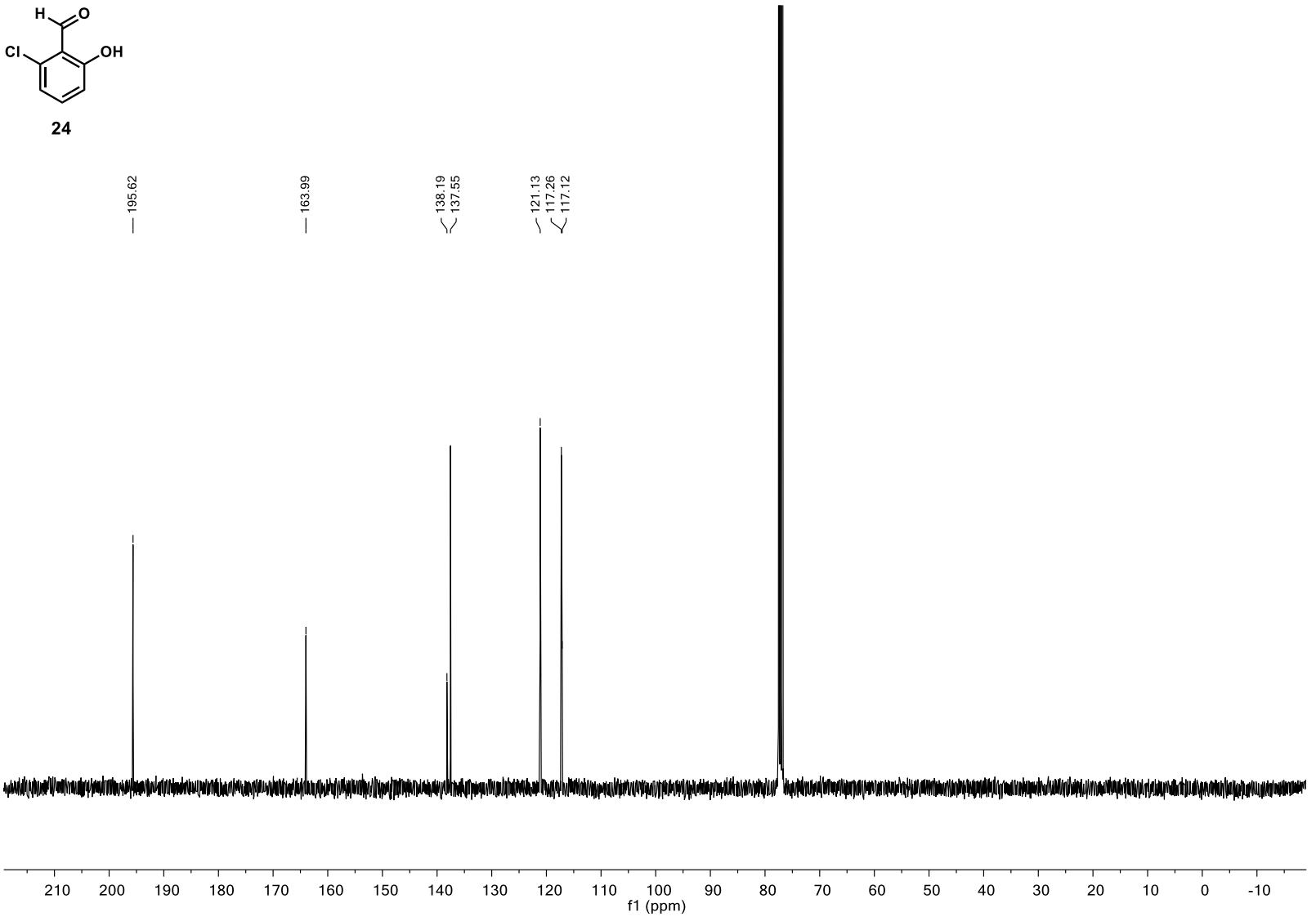
H
O
Cl
OH
24
195.62
163.99
138.19
137.55
121.13
117.26
117.12
210
200
190
180
170
160
150
140
130
120
110
100
90
80
70
60
50
40
30
20
10
0
-10
f1 (ppm)

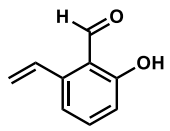
H
O
OH

20

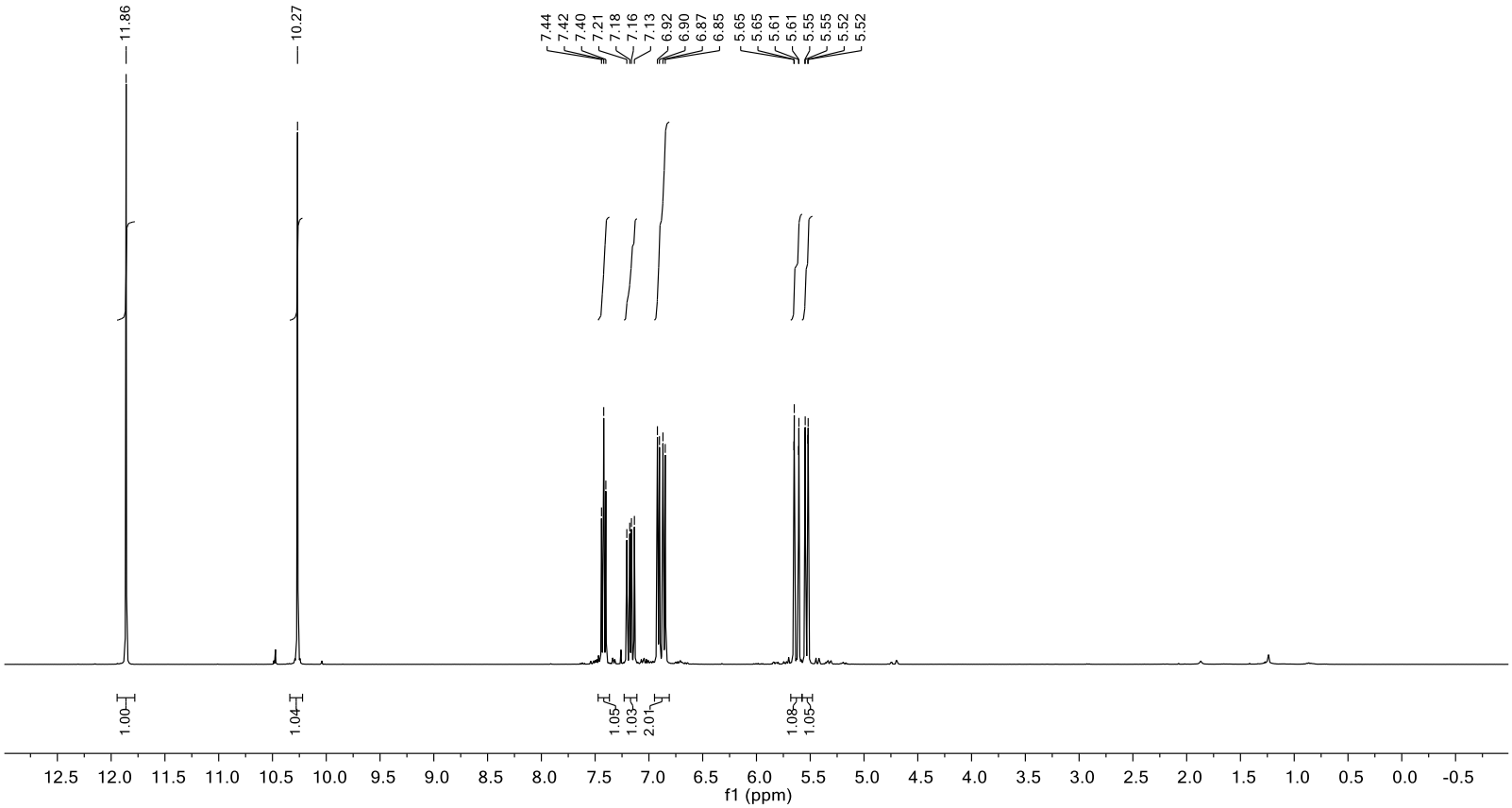
11.86
10.27
7.44
7.42
7.40
7.21
7.18
7.16
7.13
6.92
6.90
6.87
6.85
5.65
5.65
5.61
5.61
5.55
5.55
5.52
5.52
1.00
1.04
1.05
1.03
2.01
1.08
1.05
12.5 12.0 11.5 11.0 10.5 10.0 9.5 9.0 8.5 8.0 7.5 7.0 6.5 6.0 5.5 5.0 4.5 4.0 3.5 3.0 2.5 2.0 1.5 1.0 0.5 0.0 -0.5
f1 (ppm)

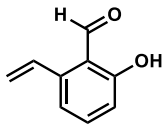
H
O
OH

20

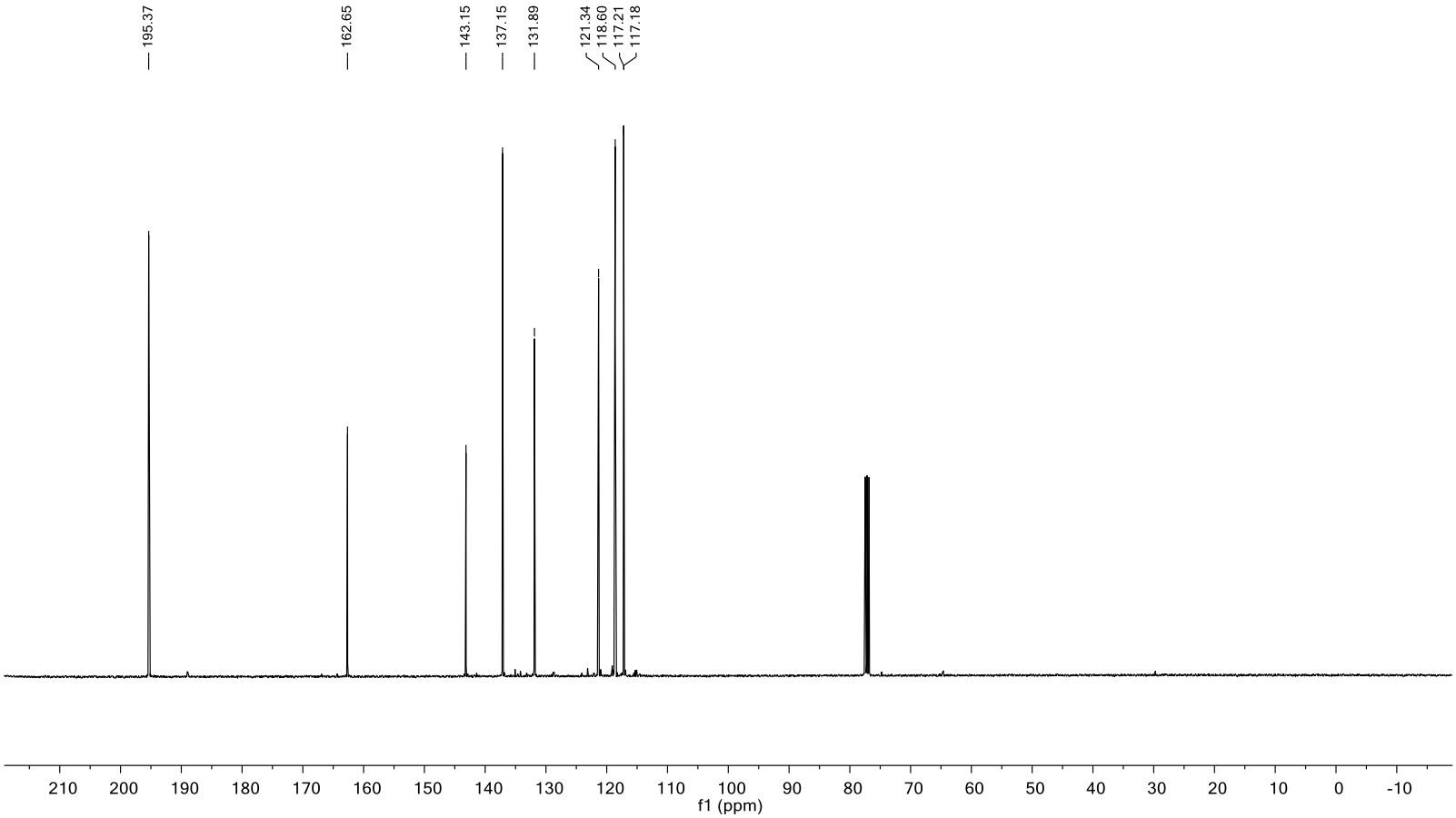
195.37
162.65
143.15
137.15
131.89
121.34
118.60
117.21
117.18
210
200
190
180
170
160
150
140
130
120
110
100
90
80
70
60
50
40
30
20
10
0
-10
f1 (ppm)

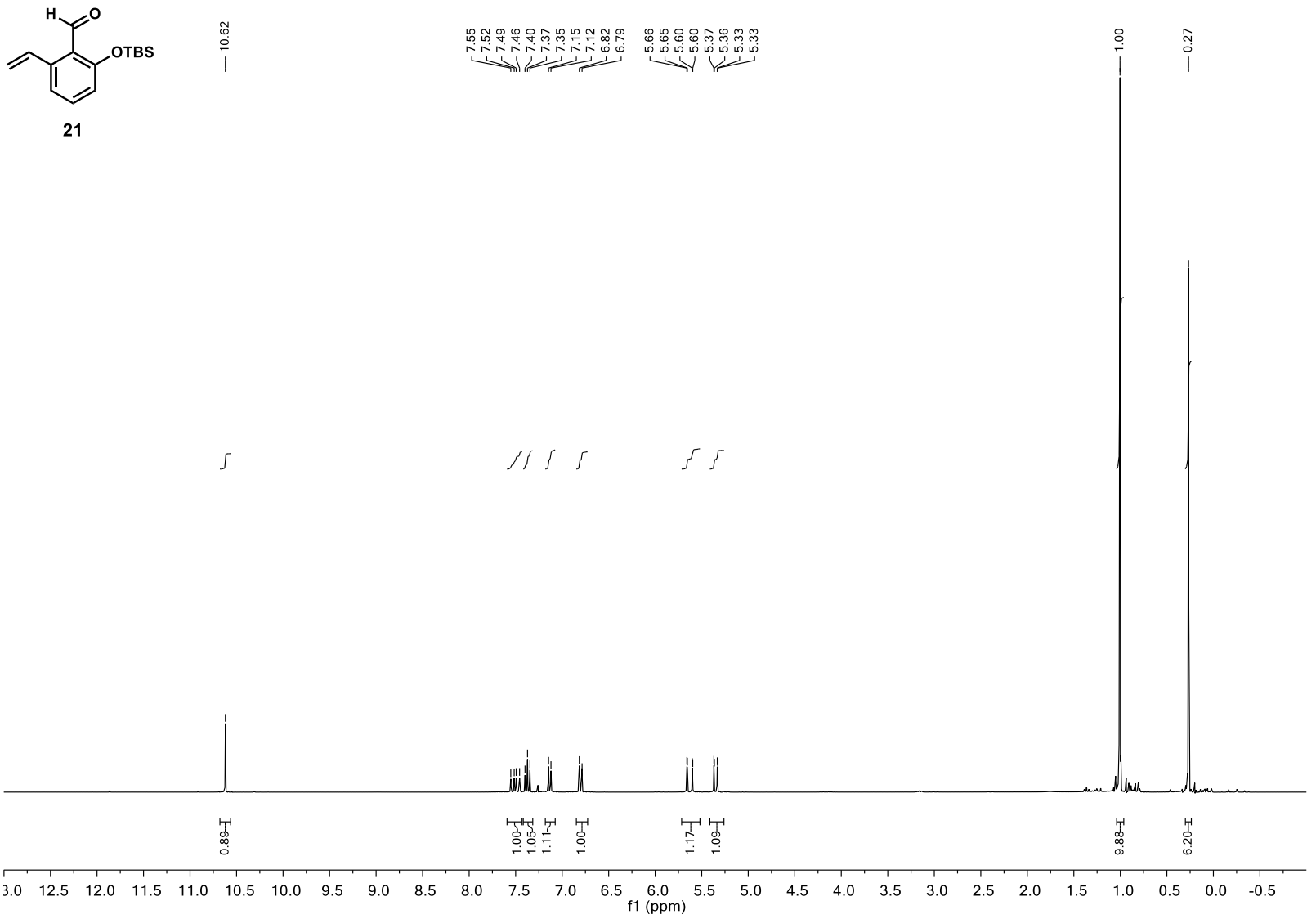
H
O
OTBS
21
10.62
7.55
7.52
7.49
7.46
7.40
7.37
7.35
7.15
7.12
6.82
6.79
5.66
5.65
5.60
5.60
5.37
5.36
5.33
5.33
1.00
0.27
0.89
1.00
1.05
1.11
1.00
1.17
1.09
9.88
6.20
f1 (ppm)

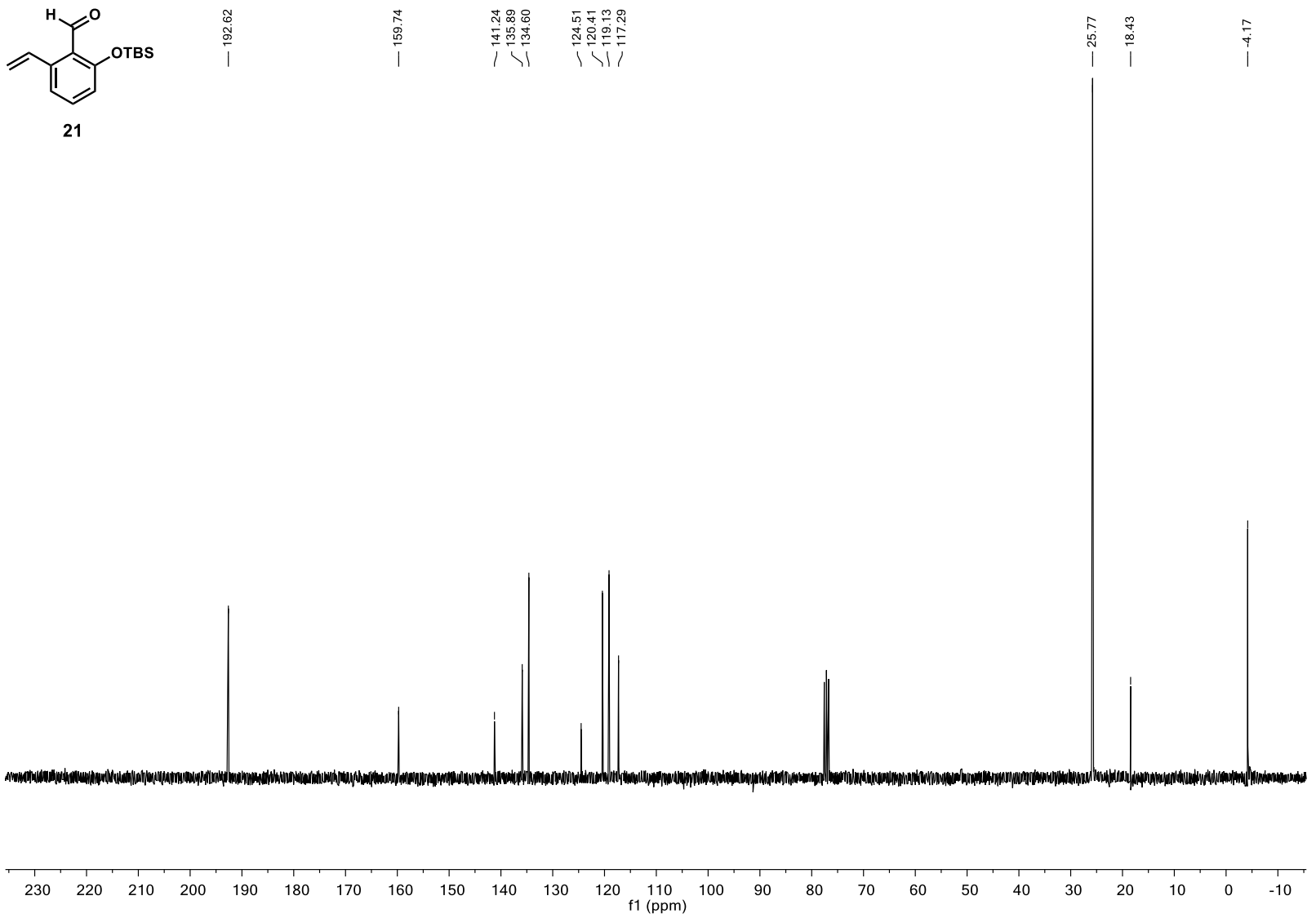
H
O
OTBS
21
192.62
159.74
141.24
135.89
134.60
124.51
120.41
119.13
117.29
25.77
18.43
-4.17
230 220 210 200 190 180 170 160 150 140 130 120 110 100 90 80 70 60 50 40 30 20 10 0 -10
f1 (ppm)

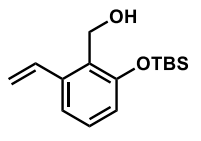
OH
OTBS

22

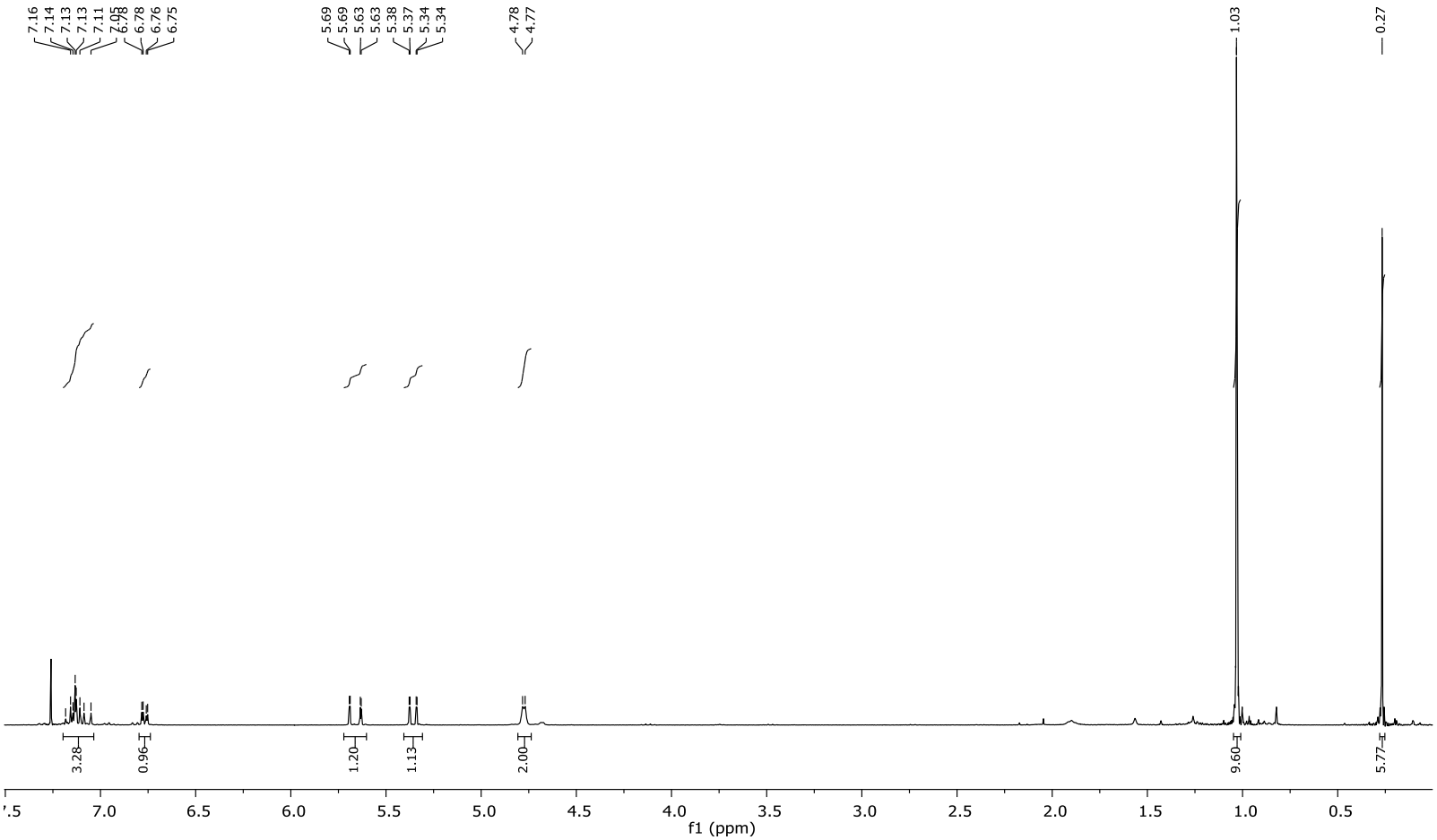
7.16
7.14
7.13
7.13
7.11
7.05
6.78
6.78
6.76
6.75
5.69
5.69
5.63
5.63
5.38
5.37
5.34
5.34
4.78
4.77
1.03
0.27
3.28
0.96
1.20
1.13
2.00
9.60
5.77
7.5
7.0
6.5
6.0
5.5
5.0
4.5
4.0
3.5
3.0
2.5
2.0
1.5
1.0
0.5
f1 (ppm)

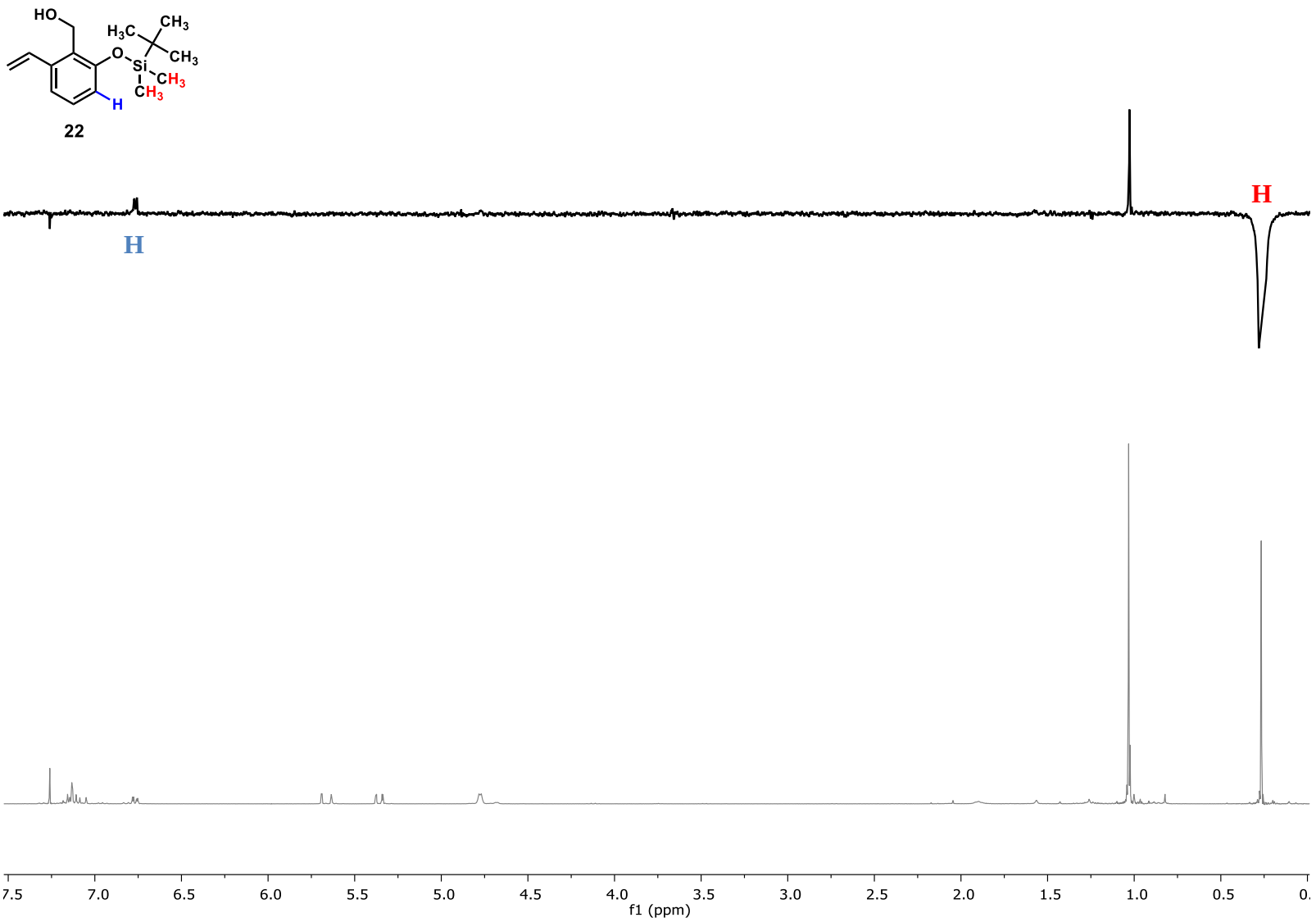
HO
H3C
CH3
CH3
O
Si
CH3
CH3
H
22
H
H
7.5
7.0
6.5
6.0
5.5
5.0
4.5
4.0
3.5
3.0
2.5
2.0
1.5
1.0
0.5
0.
f1 (ppm)

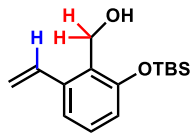

22

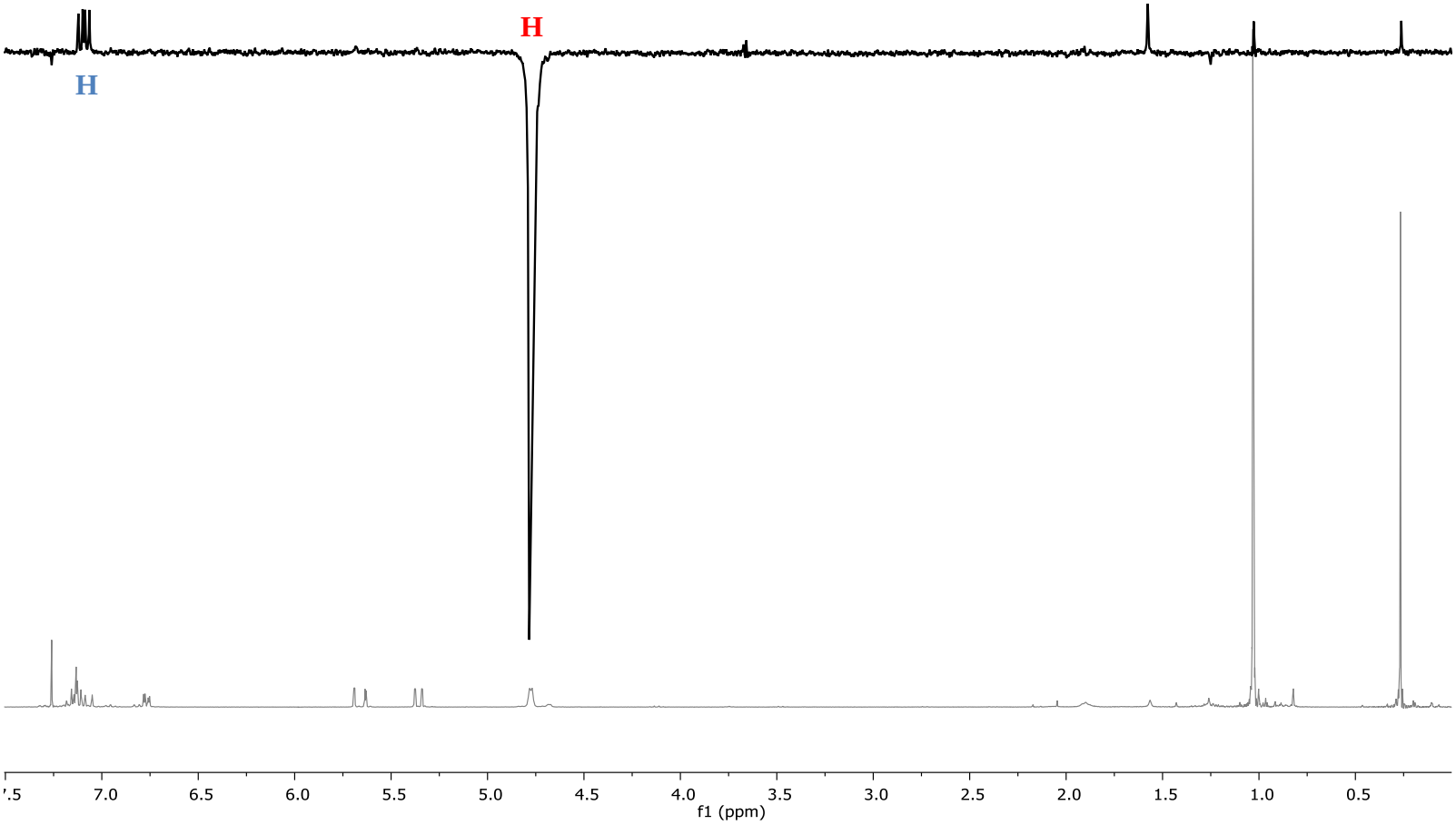

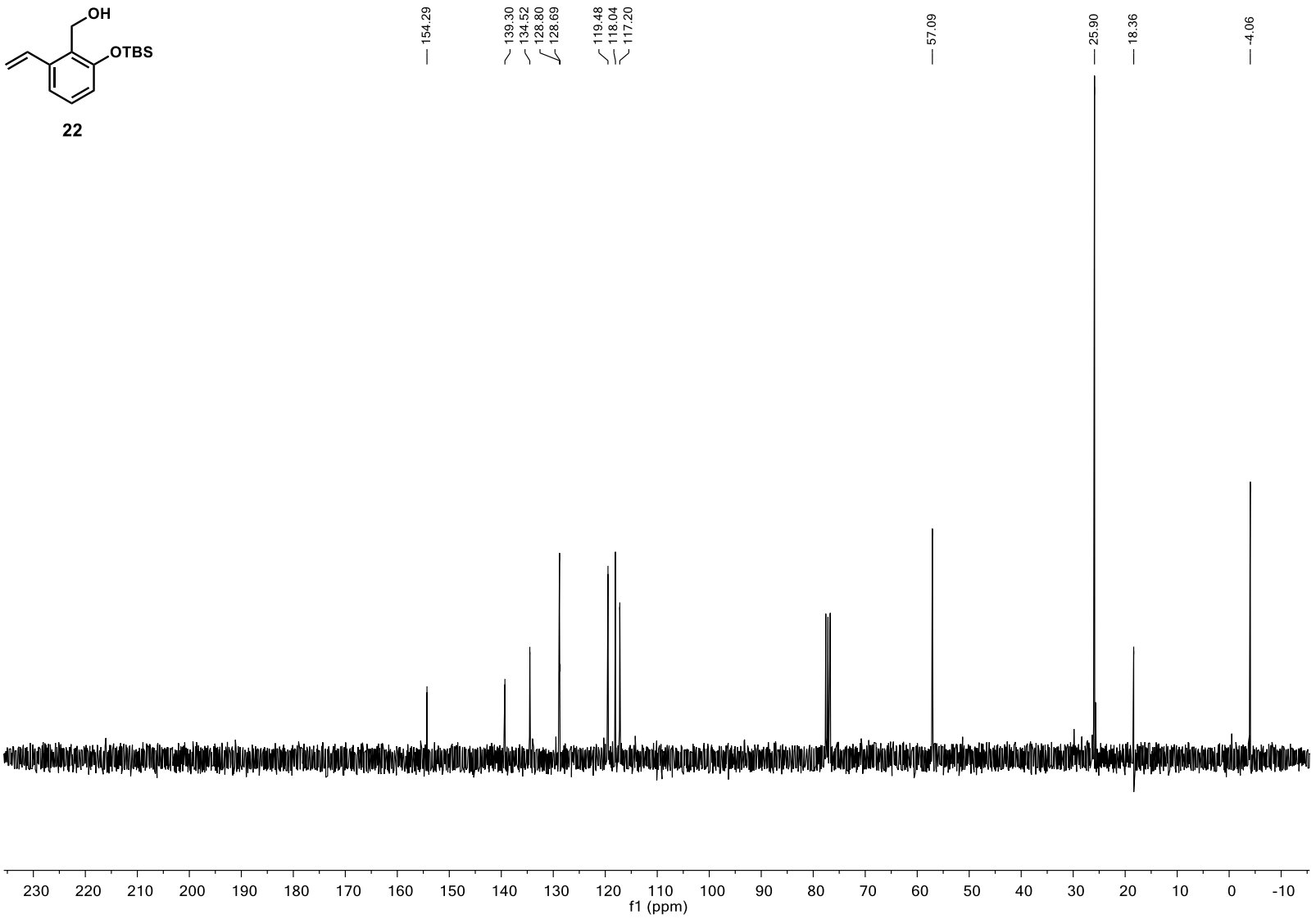
OH
OTBS
22
154.29
139.30
134.52
128.80
128.69
119.48
118.04
117.20
57.09
25.90
18.36
-4.06
230 220 210 200 190 180 170 160 150 140 130 120 110 100 90 80 70 60 50 40 30 20 10 0 -10
f1 (ppm)

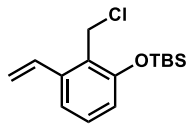
Cl
OTBS

11

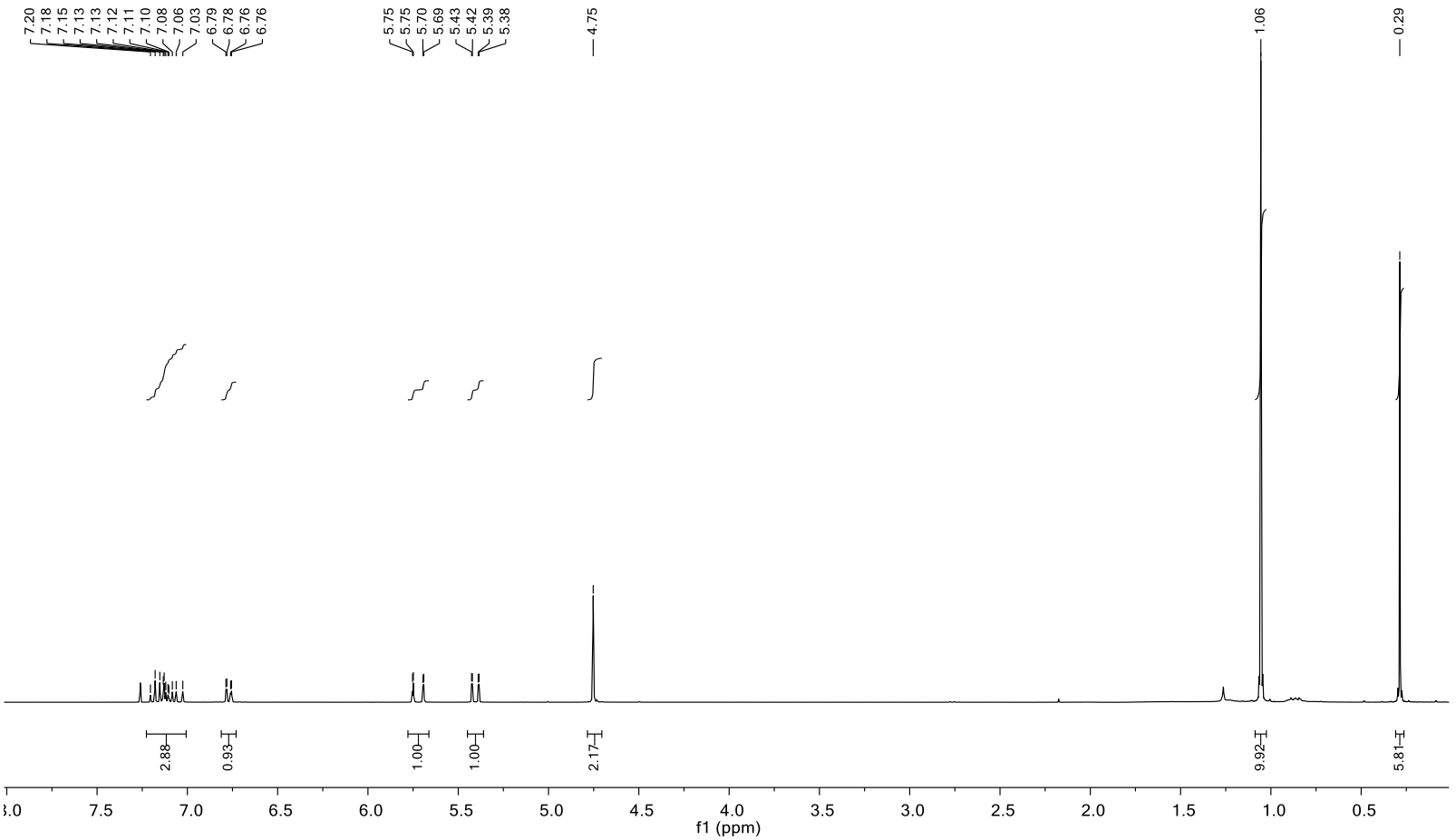
7.20
7.18
7.15
7.13
7.13
7.12
7.11
7.10
7.08
7.06
7.03
6.79
6.78
6.76
6.76
5.75
5.75
5.70
5.69
5.43
5.42
5.39
5.38
4.75
1.06
0.29
2.88
0.93
1.00
1.00
2.17
9.92
5.81
f1 (ppm)

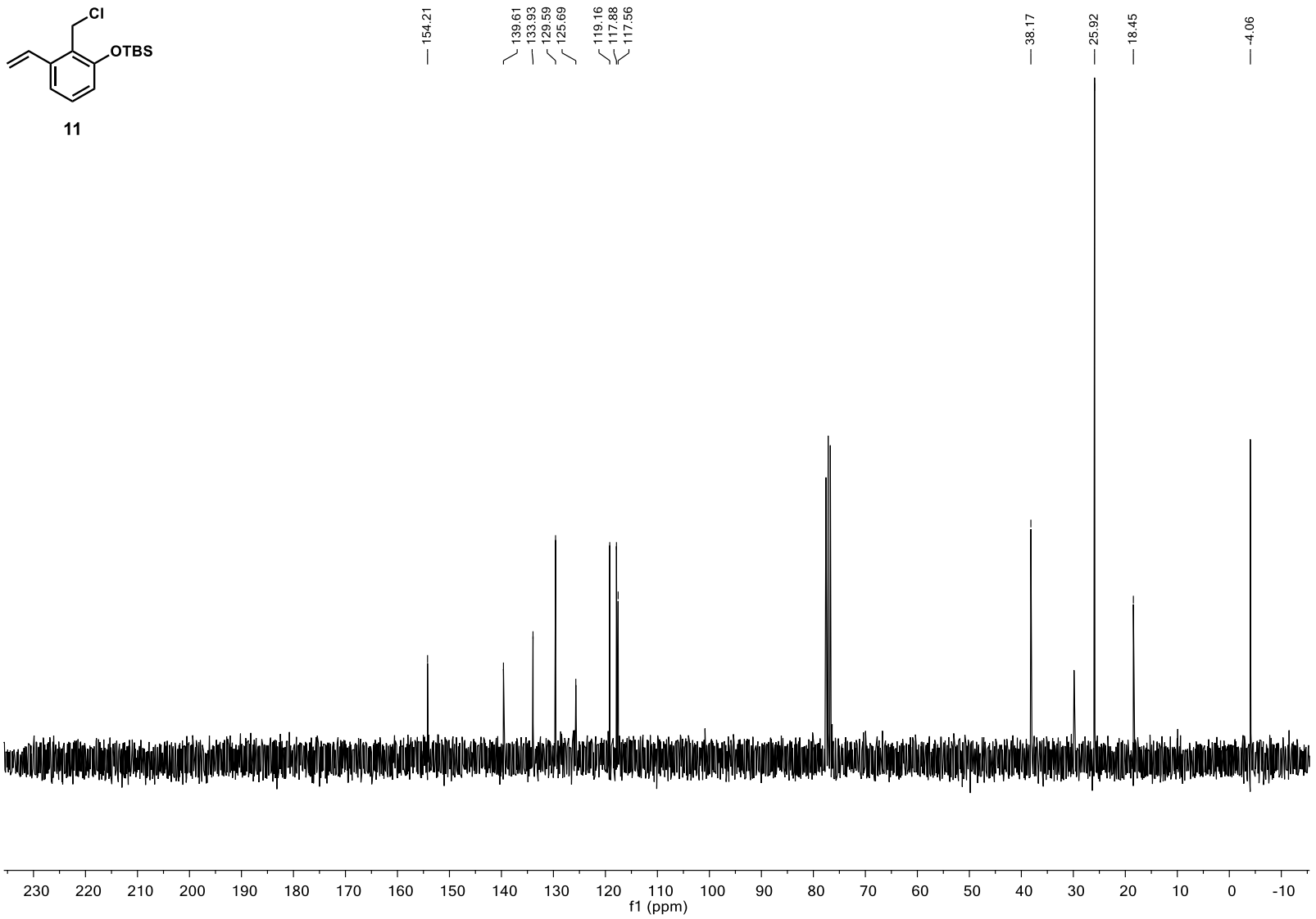
Cl
OTBS
11
154.21
139.61
133.93
129.59
125.69
119.16
117.88
117.56
38.17
25.92
18.45
-4.06
230 220 210 200 190 180 170 160 150 140 130 120 110 100 90 80 70 60 50 40 30 20 10 0 -10
f1 (ppm)

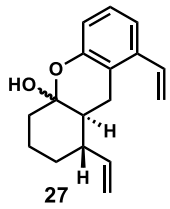
HO
O
H
H

27

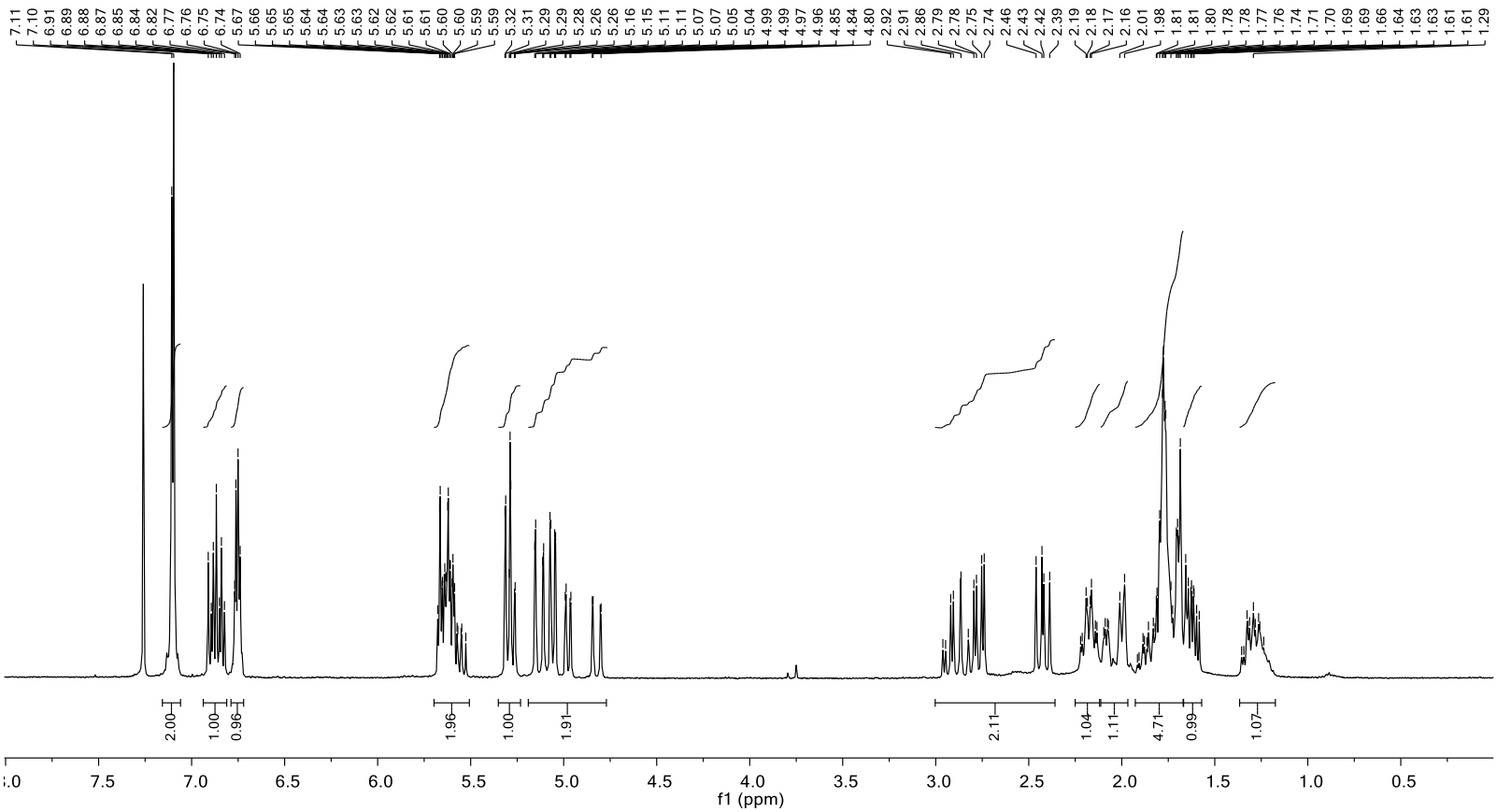
7.11 7.10 6.91 6.89 6.88 6.87 6.85 6.84 6.82 6.77 6.76 6.75 6.74 5.67 5.66 5.65 5.65 5.64 5.64 5.63 5.63 5.62 5.62 5.61 5.61 5.60 5.60 5.59 5.59 5.32 5.31 5.29 5.29 5.28 5.26 5.26 5.16 5.15 5.11 5.11 5.07 5.07 5.05 5.04 4.99 4.99 4.97 4.96 4.85 4.84 4.80 2.92 2.91 2.86 2.79 2.78 2.75 2.74 2.46 2.43 2.42 2.39 2.19 2.18 2.17 2.16 2.01 1.98 1.81 1.81 1.80 1.78 1.78 1.77 1.76 1.74 1.71 1.70 1.69 1.69 1.66 1.64 1.63 1.63 1.61 1.61 1.29
2.00
1.00
0.96
1.96
1.00
1.91
2.11
1.04
1.11
4.71
0.99
1.07
7.5
7.0
6.5
6.0
5.5
5.0
4.5
4.0
3.5
3.0
2.5
2.0
1.5
1.0
0.5
f1 (ppm)

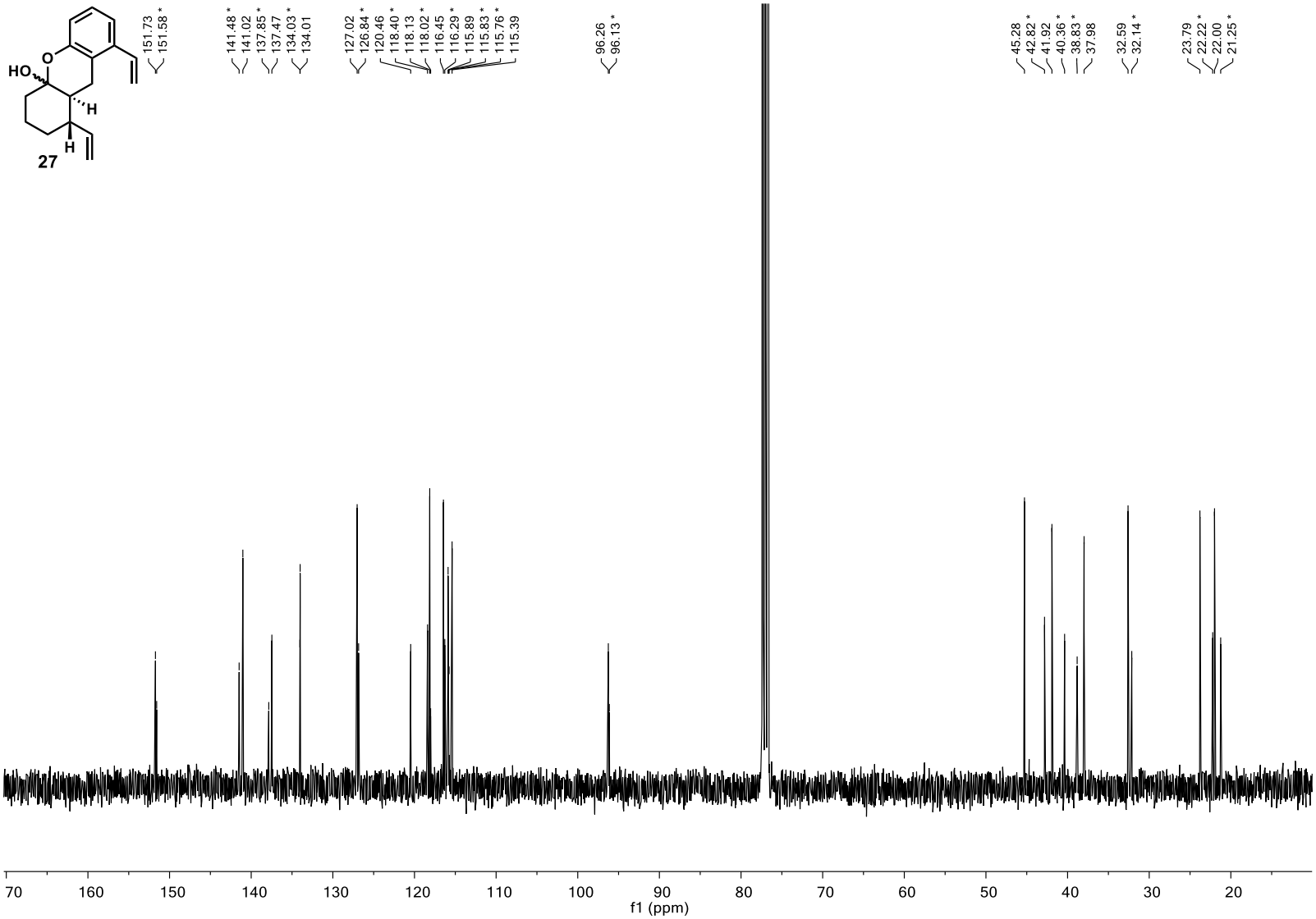
HO
O
H
H
27
151.73
151.58 *
141.48 *
141.02
137.85 *
137.47
134.03 *
134.01
127.02
126.84 *
120.46
118.40 *
118.13
118.02 *
116.45
116.29 *
115.89
115.83 *
115.76 *
115.39
96.26
96.13 *
45.28
42.82 *
41.92
40.36 *
38.83 *
37.98
32.59
32.14 *
23.79
22.22 *
22.00
21.25 *
70
160
150
140
130
120
110
100
90
80
70
60
50
40
30
20
f1 (ppm)

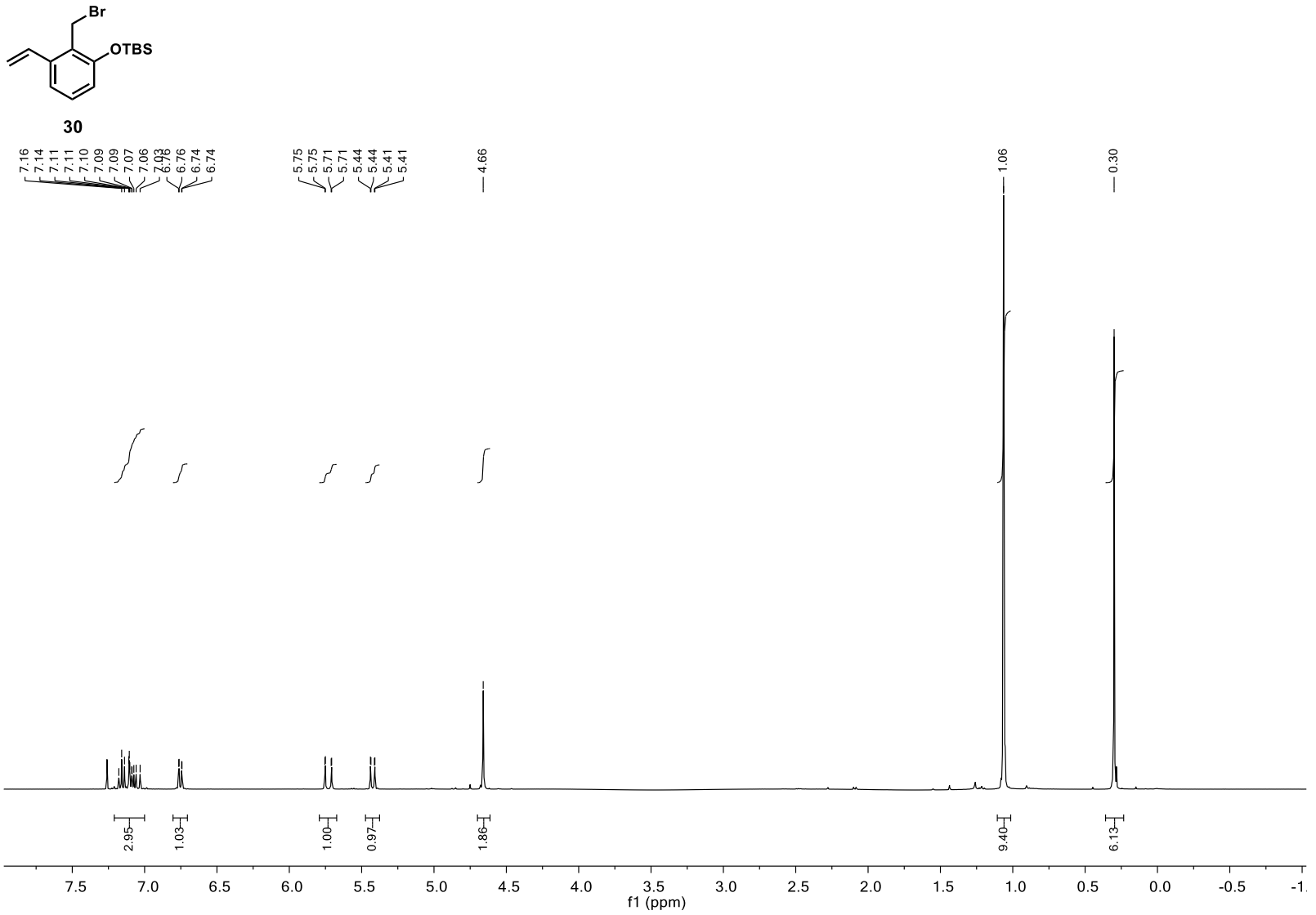
Br
OTBS
30
7.16
7.14
7.11
7.11
7.10
7.09
7.09
7.07
7.06
7.03
6.76
6.74
6.74
5.75
5.75
5.71
5.71
5.44
5.44
5.41
5.41
4.66
1.06
0.30
2.95
1.03
1.00
0.97
1.86
9.40
6.13
7.5
7.0
6.5
6.0
5.5
5.0
4.5
4.0
3.5
3.0
2.5
2.0
1.5
1.0
0.5
0.0
-0.5
f1 (ppm)

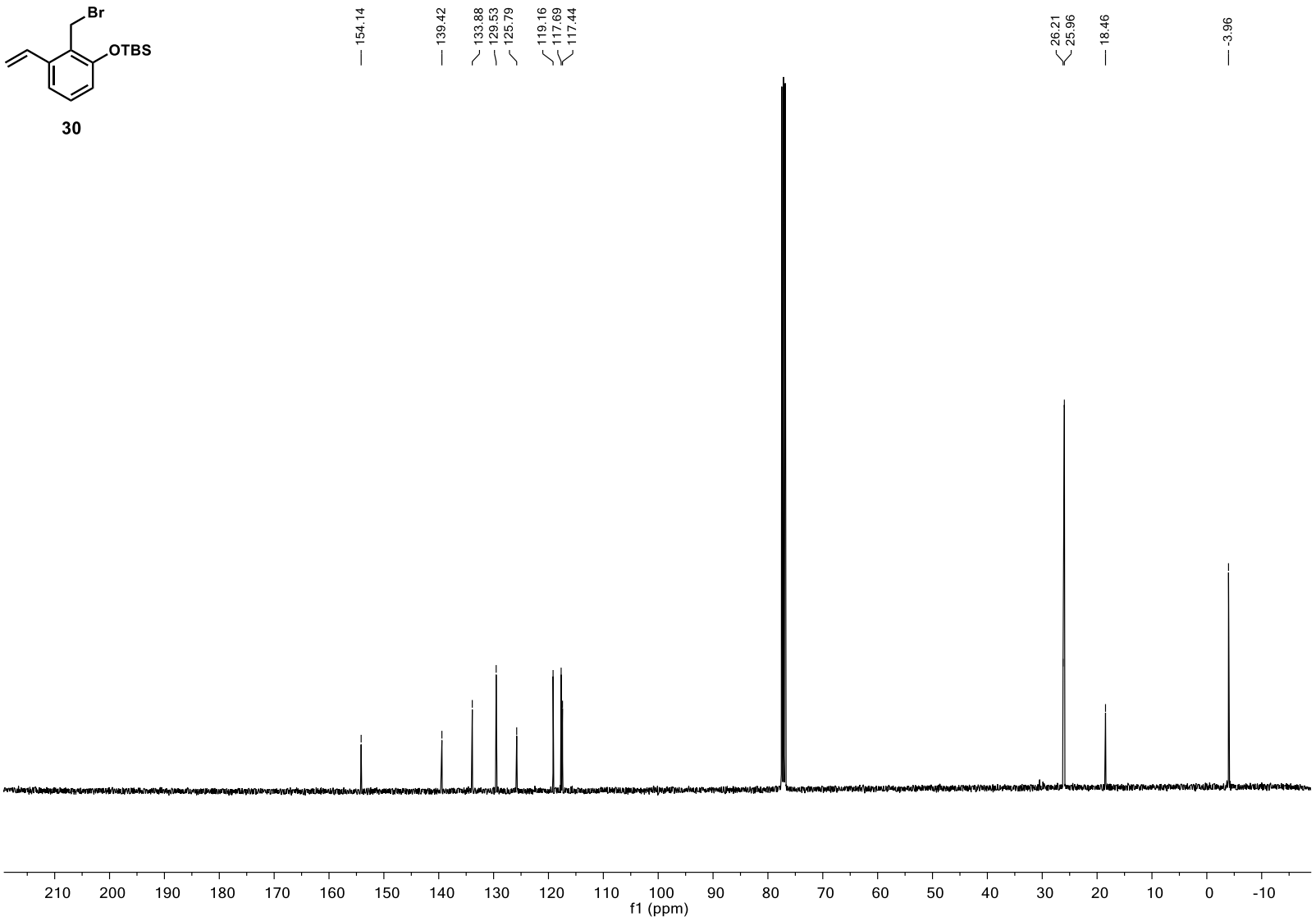
Br
OTBS
30
154.14
139.42
133.88
129.53
125.79
119.16
117.69
117.44
26.21
25.96
18.46
-3.96
210 200 190 180 170 160 150 140 130 120 110 100 90 80 70 60 50 40 30 20 10 0 -10
f1 (ppm)

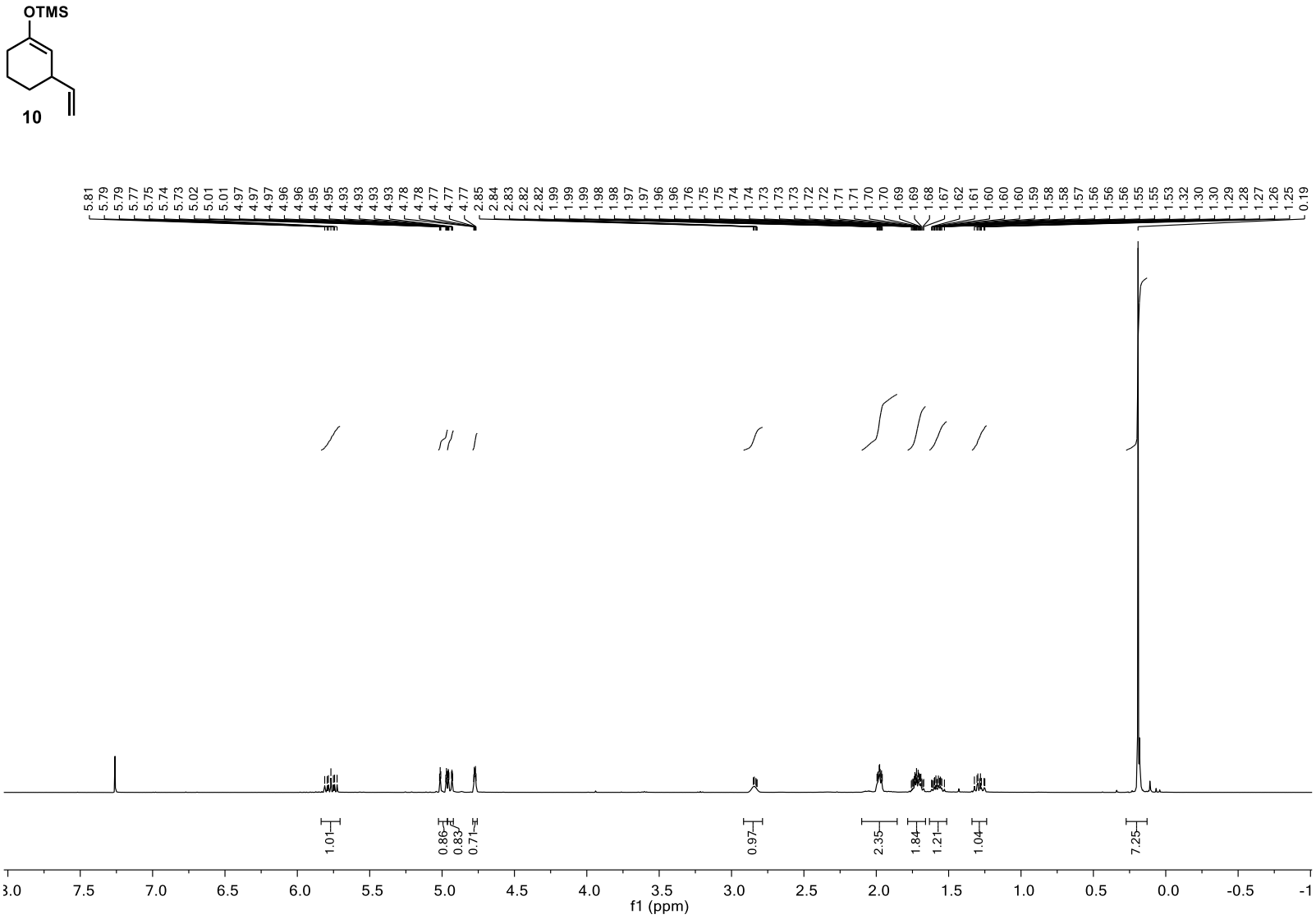
OTMS
10
5.81 5.79 5.79 5.77 5.75 5.74 5.73 5.02 5.01 5.01 4.97 4.97 4.97 4.96 4.96 4.95 4.95 4.93 4.93 4.93 4.93 4.78 4.78 4.77 4.77 4.77 2.85 2.84 2.83 2.82 2.82 1.99 1.99 1.99 1.98 1.98 1.97 1.97 1.96 1.96 1.76 1.75 1.75 1.74 1.74 1.73 1.73 1.73 1.72 1.72 1.71 1.71 1.70 1.70 1.69 1.69 1.68 1.67 1.62 1.61 1.60 1.60 1.60 1.59 1.58 1.58 1.57 1.56 1.56 1.56 1.55 1.55 1.53 1.32 1.30 1.30 1.29 1.28 1.27 1.26 1.25 0.19
1.01
0.86
0.83
0.71
0.97
2.35
1.84
1.21
1.04
7.25
3.0 7.5 7.0 6.5 6.0 5.5 5.0 4.5 4.0 3.5 3.0 2.5 2.0 1.5 1.0 0.5 0.0 -0.5 -1
f1 (ppm)

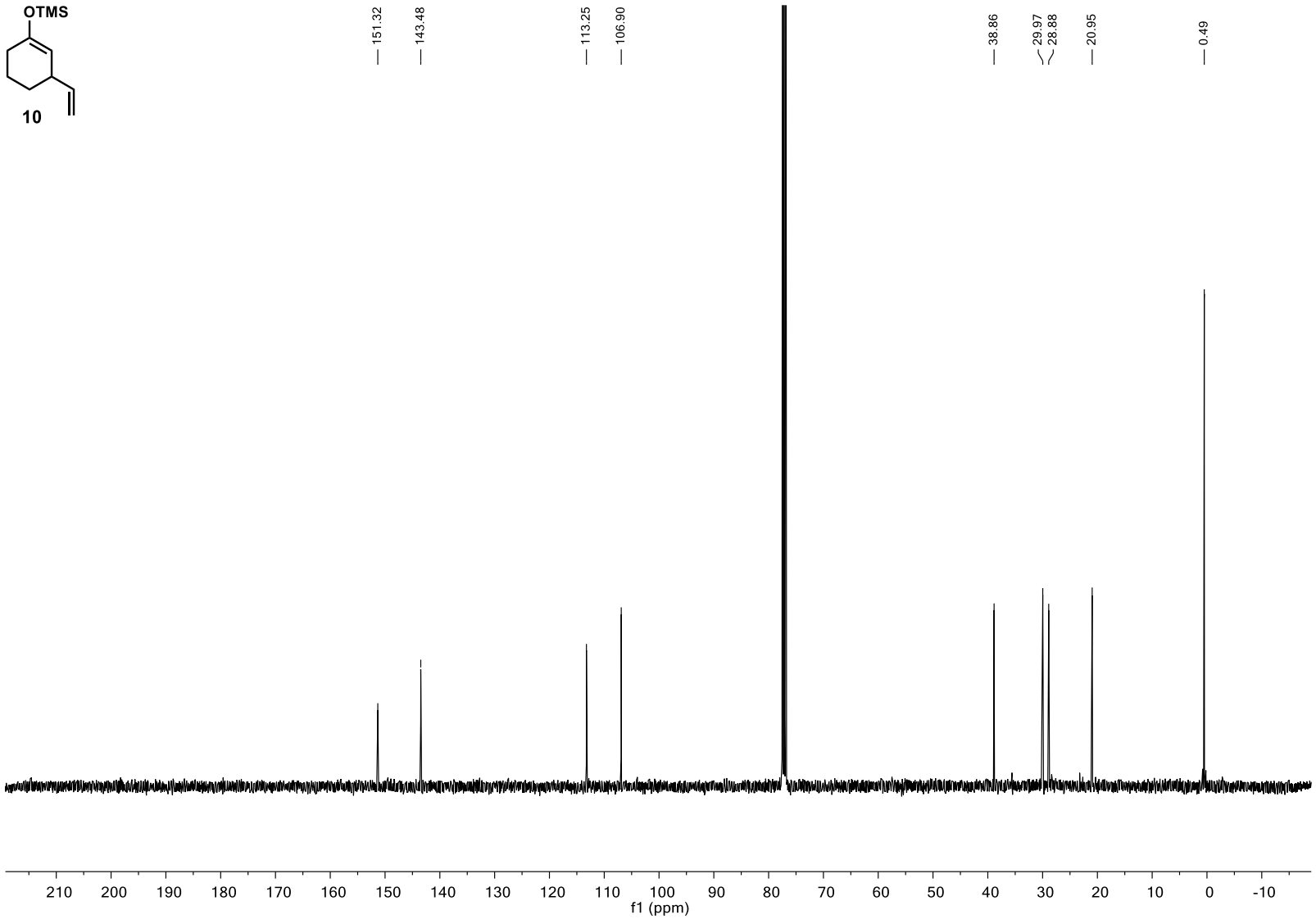
OTMS
10
151.32
143.48
113.25
106.90
38.86
29.97
28.88
20.95
0.49
210 200 190 180 170 160 150 140 130 120 110 100 90 80 70 60 50 40 30 20 10 0 -10
f1 (ppm)

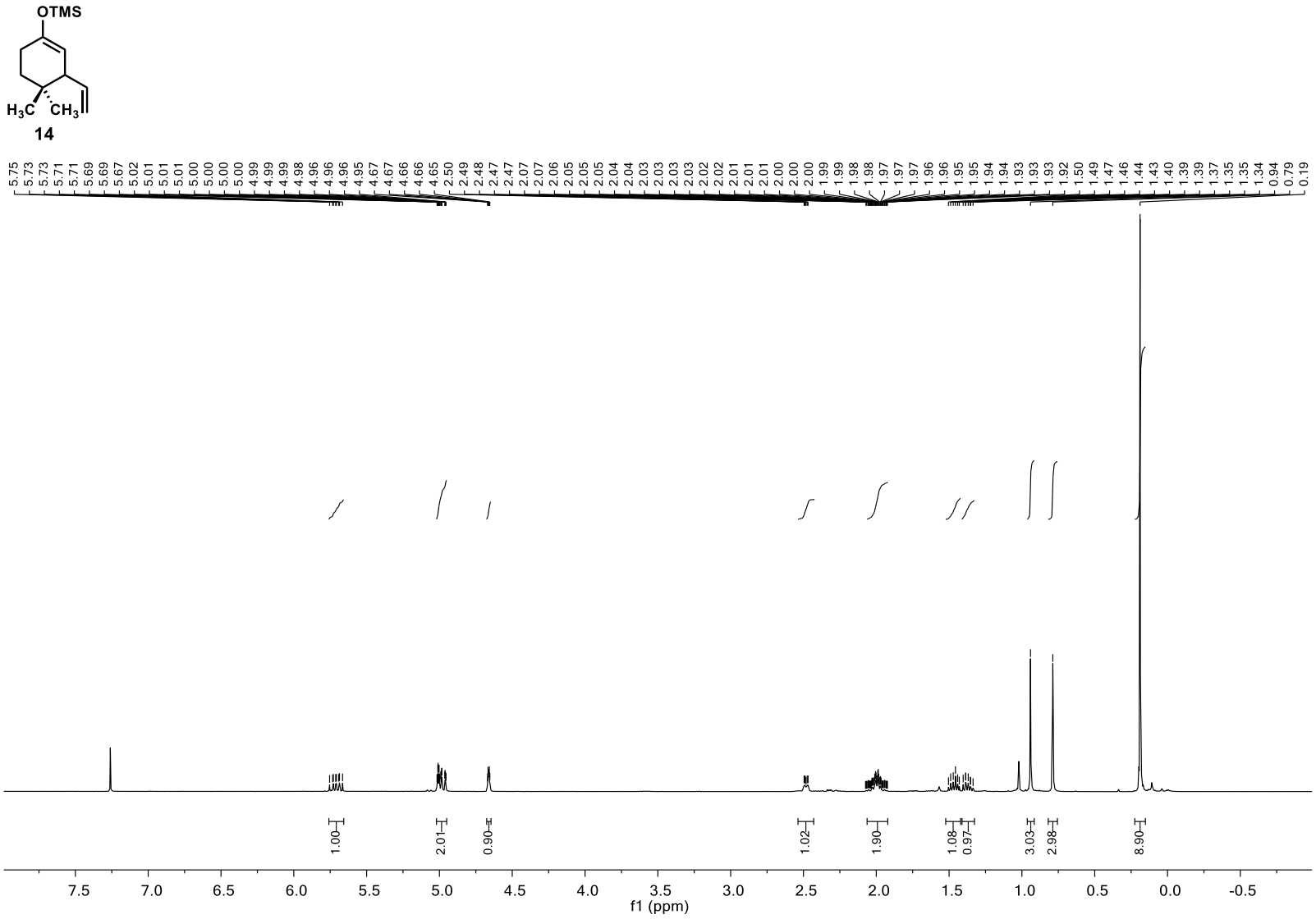
OTMS
H3C
CH3
14
f1 (ppm)

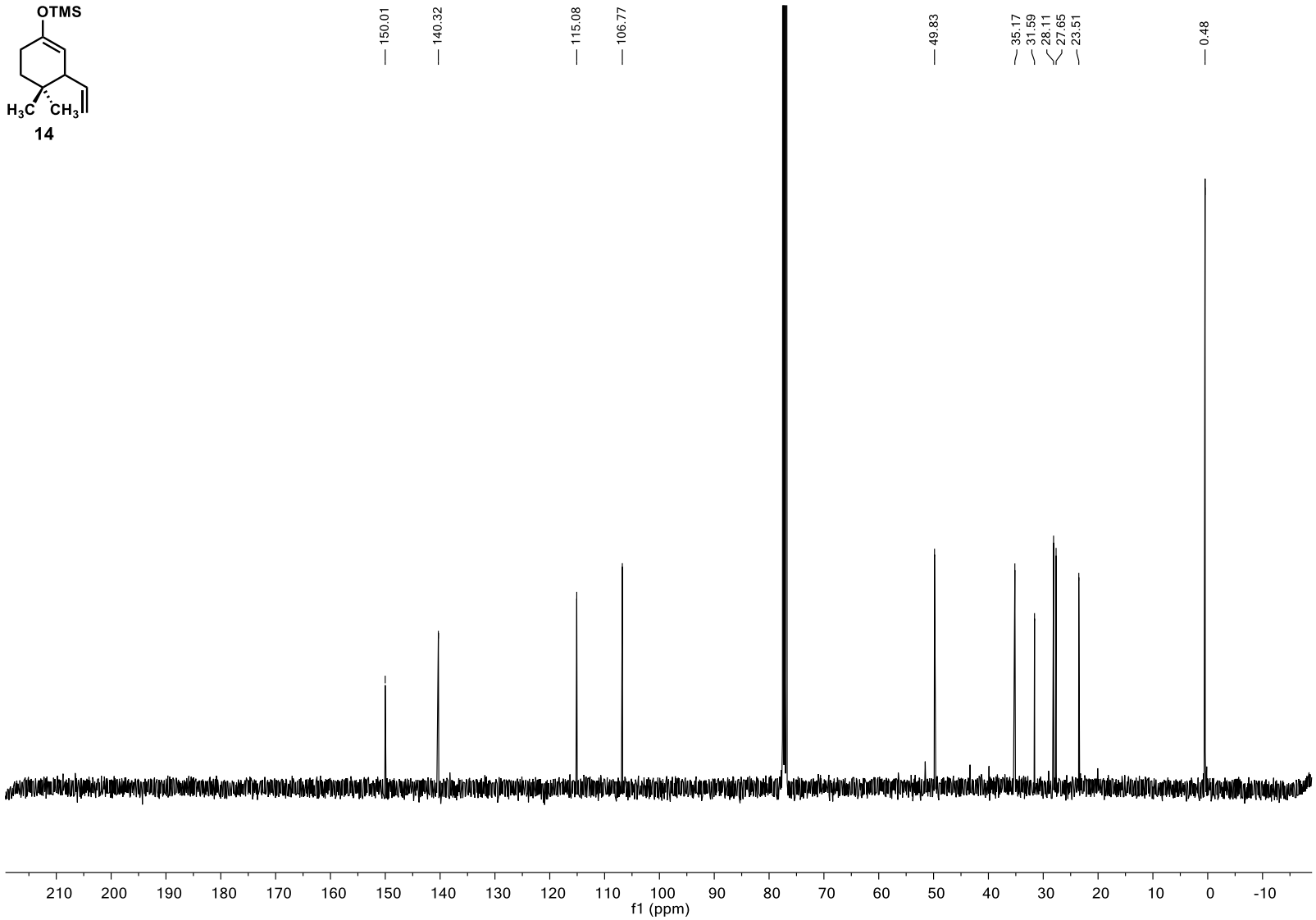
OTMS
H3C CH3
14
150.01
140.32
115.08
106.77
49.83
35.17
31.59
28.11
27.65
23.51
0.48
210 200 190 180 170 160 150 140 130 120 110 100 90 80 70 60 50 40 30 20 10 0 -10
f1 (ppm)

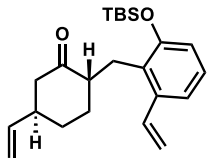
TBSO
O
H
H

31

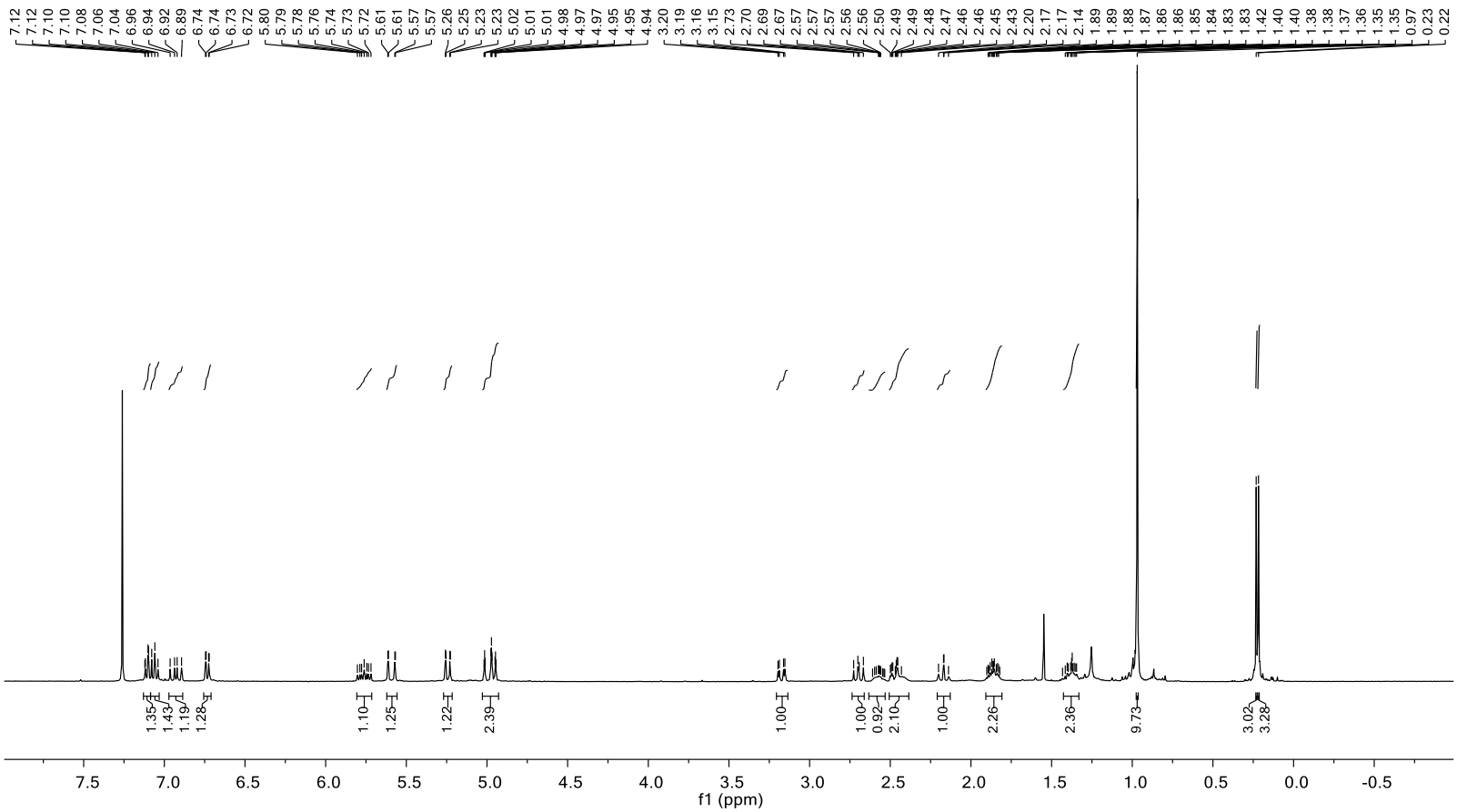
7.12 7.12 7.10 7.10 7.08 7.06 7.04 6.96 6.94 6.92 6.89 6.74 6.74 6.73 6.72 5.80 5.79 5.78 5.76 5.74 5.73 5.72 5.61 5.61 5.57 5.57 5.26 5.25 5.23 5.23 5.02 5.01 5.01 4.98 4.97 4.97 4.95 4.95 4.94 3.20 3.19 3.16 3.15 2.73 2.70 2.69 2.67 2.57 2.57 2.57 2.56 2.56 2.50 2.49 2.49 2.48 2.47 2.46 2.46 2.45 2.43 2.20 2.17 2.17 2.14 1.89 1.89 1.88 1.87 1.86 1.86 1.85 1.84 1.83 1.83 1.42 1.40 1.40 1.38 1.38 1.37 1.36 1.35 1.35 0.97 0.23 0.22
1.35 1.43 1.19 1.28 1.10 1.25 1.22 2.39 1.00 1.00 0.92 2.10 1.00 2.26 2.36 9.73 3.02 3.28
7.5 7.0 6.5 6.0 5.5 5.0 4.5 4.0 3.5 3.0 2.5 2.0 1.5 1.0 0.5 0.0 -0.5
f1 (ppm)

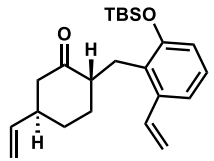
TBSO
O
H
H

31

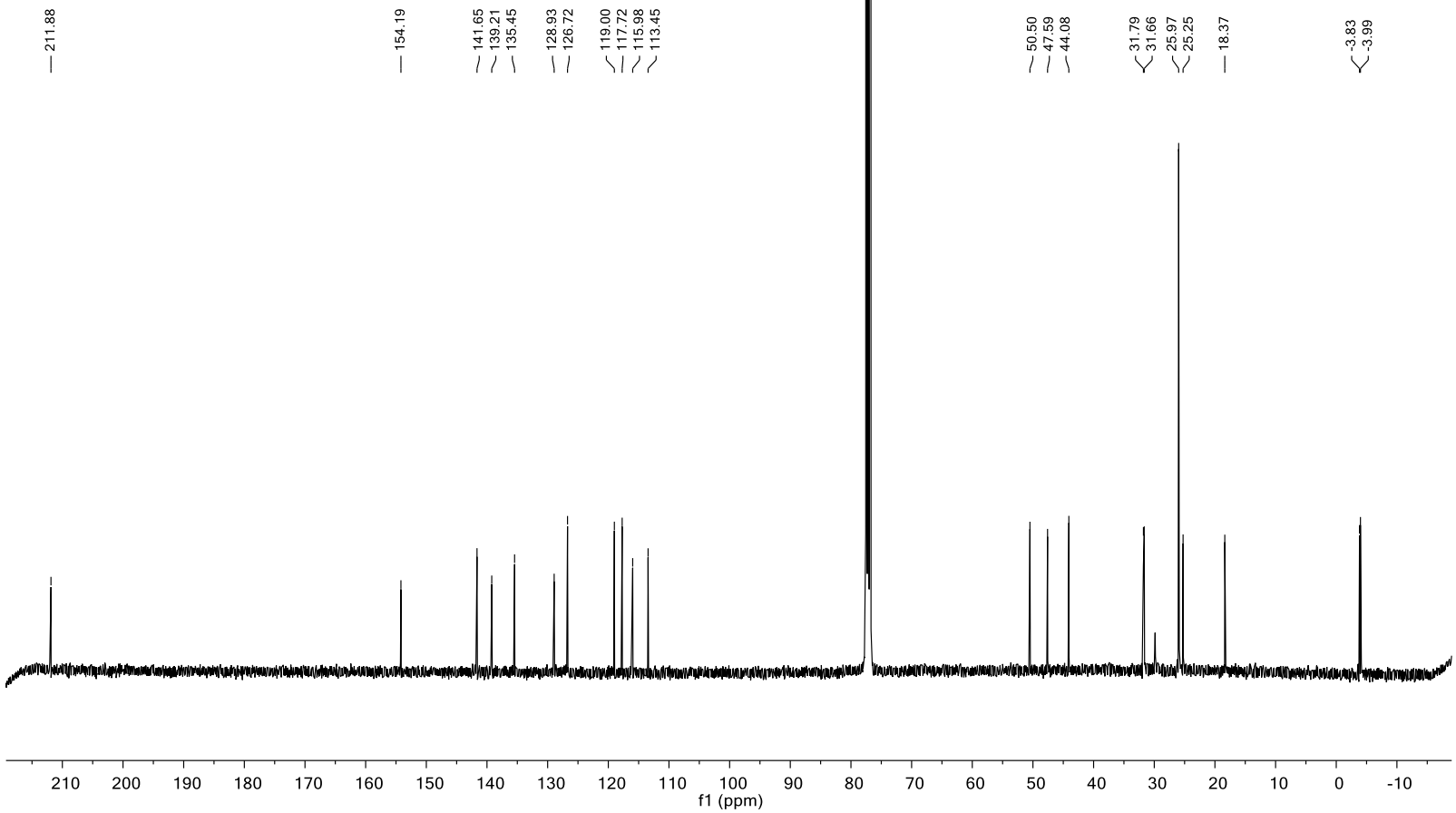
211.88
154.19
141.65
139.21
135.45
128.93
126.72
119.00
117.72
115.98
113.45
50.50
47.59
44.08
31.79
31.66
25.97
25.25
18.37
-3.83
-3.99
210 200 190 180 170 160 150 140 130 120 110 100 90 80 70 60 50 40 30 20 10 0 -10
f1 (ppm)

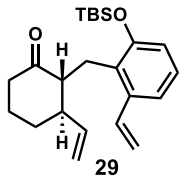
TBSO
O
H
H

29

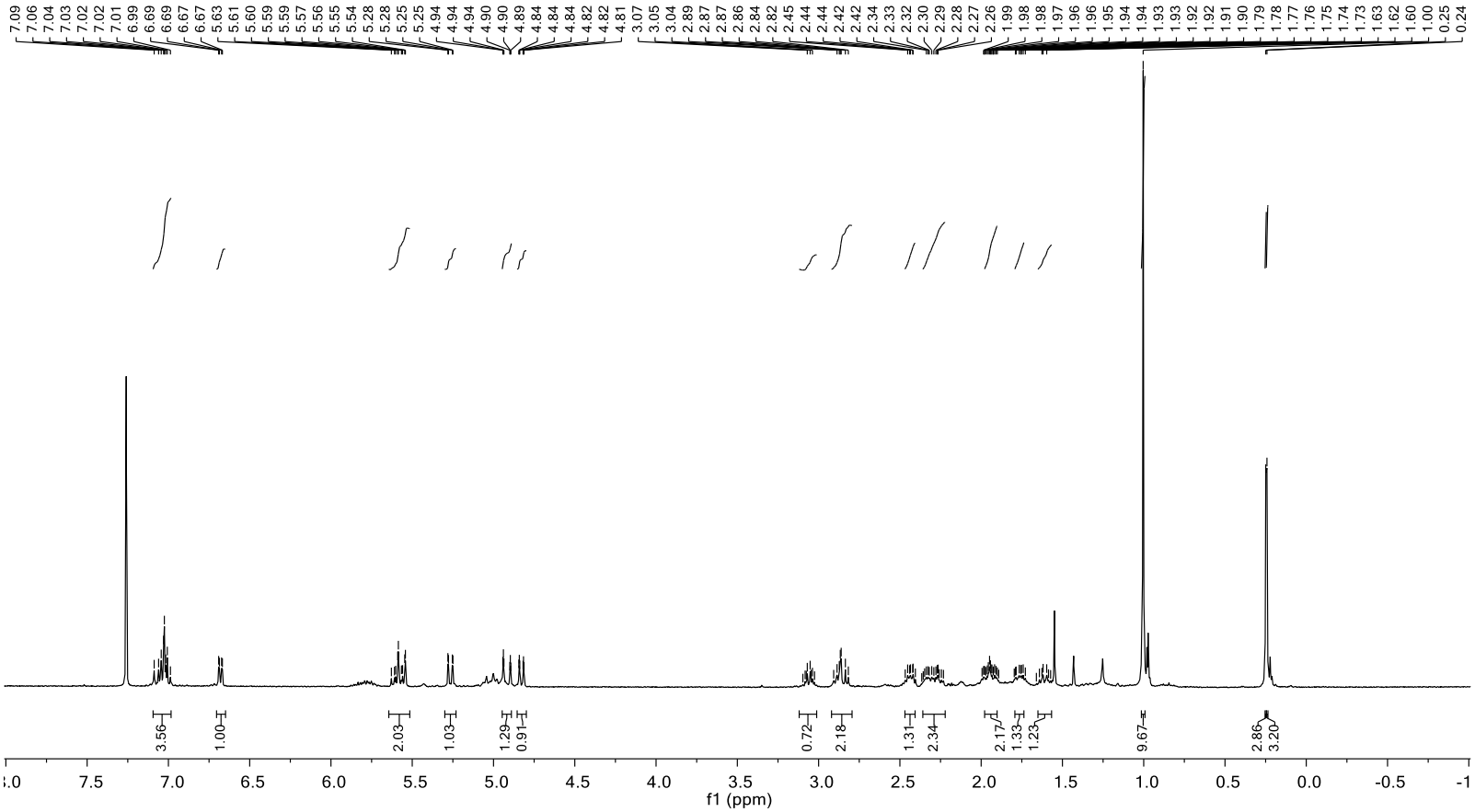
7.09 7.06 7.04 7.03 7.02 7.02 7.01 6.99 6.69 6.69 6.67 6.67 5.63 5.61 5.60 5.59 5.59 5.57 5.56 5.55 5.54 5.28 5.28 5.25 5.25 4.94 4.94 4.94 4.90 4.90 4.89 4.84 4.84 4.84 4.82 4.82 4.81 3.07 3.05 3.04 2.89 2.87 2.87 2.86 2.84 2.82 2.45 2.44 2.44 2.42 2.42 2.34 2.33 2.32 2.30 2.29 2.28 2.27 2.26 1.99 1.98 1.98 1.97 1.96 1.96 1.95 1.94 1.94 1.93 1.93 1.92 1.92 1.91 1.90 1.79 1.78 1.77 1.76 1.75 1.74 1.73 1.63 1.62 1.60 1.00 0.25 0.24
3.56 1.00 2.03 1.03 1.29 0.91 0.72 2.18 1.31 2.34 2.17 1.33 1.23 9.67 2.86 3.20
f1 (ppm)

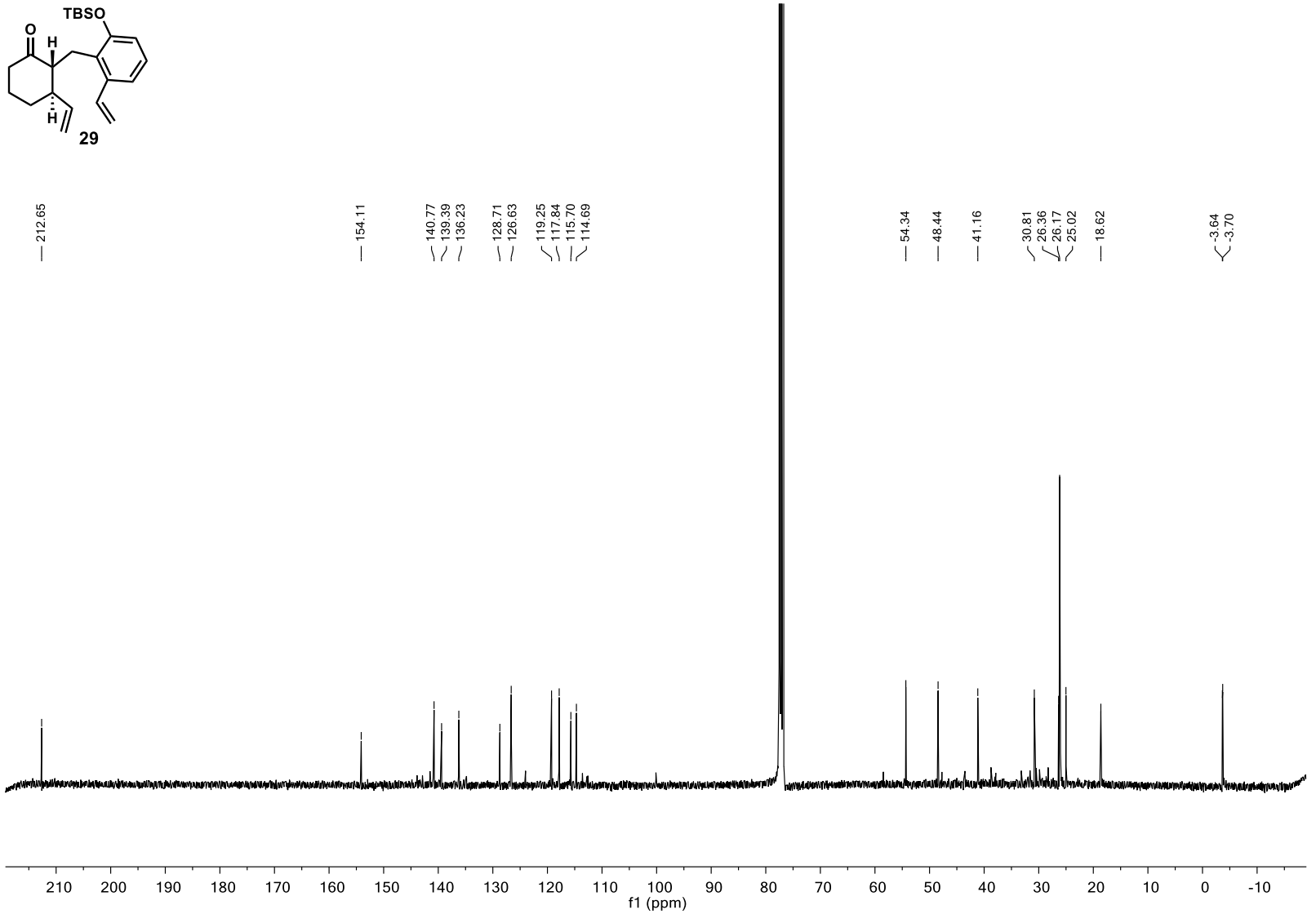
TBSO
O
H
H
29
212.65
154.11
140.77
139.39
136.23
128.71
126.63
119.25
117.84
115.70
114.69
54.34
48.44
41.16
30.81
26.36
26.17
25.02
18.62
-3.64
-3.70
210 200 190 180 170 160 150 140 130 120 110 100 90 80 70 60 50 40 30 20 10 0 -10
f1 (ppm)

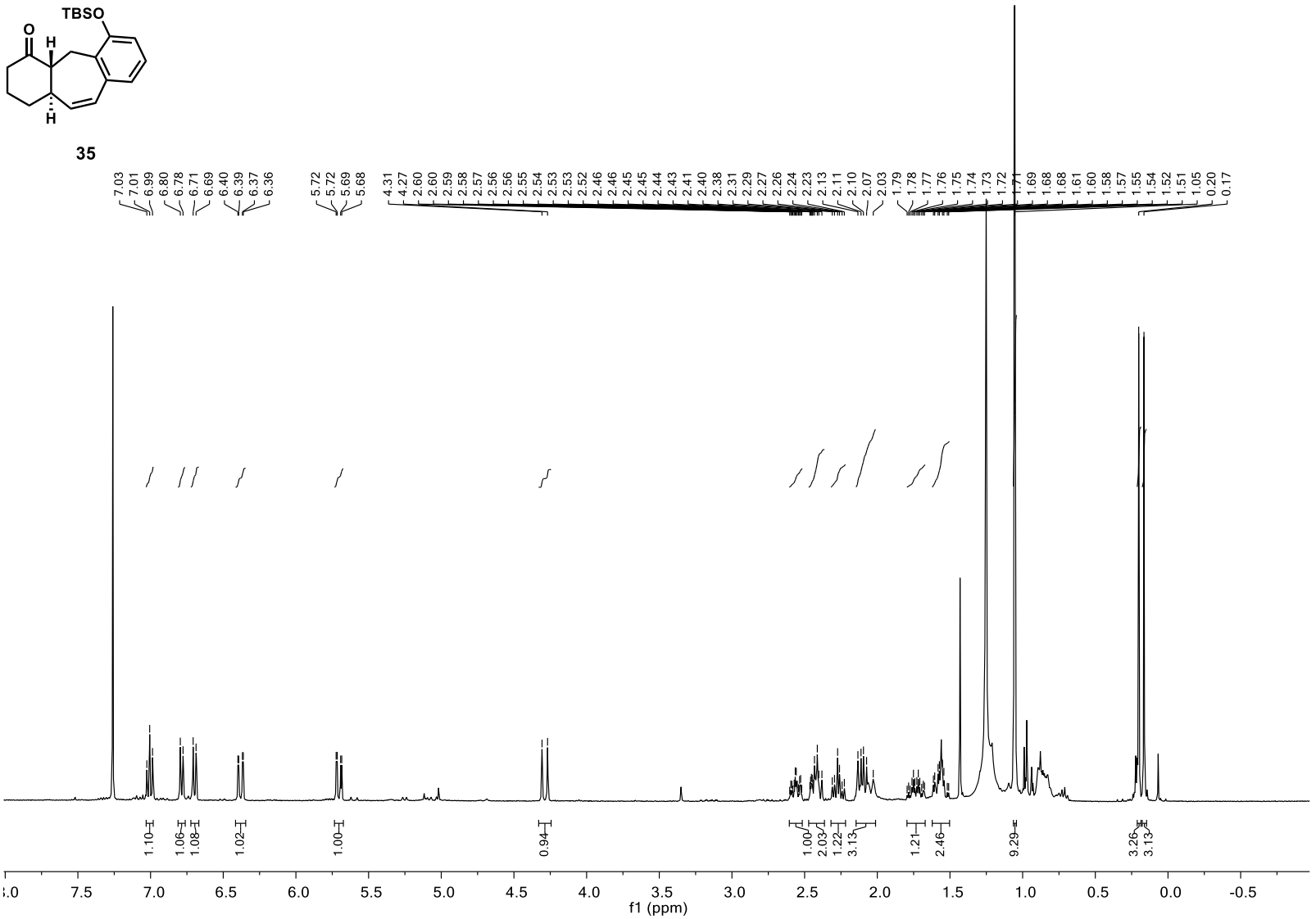
TBSO
O
H
H
35
7.03
7.01
6.99
6.80
6.78
6.71
6.69
6.40
6.39
6.37
6.36
5.72
5.72
5.69
5.68
4.31
4.27
2.60
2.60
2.59
2.58
2.57
2.56
2.56
2.55
2.54
2.53
2.53
2.52
2.46
2.46
2.45
2.45
2.44
2.43
2.41
2.40
2.38
2.31
2.29
2.27
2.26
2.24
2.23
2.13
2.11
2.10
2.07
2.03
1.79
1.78
1.77
1.76
1.75
1.74
1.73
1.72
1.71
1.69
1.68
1.68
1.61
1.60
1.58
1.57
1.55
1.54
1.52
1.51
1.05
0.20
0.17
1.10
1.06
1.08
1.02
1.00
0.94
1.00
2.03
1.22
3.13
1.21
2.46
9.29
3.26
3.13
7.5
7.0
6.5
6.0
5.5
5.0
4.5
4.0
3.5
3.0
2.5
2.0
1.5
1.0
0.5
0.0
-0.5
f1 (ppm)

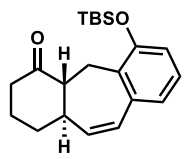
TBSO
O
H
H

35

210.64
152.45
137.05
134.58
130.69
129.30
126.37
124.55
118.55
54.43
50.47
41.24
33.08
26.51
25.93
24.08
18.40
-4.17
-4.22
210 200 190 180 170 160 150 140 130 120 110 100 90 80 70 60 50 40 30 20 10 0 -10
f1 (ppm)

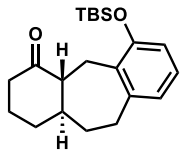
TBSO
O
H
H

37

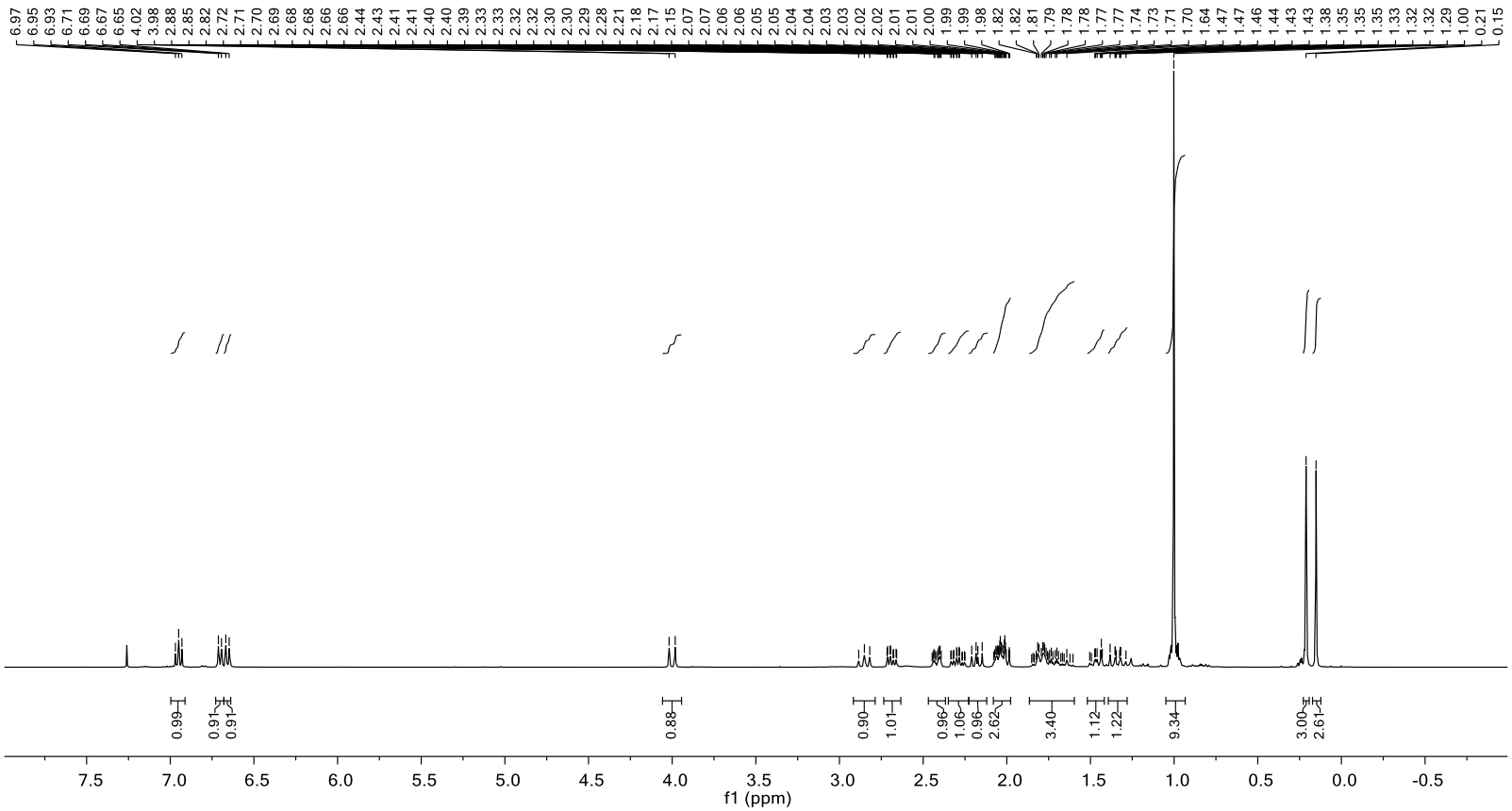
6.97 6.95 6.93 6.71 6.69 6.67 6.65 4.02 3.98 2.88 2.85 2.82 2.72 2.71 2.70 2.69 2.68 2.68 2.66 2.66 2.44 2.43 2.41 2.41 2.40 2.40 2.39 2.33 2.32 2.32 2.30 2.30 2.29 2.28 2.21 2.18 2.17 2.15 2.07 2.07 2.06 2.06 2.05 2.05 2.04 2.04 2.03 2.03 2.02 2.02 2.01 2.01 2.00 1.99 1.99 1.98 1.82 1.82 1.81 1.79 1.78 1.78 1.77 1.77 1.74 1.73 1.71 1.70 1.64 1.47 1.47 1.46 1.44 1.43 1.43 1.38 1.35 1.35 1.35 1.33 1.32 1.32 1.29 1.00 0.21 0.15
0.99 0.91 0.91 0.88 0.90 1.01 0.96 1.06 0.96 2.62 3.40 1.12 1.22 9.34 3.00 2.61
7.5 7.0 6.5 6.0 5.5 5.0 4.5 4.0 3.5 3.0 2.5 2.0 1.5 1.0 0.5 0.0 -0.5
f1 (ppm)

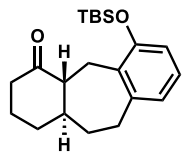
TBSO
O
H
H

37

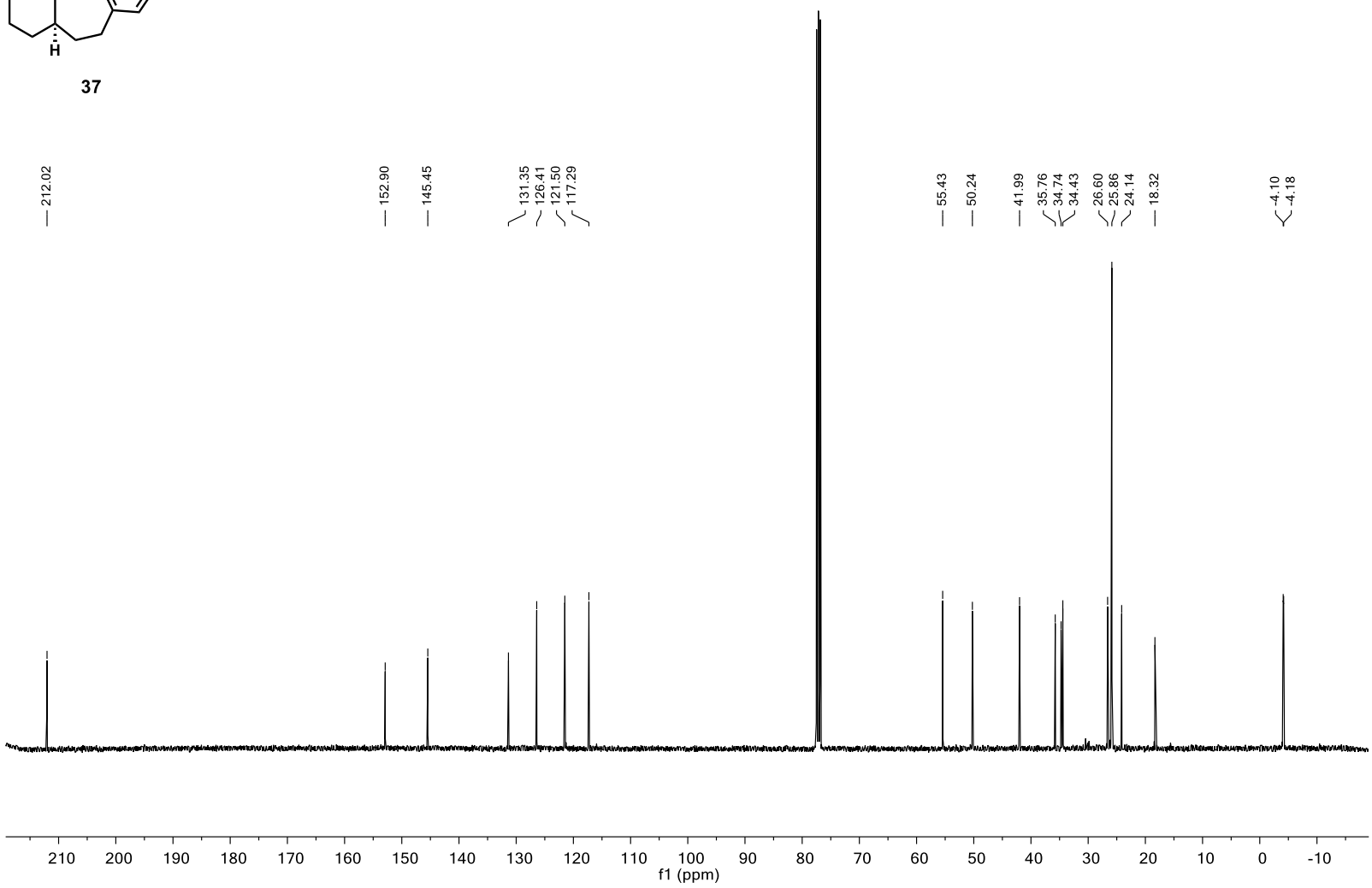
212.02
152.90
145.45
131.35
126.41
121.50
117.29
55.43
50.24
41.99
35.76
34.74
34.43
26.60
25.86
24.14
18.32
-4.10
-4.18
210 200 190 180 170 160 150 140 130 120 110 100 90 80 70 60 50 40 30 20 10 0 -10
f1 (ppm)

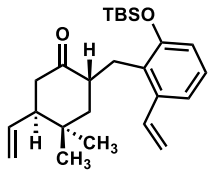
TBSO
O
H
H
CH3
CH3

33

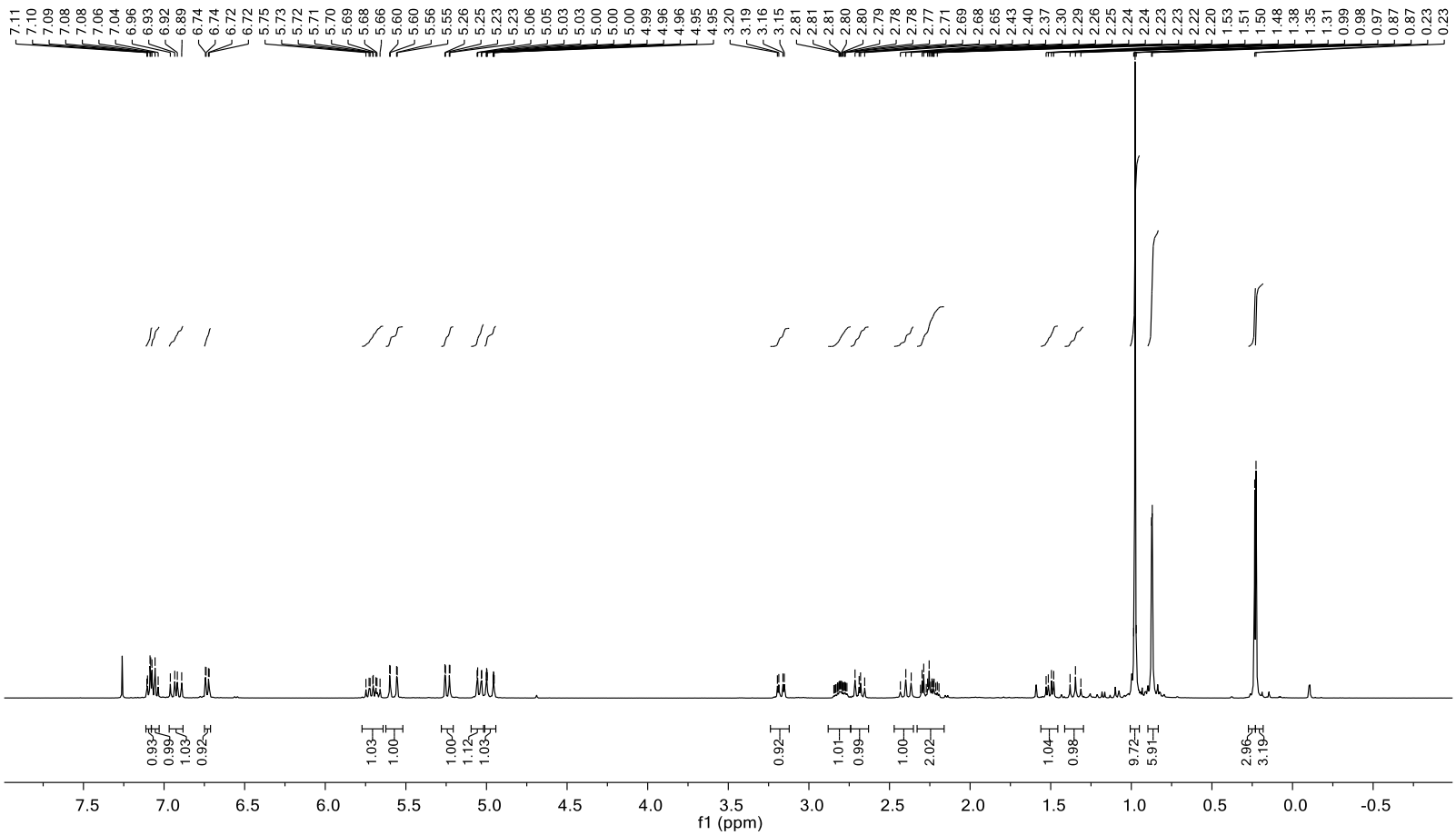
7.11 7.10 7.09 7.08 7.08 7.06 7.04 6.96 6.93 6.92 6.89 6.74 6.74 6.72 6.72 5.75 5.73 5.72 5.71 5.70 5.69 5.68 5.66 5.60 5.60 5.56 5.55 5.26 5.25 5.23 5.23 5.06 5.05 5.03 5.03 5.00 5.00 5.00 4.99 4.96 4.96 4.95 4.95 3.20 3.19 3.16 3.15 2.81 2.81 2.81 2.80 2.80 2.79 2.78 2.78 2.77 2.71 2.69 2.68 2.65 2.43 2.40 2.37 2.30 2.29 2.26 2.25 2.24 2.24 2.23 2.23 2.22 2.20 1.53 1.51 1.50 1.48 1.38 1.35 1.31 0.99 0.98 0.97 0.87 0.87 0.23 0.23
0.93 0.99 1.03 0.92 1.03 1.00 1.00 1.12 1.03 0.92 1.01 0.99 1.00 2.02 1.04 0.98 9.72 5.91 2.96 3.19
7.5 7.0 6.5 6.0 5.5 5.0 4.5 4.0 3.5 3.0 2.5 2.0 1.5 1.0 0.5 0.0 -0.5
f1 (ppm)

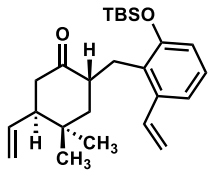
TBSO
O
H
H
CH3
CH3

33

212.15
154.14
139.29
138.21
135.61
128.68
126.66
119.03
117.55
116.10
115.95
52.72
46.89
46.83
43.61
33.64
29.33
25.99
25.15
19.25
18.37
-3.85
-3.96
210 200 190 180 170 160 150 140 130 120 110 100 90 80 70 60 50 40 30 20 10 0 -10
f1 (ppm)

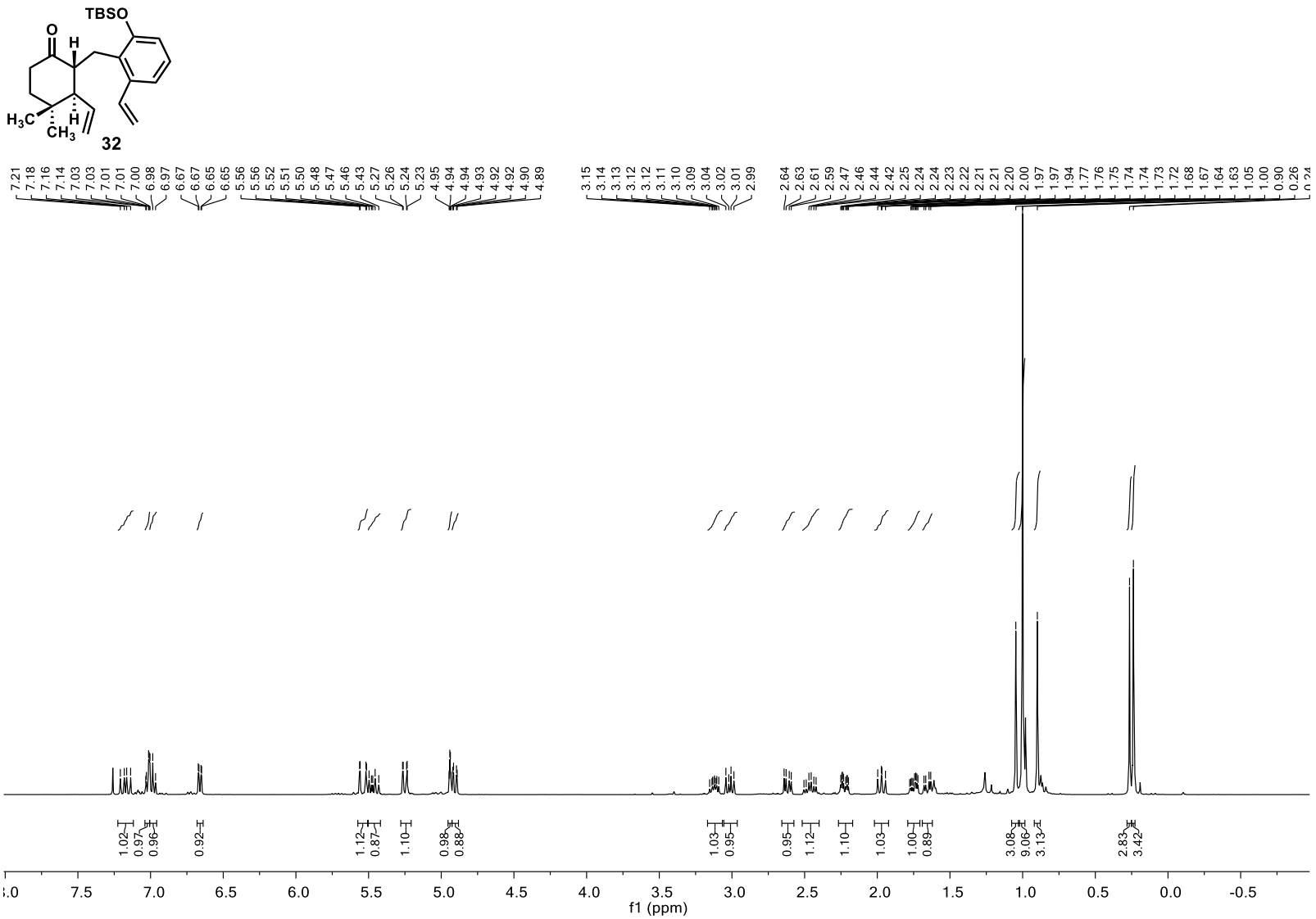
TBSO
O
H
H3C
CH3
H
32
f1 (ppm)

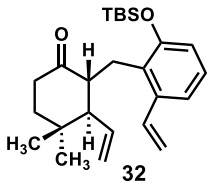
TBSO
O
H
H3C
CH3
H

32

212.39
154.04
139.65
137.12
137.08
129.45
126.23
119.21
117.73
117.39
115.04
60.46
49.64
41.81
38.83
33.93
29.83
26.23
26.08
20.53
18.69
-3.42
-3.67
210 200 190 180 170 160 150 140 130 120 110 100 90 80 70 60 50 40 30 20 10 0 -10
f1 (ppm)

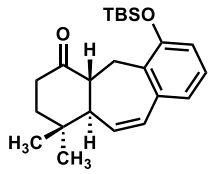
TBSO
O
H
H3C
CH3
H

36

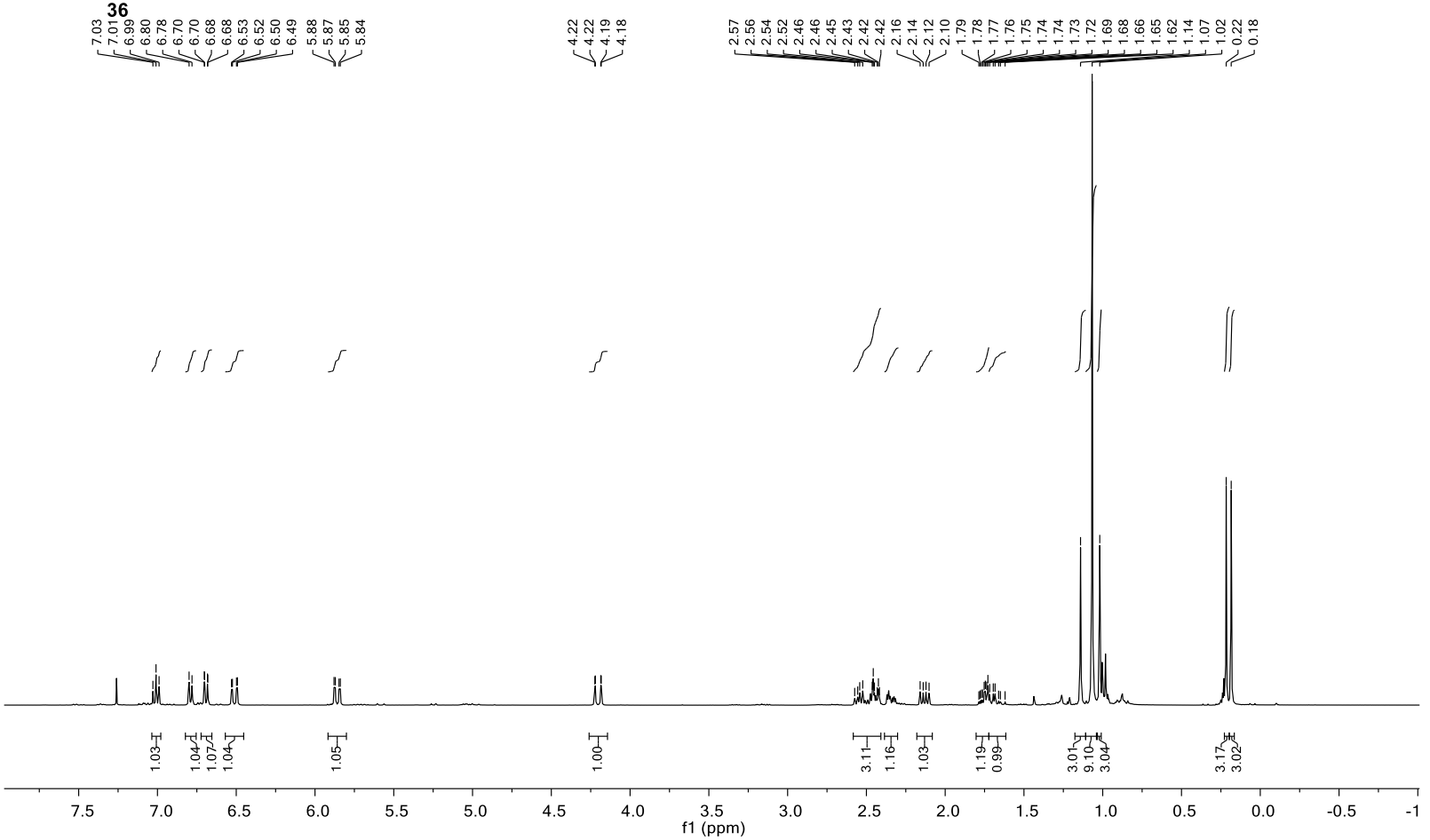
7.03
7.01
6.99
6.80
6.78
6.70
6.70
6.68
6.68
6.53
6.52
6.50
6.49
5.88
5.87
5.85
5.84
4.22
4.22
4.19
4.18
2.57
2.56
2.54
2.52
2.46
2.46
2.45
2.43
2.42
2.42
2.16
2.14
2.12
2.10
1.79
1.78
1.77
1.76
1.75
1.74
1.74
1.73
1.72
1.69
1.68
1.66
1.65
1.62
1.14
1.07
1.02
0.22
0.18
1.03
1.04
1.07
1.04
1.05
1.00
3.11
1.16
1.03
1.19
0.99
3.01
9.10
3.04
3.17
3.02
7.5
7.0
6.5
6.0
5.5
5.0
4.5
4.0
3.5
3.0
2.5
2.0
1.5
1.0
0.5
0.0
-0.5
-1
f1 (ppm)

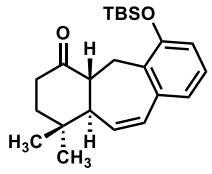
TBSO
O
H
H3C
CH3
H

36

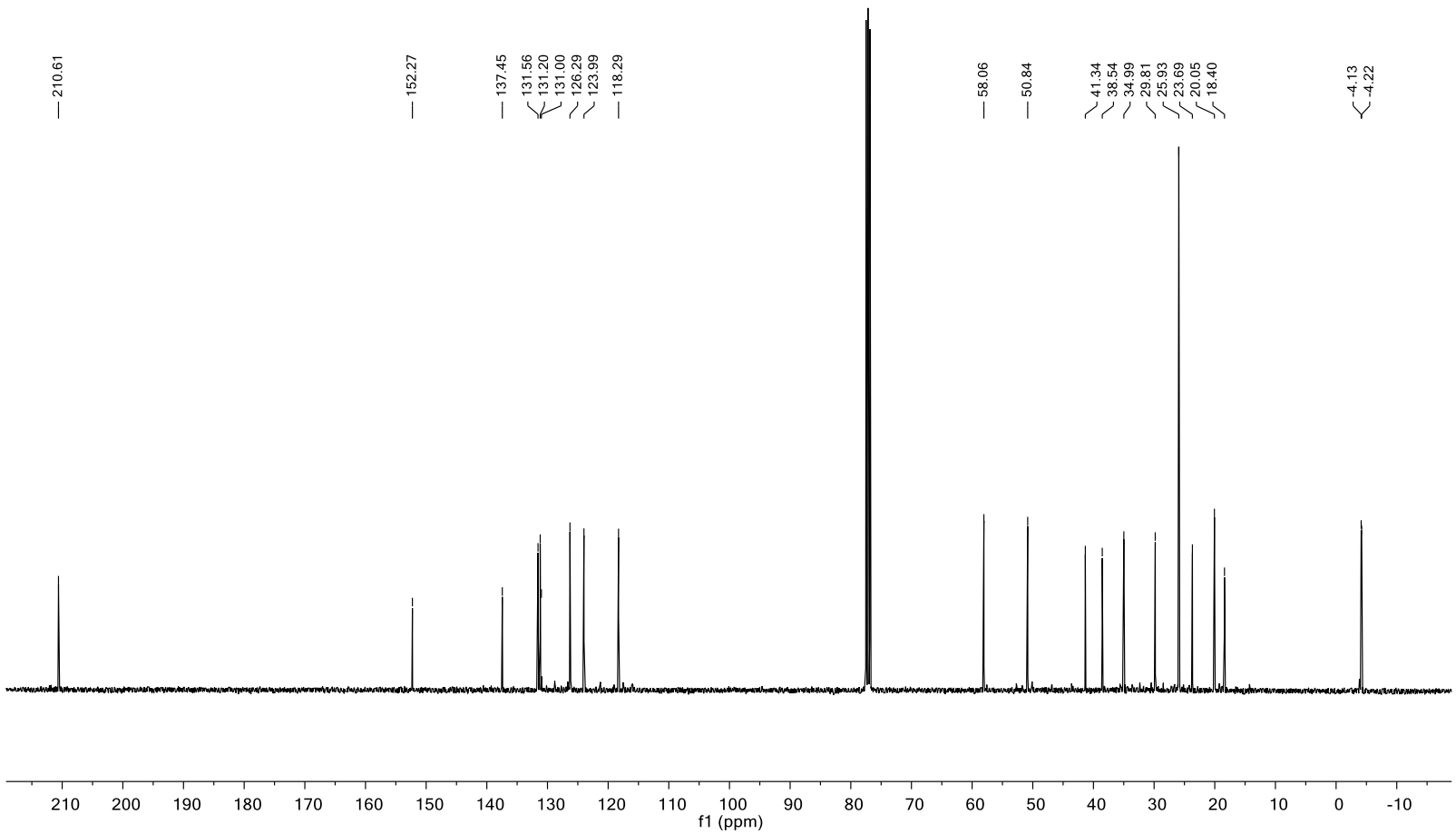
210.61
152.27
137.45
131.56
131.20
131.00
126.29
123.99
118.29
58.06
50.84
41.34
38.54
34.99
29.81
25.93
23.69
20.05
18.40
-4.13
-4.22
210 200 190 180 170 160 150 140 130 120 110 100 90 80 70 60 50 40 30 20 10 0 -10
f1 (ppm)

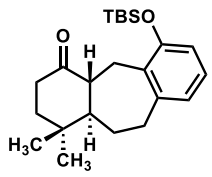
TBSO
O
H
H3C
CH3
H

38

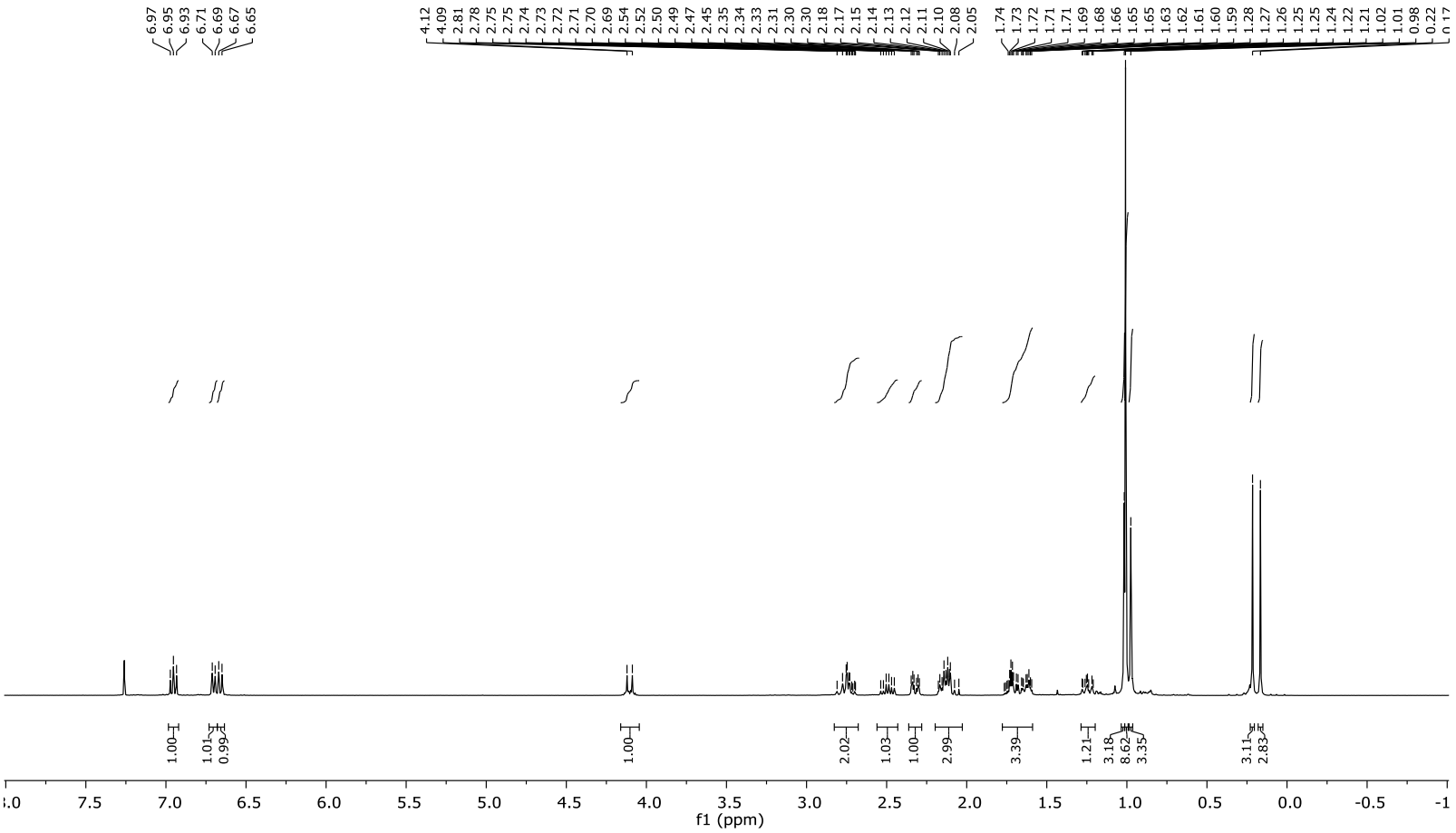
6.97
6.95
6.93
6.71
6.69
6.67
6.65
4.12
4.09
2.81
2.78
2.75
2.75
2.74
2.73
2.72
2.71
2.70
2.69
2.54
2.52
2.50
2.49
2.47
2.45
2.35
2.34
2.33
2.31
2.30
2.30
2.18
2.17
2.15
2.14
2.13
2.12
2.11
2.10
2.08
2.05
1.74
1.73
1.72
1.71
1.71
1.69
1.68
1.66
1.65
1.65
1.63
1.62
1.61
1.60
1.59
1.28
1.27
1.26
1.25
1.25
1.24
1.22
1.21
1.02
1.01
0.98
0.22
1.00
1.01
0.99
1.00
2.02
1.03
1.00
2.99
3.39
1.21
3.18
8.62
3.35
3.11
2.83
f1 (ppm)

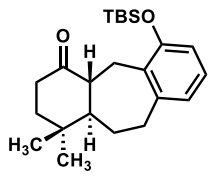
TBSO
O
H
H3C
CH3
H

38

212.07
153.01
146.16
131.09
126.43
121.02
117.22
57.98
50.56
42.55
38.75
34.76
34.36
29.61
29.36
25.87
24.45
20.17
18.34
-4.05
-4.21
210 200 190 180 170 160 150 140 130 120 110 100 90 80 70 60 50 40 30 20 10 0 -10
f1 (ppm)

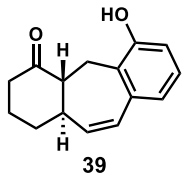
HO
O
H
H

39

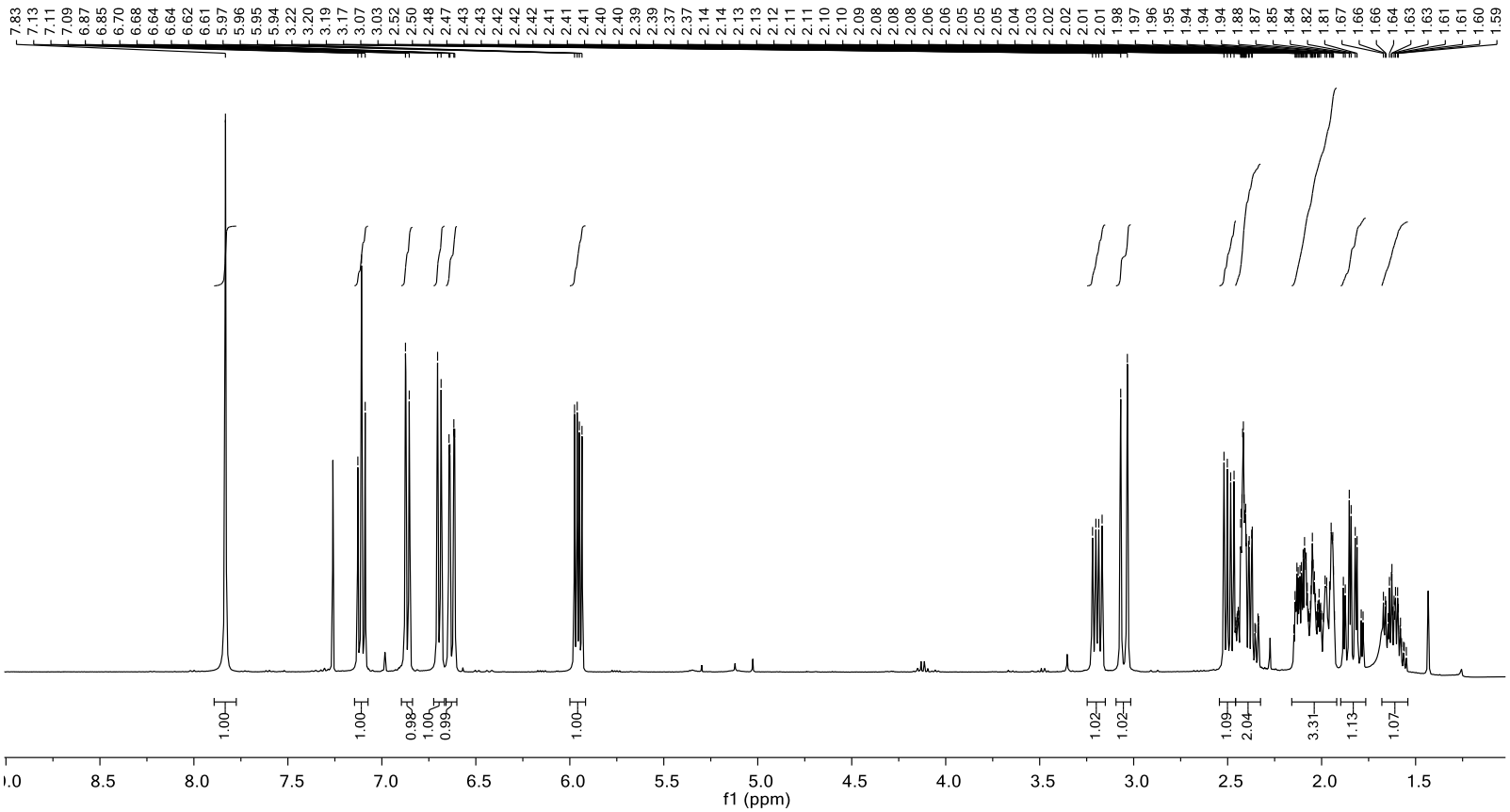
7.83 7.13 7.11 7.09 6.87 6.85 6.70 6.68 6.64 6.64 6.62 6.61 5.97 5.96 5.95 5.94 3.22 3.20 3.19 3.17 3.07 3.03 2.52 2.50 2.48 2.47 2.43 2.43 2.42 2.42 2.42 2.41 2.41 2.41 2.40 2.40 2.39 2.39 2.37 2.37 2.14 2.14 2.13 2.13 2.12 2.11 2.11 2.10 2.10 2.09 2.08 2.08 2.08 2.06 2.06 2.05 2.05 2.05 2.04 2.03 2.02 2.02 2.01 2.01 1.98 1.97 1.96 1.95 1.94 1.94 1.94 1.88 1.87 1.85 1.84 1.82 1.81 1.67 1.66 1.66 1.64 1.63 1.63 1.61 1.61 1.60 1.59
1.00 1.00 0.98 1.00 0.99 1.00 1.02 1.02 1.09 2.04 3.31 1.13 1.07
8.5 8.0 7.5 7.0 6.5 6.0 5.5 5.0 4.5 4.0 3.5 3.0 2.5 2.0 1.5
f1 (ppm)

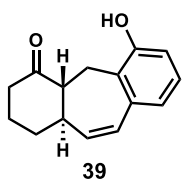
HO
O
H
H

39

215.43
154.56
139.89
134.08
131.17
127.20
125.30
120.29
115.86
65.69
44.48
40.60
30.21
26.51
24.07
210 200 190 180 170 160 150 140 130 120 110 100 90 80 70 60 50 40 30 20 10 0 -10
f1 (ppm)

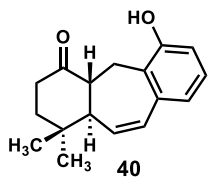
HO
O
H
H
H3C
CH3

40

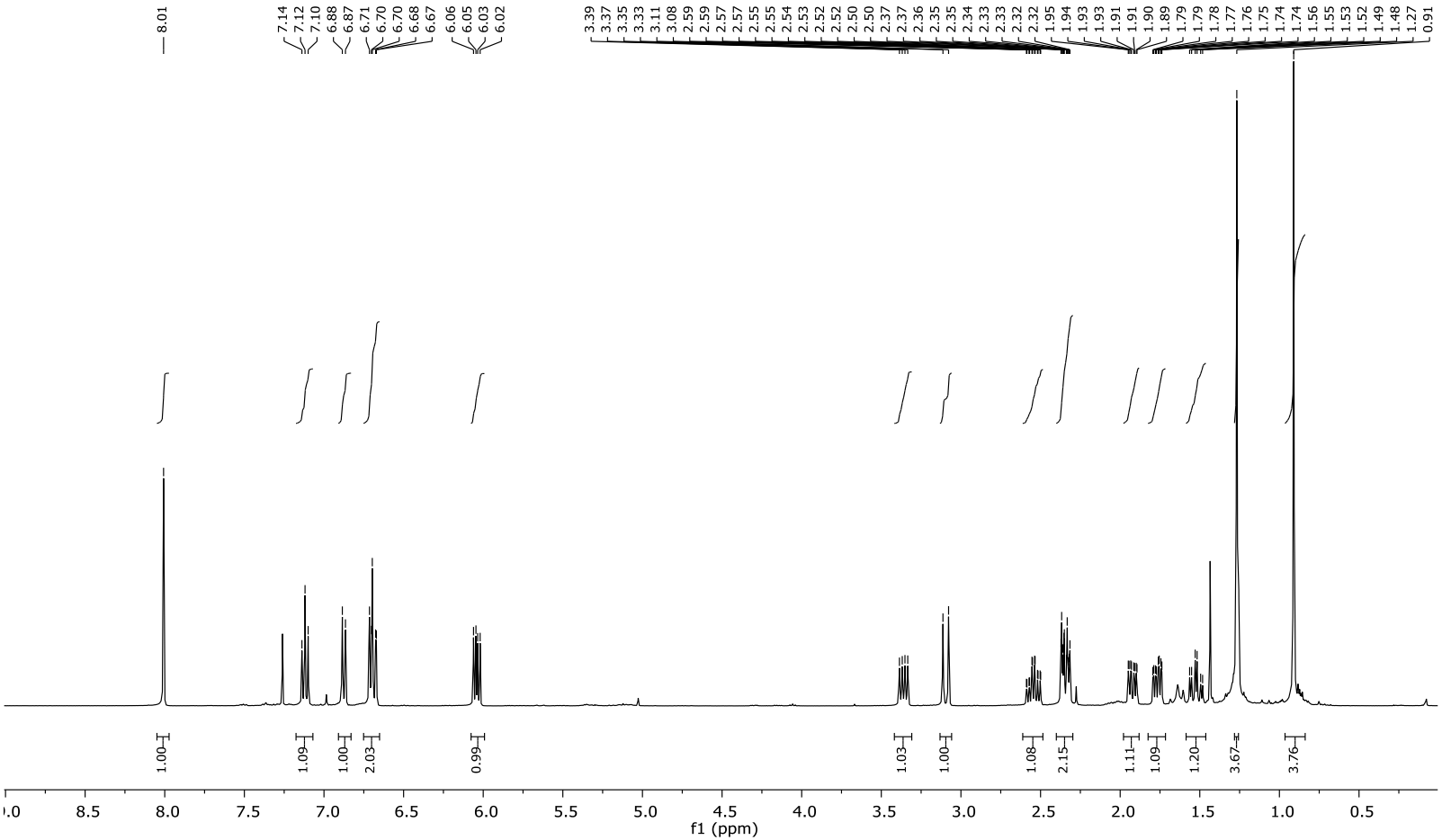
8.01
7.14
7.12
7.10
6.88
6.87
6.71
6.70
6.70
6.68
6.67
6.06
6.05
6.03
6.02
3.39
3.37
3.35
3.33
3.11
3.08
2.59
2.59
2.57
2.57
2.55
2.55
2.54
2.53
2.52
2.52
2.50
2.50
2.37
2.37
2.36
2.35
2.35
2.34
2.33
2.33
2.32
2.32
1.95
1.94
1.93
1.93
1.91
1.91
1.90
1.89
1.79
1.79
1.78
1.77
1.76
1.75
1.74
1.74
1.56
1.55
1.53
1.52
1.49
1.48
1.27
0.91
1.00
1.09
1.00
2.03
0.99
1.03
1.00
1.08
2.15
1.11
1.09
1.20
3.67
3.76
f1 (ppm)

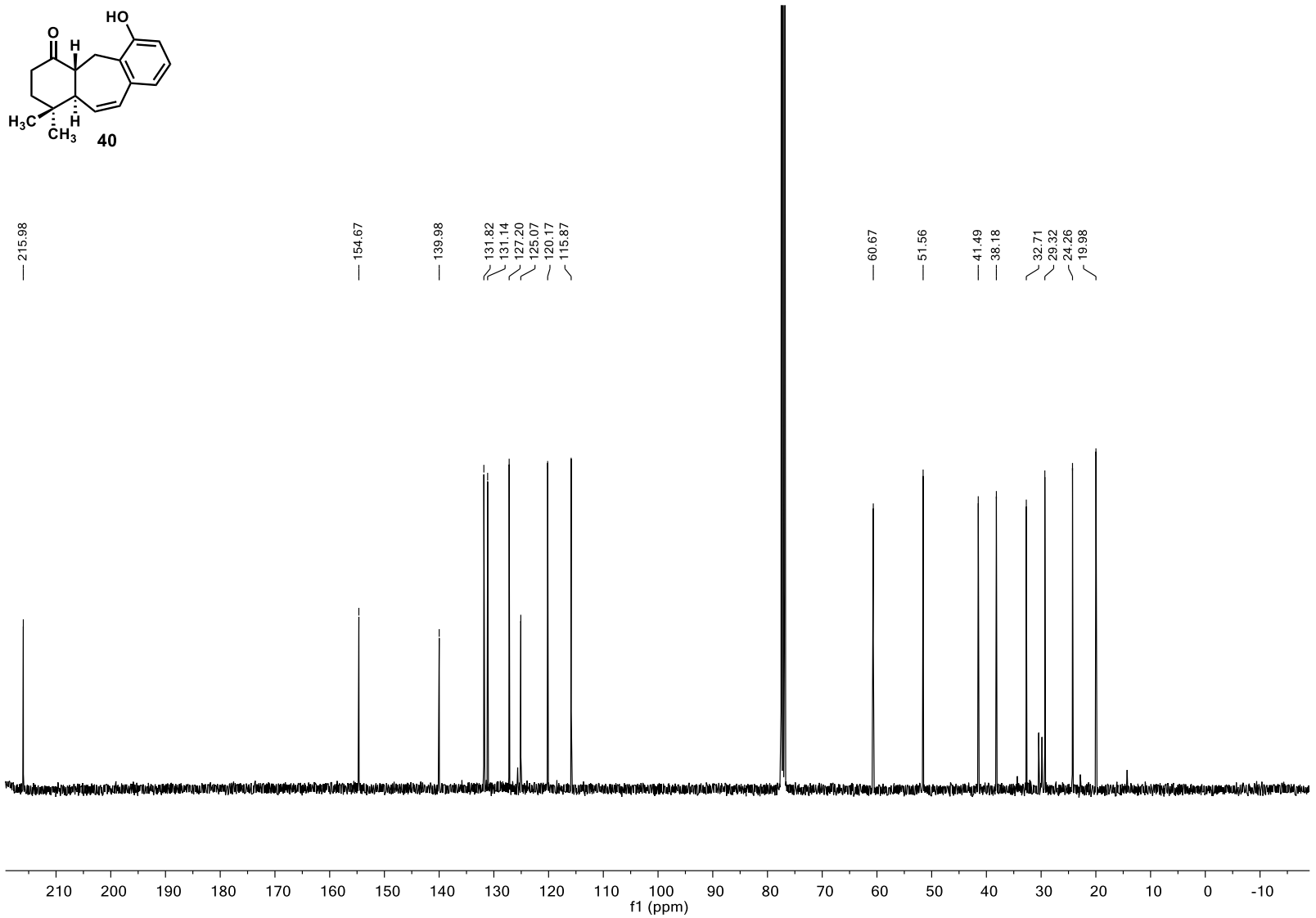
HO
O
H
H3C
CH3
H
40
215.98
154.67
139.98
131.82
131.14
127.20
125.07
120.17
115.87
60.67
51.56
41.49
38.18
32.71
29.32
24.26
19.98
210 200 190 180 170 160 150 140 130 120 110 100 90 80 70 60 50 40 30 20 10 0 -10
f1 (ppm)

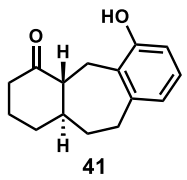
HO
O
H
H

41

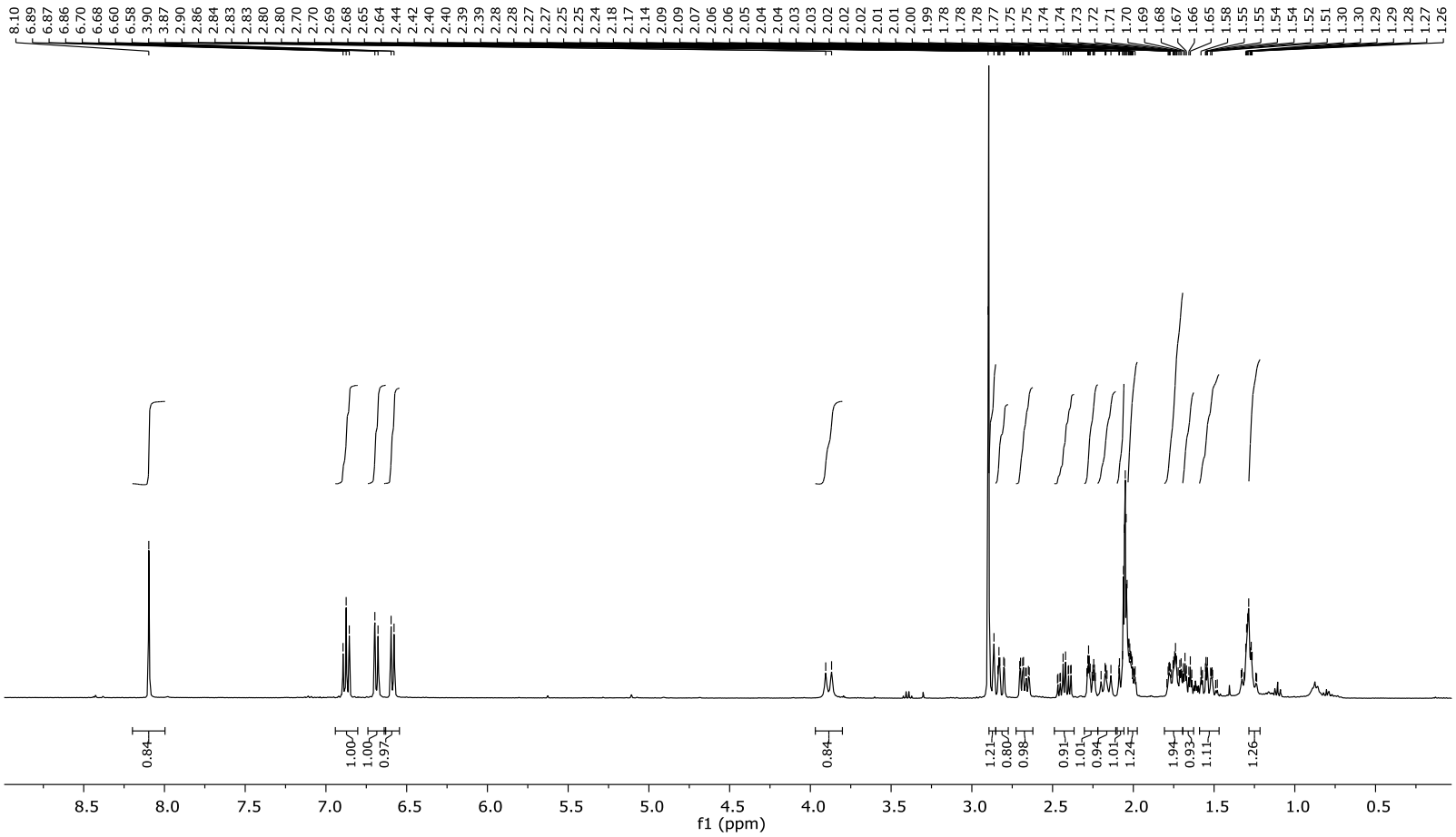
8.10 6.89 6.87 6.86 6.70 6.68 6.60 6.58 3.90 3.87 2.90 2.86 2.84 2.83 2.83 2.80 2.80 2.70 2.70 2.69 2.68 2.65 2.64 2.44 2.42 2.40 2.40 2.39 2.39 2.28 2.28 2.27 2.27 2.25 2.25 2.24 2.18 2.17 2.14 2.09 2.09 2.07 2.06 2.06 2.05 2.04 2.04 2.03 2.03 2.02 2.02 2.02 2.01 2.01 2.00 1.99 1.78 1.78 1.78 1.77 1.75 1.75 1.74 1.74 1.73 1.72 1.71 1.70 1.69 1.68 1.67 1.66 1.65 1.58 1.55 1.55 1.54 1.54 1.52 1.51 1.30 1.30 1.29 1.29 1.28 1.27 1.26
0.84 1.00 1.00 0.97 0.84 1.21 0.80 0.98 0.91 1.01 0.94 1.01 1.24 1.94 0.93 1.11 1.26
8.5 8.0 7.5 7.0 6.5 6.0 5.5 5.0 4.5 4.0 3.5 3.0 2.5 2.0 1.5 1.0 0.5
f1 (ppm)

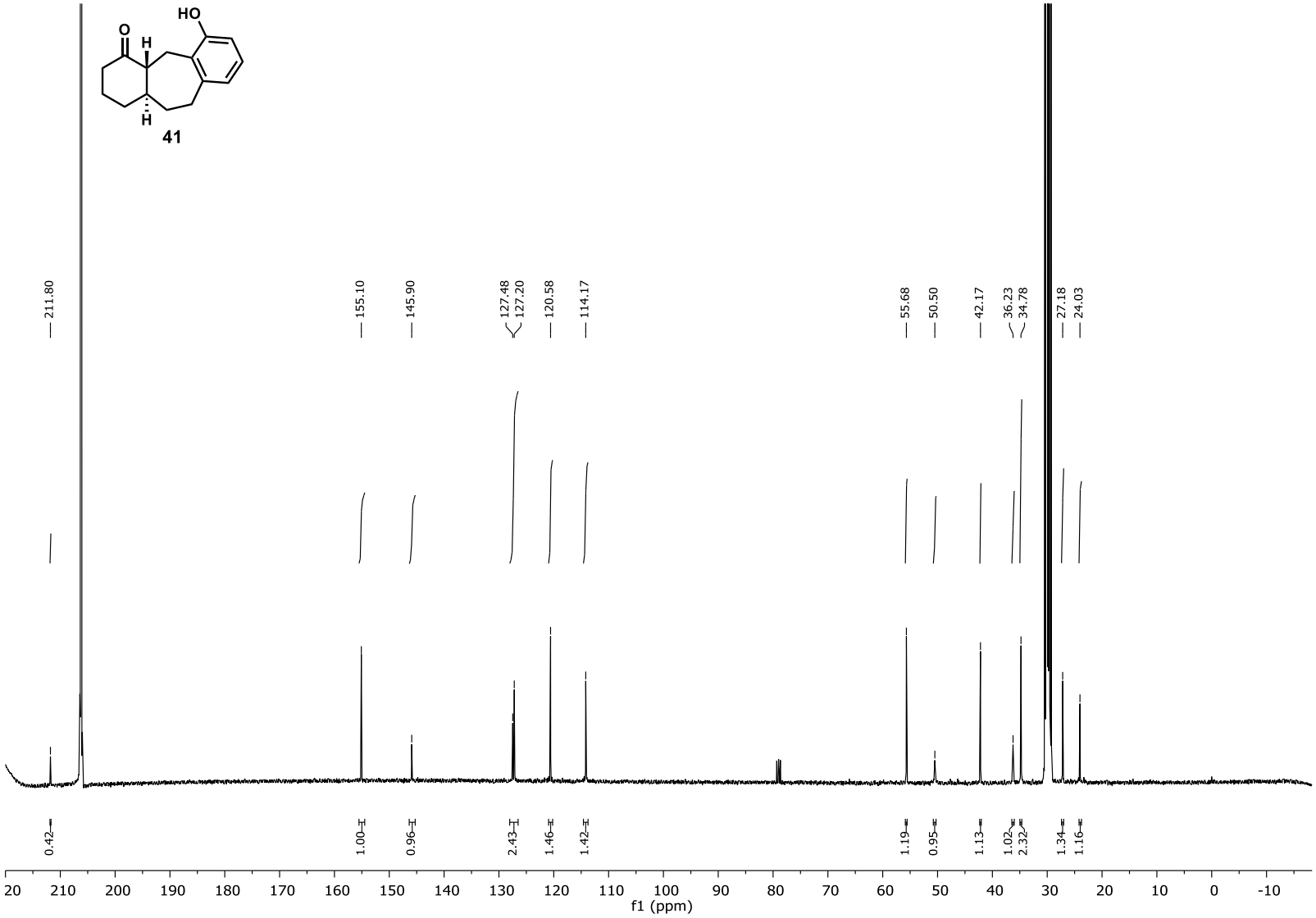
HO
O
H
H
41
211.80
155.10
145.90
127.48
127.20
120.58
114.17
55.68
50.50
42.17
36.23
34.78
27.18
24.03
0.42
1.00
0.96
2.43
1.46
1.42
1.19
0.95
1.13
1.02
2.32
1.34
1.16
f1 (ppm)

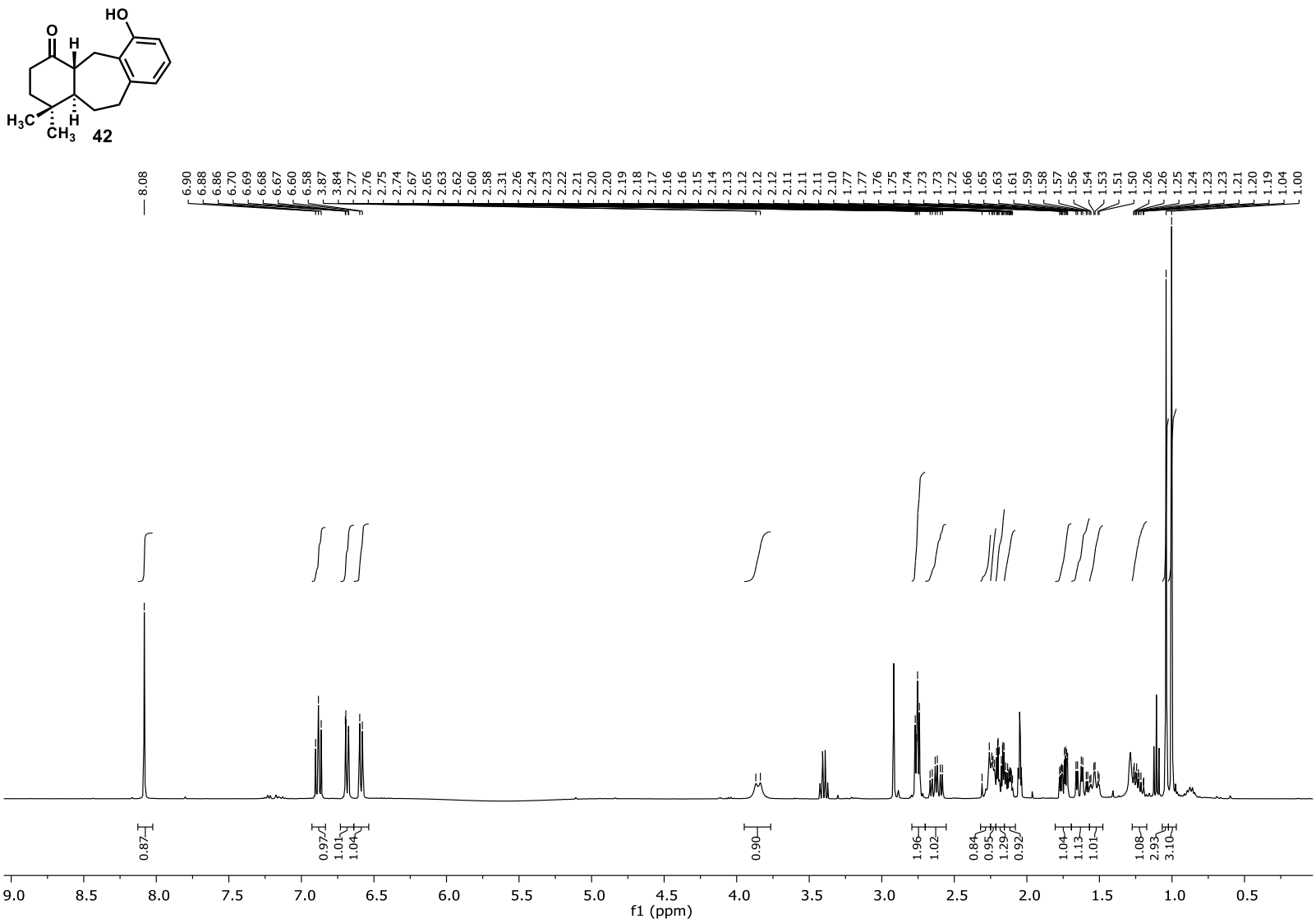
HO
O
H
H3C
CH3
H
42
8.08
6.90
6.88
6.86
6.70
6.69
6.68
6.67
6.60
6.58
3.87
3.84
2.77
2.76
2.75
2.74
2.67
2.65
2.63
2.62
2.60
2.58
2.31
2.26
2.24
2.23
2.22
2.21
2.20
2.20
2.19
2.18
2.17
2.16
2.16
2.15
2.14
2.13
2.12
2.12
2.11
2.11
2.10
1.77
1.77
1.76
1.75
1.74
1.73
1.73
1.72
1.66
1.65
1.63
1.61
1.59
1.58
1.57
1.56
1.54
1.53
1.51
1.50
1.26
1.26
1.25
1.24
1.23
1.23
1.21
1.20
1.19
1.04
1.00
0.87
0.97
1.01
1.04
0.90
1.96
1.02
0.84
0.95
1.29
0.92
1.04
1.13
1.01
1.08
2.93
3.10
9.0
8.5
8.0
7.5
7.0
6.5
6.0
5.5
5.0
4.5
4.0
3.5
3.0
2.5
2.0
1.5
1.0
0.5
f1 (ppm)

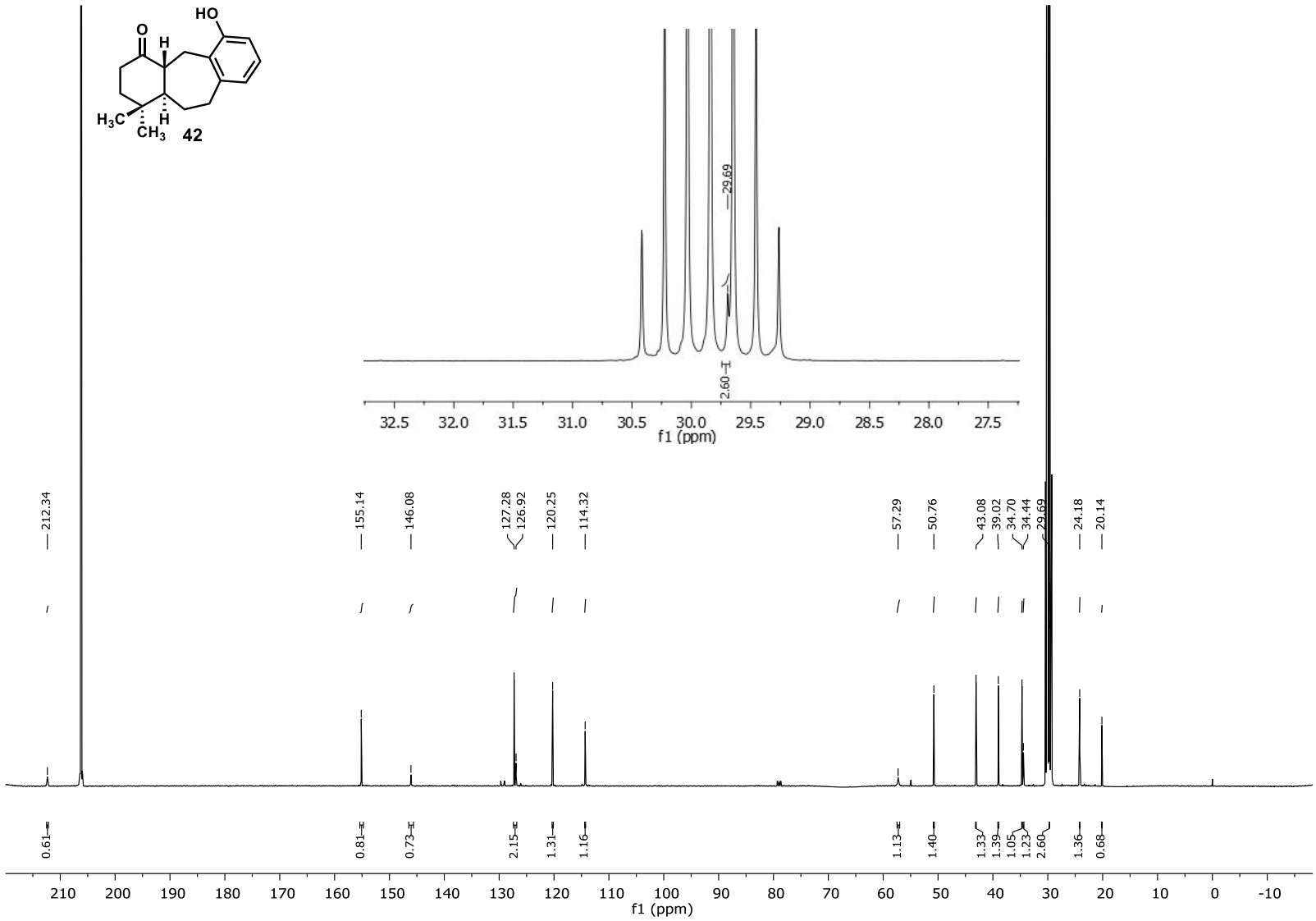
HO
O
H
H3C
CH3
H
42
29.69
2.60
32.5 32.0 31.5 31.0 30.5 30.0 29.5 29.0 28.5 28.0 27.5
f1 (ppm)
212.34
155.14
146.08
127.28
126.92
120.25
114.32
57.29
50.76
43.08
39.02
34.70
34.44
29.69
24.18
20.14
0.61
0.81
0.73
2.15
1.31
1.16
1.13
1.40
1.33
1.39
1.05
1.23
2.60
1.36
0.68
210 200 190 180 170 160 150 140 130 120 110 100 90 80 70 60 50 40 30 20 10 0 -10
f1 (ppm)

Appendix C

CRYSTAL STRUCTURE DATA

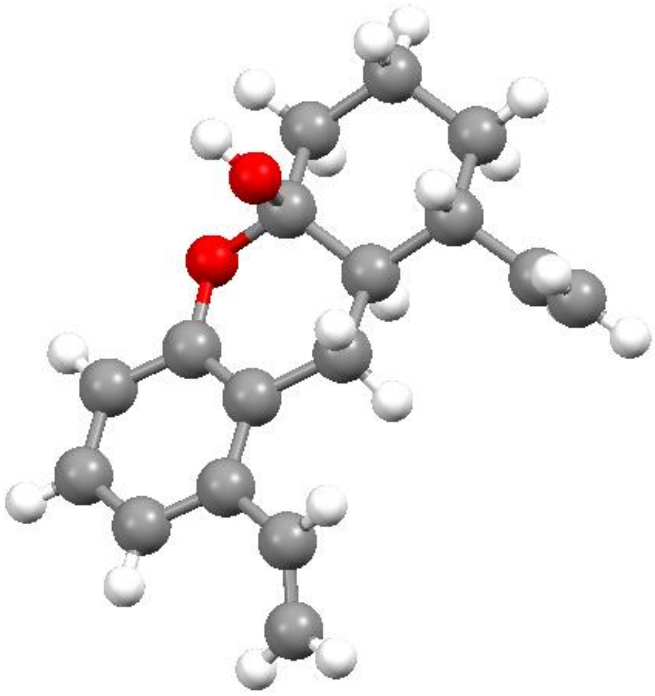

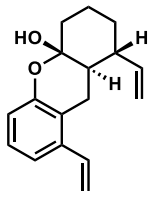

27

A clear colourless block-like specimen of $C_{17}H_{20}O_2$, approximate dimensions 0.287 mm x 0.305 mm x 0.354 mm, was used for the X-ray crystallographic analysis. The X-ray intensity data were measured.

Table 1: Data collection details.

Axis	dx/mm	2θ/°	ω/°	φ/°	χ/°	Width/°	Frames	Time/s	λ/Å	Volt./kV	*I*/mA	Temp./K
Omega	49.533	26.02	-167.98	-69.00	54.79	1.00	208	8.00	0.71073	50	30.0	200
Omega	49.533	26.02	-167.98	99.41	54.79	1.00	208	8.00	0.71073	50	30.0	200

A total of 416 frames were collected. The total exposure time was 0.92 hours. The frames were integrated with the Bruker SAINT software package using a narrow-frame algorithm. The integration of the data using a monoclinic unit cell yielded a total of 10676 reflections to a maximum θ angle of 27.65° (0.77 Å resolution), of which 3284 were independent (average redundancy 3.251, completeness = 99.8%, R_{int} = 4.40%, R_{sig} = 4.91%) and 2268 (69.06%) were greater than $2\sigma(F^2)$. The final cell constants of a = 8.9663(12) Å, b = 11.0197(14) Å, c =14.2676(19) Å, β = 90.604(2)°, volume = 1409.6(3) $Å^3$, are based upon the refinement of the XYZ-centroids of 1572 reflections above 20 σ(I) with 4.670° < 2θ < 46.99°. Data were corrected for absorption effects using the multi-scan method (SADABS). The ratio of minimum to maximum apparent transmission was 0.887. The calculated minimum and maximum transmission coefficients (based on crystal size) are 0.9730 and 0.9780.

The final anisotropic full-matrix least-squares refinement on F^2 with 173 variables converged at R1 = 5.57%, for the observed data and wR2 = 15.34% for all data. The goodness-of-fit was 1.027. The largest peak in the final difference electron density synthesis was 0.263 $e^-/Å^3$ and the largest hole was –0.21 $e^-/Å^3$ with an RMS deviation of 0.048 $e^-/Å^3$. On the basis of the final model, the calculated density was 1.208 g/cm^3 and F(000), 552 e^-.

Table 2. Sample and crystal data.

Chemical formula	$C_{17}H_{20}O_2$
Formula weight	256.33 g/mol
Temperature	200(2) K
Wavelength	0.71073 Å
Crystal size	0.287 x 0.305 x 0.354 mm
Crystal habit	clear colourless block
Crystal system	monoclinic

Space group	P 1 21/n 1	
Unit cell dimensions	a = 8.9663(12) Å	α = 90°
	b = 11.0197(14) Å	β = 90.604(2)°
	c = 14.2676(19) Å	γ = 90°
Volume	1409.6(3) $Å^3$	
Z	4	
Density (calculated)	1.208 g/cm^3	
Absorption coefficient	0.077 mm^{-1}	
F(000)	552	

Table 3. Data collection and structure refinement.

Theta range for data collection	2.33 to 27.65°	
Index ranges	-11<=h<=11, -14<=k<=14, -18<=l<=18	
Reflections collected	10676	
Independent reflections	3284 [R(int) = 0.0440]	
Coverage of independent reflections	99.8%	
Absorption correction	multi-scan	
Max. and min. transmission	0.9780 and 0.9730	
Refinement method	Full-matrix least-squares on F^2	
Refinement program	SHELXL-2014/7 (Sheldrick, 2014)	
Function minimized	$\Sigma w(F_o^2 - F_c^2)^2$	
Data / restraints / parameters	3284 / 0 / 173	
Goodness-of-fit on F^2	1.027	
Final R indices	2268 data; I>2σ(I)	R1 = 0.0557, wR2 = 0.1382
	all data	R1 = 0.0817, wR2 = 0.1534
Weighting scheme	$w=1/[\sigma^2(F_o^2)+(0.0816P)^2+0.0524P]$ where $P=(F_o^2+2F_c^2)/3$	
Largest diff. peak and hole	0.263 and -0.216 $eÅ^{-3}$	
R.M.S. deviation from mean	0.048 $eÅ^{-3}$	

Table 4. Atomic coordinates and equivalent isotropic atomic displacement parameters ($Å^2$).
U(eq) is defined as one third of the trace of the orthogonalized U_{ij} tensor.

	x/a	**y/b**	**z/c**	**U(eq)**
O1	0.59295(12)	0.61599(10)	0.92092(7)	0.0355(3)
O2	0.40499(12)	0.47899(9)	0.88463(7)	0.0336(3)
C1	0.44602(18)	0.60625(14)	0.88683(10)	0.0310(4)
C2	0.3331(2)	0.66655(16)	0.95008(11)	0.0395(4)
C3	0.3585(2)	0.80333(16)	0.95348(12)	0.0468(5)
C4	0.3570(2)	0.85871(16)	0.85551(12)	0.0436(4)
C5	0.46970(19)	0.79704(14)	0.79031(11)	0.0347(4)
C6	0.44194(18)	0.65875(14)	0.78779(10)	0.0303(4)
C7	0.55249(18)	0.59166(14)	0.72632(11)	0.0322(4)
C8	0.53838(17)	0.45593(14)	0.73701(10)	0.0290(4)
C9	0.59397(18)	0.37504(14)	0.66976(10)	0.0336(4)
C10	0.57862(19)	0.25021(15)	0.68229(12)	0.0392(4)
C11	0.50817(19)	0.20508(15)	0.76079(12)	0.0400(4)
C12	0.45247(18)	0.28309(15)	0.82740(11)	0.0366(4)
C13	0.46797(17)	0.40736(14)	0.81532(10)	0.0306(4)
C14	0.4615(2)	0.85200(15)	0.69415(11)	0.0374(4)
C15	0.5719(2)	0.90050(17)	0.64819(14)	0.0505(5)
C16	0.6695(2)	0.42254(16)	0.58589(12)	0.0447(5)
C17	0.6776(3)	0.37145(19)	0.50478(13)	0.0600(6)

Table 5. Bond lengths (Å).

O1-C1	1.4036(19)	O1-H1	0.84
O2-C13	1.3898(17)	O2-C1	1.4500(18)
C1-C2	1.517(2)	C1-C6	1.527(2)
C2-C3	1.525(2)	C2-H2A	0.99
C2-H2B	0.99	C3-C4	1.525(2)
C3-H3A	0.99	C3-H3B	0.99
C4-C5	1.539(2)	C4-H4A	0.99
C4-H4B	0.99	C5-C14	1.501(2)
C5-C6	1.544(2)	C5-H5	1.0

C6-C7	1.522(2)	C6-H6	1.0
C7-C8	1.509(2)	C7-H7A	0.99
C7-H7B	0.99	C8-C13	1.396(2)
C8-C9	1.405(2)	C9-C10	1.394(2)
C9-C16	1.477(2)	C10-C11	1.384(2)
C10-H10	0.95	C11-C12	1.379(2)
C11-H11	0.95	C12-C13	1.387(2)
C12-H12	0.95	C14-C15	1.307(2)
C14-H14	0.95	C15-H15A	0.95
C15-H15B	0.95	C16-C17	1.290(3)
C16-H16	0.95	C17-H17A	0.95
C17-H17B	0.95		

Table 6. Bond angles (°).

C1-O1-H1	109.5	C13-O2-C1	117.37(11)
O1-C1-O2	108.57(12)	O1-C1-C2	112.98(13)
O2-C1-C2	105.40(12)	O1-C1-C6	107.75(12)
O2-C1-C6	110.05(12)	C2-C1-C6	112.02(13)
C1-C2-C3	110.57(14)	C1-C2-H2A	109.5
C3-C2-H2A	109.5	C1-C2-H2B	109.5
C3-C2-H2B	109.5	H2A-C2-H2B	108.1
C4-C3-C2	111.50(14)	C4-C3-H3A	109.3
C2-C3-H3A	109.3	C4-C3-H3B	109.3
C2-C3-H3B	109.3	H3A-C3-H3B	108.0
C3-C4-C5	112.22(14)	C3-C4-H4A	109.2
C5-C4-H4A	109.2	C3-C4-H4B	109.2
C5-C4-H4B	109.2	H4A-C4-H4B	107.9
C14-C5-C4	110.38(13)	C14-C5-C6	111.75(13)
C4-C5-C6	110.08(13)	C14-C5-H5	108.2
C4-C5-H5	108.2	C6-C5-H5	108.2
C7-C6-C1	109.86(12)	C7-C6-C5	112.77(12)
C1-C6-C5	110.49(12)	C7-C6-H6	107.8
C1-C6-H6	107.8	C5-C6-H6	107.8
C8-C7-C6	111.56(12)	C8-C7-H7A	109.3
C6-C7-H7A	109.3	C8-C7-H7B	109.3

C6-C7-H7B	109.3	H7A-C7-H7B	108.0
C13-C8-C9	118.04(14)	C13-C8-C7	120.01(13)
C9-C8-C7	121.95(13)	C10-C9-C8	120.15(14)
C10-C9-C16	120.02(14)	C8-C9-C16	119.83(14)
C11-C10-C9	120.32(15)	C11-C10-H10	119.8
C9-C10-H10	119.8	C12-C11-C10	120.36(15)
C12-C11-H11	119.8	C10-C11-H11	119.8
C11-C12-C13	119.48(15)	C11-C12-H12	120.3
C13-C12-H12	120.3	C12-C13-O2	115.48(13)
C12-C13-C8	121.64(14)	O2-C13-C8	122.84(14)
C15-C14-C5	126.40(17)	C15-C14-H14	116.8
C5-C14-H14	116.8	C14-C15-H15A	120.0
C14-C15-H15B	120.0	H15A-C15-H15B	120.0
C17-C16-C9	127.09(18)	C17-C16-H16	116.5
C9-C16-H16	116.5	C16-C17-H17A	120.0
C16-C17-H17B	120.0	H17A-C17-H17B	120.0

Table 7. Torsion angles (°).

C13-O2-C1-O1	-73.20(15)	C13-O2-C1-C2	165.48(12)
C13-O2-C1-C6	44.51(17)	O1-C1-C2-C3	65.08(17)
O2-C1-C2-C3	-176.52(13)	C6-C1-C2-C3	-56.84(19)
C1-C2-C3-C4	55.0(2)	C2-C3-C4-C5	-54.9(2)
C3-C4-C5-C14	178.44(15)	C3-C4-C5-C6	54.6(2)
O1-C1-C6-C7	57.50(16)	O2-C1-C6-C7	-60.72(16)
C2-C1-C6-C7	-177.63(13)	O1-C1-C6-C5	-67.55(16)
O2-C1-C6-C5	174.23(12)	C2-C1-C6-C5	57.32(18)
C14-C5-C6-C7	58.45(18)	C4-C5-C6-C7	-178.53(13)
C14-C5-C6-C1	-178.17(13)	C4-C5-C6-C1	-55.15(17)
C1-C6-C7-C8	47.33(17)	C5-C6-C7-C8	171.06(13)
C6-C7-C8-C13	-19.0(2)	C6-C7-C8-C9	160.79(14)
C13-C8-C9-C10	-0.2(2)	C7-C8-C9-C10	-179.99(15)
C13-C8-C9-C16	-179.89(15)	C7-C8-C9-C16	0.3(2)
C8-C9-C10-C11	0.2(3)	C16-C9-C10-C11	179.90(16)
C9-C10-C11-C12	0.0(3)	C10-C11-C12-C13	-0.2(3)
C11-C12-C13-O2	178.34(14)	C11-C12-C13-C8	0.2(2)

C1-O2-C13-C12	166.60(13)	C1-O2-C13-C8	-15.3(2)
C9-C8-C13-C12	0.0(2)	C7-C8-C13-C12	179.78(15)
C9-C8-C13-O2	-178.00(13)	C7-C8-C13-O2	1.8(2)
C4-C5-C14-C15	123.95(19)	C6-C5-C14-C15	-113.20(19)
C10-C9-C16-C17	27.9(3)	C8-C9-C16-C17	-152.5(2)

Table 8. Anisotropic atomic displacement parameters ($Å^2$).

The anisotropic atomic displacement factor exponent takes the form:
$-2\pi^2[h^2 a^{*2} U_{11} + ... + 2 h k a^* b^* U_{12}]$

	U_{11}	**U_{22}**	**U_{33}**	**U_{23}**	**U_{13}**	**U_{12}**
O1	0.0396(7)	0.0361(7)	0.0308(6)	0.0013(5)	-0.0005(5)	-0.0021(5)
O2	0.0409(7)	0.0302(6)	0.0298(6)	-0.0004(5)	0.0079(5)	-0.0037(5)
C1	0.0342(9)	0.0291(9)	0.0297(8)	-0.0004(6)	0.0034(6)	-0.0007(7)
C2	0.0461(10)	0.0414(10)	0.0312(8)	0.0001(7)	0.0097(7)	0.0054(8)
C3	0.0655(13)	0.0379(10)	0.0374(9)	-0.0057(8)	0.0101(8)	0.0121(9)
C4	0.0564(12)	0.0333(10)	0.0411(9)	-0.0038(8)	0.0075(8)	0.0104(8)
C5	0.0415(9)	0.0287(9)	0.0340(8)	-0.0006(7)	0.0012(7)	0.0025(7)
C6	0.0341(9)	0.0292(8)	0.0276(7)	-0.0018(6)	0.0030(6)	0.0006(7)
C7	0.0391(9)	0.0277(9)	0.0299(8)	0.0000(6)	0.0054(7)	0.0005(7)
C8	0.0319(8)	0.0271(8)	0.0279(8)	0.0003(6)	0.0011(6)	-0.0009(6)
C9	0.0380(9)	0.0295(9)	0.0333(8)	-0.0006(7)	0.0031(7)	0.0029(7)
C10	0.0500(11)	0.0297(9)	0.0380(9)	-0.0045(7)	0.0058(8)	0.0044(8)
C11	0.0511(11)	0.0244(9)	0.0446(10)	0.0016(7)	0.0024(8)	-0.0020(7)
C12	0.0414(9)	0.0329(9)	0.0356(9)	0.0056(7)	0.0026(7)	-0.0061(7)
C13	0.0304(8)	0.0313(9)	0.0300(8)	-0.0018(6)	0.0003(6)	-0.0010(6)
C14	0.0452(10)	0.0292(9)	0.0378(9)	-0.0014(7)	0.0024(7)	0.0060(7)
C15	0.0570(12)	0.0483(12)	0.0463(10)	0.0044(9)	0.0087(9)	-0.0034(9)
C16	0.0591(12)	0.0310(9)	0.0443(10)	0.0006(8)	0.0176(9)	0.0053(8)
C17	0.0940(17)	0.0460(12)	0.0403(10)	-0.0010(9)	0.0198(10)	0.0021(11)

Table 9. Hydrogen atomic coordinates and isotropic atomic displacement parameters ($Å^2$).

	x/a	y/b	z/c	U(eq)
H1	0.5967	0.5923	0.9769	0.053
H2A	0.3421	0.6325	1.0141	0.047
H2B	0.2310	0.6496	0.9263	0.047
H3A	0.2795	0.8416	0.9914	0.056
H3B	0.4557	0.8203	0.9843	0.056
H4A	0.3809	0.9462	0.8602	0.052
H4B	0.2557	0.8510	0.8280	0.052
H5	0.5722	0.8114	0.8164	0.042
H6	0.3397	0.6449	0.7612	0.036
H7A	0.5347	0.6140	0.6599	0.039
H7B	0.6552	0.6168	0.7436	0.039
H10	0.6167	0.1959	0.6367	0.047
H11	0.4981	0.1199	0.7688	0.048
H12	0.4039	0.2520	0.8811	0.044
H14	0.3668	0.8515	0.6637	0.045
H15A	0.6688	0.9032	0.6757	0.061
H15B	0.5552	0.9331	0.5873	0.061
H16	0.7173	0.4991	0.5924	0.054
H17A	0.6318	0.2948	0.4944	0.072
H17B	0.7294	0.4104	0.4555	0.072

Table 10. Hydrogen bond distances (Å) and angles (°).

	Donor-H	Acceptor-H	Donor-Acceptor	Angle
O1-H1···O2	0.84	2.13	2.9650(15)	175.5

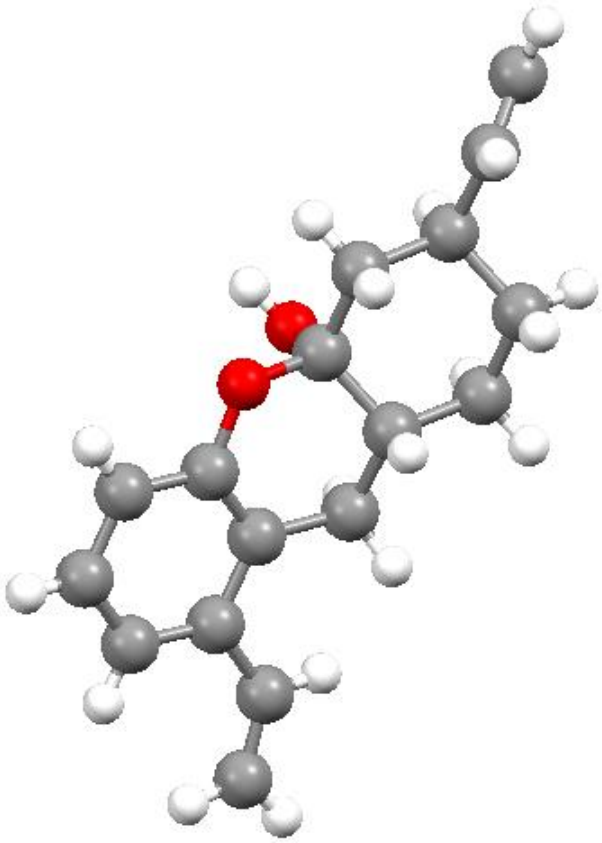

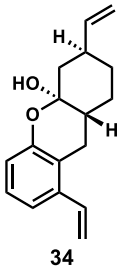

34

A specimen of $C_{17}H_{20}O_2$, approximate dimensions 0.144 mm x 0.431 mm x 0.507 mm, was used for the X-ray crystallographic analysis. The X-ray intensity data were measured.

The total exposure time was 2.02 hours. The frames were integrated with the Bruker SAINT software package using a narrow-frame algorithm. The integration of the data using a triclinic unit cell yielded a total of 31588 reflections to a maximum θ angle of 27.63° (0.77 Å resolution), of which 6529 were independent (average redundancy 4.838, completeness = 99.7%, R_{int} = 6.96%, R_{sig} = 6.21%) and 4670 (71.53%) were greater than $2\sigma(F^2)$. The final cell constants of a = 10.359(2) Å, b = 11.455(3) Å, c =13.302(3) Å, α = 73.297(3)°, β = 70.225(3)°, γ = 76.414(3)°, volume = 1406.0(6) $Å^3$, are based upon the refinement of the XYZ-centroids of 4734 reflections above 20 σ(I) with 4.423° < 2θ < 47.14°. Data were corrected for absorption effects using the multi-scan method (SADABS). The ratio of minimum to maximum apparent transmission was 0.928. The calculated minimum and maximum transmission coefficients (based on crystal size) are 0.6919 and 0.7456.

The structure was solved and refined using the Bruker SHELXTL Software Package, using the space group P –1, with Z = 4 for the formula unit, $C_{17}H_{20}O_2$. The final anisotropic full-matrix least-squares refinement on F^2 with 345 variables converged at R1 = 11.18%, for the observed data and wR2 = 41.50% for all data. The goodness-of-fit was 1.162. The largest peak in the final difference electron density synthesis was 0.556 $e^-/Å^3$ and the largest hole was –0.417 $e^-/Å^3$ with an RMS deviation of 0.105 $e^-/Å^3$. On the basis of the final model, the calculated density was 1.211 g/cm^3 and F(000), 552 e^-.

Table 1. Sample and crystal data.

Chemical formula	$C_{17}H_{20}O_2$
Formula weight	256.33 g/mol
Temperature	200(2) K
Wavelength	0.71073 Å

Crystal size	0.144 x 0.431 x 0.507 mm	
Crystal system	triclinic	
Space group	P -1	
Unit cell dimensions	a = 10.359(2) Å	α = 73.297(3)°
	b = 11.455(3) Å	β = 70.225(3)°
	c = 13.302(3) Å	γ = 76.414(3)°
Volume	1406.0(6) $Å^3$	
Z	4	
Density (calculated)	1.211 g/cm^3	
Absorption coefficient	0.078 mm^{-1}	
F(000)	552	

Table 2. Data collection and structure refinement.

Theta range for data collection	1.67 to 27.63°	
Index ranges	-13<=h<=13, -14<=k<=14, -17<=l<=17	
Reflections collected	31588	
Independent reflections	6529 [R(int) = 0.0696]	
Coverage of independent reflections	99.7%	
Absorption correction	multi-scan	
Max. and min. transmission	0.7456 and 0.6919	
Structure solution technique	direct methods	
Structure solution program	SHELXS-97 (Sheldrick 2008)	
Refinement method	Full-matrix least-squares on F^2	
Refinement program	SHELXL-2014/7 (Sheldrick, 2014)	
Function minimized	$\Sigma w(F_o^2 - F_c^2)^2$	
Data / restraints / parameters	6529 / 0 / 345	
Goodness-of-fit on F^2	1.162	
Final R indices	4670 data; I>2σ(I)	R1 = 0.1118, wR2 = 0.3994

	all data	R1 = 0.1366, wR2 = 0.4150
Weighting scheme	$w=1/[\sigma^2(F_o^2)+(0.1800P)^2+4.8216P]$ where $P=(F_o^2+2F_c^2)/3$	
Largest diff. peak and hole	0.556 and -0.417 eÅ^{-3}	
R.M.S. deviation from mean	0.105 eÅ^{-3}	

Table 3. Atomic coordinates and equivalent isotropic atomic displacement parameters (Å^2).

U(eq) is defined as one third of the trace of the orthogonalized U_{ij} tensor.

	x/a	**y/b**	**z/c**	**U(eq)**
C1	0.7054(5)	0.8019(4)	0.4952(4)	0.0288(9)
C2	0.7108(5)	0.8760(4)	0.3796(4)	0.0338(10)
C3	0.7517(5)	0.7903(5)	0.3006(4)	0.0351(10)
C4	0.8928(6)	0.7112(5)	0.3042(5)	0.0433(12)
C5	0.8932(5)	0.6393(5)	0.4199(4)	0.0389(11)
C6	0.8432(5)	0.7218(4)	0.5020(4)	0.0302(10)
C7	0.8286(5)	0.6473(4)	0.6199(4)	0.0335(10)
C8	0.7479(5)	0.7240(4)	0.7030(4)	0.0322(10)
C9	0.7436(5)	0.6802(5)	0.8143(4)	0.0361(11)
C10	0.6688(6)	0.7537(5)	0.8888(4)	0.0442(12)
C11	0.5992(6)	0.8697(5)	0.8543(5)	0.0454(13)
C12	0.6011(6)	0.9137(5)	0.7447(4)	0.0401(12)
C13	0.6746(5)	0.8399(4)	0.6708(4)	0.0312(10)
C14	0.7568(6)	0.8614(5)	0.1854(4)	0.0440(13)
C15	0.6812(8)	0.8517(7)	0.1282(5)	0.0629(18)
C16	0.8143(6)	0.5554(5)	0.8526(5)	0.0426(12)
C17	0.8586(7)	0.5171(6)	0.9409(6)	0.0595(17)
C18	0.2214(5)	0.8053(4)	0.5184(4)	0.0293(9)
C19	0.1183(5)	0.8414(4)	0.6202(4)	0.0319(10)
C20	0.1663(5)	0.7749(5)	0.7232(4)	0.0346(10)
C21	0.1910(6)	0.6346(4)	0.7336(4)	0.0378(11)
C22	0.2950(5)	0.5982(4)	0.6308(4)	0.0331(10)

C23	0.2496(5)	0.6663(4)	0.5279(4)	0.0305(10)
C24	0.3526(5)	0.6356(4)	0.4234(4)	0.0333(10)
C25	0.3099(5)	0.7160(5)	0.3244(4)	0.0350(10)
C26	0.3587(6)	0.6831(6)	0.2220(4)	0.0436(12)
C27	0.3138(6)	0.7589(6)	0.1344(5)	0.0502(14)
C28	0.2229(6)	0.8674(6)	0.1457(5)	0.0475(13)
C29	0.1749(6)	0.9012(5)	0.2455(4)	0.0410(12)
C30	0.2183(5)	0.8248(5)	0.3342(4)	0.0329(10)
C31	0.0636(6)	0.8066(5)	0.8261(5)	0.0455(13)
C32	0.0948(9)	0.8388(6)	0.9008(5)	0.0626(18)
C33	0.4549(7)	0.5669(7)	0.2109(5)	0.0627(19)
C34	0.5044(7)	0.5164(7)	0.1281(6)	0.0583(16)
O1	0.6711(4)	0.8899(3)	0.5633(3)	0.0323(8)
O2	0.6037(3)	0.7243(3)	0.5364(3)	0.0332(8)
O3	0.1615(3)	0.8658(3)	0.4304(3)	0.0345(8)
O4	0.3501(3)	0.8463(3)	0.4934(3)	0.0320(8)

Table 4. Bond lengths (Å).

C1-O2	1.403(5)	C1-O1	1.449(5)
C1-C2	1.518(6)	C1-C6	1.521(6)
C2-C3	1.531(7)	C2-H2A	0.99
C2-H2B	0.99	C3-C14	1.505(7)
C3-C4	1.536(7)	C3-H3	1.0
C4-C5	1.524(8)	C4-H4A	0.99
C4-H4B	0.99	C5-C6	1.528(7)
C5-H5A	0.99	C5-H5B	0.99
C6-C7	1.530(7)	C6-H6	1.0
C7-C8	1.510(7)	C7-H7A	0.99
C7-H7B	0.99	C8-C13	1.394(7)
C8-C9	1.409(7)	C9-C10	1.394(8)
C9-C16	1.477(7)	C10-C11	1.386(8)
C10-H10	0.95	C11-C12	1.394(7)
C11-H11	0.95	C12-C13	1.388(7)
C12-H12	0.95	C13-O1	1.389(5)
C14-C15	1.303(9)	C14-H14	0.95

C15-H15A	0.95	C15-H15B	0.95
C16-C17	1.325(8)	C16-H16	0.95
C17-H17A	0.95	C17-H17B	0.95
C18-O4	1.419(5)	C18-O3	1.434(5)
C18-C19	1.510(6)	C18-C23	1.526(6)
C19-C20	1.546(7)	C19-H19A	0.99
C19-H19B	0.99	C20-C31	1.503(7)
C20-C21	1.540(7)	C20-H20	1.0
C21-C22	1.524(7)	C21-H21A	0.99
C21-H21B	0.99	C22-C23	1.535(6)
C22-H22A	0.99	C22-H22B	0.99
C23-C24	1.515(7)	C23-H23	1.0
C24-C25	1.512(7)	C24-H24A	0.99
C24-H24B	0.99	C25-C30	1.387(7)
C25-C26	1.411(7)	C26-C27	1.387(8)
C26-C33	1.475(9)	C27-C28	1.384(9)
C27-H27	0.95	C28-C29	1.386(8)
C28-H28	0.95	C29-C30	1.394(7)
C29-H29	0.95	C30-O3	1.382(6)
C31-C32	1.308(9)	C31-H31	0.95
C32-H32A	0.95	C32-H32B	0.95
C33-C34	1.286(9)	C33-H33	0.95
C34-H34A	0.95	C34-H34B	0.95
O2-H2	0.84	O4-H4	0.84

Table 5. Bond angles (°).

O2-C1-O1	109.0(4)	O2-C1-C2	111.8(4)
O1-C1-C2	106.9(3)	O2-C1-C6	107.6(4)
O1-C1-C6	109.1(4)	C2-C1-C6	112.4(4)
C1-C2-C3	110.6(4)	C1-C2-H2A	109.5
C3-C2-H2A	109.5	C1-C2-H2B	109.5
C3-C2-H2B	109.5	H2A-C2-H2B	108.1
C14-C3-C4	110.6(4)	C14-C3-C2	111.6(4)
C4-C3-C2	109.3(4)	C14-C3-H3	108.4
C4-C3-H3	108.4	C2-C3-H3	108.4

C5-C4-C3	112.4(4)	C5-C4-H4A	109.1
C3-C4-H4A	109.1	C5-C4-H4B	109.1
C3-C4-H4B	109.1	H4A-C4-H4B	107.9
C4-C5-C6	112.5(4)	C4-C5-H5A	109.1
C6-C5-H5A	109.1	C4-C5-H5B	109.1
C6-C5-H5B	109.1	H5A-C5-H5B	107.8
C1-C6-C5	111.0(4)	C1-C6-C7	109.4(4)
C5-C6-C7	112.2(4)	C1-C6-H6	108.1
C5-C6-H6	108.1	C7-C6-H6	108.1
C8-C7-C6	112.1(4)	C8-C7-H7A	109.2
C6-C7-H7A	109.2	C8-C7-H7B	109.2
C6-C7-H7B	109.2	H7A-C7-H7B	107.9
C13-C8-C9	118.6(5)	C13-C8-C7	120.3(4)
C9-C8-C7	121.2(4)	C10-C9-C8	119.7(5)
C10-C9-C16	120.1(5)	C8-C9-C16	120.1(5)
C11-C10-C9	120.7(5)	C11-C10-H10	119.7
C9-C10-H10	119.7	C10-C11-C12	120.3(5)
C10-C11-H11	119.9	C12-C11-H11	119.9
C13-C12-C11	119.0(5)	C13-C12-H12	120.5
C11-C12-H12	120.5	O1-C13-C12	115.6(4)
O1-C13-C8	122.6(4)	C12-C13-C8	121.8(4)
C15-C14-C3	125.8(6)	C15-C14-H14	117.1
C3-C14-H14	117.1	C14-C15-H15A	120.0
C14-C15-H15B	120.0	H15A-C15-H15B	120.0
C17-C16-C9	126.2(6)	C17-C16-H16	116.9
C9-C16-H16	116.9	C16-C17-H17A	120.0
C16-C17-H17B	120.0	H17A-C17-H17B	120.0
O4-C18-O3	108.5(4)	O4-C18-C19	111.7(4)
O3-C18-C19	106.1(4)	O4-C18-C23	108.1(4)
O3-C18-C23	109.6(4)	C19-C18-C23	112.7(4)
C18-C19-C20	111.3(4)	C18-C19-H19A	109.4
C20-C19-H19A	109.4	C18-C19-H19B	109.4
C20-C19-H19B	109.4	H19A-C19-H19B	108.0
C31-C20-C21	110.0(4)	C31-C20-C19	112.4(4)
C21-C20-C19	109.3(4)	C31-C20-H20	108.4

C21-C20-H20	108.4	C19-C20-H20	108.4
C22-C21-C20	111.8(4)	C22-C21-H21A	109.3
C20-C21-H21A	109.3	C22-C21-H21B	109.3
C20-C21-H21B	109.3	H21A-C21-H21B	107.9
C21-C22-C23	111.6(4)	C21-C22-H22A	109.3
C23-C22-H22A	109.3	C21-C22-H22B	109.3
C23-C22-H22B	109.3	H22A-C22-H22B	108.0
C24-C23-C18	110.4(4)	C24-C23-C22	113.2(4)
C18-C23-C22	110.6(4)	C24-C23-H23	107.5
C18-C23-H23	107.5	C22-C23-H23	107.5
C25-C24-C23	110.4(4)	C25-C24-H24A	109.6
C23-C24-H24A	109.6	C25-C24-H24B	109.6
C23-C24-H24B	109.6	H24A-C24-H24B	108.1
C30-C25-C26	118.6(5)	C30-C25-C24	119.3(4)
C26-C25-C24	122.1(4)	C27-C26-C25	119.7(5)
C27-C26-C33	121.1(5)	C25-C26-C33	119.1(5)
C28-C27-C26	120.8(5)	C28-C27-H27	119.6
C26-C27-H27	119.6	C27-C28-C29	120.1(5)
C27-C28-H28	120.0	C29-C28-H28	120.0
C28-C29-C30	119.4(5)	C28-C29-H29	120.3
C30-C29-H29	120.3	O3-C30-C25	124.1(4)
O3-C30-C29	114.6(4)	C25-C30-C29	121.3(5)
C32-C31-C20	125.0(6)	C32-C31-H31	117.5
C20-C31-H31	117.5	C31-C32-H32A	120.0
C31-C32-H32B	120.0	H32A-C32-H32B	120.0
C34-C33-C26	129.1(6)	C34-C33-H33	115.4
C26-C33-H33	115.4	C33-C34-H34A	120.0
C33-C34-H34B	120.0	H34A-C34-H34B	120.0
C13-O1-C1	115.5(3)	C1-O2-H2	109.5
C30-O3-C18	117.3(3)	C18-O4-H4	109.5

Table 6. Torsion angles (°).

O2-C1-C2-C3	-62.8(5)	O1-C1-C2-C3	178.0(4)
C6-C1-C2-C3	58.3(5)	C1-C2-C3-C14	179.6(4)
C1-C2-C3-C4	-57.8(5)	C14-C3-C4-C5	178.9(4)

C2-C3-C4-C5	55.6(6)	C3-C4-C5-C6	-52.9(6)
O2-C1-C6-C5	69.5(5)	O1-C1-C6-C5	-172.4(4)
C2-C1-C6-C5	-54.0(5)	O2-C1-C6-C7	-54.8(5)
O1-C1-C6-C7	63.3(5)	C2-C1-C6-C7	-178.3(4)
C4-C5-C6-C1	51.0(6)	C4-C5-C6-C7	173.7(4)
C1-C6-C7-C8	-42.8(5)	C5-C6-C7-C8	-166.4(4)
C6-C7-C8-C13	12.1(6)	C6-C7-C8-C9	-168.5(4)
C13-C8-C9-C10	-1.0(7)	C7-C8-C9-C10	179.6(5)
C13-C8-C9-C16	177.0(5)	C7-C8-C9-C16	-2.3(7)
C8-C9-C10-C11	-0.3(8)	C16-C9-C10-C11	-178.4(5)
C9-C10-C11-C12	1.1(9)	C10-C11-C12-C13	-0.5(9)
C11-C12-C13-O1	179.8(5)	C11-C12-C13-C8	-0.9(8)
C9-C8-C13-O1	-179.0(4)	C7-C8-C13-O1	0.3(7)
C9-C8-C13-C12	1.6(7)	C7-C8-C13-C12	-179.0(5)
C4-C3-C14-C15	118.8(7)	C2-C3-C14-C15	-119.2(7)
C10-C9-C16-C17	-25.8(9)	C8-C9-C16-C17	156.1(6)
O4-C18-C19-C20	-65.7(5)	O3-C18-C19-C20	176.2(4)
C23-C18-C19-C20	56.3(5)	C18-C19-C20-C31	-178.5(4)
C18-C19-C20-C21	-56.0(5)	C31-C20-C21-C22	-179.9(4)
C19-C20-C21-C22	56.3(5)	C20-C21-C22-C23	-56.1(5)
O4-C18-C23-C24	-56.5(5)	O3-C18-C23-C24	61.7(5)
C19-C18-C23-C24	179.6(4)	O4-C18-C23-C22	69.6(5)
O3-C18-C23-C22	-172.3(4)	C19-C18-C23-C22	-54.4(5)
C21-C22-C23-C24	178.2(4)	C21-C22-C23-C18	53.8(5)
C18-C23-C24-C25	-49.1(5)	C22-C23-C24-C25	-173.6(4)
C23-C24-C25-C30	19.5(6)	C23-C24-C25-C26	-159.6(5)
C30-C25-C26-C27	-0.5(8)	C24-C25-C26-C27	178.5(5)
C30-C25-C26-C33	-179.3(6)	C24-C25-C26-C33	-0.2(8)
C25-C26-C27-C28	0.9(9)	C33-C26-C27-C28	179.6(6)
C26-C27-C28-C29	-0.4(9)	C27-C28-C29-C30	-0.3(9)
C26-C25-C30-O3	178.8(5)	C24-C25-C30-O3	-0.3(7)
C26-C25-C30-C29	-0.3(8)	C24-C25-C30-C29	-179.3(5)
C28-C29-C30-O3	-178.5(5)	C28-C29-C30-C25	0.7(8)
C21-C20-C31-C32	105.7(7)	C19-C20-C31-C32	-132.3(6)
C27-C26-C33-C34	-3.5(12)	C25-C26-C33-C34	175.3(7)

C12-C13-O1-C1	-160.0(4)	C8-C13-O1-C1	20.6(6)
O2-C1-O1-C13	65.0(5)	C2-C1-O1-C13	-174.0(4)
C6-C1-O1-C13	-52.2(5)	C25-C30-O3-C18	12.7(7)
C29-C30-O3-C18	-168.1(4)	O4-C18-O3-C30	75.2(5)
C19-C18-O3-C30	-164.6(4)	C23-C18-O3-C30	-42.6(5)

Table 7. Anisotropic atomic displacement parameters ($Å^2$).

The anisotropic atomic displacement factor exponent takes the form: $-2\pi^2[h^2 a^{*2} U_{11} + ... + 2 h k a^* b^* U_{12}]$

	U_{11}	**U_{22}**	**U_{33}**	**U_{23}**	**U_{13}**	**U_{12}**
C1	0.031(2)	0.023(2)	0.034(2)	-0.0088(17)	-0.0083(18)	-0.0052(17)
C2	0.039(3)	0.030(2)	0.034(2)	-0.0088(19)	-0.011(2)	-0.0058(19)
C3	0.039(3)	0.034(2)	0.035(2)	-0.010(2)	-0.010(2)	-0.010(2)
C4	0.041(3)	0.045(3)	0.043(3)	-0.020(2)	-0.004(2)	-0.005(2)
C5	0.036(3)	0.036(3)	0.043(3)	-0.015(2)	-0.010(2)	0.002(2)
C6	0.025(2)	0.028(2)	0.038(2)	-0.0097(19)	-0.0082(18)	-0.0035(17)
C7	0.030(2)	0.030(2)	0.042(3)	-0.010(2)	-0.016(2)	0.0025(18)
C8	0.029(2)	0.033(2)	0.037(2)	-0.0062(19)	-0.0104(19)	-0.0082(18)
C9	0.037(3)	0.035(2)	0.038(3)	-0.004(2)	-0.015(2)	-0.009(2)
C10	0.054(3)	0.047(3)	0.033(3)	-0.005(2)	-0.015(2)	-0.011(2)
C11	0.059(4)	0.043(3)	0.036(3)	-0.013(2)	-0.014(2)	-0.006(3)
C12	0.051(3)	0.032(2)	0.037(3)	-0.011(2)	-0.014(2)	0.001(2)
C13	0.035(2)	0.030(2)	0.031(2)	-0.0069(18)	-0.0116(19)	-0.0069(18)
C14	0.056(3)	0.042(3)	0.035(3)	-0.011(2)	-0.009(2)	-0.013(2)
C15	0.086(5)	0.069(4)	0.041(3)	-0.011(3)	-0.025(3)	-0.017(4)
C16	0.042(3)	0.039(3)	0.043(3)	0.004(2)	-0.017(2)	-0.007(2)
C17	0.060(4)	0.055(4)	0.058(4)	0.005(3)	-0.028(3)	-0.004(3)
C18	0.026(2)	0.027(2)	0.034(2)	-0.0048(18)	-0.0092(18)	-0.0043(17)
C19	0.029(2)	0.031(2)	0.037(3)	-0.0112(19)	-0.0098(19)	-0.0019(18)
C20	0.036(3)	0.035(2)	0.032(2)	-0.0095(19)	-0.008(2)	-0.0062(19)
C21	0.042(3)	0.030(2)	0.037(3)	-0.003(2)	-0.011(2)	-0.006(2)
C22	0.037(2)	0.025(2)	0.034(2)	-0.0029(18)	-0.011(2)	-0.0042(18)
C23	0.029(2)	0.028(2)	0.034(2)	-0.0072(18)	-0.0110(19)	-0.0020(17)
C24	0.033(2)	0.030(2)	0.037(3)	-0.0118(19)	-0.010(2)	-0.0009(18)
C25	0.033(2)	0.039(3)	0.034(2)	-0.009(2)	-0.012(2)	-0.004(2)

C26	0.040(3)	0.056(3)	0.036(3)	-0.013(2)	-0.011(2)	-0.004(2)
C27	0.048(3)	0.066(4)	0.038(3)	-0.016(3)	-0.014(2)	-0.005(3)
C28	0.050(3)	0.053(3)	0.039(3)	0.000(2)	-0.019(2)	-0.012(3)
C29	0.043(3)	0.040(3)	0.042(3)	-0.004(2)	-0.019(2)	-0.005(2)
C30	0.030(2)	0.036(2)	0.034(2)	-0.0067(19)	-0.0104(19)	-0.0078(19)
C31	0.049(3)	0.037(3)	0.042(3)	-0.009(2)	-0.006(2)	-0.001(2)
C32	0.085(5)	0.056(4)	0.043(3)	-0.021(3)	-0.013(3)	0.000(3)
C33	0.060(4)	0.079(5)	0.047(3)	-0.029(3)	-0.023(3)	0.022(3)
C34	0.067(4)	0.060(4)	0.054(4)	-0.027(3)	-0.016(3)	-0.006(3)
O1	0.0414(19)	0.0260(16)	0.0304(17)	-0.0066(13)	-0.0136(14)	-0.0018(13)
O2	0.0275(16)	0.0322(17)	0.0419(19)	-0.0065(14)	-0.0127(14)	-0.0069(13)
O3	0.0324(17)	0.0332(17)	0.0373(18)	-0.0084(14)	-0.0156(14)	0.0046(13)
O4	0.0289(16)	0.0252(15)	0.0413(19)	-0.0053(14)	-0.0110(14)	-0.0047(12)

Table 8. Hydrogen atomic coordinates and isotropic atomic displacement parameters ($Å^2$).

	x/a	**y/b**	**z/c**	**U(eq)**
H2A	0.7792	0.9334	0.3551	0.041
H2B	0.6188	0.9256	0.3789	0.041
H3	0.6806	0.7342	0.3258	0.042
H4A	0.9164	0.6526	0.2563	0.052
H4B	0.9651	0.7654	0.2750	0.052
H5A	0.9886	0.5970	0.4189	0.047
H5B	0.8325	0.5753	0.4443	0.047
H6	0.9135	0.7774	0.4828	0.036
H7A	0.7808	0.5764	0.6336	0.04
H7B	0.9221	0.6142	0.6293	0.04
H10	0.6655	0.7239	0.9639	0.053
H11	0.5499	0.9195	0.9056	0.055
H12	0.5528	0.9929	0.7209	0.048
H14	0.8208	0.9185	0.1513	0.053
H15A	0.6158	0.7958	0.1589	0.075
H15B	0.6915	0.9006	0.0557	0.075
H16	0.8295	0.4970	0.8099	0.051
H17A	0.8458	0.5721	0.9862	0.071

H17B	0.9032	0.4346	0.9589	0.071
H19A	0.0269	0.8201	0.6300	0.038
H19B	0.1073	0.9317	0.6111	0.038
H20	0.2563	0.8007	0.7136	0.042
H21A	0.2260	0.5922	0.7976	0.045
H21B	0.1018	0.6071	0.7466	0.045
H22A	0.3043	0.5082	0.6392	0.04
H22B	0.3870	0.6176	0.6221	0.04
H23	0.1603	0.6400	0.5365	0.037
H24A	0.4461	0.6486	0.4181	0.04
H24B	0.3572	0.5477	0.4251	0.04
H27	0.3458	0.7360	0.0658	0.06
H28	0.1934	0.9187	0.0849	0.057
H29	0.1129	0.9759	0.2534	0.049
H31	-0.0312	0.8031	0.8379	0.055
H32A	0.1885	0.8434	0.8920	0.075
H32B	0.0238	0.8576	0.9638	0.075
H33	0.4844	0.5232	0.2737	0.075
H34A	0.4793	0.5550	0.0625	0.07
H34B	0.5660	0.4405	0.1326	0.07
H2	0.5274	0.7657	0.5296	0.05
H4	0.3375	0.9236	0.4825	0.048

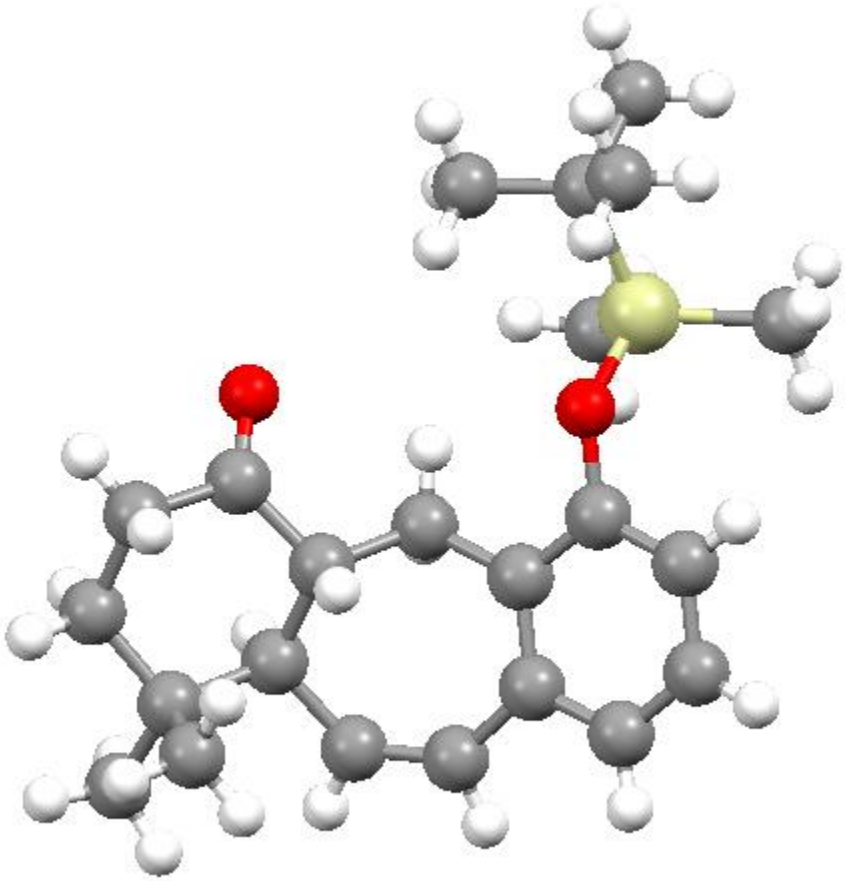

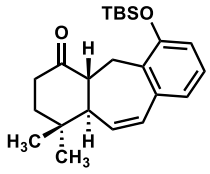

36

A specimen of $C_{23}H_{34}O_2Si$, approximate dimensions 0.126 mm x 0.214 mm x 0.304 mm, was used for the X-ray crystallographic analysis. The X-ray intensity data were measured.

The integration of the data using a monoclinic unit cell yielded a total of 49271 reflections to a maximum θ angle of 27.59° (0.77Å resolution), of which 10144 were independent (average redundancy 4.857, completeness = 99.6%, R_{int} = 4.22%, R_{sig} = 3.65%) and 6458 (63.66%) were greater than $2\sigma(F^2)$. The final cell constants of a = 21.374(2) Å, b = 11.8926(11) Å, c = 18.8889(17) Å, β = 113.973(2)°, volume = 4387.2(7) $Å^3$, are based upon the refinement of the XYZ-centroids of reflections above 20 σ(I). The calculated minimum and maximum transmission coefficients (based on crystal size) are 0.6881 and 0.7456.

The structure was solved and refined using the Bruker SHELXTL Software Package, using the space group P 1 21/c 1, with Z = 8 for the formula unit, $C_{23}H_{34}O_2Si$. The final anisotropic full-matrix least-squares refinement on F^2 with 510 variables converged at R1 = 4.62%, for the observed data and wR2 = 13.68% for all data. The goodness-of-fit was 1.015. The largest peak in the final difference electron density synthesis was 0.431 $e^-/Å^3$ and the largest hole was –0.199 $e^-/Å^3$ with an RMS deviation of 0.042 $e^-/Å^3$. On the basis of the final model, the calculated density was 1.122 g/cm^3 and F(000), 1616 e^-.

Table 1. Sample and crystal data.

Chemical formula	$C_{23}H_{34}O_2Si$	
Formula weight	370.59 g/mol	
Temperature	200(2) K	
Wavelength	0.71073 Å	
Crystal size	0.126 x 0.214 x 0.304 mm	
Crystal system	monoclinic	
Space group	P 1 21/c 1	
Unit cell dimensions	a = 21.374(2) Å	α = 90°
	b = 11.8926(11) Å	β = 113.973(2)°

	c = 18.8889(17) Å	γ = 90°
Volume	4387.2(7) $Å^3$	
Z	8	
Density (calculated)	1.122 g/cm^3	
Absorption coefficient	0.120 mm^{-1}	
F(000)	1616	

Table 2. Data collection and structure refinement.

Theta range for data collection	1.04 to 27.59°	
Index ranges	-27<=h<=27, -15<=k<=15, -24<=l<=24	
Reflections collected	49271	
Independent reflections	10144 [R(int) = 0.0422]	
Max. and min. transmission	0.7456 and 0.6881	
Structure solution technique	direct methods	
Structure solution program	SHELXS-97 (Sheldrick 2008)	
Refinement method	Full-matrix least-squares on F^2	
Refinement program	SHELXL-2014/7 (Sheldrick, 2014)	
Function minimized	$\Sigma\ w(F_o^2 - F_c^2)^2$	
Data / restraints / parameters	10144 / 38 / 510	
Goodness-of-fit on F^2	1.015	
Δ/σ_{max}	0.001	
Final R indices	6458 data; I>2σ(I)	R1 = 0.0462, wR2 = 0.1156
	all data	R1 = 0.0840, wR2 = 0.1368
Weighting scheme	$w=1/[\sigma^2(F_o^2)+(0.0648P)^2+0.8760P]$ where $P=(F_o^2+2F_c^2)/3$	
Largest diff. peak and hole	0.431 and -0.199 $eÅ^{-3}$	
R.M.S. deviation from mean	0.042 $eÅ^{-3}$	

Table 3. Atomic coordinates and equivalent isotropic atomic displacement parameters ($Å^2$).

U(eq) is defined as one third of the trace of the orthogonalized U_{ij} tensor.

	x/a	**y/b**	**z/c**	**U(eq)**
Si1	0.86745(2)	0.85277(4)	0.72854(3)	0.03065(12)
Si2A	0.62659(3)	0.59908(5)	0.26961(3)	0.03217(16)
Si2B	0.60037(16)	0.6101(3)	0.29253(19)	0.03217(16)
O1	0.84197(6)	0.43049(12)	0.71304(8)	0.0499(3)
O2	0.82346(5)	0.78811(9)	0.64475(6)	0.0335(3)
O3	0.66283(7)	0.17810(12)	0.27761(8)	0.0546(4)
O4	0.66954(6)	0.52863(10)	0.34959(7)	0.0385(3)
C1	0.79457(8)	0.41058(14)	0.65174(10)	0.0342(4)
C2	0.78908(9)	0.30142(15)	0.60949(12)	0.0452(5)
C3	0.72256(9)	0.24200(15)	0.59982(12)	0.0454(5)
C4	0.65800(9)	0.31379(15)	0.56191(10)	0.0385(4)
C5	0.66885(8)	0.42694(14)	0.60786(10)	0.0346(4)
C6	0.60612(9)	0.50034(16)	0.57801(12)	0.0442(5)
C7	0.59641(9)	0.60781(16)	0.55625(11)	0.0451(5)
C8	0.64346(8)	0.69831(14)	0.55543(10)	0.0359(4)
C9	0.61575(9)	0.78875(16)	0.50489(11)	0.0431(4)
C10	0.65645(9)	0.87701(16)	0.50175(11)	0.0428(4)
C11	0.72563(9)	0.87726(15)	0.54934(10)	0.0377(4)
C12	0.75386(8)	0.78902(14)	0.60055(9)	0.0309(4)
C13	0.71376(8)	0.69840(13)	0.60454(9)	0.0299(3)
C14	0.74461(8)	0.60115(13)	0.65793(9)	0.0327(4)
C15	0.73446(8)	0.48918(13)	0.61420(9)	0.0302(4)
C16	0.59898(10)	0.24687(17)	0.56854(14)	0.0576(6)
C17	0.64159(11)	0.33444(18)	0.47589(11)	0.0544(5)
C18	0.85389(10)	0.00733(15)	0.71576(11)	0.0441(5)
C19	0.83831(10)	0.80192(17)	0.80288(11)	0.0474(5)
C20	0.95870(9)	0.81297(15)	0.75235(10)	0.0394(4)
C21	0.00477(10)	0.8709(2)	0.82906(12)	0.0628(6)
C22	0.96741(11)	0.68488(19)	0.76130(17)	0.0724(7)

C23	0.98060(10)	0.8524(2)	0.68858(12)	0.0558(6)
C24	0.71175(9)	0.15669(14)	0.33712(11)	0.0375(4)
C25	0.72116(10)	0.04356(16)	0.37555(13)	0.0512(5)
C26	0.78979(10)	0.99309(16)	0.38410(12)	0.0497(5)
C27	0.85190(10)	0.06954(15)	0.42477(10)	0.0417(4)
C28	0.83760(9)	0.18665(14)	0.38352(10)	0.0362(4)
C29	0.89739(9)	0.26531(16)	0.41849(11)	0.0431(4)
C30	0.90272(9)	0.37117(16)	0.44411(11)	0.0419(4)
C31	0.85166(9)	0.45427(14)	0.44449(10)	0.0347(4)
C32	0.87484(10)	0.54397(16)	0.49675(11)	0.0427(4)
C33	0.83080(10)	0.62679(16)	0.49956(11)	0.0457(5)
C34	0.76230(10)	0.62229(15)	0.44979(10)	0.0408(4)
C35	0.73829(8)	0.53465(14)	0.39683(9)	0.0333(4)
C36	0.78217(8)	0.44971(13)	0.39325(9)	0.0309(4)
C37	0.75539(9)	0.35388(13)	0.33689(10)	0.0341(4)
C38	0.76928(8)	0.23902(14)	0.37709(10)	0.0326(4)
C39	0.91281(11)	0.01242(18)	0.41566(13)	0.0568(6)
C40	0.86780(12)	0.08037(18)	0.51144(11)	0.0552(5)
C41A	0.6433(3)	0.7521(3)	0.2847(4)	0.0468(9)
C42A	0.65349(13)	0.5498(2)	0.19288(14)	0.0472(6)
C43A	0.53516(10)	0.56162(19)	0.24637(13)	0.0422(5)
C44A	0.51546(13)	0.5995(3)	0.31246(16)	0.0643(8)
C45A	0.48771(14)	0.6209(3)	0.17130(16)	0.0611(8)
C46A	0.52523(17)	0.4335(2)	0.2348(2)	0.0740(11)
C41B	0.6320(19)	0.7552(16)	0.291(3)	0.0468(9)
C42B	0.5429(7)	0.6116(13)	0.3449(8)	0.0472(6)
C43B	0.5595(5)	0.5482(9)	0.1942(6)	0.0422(5)
C44B	0.6099(6)	0.5397(14)	0.1549(9)	0.0643(8)
C45B	0.5003(7)	0.6259(15)	0.1429(10)	0.0611(8)
C46B	0.5313(10)	0.4309(12)	0.1970(13)	0.0740(11)

Table 4. Bond lengths (Å).

Si1-O2	1.6646(12)	Si1-C19	1.8535(19)
Si1-C18	1.8612(18)	Si1-C20	1.8756(18)
Si2A-O4	1.6432(13)	Si2A-C41A	1.855(3)

Si2A-C42A	1.858(2)	Si2A-C43A	1.874(2)
Si2B-O4	1.730(3)	Si2B-C41B	1.859(14)
Si2B-C43B	1.854(10)	Si2B-C42B	1.864(11)
O1-C1	1.212(2)	O2-C12	1.3788(19)
O3-C24	1.211(2)	O4-C35	1.3767(19)
C1-C2	1.503(2)	C1-C15	1.512(2)
C2-C3	1.531(3)	C2-H2A	0.99
C2-H2B	0.99	C3-C4	1.531(2)
C3-H3A	0.99	C3-H3B	0.99
C4-C17	1.536(3)	C4-C16	1.539(2)
C4-C5	1.567(2)	C5-C6	1.504(2)
C5-C15	1.547(2)	C5-H5	1.0
C6-C7	1.333(3)	C6-H6	0.95
C7-C8	1.477(2)	C7-H7	0.95
C8-C9	1.400(2)	C8-C13	1.409(2)
C9-C10	1.380(3)	C9-H9	0.95
C10-C11	1.384(2)	C10-H10	0.95
C11-C12	1.388(2)	C11-H11	0.95
C12-C13	1.398(2)	C13-C14	1.500(2)
C14-C15	1.535(2)	C14-H14A	0.99
C14-H14B	0.99	C15-H15	1.0
C16-H16A	0.98	C16-H16B	0.98
C16-H16C	0.98	C17-H17A	0.98
C17-H17B	0.98	C17-H17C	0.98
C18-H18A	0.98	C18-H18B	0.98
C18-H18C	0.98	C19-H19A	0.98
C19-H19B	0.98	C19-H19C	0.98
C20-C23	1.533(3)	C20-C22	1.536(3)
C20-C21	1.544(3)	C21-H21A	0.98
C21-H21B	0.98	C21-H21C	0.98
C22-H22A	0.98	C22-H22B	0.98
C22-H22C	0.98	C23-H23A	0.98
C23-H23B	0.98	C23-H23C	0.98
C24-C25	1.503(3)	C24-C38	1.512(2)
C25-C26	1.532(3)	C25-H25A	0.99

C25-H25B	0.99	C26-C27	1.533(3)
C26-H26A	0.99	C26-H26B	0.99
C27-C40	1.536(3)	C27-C39	1.539(3)
C27-C28	1.564(2)	C28-C29	1.503(3)
C28-C38	1.546(2)	C28-H28	1.0
C29-C30	1.337(3)	C29-H29	0.95
C30-C31	1.474(2)	C30-H30	0.95
C31-C32	1.400(2)	C31-C36	1.406(2)
C32-C33	1.378(3)	C32-H32	0.95
C33-C34	1.383(3)	C33-H33	0.95
C34-C35	1.390(2)	C34-H34	0.95
C35-C36	1.399(2)	C36-C37	1.505(2)
C37-C38	1.532(2)	C37-H37A	0.99
C37-H37B	0.99	C38-H38	1.0
C39-H39A	0.98	C39-H39B	0.98
C39-H39C	0.98	C40-H40A	0.98
C40-H40B	0.98	C40-H40C	0.98
C41A-H41A	0.98	C41A-H41B	0.98
C41A-H41C	0.98	C42A-H42A	0.98
C42A-H42B	0.98	C42A-H42C	0.98
C43A-C45A	1.539(3)	C43A-C44A	1.538(3)
C43A-C46A	1.542(3)	C44A-H44A	0.98
C44A-H44B	0.98	C44A-H44C	0.98
C45A-H45A	0.98	C45A-H45B	0.98
C45A-H45C	0.98	C46A-H46A	0.98
C46A-H46B	0.98	C46A-H46C	0.98
C41B-H41D	0.98	C41B-H41E	0.98
C41B-H41F	0.98	C42B-H42D	0.98
C42B-H42E	0.98	C42B-H42F	0.98
C43B-C46B	1.528(12)	C43B-C44B	1.540(11)
C43B-C45B	1.550(11)	C44B-H44D	0.98
C44B-H44E	0.98	C44B-H44F	0.98
C45B-H45D	0.98	C45B-H45E	0.98
C45B-H45F	0.98	C46B-H46D	0.98
C46B-H46E	0.98	C46B-H46F	0.98

Table 5. Bond angles (°).

O2-Si1-C19	109.62(8)	O2-Si1-C18	109.57(8)
C19-Si1-C18	109.75(9)	O2-Si1-C20	104.00(7)
C19-Si1-C20	111.88(9)	C18-Si1-C20	111.86(9)
O4-Si2A-C41A	111.0(2)	O4-Si2A-C42A	108.78(9)
C41A-Si2A-C42A	109.16(17)	O4-Si2A-C43A	103.53(8)
C41A-Si2A-C43A	112.75(17)	C42A-Si2A-C43A	111.46(11)
O4-Si2B-C41B	107.8(13)	O4-Si2B-C43B	109.7(3)
C41B-Si2B-C43B	112.2(14)	O4-Si2B-C42B	104.8(5)
C41B-Si2B-C42B	108.9(10)	C43B-Si2B-C42B	113.0(6)
C12-O2-Si1	128.73(10)	C35-O4-Si2A	128.30(11)
C35-O4-Si2B	142.35(15)	O1-C1-C2	122.02(16)
O1-C1-C15	123.25(16)	C2-C1-C15	114.63(14)
C1-C2-C3	109.29(15)	C1-C2-H2A	109.8
C3-C2-H2A	109.8	C1-C2-H2B	109.8
C3-C2-H2B	109.8	H2A-C2-H2B	108.3
C2-C3-C4	114.55(15)	C2-C3-H3A	108.6
C4-C3-H3A	108.6	C2-C3-H3B	108.6
C4-C3-H3B	108.6	H3A-C3-H3B	107.6
C3-C4-C17	111.04(16)	C3-C4-C16	106.65(15)
C17-C4-C16	109.04(16)	C3-C4-C5	108.51(14)
C17-C4-C5	111.56(15)	C16-C4-C5	109.92(15)
C6-C5-C15	113.16(14)	C6-C5-C4	112.45(14)
C15-C5-C4	112.29(14)	C6-C5-H5	106.1
C15-C5-H5	106.1	C4-C5-H5	106.1
C7-C6-C5	132.49(16)	C7-C6-H6	113.8
C5-C6-H6	113.8	C6-C7-C8	132.88(17)
C6-C7-H7	113.6	C8-C7-H7	113.6
C9-C8-C13	119.40(16)	C9-C8-C7	117.76(15)
C13-C8-C7	122.81(16)	C10-C9-C8	120.95(16)
C10-C9-H9	119.5	C8-C9-H9	119.5
C9-C10-C11	119.98(17)	C9-C10-H10	120.0
C11-C10-H10	120.0	C10-C11-C12	119.89(16)
C10-C11-H11	120.1	C12-C11-H11	120.1
O2-C12-C11	118.98(14)	O2-C12-C13	119.71(14)

C11-C12-C13	121.19(15)	C12-C13-C8	118.57(15)
C12-C13-C14	121.27(14)	C8-C13-C14	120.14(15)
C13-C14-C15	112.31(13)	C13-C14-H14A	109.1
C15-C14-H14A	109.1	C13-C14-H14B	109.1
C15-C14-H14B	109.1	H14A-C14-H14B	107.9
C1-C15-C14	112.11(13)	C1-C15-C5	108.14(13)
C14-C15-C5	112.47(13)	C1-C15-H15	108.0
C14-C15-H15	108.0	C5-C15-H15	108.0
C4-C16-H16A	109.5	C4-C16-H16B	109.5
H16A-C16-H16B	109.5	C4-C16-H16C	109.5
H16A-C16-H16C	109.5	H16B-C16-H16C	109.5
C4-C17-H17A	109.5	C4-C17-H17B	109.5
H17A-C17-H17B	109.5	C4-C17-H17C	109.5
H17A-C17-H17C	109.5	H17B-C17-H17C	109.5
Si1-C18-H18A	109.5	Si1-C18-H18B	109.5
H18A-C18-H18B	109.5	Si1-C18-H18C	109.5
H18A-C18-H18C	109.5	H18B-C18-H18C	109.5
Si1-C19-H19A	109.5	Si1-C19-H19B	109.5
H19A-C19-H19B	109.5	Si1-C19-H19C	109.5
H19A-C19-H19C	109.5	H19B-C19-H19C	109.5
C23-C20-C22	109.16(18)	C23-C20-C21	108.59(16)
C22-C20-C21	109.69(18)	C23-C20-Si1	110.75(13)
C22-C20-Si1	110.15(13)	C21-C20-Si1	108.48(13)
C20-C21-H21A	109.5	C20-C21-H21B	109.5
H21A-C21-H21B	109.5	C20-C21-H21C	109.5
H21A-C21-H21C	109.5	H21B-C21-H21C	109.5
C20-C22-H22A	109.5	C20-C22-H22B	109.5
H22A-C22-H22B	109.5	C20-C22-H22C	109.5
H22A-C22-H22C	109.5	H22B-C22-H22C	109.5
C20-C23-H23A	109.5	C20-C23-H23B	109.5
H23A-C23-H23B	109.5	C20-C23-H23C	109.5
H23A-C23-H23C	109.5	H23B-C23-H23C	109.5
O3-C24-C25	122.15(17)	O3-C24-C38	123.20(16)
C25-C24-C38	114.61(16)	C24-C25-C26	109.64(16)
C24-C25-H25A	109.7	C26-C25-H25A	109.7

C24-C25-H25B	109.7	C26-C25-H25B	109.7
H25A-C25-H25B	108.2	C25-C26-C27	114.69(16)
C25-C26-H26A	108.6	C27-C26-H26A	108.6
C25-C26-H26B	108.6	C27-C26-H26B	108.6
H26A-C26-H26B	107.6	C26-C27-C40	110.81(17)
C26-C27-C39	106.37(16)	C40-C27-C39	108.99(16)
C26-C27-C28	108.91(14)	C40-C27-C28	111.72(15)
C39-C27-C28	109.89(16)	C29-C28-C38	113.02(14)
C29-C28-C27	112.09(14)	C38-C28-C27	112.64(14)
C29-C28-H28	106.1	C38-C28-H28	106.1
C27-C28-H28	106.1	C30-C29-C28	132.65(17)
C30-C29-H29	113.7	C28-C29-H29	113.7
C29-C30-C31	132.73(17)	C29-C30-H30	113.6
C31-C30-H30	113.6	C32-C31-C36	119.13(16)
C32-C31-C30	117.62(16)	C36-C31-C30	123.20(16)
C33-C32-C31	121.34(17)	C33-C32-H32	119.3
C31-C32-H32	119.3	C32-C33-C34	119.81(17)
C32-C33-H33	120.1	C34-C33-H33	120.1
C33-C34-C35	119.84(17)	C33-C34-H34	120.1
C35-C34-H34	120.1	O4-C35-C34	119.35(15)
O4-C35-C36	119.43(15)	C34-C35-C36	121.16(16)
C35-C36-C31	118.71(15)	C35-C36-C37	120.76(15)
C31-C36-C37	120.52(15)	C36-C37-C38	112.53(13)
C36-C37-H37A	109.1	C38-C37-H37A	109.1
C36-C37-H37B	109.1	C38-C37-H37B	109.1
H37A-C37-H37B	107.8	C24-C38-C37	112.05(14)
C24-C38-C28	109.20(14)	C37-C38-C28	112.62(14)
C24-C38-H38	107.6	C37-C38-H38	107.6
C28-C38-H38	107.6	C27-C39-H39A	109.5
C27-C39-H39B	109.5	H39A-C39-H39B	109.5
C27-C39-H39C	109.5	H39A-C39-H39C	109.5
H39B-C39-H39C	109.5	C27-C40-H40A	109.5
C27-C40-H40B	109.5	H40A-C40-H40B	109.5
C27-C40-H40C	109.5	H40A-C40-H40C	109.5
H40B-C40-H40C	109.5	Si2A-C41A-H41A	109.5

Si2A-C41A-H41B	109.5	H41A-C41A-H41B	109.5
Si2A-C41A-H41C	109.5	H41A-C41A-H41C	109.5
H41B-C41A-H41C	109.5	Si2A-C42A-H42A	109.5
Si2A-C42A-H42B	109.5	H42A-C42A-H42B	109.5
Si2A-C42A-H42C	109.5	H42A-C42A-H42C	109.5
H42B-C42A-H42C	109.5	C45A-C43A-C44A	108.5(2)
C45A-C43A-C46A	108.8(2)	C44A-C43A-C46A	109.7(2)
C45A-C43A-Si2A	109.93(16)	C44A-C43A-Si2A	110.08(16)
C46A-C43A-Si2A	109.79(17)	C43A-C44A-H44A	109.5
C43A-C44A-H44B	109.5	H44A-C44A-H44B	109.5
C43A-C44A-H44C	109.5	H44A-C44A-H44C	109.5
H44B-C44A-H44C	109.5	C43A-C45A-H45A	109.5
C43A-C45A-H45B	109.5	H45A-C45A-H45B	109.5
C43A-C45A-H45C	109.5	H45A-C45A-H45C	109.5
H45B-C45A-H45C	109.5	C43A-C46A-H46A	109.5
C43A-C46A-H46B	109.5	H46A-C46A-H46B	109.5
C43A-C46A-H46C	109.5	H46A-C46A-H46C	109.5
H46B-C46A-H46C	109.5	Si2B-C41B-H41D	109.5
Si2B-C41B-H41E	109.5	H41D-C41B-H41E	109.5
Si2B-C41B-H41F	109.5	H41D-C41B-H41F	109.5
H41E-C41B-H41F	109.5	Si2B-C42B-H42D	109.5
Si2B-C42B-H42E	109.5	H42D-C42B-H42E	109.5
Si2B-C42B-H42F	109.5	H42D-C42B-H42F	109.5
H42E-C42B-H42F	109.5	C46B-C43B-C44B	108.6(9)
C46B-C43B-C45B	109.4(10)	C44B-C43B-C45B	106.9(8)
C46B-C43B-Si2B	111.1(10)	C44B-C43B-Si2B	111.8(8)
C45B-C43B-Si2B	108.8(9)	C43B-C44B-H44D	109.5
C43B-C44B-H44E	109.5	H44D-C44B-H44E	109.5
C43B-C44B-H44F	109.5	H44D-C44B-H44F	109.5
H44E-C44B-H44F	109.5	C43B-C45B-H45D	109.5
C43B-C45B-H45E	109.5	H45D-C45B-H45E	109.5
C43B-C45B-H45F	109.5	H45D-C45B-H45F	109.5
H45E-C45B-H45F	109.5	C43B-C46B-H46D	109.5
C43B-C46B-H46E	109.5	H46D-C46B-H46E	109.5
C43B-C46B-H46F	109.5	H46D-C46B-H46F	109.5

H46E-C46B-H46F 109.5

Table 6. Torsion angles (°).

C19-Si1-O2-C12	60.60(15)	C18-Si1-O2-C12	-59.90(15)
C20-Si1-O2-C12	-179.62(13)	C41A-Si2A-O4-C35	-51.00(19)
C42A-Si2A-O4-C35	69.13(17)	C43A-Si2A-O4-C35	-172.23(15)
C41B-Si2B-O4-C35	4.7(12)	C43B-Si2B-O4-C35	127.2(4)
C42B-Si2B-O4-C35	-111.2(5)	O1-C1-C2-C3	120.34(19)
C15-C1-C2-C3	-56.0(2)	C1-C2-C3-C4	53.6(2)
C2-C3-C4-C17	69.7(2)	C2-C3-C4-C16	-171.65(17)
C2-C3-C4-C5	-53.3(2)	C3-C4-C5-C6	-176.25(15)
C17-C4-C5-C6	61.11(19)	C16-C4-C5-C6	-59.97(19)
C3-C4-C5-C15	54.75(19)	C17-C4-C5-C15	-67.90(19)
C16-C4-C5-C15	171.02(15)	C15-C5-C6-C7	-0.1(3)
C4-C5-C6-C7	-128.6(2)	C5-C6-C7-C8	-2.6(4)
C6-C7-C8-C9	157.7(2)	C6-C7-C8-C13	-24.2(3)
C13-C8-C9-C10	0.9(3)	C7-C8-C9-C10	179.13(17)
C8-C9-C10-C11	-0.4(3)	C9-C10-C11-C12	-0.4(3)
Si1-O2-C12-C11	83.94(18)	Si1-O2-C12-C13	-99.91(16)
C10-C11-C12-O2	176.86(15)	C10-C11-C12-C13	0.8(3)
O2-C12-C13-C8	-176.30(14)	C11-C12-C13-C8	-0.2(2)
O2-C12-C13-C14	1.9(2)	C11-C12-C13-C14	177.93(15)
C9-C8-C13-C12	-0.6(2)	C7-C8-C13-C12	-178.71(16)
C9-C8-C13-C14	-178.79(16)	C7-C8-C13-C14	3.1(3)
C12-C13-C14-C15	-120.24(16)	C8-C13-C14-C15	57.9(2)
O1-C1-C15-C14	6.3(2)	C2-C1-C15-C14	-177.37(15)
O1-C1-C15-C5	-118.26(18)	C2-C1-C15-C5	58.08(18)
C13-C14-C15-C1	145.55(14)	C13-C14-C15-C5	-92.33(16)
C6-C5-C15-C1	174.68(14)	C4-C5-C15-C1	-56.68(18)
C6-C5-C15-C14	50.33(19)	C4-C5-C15-C14	178.97(13)
O2-Si1-C20-C23	59.78(15)	C19-Si1-C20-C23	178.01(13)
C18-Si1-C20-C23	-58.38(16)	O2-Si1-C20-C22	-61.07(17)
C19-Si1-C20-C22	57.16(18)	C18-Si1-C20-C22	-179.23(15)
O2-Si1-C20-C21	178.85(13)	C19-Si1-C20-C21	-62.91(16)
C18-Si1-C20-C21	60.69(16)	O3-C24-C25-C26	122.7(2)

C38-C24-C25-C26	-55.2(2)	C24-C25-C26-C27	53.4(2)
C25-C26-C27-C40	70.7(2)	C25-C26-C27-C39	-171.02(17)
C25-C26-C27-C28	-52.6(2)	C26-C27-C28-C29	-178.02(15)
C40-C27-C28-C29	59.2(2)	C39-C27-C28-C29	-61.9(2)
C26-C27-C28-C38	53.19(19)	C40-C27-C28-C38	-69.5(2)
C39-C27-C28-C38	169.34(15)	C38-C28-C29-C30	-0.8(3)
C27-C28-C29-C30	-129.4(2)	C28-C29-C30-C31	-3.7(4)
C29-C30-C31-C32	160.0(2)	C29-C30-C31-C36	-22.5(3)
C36-C31-C32-C33	0.8(3)	C30-C31-C32-C33	178.41(17)
C31-C32-C33-C34	-0.3(3)	C32-C33-C34-C35	-0.4(3)
Si2A-O4-C35-C34	79.95(19)	Si2B-O4-C35-C34	43.3(3)
Si2A-O4-C35-C36	-103.06(17)	Si2B-O4-C35-C36	-139.7(2)
C33-C34-C35-O4	177.53(16)	C33-C34-C35-C36	0.6(3)
O4-C35-C36-C31	-176.98(14)	C34-C35-C36-C31	0.0(2)
O4-C35-C36-C37	1.7(2)	C34-C35-C36-C37	178.67(15)
C32-C31-C36-C35	-0.6(2)	C30-C31-C36-C35	-178.09(15)
C32-C31-C36-C37	-179.37(15)	C30-C31-C36-C37	3.2(2)
C35-C36-C37-C38	-122.19(16)	C31-C36-C37-C38	56.5(2)
O3-C24-C38-C37	4.3(2)	C25-C24-C38-C37	-177.88(15)
O3-C24-C38-C28	-121.19(18)	C25-C24-C38-C28	56.63(19)
C36-C37-C38-C24	144.64(14)	C36-C37-C38-C28	-91.78(17)
C29-C28-C38-C24	176.68(14)	C27-C28-C38-C24	-55.02(18)
C29-C28-C38-C37	51.52(19)	C27-C28-C38-C37	179.83(14)
O4-Si2A-C43A-C45A	-179.43(18)	C41A-Si2A-C43A-C45A	60.5(3)
C42A-Si2A-C43A-C45A	-62.7(2)	O4-Si2A-C43A-C44A	61.04(19)
C41A-Si2A-C43A-C44A	-59.0(3)	C42A-Si2A-C43A-C44A	177.81(18)
O4-Si2A-C43A-C46A	-59.8(2)	C41A-Si2A-C43A-C46A	-179.9(3)
C42A-Si2A-C43A-C46A	56.9(2)	O4-Si2B-C43B-C46B	62.5(9)
C41B-Si2B-C43B-C46B	-177.7(13)	C42B-Si2B-C43B-C46B	-54.0(10)
O4-Si2B-C43B-C44B	-59.0(8)	C41B-Si2B-C43B-C44B	60.8(14)
C42B-Si2B-C43B-C44B	-175.6(9)	O4-Si2B-C43B-C45B	-176.9(7)
C41B-Si2B-C43B-C45B	-57.1(14)	C42B-Si2B-C43B-C45B	66.5(9)

Table 7. Anisotropic atomic displacement parameters ($Å^2$).

The anisotropic atomic displacement factor exponent takes the form:
$-2\pi^2[h^2 a^{*2} U_{11} + ... + 2 h k a^* b^* U_{12}]$

	U_{11}	U_{22}	U_{33}	U_{23}	U_{13}	U_{12}
Si1	0.0311(2)	0.0273(2)	0.0334(3)	-0.00358(19)	0.0129(2)	-0.00249(18)
Si2A	0.0306(3)	0.0271(3)	0.0388(3)	0.0028(2)	0.0140(2)	0.0006(2)
Si2B	0.0306(3)	0.0271(3)	0.0388(3)	0.0028(2)	0.0140(2)	0.0006(2)
O1	0.0385(7)	0.0497(8)	0.0459(8)	-0.0020(6)	0.0011(6)	0.0069(6)
O2	0.0284(6)	0.0344(6)	0.0361(6)	-0.0073(5)	0.0116(5)	-0.0032(5)
O3	0.0463(8)	0.0496(8)	0.0517(9)	-0.0024(7)	0.0034(7)	-0.0046(7)
O4	0.0325(6)	0.0344(6)	0.0471(7)	0.0060(6)	0.0148(6)	0.0025(5)
C1	0.0301(8)	0.0338(9)	0.0366(10)	0.0028(8)	0.0114(8)	-0.0012(7)
C2	0.0410(10)	0.0365(10)	0.0535(12)	-0.0034(9)	0.0143(9)	0.0043(8)
C3	0.0464(11)	0.0311(9)	0.0512(12)	-0.0024(9)	0.0121(9)	-0.0041(8)
C4	0.0369(9)	0.0302(9)	0.0402(10)	0.0009(8)	0.0073(8)	-0.0064(7)
C5	0.0330(9)	0.0334(9)	0.0357(9)	0.0031(7)	0.0122(8)	-0.0037(7)
C6	0.0288(9)	0.0427(11)	0.0609(12)	0.0010(9)	0.0179(9)	-0.0069(8)
C7	0.0252(9)	0.0424(10)	0.0612(12)	0.0025(9)	0.0109(8)	0.0002(8)
C8	0.0302(8)	0.0337(9)	0.0411(10)	0.0002(8)	0.0115(8)	0.0014(7)
C9	0.0324(9)	0.0423(11)	0.0451(11)	0.0033(9)	0.0061(8)	0.0059(8)
C10	0.0451(10)	0.0374(10)	0.0409(11)	0.0091(8)	0.0123(9)	0.0053(8)
C11	0.0417(10)	0.0334(9)	0.0384(10)	0.0017(8)	0.0166(8)	-0.0029(8)
C12	0.0306(8)	0.0314(9)	0.0315(9)	-0.0053(7)	0.0134(7)	-0.0012(7)
C13	0.0311(8)	0.0288(8)	0.0287(8)	-0.0010(7)	0.0110(7)	0.0009(7)
C14	0.0317(8)	0.0305(9)	0.0322(9)	-0.0008(7)	0.0092(7)	-0.0016(7)
C15	0.0295(8)	0.0294(8)	0.0285(8)	0.0003(7)	0.0086(7)	-0.0027(7)
C16	0.0435(11)	0.0386(11)	0.0800(16)	0.0079(11)	0.0141(11)	-0.0100(9)
C17	0.0606(13)	0.0480(12)	0.0403(11)	-0.0042(9)	0.0058(10)	-0.0067(10)
C18	0.0481(11)	0.0309(9)	0.0515(12)	-0.0043(8)	0.0183(9)	-0.0003(8)
C19	0.0579(12)	0.0466(11)	0.0451(11)	-0.0064(9)	0.0284(10)	-0.0068(9)
C20	0.0323(9)	0.0392(10)	0.0427(10)	-0.0016(8)	0.0112(8)	-0.0003(8)
C21	0.0384(11)	0.0880(18)	0.0472(12)	-0.0070(12)	0.0023(9)	-0.0053(11)
C22	0.0496(13)	0.0487(13)	0.118(2)	0.0112(14)	0.0327(14)	0.0162(10)
C23	0.0366(10)	0.0764(16)	0.0586(13)	-0.0050(11)	0.0235(10)	-0.0045(10)

C24	0.0404(10)	0.0327(9)	0.0397(10)	-0.0048(8)	0.0166(9)	0.0004(8)
C25	0.0587(13)	0.0309(10)	0.0626(13)	-0.0024(9)	0.0233(11)	-0.0053(9)
C26	0.0632(13)	0.0312(10)	0.0473(12)	0.0018(9)	0.0149(10)	0.0076(9)
C27	0.0497(11)	0.0355(10)	0.0338(10)	0.0045(8)	0.0107(8)	0.0092(8)
C28	0.0414(10)	0.0355(9)	0.0318(9)	0.0024(7)	0.0151(8)	0.0066(8)
C29	0.0343(9)	0.0452(11)	0.0501(11)	0.0042(9)	0.0173(9)	0.0088(8)
C30	0.0322(9)	0.0454(11)	0.0456(11)	0.0042(9)	0.0130(8)	-0.0004(8)
C31	0.0347(9)	0.0347(9)	0.0325(9)	0.0038(7)	0.0112(7)	-0.0018(7)
C32	0.0410(10)	0.0446(11)	0.0353(10)	0.0005(8)	0.0080(8)	-0.0045(8)
C33	0.0558(12)	0.0441(11)	0.0347(10)	-0.0095(8)	0.0160(9)	-0.0065(9)
C34	0.0523(11)	0.0379(10)	0.0363(10)	-0.0013(8)	0.0222(9)	0.0027(8)
C35	0.0350(9)	0.0347(9)	0.0308(9)	0.0051(7)	0.0141(7)	0.0013(7)
C36	0.0354(9)	0.0296(8)	0.0282(8)	0.0042(7)	0.0134(7)	-0.0012(7)
C37	0.0369(9)	0.0298(9)	0.0318(9)	0.0015(7)	0.0099(7)	0.0021(7)
C38	0.0361(9)	0.0294(8)	0.0302(9)	-0.0002(7)	0.0114(7)	0.0020(7)
C39	0.0600(13)	0.0466(12)	0.0568(13)	0.0030(10)	0.0163(11)	0.0192(10)
C40	0.0738(15)	0.0485(12)	0.0366(11)	0.0070(9)	0.0158(10)	0.0053(11)
C41A	0.044(3)	0.0336(10)	0.0617(18)	0.0019(10)	0.0210(18)	0.0012(11)
C42A	0.0545(14)	0.0459(13)	0.0481(14)	0.0041(11)	0.0279(12)	0.0028(11)
C43A	0.0308(10)	0.0436(12)	0.0484(13)	0.0070(10)	0.0121(10)	0.0006(9)
C44A	0.0404(14)	0.097(2)	0.0600(18)	0.0095(18)	0.0252(13)	0.0083(16)
C45A	0.0393(13)	0.0802(19)	0.0519(19)	0.0115(15)	0.0062(12)	0.0064(13)
C46A	0.0523(16)	0.0506(15)	0.112(3)	-0.0001(18)	0.0265(19)	-0.0195(12)
C41B	0.044(3)	0.0336(10)	0.0617(18)	0.0019(10)	0.0210(18)	0.0012(11)
C42B	0.0545(14)	0.0459(13)	0.0481(14)	0.0041(11)	0.0279(12)	0.0028(11)
C43B	0.0308(10)	0.0436(12)	0.0484(13)	0.0070(10)	0.0121(10)	0.0006(9)
C44B	0.0404(14)	0.097(2)	0.0600(18)	0.0095(18)	0.0252(13)	0.0083(16)
C45B	0.0393(13)	0.0802(19)	0.0519(19)	0.0115(15)	0.0062(12)	0.0064(13)
C46B	0.0523(16)	0.0506(15)	0.112(3)	-0.0001(18)	0.0265(19)	-0.0195(12)

Table 8. Hydrogen atomic coordinates and isotropic atomic displacement parameters ($Å^2$).

	x/a	y/b	z/c	U(eq)
H2A	0.8288	0.2529	0.6391	0.054
H2B	0.7893	0.3161	0.5580	0.054
H3A	0.7262	0.2177	0.6515	0.054
H3B	0.7175	0.1736	0.5681	0.054
H5	0.6764	0.4059	0.6620	0.041
H6	0.5655	0.4628	0.5739	0.053
H7	0.5499	0.6308	0.5375	0.054
H9	0.5682	0.7894	0.4723	0.052
H10	0.6370	0.9376	0.4669	0.051
H11	0.7538	0.9377	0.5470	0.045
H14A	0.7235	0.5960	0.6957	0.039
H14B	0.7942	0.6148	0.6872	0.039
H15	0.7301	0.5058	0.5605	0.036
H16A	0.5996	0.1695	0.5510	0.086
H16B	0.5552	0.2822	0.5362	0.086
H16C	0.6045	0.2463	0.6226	0.086
H17A	0.6798	0.3743	0.4712	0.082
H17B	0.5999	0.3800	0.4529	0.082
H17C	0.6345	0.2622	0.4488	0.082
H18A	0.8710	1.0343	0.6779	0.066
H18B	0.8787	1.0451	0.7655	0.066
H18C	0.8049	1.0240	0.6972	0.066
H19A	0.7887	0.8125	0.7842	0.071
H19B	0.8615	0.8445	0.8509	0.071
H19C	0.8493	0.7219	0.8128	0.071
H21A	1.0527	0.8509	0.8423	0.094
H21B	0.9915	0.8461	0.8705	0.094
H21C	0.9993	0.9527	0.8230	0.094
H22A	0.9366	0.6482	0.7133	0.109
H22B	0.9563	0.6598	0.8043	0.109
H22C	1.0149	0.6648	0.7720	0.109
H23A	1.0286	0.8320	0.7025	0.084

H23B	0.9755	0.9342	0.6829	0.084
H23C	0.9517	0.8163	0.6395	0.084
H25A	0.6833	-0.0071	0.3440	0.061
H25B	0.7201	0.0516	0.4272	0.061
H26A	0.7872	-0.0255	0.3319	0.06
H26B	0.7971	-0.0781	0.4136	0.06
H28	0.8323	0.1724	0.3292	0.043
H29	0.9397	0.2336	0.4234	0.052
H30	0.9485	0.3982	0.4665	0.05
H32	0.9219	0.5478	0.5310	0.051
H33	0.8475	0.6868	0.5356	0.055
H34	0.7317	0.6789	0.4518	0.049
H37A	0.7772	0.3564	0.2996	0.041
H37B	0.7054	0.3632	0.3073	0.041
H38	0.7725	0.2505	0.4309	0.039
H39A	0.9548	0.0546	0.4450	0.085
H39B	0.9048	0.0110	0.3608	0.085
H39C	0.9176	-0.0647	0.4354	0.085
H40A	0.8282	0.1128	0.5177	0.083
H40B	0.9076	0.1294	0.5363	0.083
H40C	0.8777	0.0059	0.5356	0.083
H41A	0.6309	0.7780	0.3265	0.07
H41B	0.6159	0.7925	0.2368	0.07
H41C	0.6920	0.7668	0.2986	0.07
H42A	0.7031	0.5586	0.2107	0.071
H42B	0.6302	0.5944	0.1458	0.071
H42C	0.6413	0.4703	0.1817	0.071
H44A	0.4670	0.5828	0.2987	0.096
H44B	0.5231	0.6806	0.3207	0.096
H44C	0.5437	0.5594	0.3601	0.096
H45A	0.5003	0.5987	0.1288	0.092
H45B	0.4925	0.7026	0.1785	0.092
H45C	0.4401	0.5994	0.1588	0.092
H46A	0.4783	0.4136	0.2268	0.111
H46B	0.5576	0.3946	0.2809	0.111

H46C	0.5335	0.4107	0.1895	0.111
H41D	0.5987	0.8096	0.2936	0.07
H41E	0.6381	0.7667	0.2425	0.07
H41F	0.6759	0.7658	0.3351	0.07
H42D	0.5131	0.5452	0.3302	0.071
H42E	0.5147	0.6798	0.3311	0.071
H42F	0.5705	0.6106	0.4009	0.071
H44D	0.5846	0.5226	0.0998	0.096
H44E	0.6431	0.4797	0.1795	0.096
H44F	0.6341	0.6114	0.1605	0.096
H45D	0.5187	0.6998	0.1385	0.092
H45E	0.4673	0.6345	0.1664	0.092
H45F	0.4773	0.5926	0.0912	0.092
H46D	0.5694	0.3787	0.2221	0.111
H46E	0.5037	0.4051	0.1441	0.111
H46F	0.5028	0.4337	0.2265	0.111

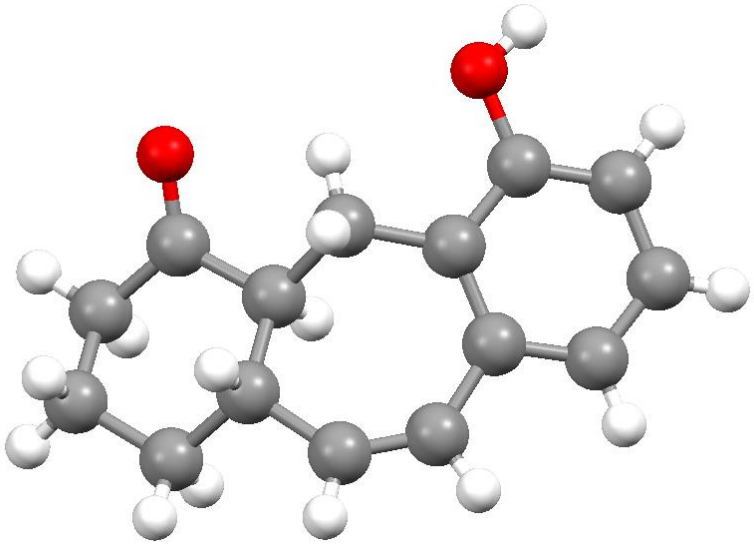

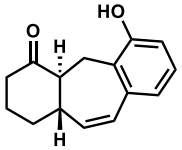

39

A clear colourless block-like specimen of $C_{15}H_{16}O_2$, approximate dimensions 0.304 mm x 0.354 mm x 0.406 mm, was used for the X-ray crystallographic analysis. The X-ray intensity data were measured.

Table 1: Data collection details.

Axis	**dx/mm**	**2θ/°**	**ω/°**	**φ/°**	**χ/°**	**Width/°**	**Frames**	**Time/s**	**λ/Å**	**Volt./kV**	***I*/mA**	**Temp./K**
Omega	49.484	26.02	-167.98	-73.16	54.79	1.00	208	5.00	0.71073	50	30.0	200
Phi	49.484	24.92	-169.08	41.00	54.79	1.00	150	5.00	0.71073	50	30.0	200

A clear colourless block-like specimen of $C_{15}H_{16}O_2$, approximate dimensions 0.304 mm x 0.354 mm x 0.406 mm, was used for the X-ray crystallographic analysis. The X-ray intensity data were measured.

A total of 358 frames were collected. The total exposure time was 0.50 hours. The frames were integrated with the Bruker SAINT software package using a narrow-frame algorithm. The integration of the data using an orthorhombic unit cell yielded a total of 7034 reflections to a maximum θ angle of 27.67° (0.77 Å resolution), of which 2762 were independent (average redundancy 2.547, completeness = 99.5%, R_{int} =3.12%, R_{sig}= 3.65%) and 2470 (89.43%) were greater than $2\sigma(F^2)$. The final cell constants of $\underline{a}$ = 8.8464(11) Å, $\underline{b}$ = 10.4228(13) Å, $\underline{c}$ = 12.8370(16) Å, volume = 1183.6(3) $Å^3$, are based upon the refinement of the XYZ-centroids of 2783 reflections above 20 σ(I) with 5.034° < 2θ < 54.68°. Data were corrected for absorption effects using the multi-scan method (SADABS). The ratio of minimum to maximum apparent transmission was 0.899. The calculated minimum and maximum transmission coefficients (based on crystal size) are 0.6700 and 0.7456.

The structure was solved and refined using the Bruker SHELXTL Software Package, using the space group P 21 21 21, with Z = 4 for the formula unit, $C_{15}H_{16}O_2$. The final anisotropic full-matrix least-squares refinement on F^2 with 157 variables converged at R1 = 3.92%, for the observed data and wR2 = 10.12% for all data. The goodness-of-fit was 1.055. The largest peak in the final difference electron density synthesis was 0.185 $e^-/Å^3$ and the largest hole was –0.186 $e^-/Å^3$ with an RMS deviation of 0.037 $e^-/Å^3$. On the basis of the final model, the calculated density was 1.281 g/cm^3 and F(000), 488 e^-.

Table 2. Sample and crystal data.

Chemical formula	$C_{15}H_{16}O_2$	
Formula weight	228.28 g/mol	
Temperature	200(2) K	
Wavelength	0.71073 Å	
Crystal size	0.304 x 0.354 x 0.406 mm	
Crystal habit	clear colourless block	
Crystal system	orthorhombic	
Space group	P 21 21 21	
Unit cell dimensions	a = 8.8464(11) Å	α = 90°
	b = 10.4228(13) Å	β = 90°
	c = 12.8370(16) Å	γ = 90°
Volume	1183.6(3) $Å^3$	
Z	4	
Density (calculated)	1.281 g/cm^3	
Absorption coefficient	0.084 mm^{-1}	
F(000)	488	

Table 3. Data collection and structure refinement.

Theta range for data collection	2.52 to 27.67°
Index ranges	-9<=h<=11, -9<=k<=13, -16<=l<=16
Reflections collected	7034
Independent reflections	2762 [R(int) = 0.0312]
Coverage of independent reflections	99.5%
Absorption correction	multi-scan
Max. and min. transmission	0.7456 and 0.6700
Structure solution technique	direct methods
Structure solution program	SHELXS-97 (Sheldrick 2008)
Refinement method	Full-matrix least-squares on F^2
Refinement program	SHELXL-2014/7 (Sheldrick, 2014)
Function minimized	$\Sigma\ w(F_o^2 - F_c^2)^2$
Data / restraints / parameters	2762 / 0 / 157

Goodness-of-fit on F^2	1.055
Final R indices	2470 data; R1 = 0.0392, wR2 = 0.0973 $I>2\sigma(I)$
	all data R1 = 0.0449, wR2 = 0.1012
Weighting scheme	$w=1/[\sigma^2(F_o^2)+(0.0569P)^2+0.0606P]$ where $P=(F_o^2+2F_c^2)/3$
Absolute structure parameter	0.0(6)
Largest diff. peak and hole	0.185 and -0.186 eÅ^{-3}
R.M.S. deviation from mean	0.037 eÅ^{-3}

Table 4. Atomic coordinates and equivalent isotropic atomic displacement parameters (Å^2).

U(eq) is defined as one third of the trace of the orthogonalized U_{ij} tensor.

	x/a	**y/b**	**z/c**	**U(eq)**
O1	0.40749(19)	0.68354(13)	0.74900(11)	0.0380(4)
O2	0.4462(2)	0.05271(14)	0.59098(11)	0.0434(4)
C1	0.4042(2)	0.60749(18)	0.66180(15)	0.0292(4)
C2	0.4431(2)	0.47875(19)	0.66681(15)	0.0318(4)
C3	0.4351(3)	0.4039(2)	0.57846(16)	0.0362(5)
C4	0.3875(3)	0.4570(2)	0.48579(16)	0.0358(5)
C5	0.3497(2)	0.58712(19)	0.47873(16)	0.0301(4)
C6	0.2913(2)	0.6312(2)	0.37712(16)	0.0354(5)
C7	0.2675(2)	0.7464(2)	0.33710(16)	0.0370(5)
C8	0.3040(2)	0.8789(2)	0.37598(16)	0.0321(5)
C9	0.3731(3)	0.9582(2)	0.28758(17)	0.0426(5)
C10	0.4062(3)	0.0944(2)	0.32265(18)	0.0427(5)
C11	0.5155(3)	0.0922(2)	0.41446(17)	0.0375(5)
C12	0.4540(2)	0.01184(19)	0.50233(15)	0.0311(4)
C13	0.4043(2)	0.87672(17)	0.47398(14)	0.0273(4)
C14	0.3271(3)	0.80705(19)	0.56492(15)	0.0311(5)
C15	0.3600(2)	0.66487(19)	0.56794(15)	0.0275(4)

Table 5. Bond lengths (Å).

O1-C1	1.372(2)	O1-H1	0.87(3)
O2-C12	1.217(2)	C1-C2	1.387(3)
C1-C15	1.401(3)	C2-C3	1.379(3)
C2-H2	0.95	C3-C4	1.378(3)
C3-H3	0.95	C4-C5	1.400(3)
C4-H4	0.95	C5-C15	1.406(3)
C5-C6	1.476(3)	C6-C7	1.323(3)
C6-H6	0.95	C7-C8	1.504(3)
C7-H7	0.95	C8-C9	1.531(3)
C8-C13	1.539(3)	C8-H8	1.0
C9-C10	1.518(3)	C9-H9A	0.99
C9-H9B	0.99	C10-C11	1.525(3)
C10-H10A	0.99	C10-H10B	0.99
C11-C12	1.507(3)	C11-H11A	0.99
C11-H11B	0.99	C12-C13	1.520(3)
C13-C14	1.535(3)	C13-H13	1.0
C14-C15	1.511(3)	C14-H14A	0.99
C14-H14B	0.99		

Table 6. Bond angles (°).

C1-O1-H1	110.8(17)	O1-C1-C2	121.07(17)
O1-C1-C15	117.45(16)	C2-C1-C15	121.48(18)
C3-C2-C1	119.81(18)	C3-C2-H2	120.1
C1-C2-H2	120.1	C2-C3-C4	119.89(18)
C2-C3-H3	120.1	C4-C3-H3	120.1
C3-C4-C5	121.21(19)	C3-C4-H4	119.4
C5-C4-H4	119.4	C4-C5-C15	119.36(18)
C4-C5-C6	116.24(19)	C15-C5-C6	124.28(18)
C7-C6-C5	132.9(2)	C7-C6-H6	113.5
C5-C6-H6	113.5	C6-C7-C8	132.14(19)
C6-C7-H7	113.9	C8-C7-H7	113.9
C7-C8-C9	109.59(17)	C7-C8-C13	112.41(16)
C9-C8-C13	112.57(17)	C7-C8-H8	107.3

C9-C8-H8	107.3	C13-C8-H8	107.3
C10-C9-C8	111.21(18)	C10-C9-H9A	109.4
C8-C9-H9A	109.4	C10-C9-H9B	109.4
C8-C9-H9B	109.4	H9A-C9-H9B	108.0
C9-C10-C11	109.70(18)	C9-C10-H10A	109.7
C11-C10-H10A	109.7	C9-C10-H10B	109.7
C11-C10-H10B	109.7	H10A-C10-H10B	108.2
C12-C11-C10	110.99(18)	C12-C11-H11A	109.4
C10-C11-H11A	109.4	C12-C11-H11B	109.4
C10-C11-H11B	109.4	H11A-C11-H11B	108.0
O2-C12-C11	121.73(19)	O2-C12-C13	122.13(18)
C11-C12-C13	116.14(16)	C12-C13-C14	112.65(15)
C12-C13-C8	110.40(15)	C14-C13-C8	111.86(16)
C12-C13-H13	107.2	C14-C13-H13	107.2
C8-C13-H13	107.2	C15-C14-C13	113.45(16)
C15-C14-H14A	108.9	C13-C14-H14A	108.9
C15-C14-H14B	108.9	C13-C14-H14B	108.9
H14A-C14-H14B	107.7	C1-C15-C5	118.20(17)
C1-C15-C14	119.65(17)	C5-C15-C14	122.15(17)

Table 7. Anisotropic atomic displacement parameters ($Å^2$).

The anisotropic atomic displacement factor exponent takes the form:
$-2\pi^2[h^2 a^{*2} U_{11} + ... + 2 h k a^* b^* U_{12}]$

	U_{11}	**U_{22}**	**U_{33}**	**U_{23}**	**U_{13}**	**U_{12}**
O1	0.0557(10)	0.0316(7)	0.0266(7)	-0.0001(6)	-0.0042(7)	0.0008(7)
O2	0.0660(11)	0.0308(8)	0.0336(8)	-0.0030(6)	-0.0053(7)	-0.0046(7)
C1	0.0296(10)	0.0287(10)	0.0294(10)	-0.0003(7)	0.0032(8)	-0.0031(8)
C2	0.0316(10)	0.0316(10)	0.0324(10)	0.0054(8)	0.0016(8)	-0.0012(8)
C3	0.0443(13)	0.0251(9)	0.0392(12)	0.0021(8)	0.0055(9)	0.0021(9)
C4	0.0433(13)	0.0294(10)	0.0347(10)	-0.0055(8)	0.0061(9)	-0.0024(9)
C5	0.0305(10)	0.0305(10)	0.0293(10)	0.0015(7)	0.0012(8)	-0.0036(8)
C6	0.0405(12)	0.0342(11)	0.0316(10)	-0.0050(8)	-0.0054(9)	-0.0056(9)
C7	0.0411(12)	0.0379(11)	0.0320(10)	-0.0007(9)	-0.0112(9)	-0.0046(10)
C8	0.0340(11)	0.0321(10)	0.0302(10)	0.0026(8)	-0.0075(8)	-0.0003(9)
C9	0.0532(14)	0.0417(12)	0.0328(11)	0.0078(9)	-0.0075(10)	-0.0049(11)

C10	0.0496(14)	0.0375(11)	0.0410(12)	0.0119(9)	-0.0035(10)	-0.0026(11)
C11	0.0429(13)	0.0300(10)	0.0396(12)	0.0027(8)	0.0005(9)	-0.0052(9)
C12	0.0330(11)	0.0270(10)	0.0333(11)	0.0012(8)	-0.0052(8)	0.0041(8)
C13	0.0295(10)	0.0255(9)	0.0269(9)	0.0004(7)	-0.0044(7)	0.0017(8)
C14	0.0383(11)	0.0277(10)	0.0274(10)	0.0002(8)	0.0007(8)	0.0020(8)
C15	0.0268(9)	0.0250(9)	0.0306(10)	0.0006(8)	0.0024(7)	-0.0022(8)

Table 8. Hydrogen atomic coordinates and isotropic atomic displacement parameters ($Å^2$).

	x/a	**y/b**	**z/c**	**U(eq)**
H1	0.441(3)	0.641(3)	0.802(2)	0.057
H2	0.4751	0.4423	0.7309	0.038
H3	0.4624	0.3158	0.5815	0.043
H4	0.3803	0.4043	0.4256	0.043
H6	0.2655	0.5631	0.3312	0.043
H7	0.2181	0.7452	0.2714	0.044
H8	0.2063	0.9207	0.3957	0.038
H9A	0.4681	0.9171	0.2640	0.051
H9B	0.3023	0.9601	0.2279	0.051
H10A	0.3109	1.1372	0.3435	0.051
H10B	0.4511	1.1436	0.2644	0.051
H11A	0.6138	1.0568	0.3915	0.045
H11B	0.5326	1.1809	0.4394	0.045
H13	0.4975	0.8271	0.4562	0.033
H14A	0.3611	0.8462	0.6312	0.037
H14B	0.2165	0.8198	0.5596	0.037

Table 9. Hydrogen bond distances (Å) and angles (°).

	Donor-H	**Acceptor-H**	**Donor-Acceptor**	**Angle**
O1-H1···O2	0.87(3)	1.93(3)	2.785(2)	169.(3)